Purinergic signalling in testicular peritubular cells

Annika Missel

Dissertation der Fakultät für Biologie
Ludwig-Maximilians-Universität München

München, 2021

Diese Dissertation wurde unter der Leitung
von Prof. Dr. Artur Mayerhofer und PD Dr. Lars Kunz
im Zeitraum von Oktober 2018 bis November 2021
im Bereich Zellbiologie – Anatomie III
des Biomedizinischen Centrums München
der Ludwig-Maximilians-Universität München
durchgeführt.

Erstgutachter:	PD Dr. Lars Kunz
Zweitgutachter:	Prof. Dr. Heinrich Leonhardt
Tag der Abgabe:	25.11.2021
Tag der mündlichen Prüfung:	25.04.2022

Eidesstattliche Erklärung

Ich versichere hiermit an Eides statt, dass die vorgelegte Dissertation von mir selbstständig und ohne unerlaubte Hilfe angefertigt wurde. Außerdem erkläre ich, dass die Dissertation weder ganz, noch in wesentlichen Teilen einer anderen Prüfungskommission vorgelegt worden ist. Ich habe mich anderweitig keiner Doktorprüfung ohne Erfolg unterzogen.

München, den 25.11.2021

_____

Annika Missel

CONTENT

ABBREVIATIONS

3R rule	Replacement, reduction and refinement
ADORA	Adenosine receptor
ACTA2	Smooth muscle actin
ADA	Adenosine deaminase
ADK	Adenosine kinase
ADP	Adenosine 5'diphosphate
AMP	Adenosine 5'monophosphate
AR	Androgen receptor
ATP	Adenosine 5'triphosphate
Ca^{2+}	Calcium
CD	Cluster of differentiation
CD26	Dipeptidyl peptidase IV (also called DPP4)
CD39	Ectonucleoside triphosphate diphosphohydrolase-1 (also called ENTPD1)
CD73	Ecto-5'-Nucleotidase (also called NT5E)
cDNA	Complementary deoxyribonucleic acid
CNN1	Calponin
CNT	Cation-linked concentrative nucleoside transporters
CRISPR/Cas9	Clustered regularly interspaced short palindromic repeats and CRISPR associated protein 9
ECM	Extracellular matrix
ENT	Equilibrative nucleoside transporters
ENTPD1	Ectonucleoside triphosphate diphosphohydrolase-1
et al.	Et aliae / et alii
FCS	Fetal calf serum
FSH	Follicle-stimulating hormone
g	Gram
GDNF	Glial cell line-derived neutrophic factor
GnRH	Gonadotropin releasing hormone
hTERT	Human telomerase reverse transcriptase
HTPC	Human testicular peritubular cell

IL	Interleukin
iMKTPC	Immortalized monkey testicular peritubular cell
LH	Luteinizing hormone
MCP	Monocyte chemotactic protein
MKTPC	Monkey testicular peritubular cell
ml	Millilitres
mM	Millimolar
MTPC	Mouse testicular peritubular cells
MYH11	Myosin-heavy chain 11
nM	Nanomolar
NOA	Non-obstructive azoospermia
NT5E	Ecto-5′-Nucleotidase
OA	Obstructive azoospermia
p53	Tumour suppressor protein p53
POM	Polyoxometalate
POM-1	Polyoxotungstate-1
siRNA	Small interfering ribonucleic acid
SMA	Smooth muscle actin
SSC	Spermatogonial stem cells
TGF-β	Transforming growth factor β
TLR	Toll-like receptor
TNF	Tumour necrosis factor
TPC	Testicular peritubular cell
UMAP	Uniform manifold approximation and projection for dimension reduction
μM	Micromolar

PUBLICATIONS AND CONTRIBUTIONS

PUBLICATION I

ATP activation of peritubular cells drives testicular sperm transport

David Fleck, Lina Kenzler, Nadine Mundt, Martin Strauch, Naofumi Uesaka, Robert Moosmann, Felicitas Bruentgens, **Annika Missel**, Artur Mayerhofer, Dorit Merhof, Jennifer Spehr & Marc Spehr

Elife, 10., 2021, doi:10.7554/eLife.62885

D. Fleck, L. Kenzler, A. Mayerhofer, J. Spehr and M. Spehr contributed substantially to the conception of this work. Experiments were designed by D. Fleck, L. Kenzler, N. Mundt, N. Uesaka, J. Spehr and M. Spehr. Data acquisition and analysis was performed by D. Fleck, L. Kenzler, N. Mundt, F. Bruentgens, **A. Missel**, R. Moosmann, N. Uesaka, M. Strauch and J. Spehr. **A. Missel** implemented all cellular studies on human testicular peritubular cells. D. Fleck, L. Kenzler, N. Mundt, M. Strauch, F. Bruentgens, A. Mayerhofer, J. Spehr and M. Spehr contributed to data interpretation. M. Strauch and D. Merhof created a new software, which was used for contraction analysis. All authors have drafted the work and / or substantively revised it. All authors have approved the submitted version of the manuscript.

We hereby confirm the above statement concerning this publication

_____ _____

Annika Missel Prof. Dr. Artur Mayerhofer

_____

PD Dr. Lars Kunz

PUBLICATION II

Testicular adenosine acts as a pro-inflammatory molecule: role of testicular peritubular cells

Annika Missel, Lena Walenta, Katja Eubler, Nadine Mundt, Hanna Heikelä, Ulrich Pickl, Matthias Trottmann, Bastian Popper, Matti Poutanen, Leena Strauss, Frank-Michael Köhn, Lars Kunz, Marc Spehr & Artur Mayerhofer

Mol Hum Reprod., 27., 2021, doi:10.1093/molehr/gaab037

A. Mayerhofer conceived of the study. **A. Missel** conducted the majority of the experiments, subsequent analyses and interpretation of the results. **A. Missel**, L. Walenta, L. Kunz, M Spehr and A. Mayerhofer contributed substantially to the implementation of this study. L. Walenta, K. Eubler, N. Mundt and H. Heikelä participated in sample generation and analysis. U. Pickl, M. Trottmann, F-M. Köhn, B. Popper, L. Strauss and M. Poutanen provided biopsies of human testes or mouse testes samples, respectively. **A. Missel** and A. Mayerhofer drafted the manuscript. All authors contributed to the writing of the final version and approved it.

We hereby confirm the above statement concerning this publication

_____ _____

Annika Missel Prof. Dr. Artur Mayerhofer

_____

PD Dr. Lars Kunz

PUBLICATION III

A translational cellular model for the study of peritubular cells of the testis

Nina Schmid*, **Annika Missel***, Stoyan Petkov*, Jan Bernd Stöckl, Florian Flenkenthaler, Georg J. Arnold, Thomas Fröhlich, Rüdiger Behr*
& Artur Mayerhofer*
(*shared first/last authorship)

Reproduction, 160(2), 259-268., 2020, doi:10.1530/REP-20-0100

A. Mayerhofer conceived of the study, directed the work and supervised the experiments. **A. Missel** and N. Schmid performed the majority of the cellular experiments. S. Petkov and R. Behr designed the immortalization experiments and S. Petkov conducted them. J. B. Stöckl, F. Flenkenthaler, T. Fröhlich and G. J. Arnold performed proteomic studies and evaluated the results. N. Schmid, **A. Missel** and A. Mayerhofer drafted the manuscript. All authors contributed to the manuscript and approved the final version.

We hereby confirm the above statement concerning this publication

_____ _____

Annika Missel Dr. Nina Schmid

_____ _____

Dr. Stoyan Petkov Prof. Dr. Artur Mayerhofer

_____

PD Dr. Lars Kunz

ABSTRACT

Extracellular ATP and its metabolites, as part of the purinergic signalling system, act *via* membrane receptors and fulfil important roles in the body. However, in the testis this signalling system is still poorly examined, but evidence for paracrine communication is increasing. Spermatogenesis takes place in the seminiferous tubules, which are surrounded by smooth-muscle like peritubular cells. The physiologic principles of luminal transport through the testis were so far unknown. The present study, now, indicates that extracellular ATP, acting through P2 receptor-dependent pathways, is a physiological trigger of contractile forces in peritubular cells, resulting in sperm transport.

Adenosine is the final metabolite of ATP, can act *via* adenosine receptors, and was found to be a pro-inflammatory molecule in the human testis. In human testicular peritubular cells (HTPCs), adenosine receptors as well as the ectonucleotidases CD39 and CD73, which can generate adenosine, are present *in situ* and *in vitro.* A malachite green assay, measuring free phosphate, identified both ectonucleotidases as being able to dephosphorylate extracellular ATP into its metabolites. Pharmacological inhibition of CD39 reduced not only the formation of extracellular phosphate, but also decreased pro-inflammatory cytokine levels, which were evoked after ATP exposure. Indeed, adenosine and its analogues elevated pro-inflammatory cytokines. Further studies, including a siRNA-mediated knock-down, identified the adenosine receptor A2B as the main mediator for adenosine-evoked production of pro-inflammatory cytokines in peritubular cells.

HTPCs are primary cells and their use is limited due to availability, heterogeneity and replicative senescence *in vitro*. Therefore, peritubular cells from the common marmoset monkey, *callithrix jacchus*, (MKTPCs) were immortalized with a piggyBac transposon containing the human telomerase gene *hTERT*. The generated iMTKPCs retained their phenotype after immortalization and grew continuously in cell culture without discernible changes. The cells revealed the typical gene expression pattern of MKTPCs and HTPCs. Like HTPCs, iMKTPCs express purinergic receptors and ATP exposure resulted in a comparable increase of pro-inflammatory cytokines. They are therefore a

promising tool for future in-depth studies concerning purinergic signalling and a translational model for human peritubular cells.

The results indicated that different parts of the testicular purinergic system are involved in the regulation of various testicular functions. One is coordinating contraction of peritubular cells in the context of sperm transport, another one is involved in the regulation of inflammatory events. If transferable to the *in vivo* situation, pharmacological interference with receptors and ectonucleotidases of this system might represent new approaches in the treatment of male infertility.

ZUSAMMENFASSUNG

Die Reaktion von extrazellulärem ATP und zugehörigen Metaboliten ist Teil der purinergen Signalmechanismen und wird über membranständige Rezeptoren vermittelt. Dieses Signalweg-System ist im Hoden noch immer unzureichend untersucht, es gibt aber zunehmend Anzeichen dafür, dass es in die parakrine Kommunikation von Zellen involviert ist. Die Spermatogenese findet in den Hodenkanälchen statt, welche von glattmuskelzellähnlichen peritubulären Zellen umgeben sind. Bisher ist es aber noch weitestgehend unbekannt, wie Spermien durch das Lumen der Hodenkanälchen transportiert werden. Die vorliegende Studie beschreibt Hinweise auf eine Beteiligung von extrazellulärem ATP, vermittelt durch P2-Rezeptor Signalwege, als physiologischer Auslöser von kontraktilen Kräften in peritubulären Zellen, und einem daraus resultierenden Spermientransport.

Adenosin ist der finale Metabolit von ATP, wirkt über Adenosin-Rezeptoren, und es wurde festgestellt, dass es als ein pro-inflammatorisches Molekül im humanen Hoden agiert. In humanen testikulären peritubulären Zellen (HTPC) sind sowohl die Adenosin-Rezeptoren als auch die Ektonukleotidasen CD39 und CD73, welche Adenosin generieren, *in situ* und *in vitro* vorhanden. Anhand des *Malachite Green Assays,* welcher freie Phosphate nachweist, wurde gezeigt, dass beide Ektonukleotidasen dazu fähig sind, extrazelluläres ATP zu ATP-Metaboliten zu dephosphorylieren. Eine pharmakologische Blockierung von CD39 reduzierte nicht nur die Entstehung von extrazellulärem Phosphat, es verringerte auch pro-inflammatorische Zytokinlevel, welche nach ATP-Stimulation erhöht waren. Tatsächlich erhöhten sich auch durch Adenosin und analoge Moleküle pro-inflammatorische Zytokinlevel. Weitere Untersuchungen, wie eine Herunterregulierung mithilfe von siRNA, identifizierten den Rezeptor A2B als hauptverantwortlichen Mediator für Adenosin-abhängige pro-inflammatorische Zytokinproduktion in peritubulären Zellen.

HTPCs sind primäre Zellen und *in vitro* in ihrem Nutzen aufgrund von Verfügbarkeit, Heterogenität und replikativer Seneszenz eingeschränkt. Daher wurden peritubuläre Zellen des Weißbüschelaffen *Callithrix jacchus* (MKTPC) mit Hilfe des PiggyBac-

Transposons und einem darin enthaltenen Gen der humanen Telomerase (*hTERT*), immortalisiert. Diese erzeugten iMKTPCs behielten ihren Phänotypen nach Immortalisierung bei und konnten in der Zellkultur kontinuierlich und ohne erkennbare Veränderungen kultiviert werden. Die Zellen zeigten typische Expressionsmuster wie sie von MKTPCs und HTPCs bekannt sind. Verglichen mit HTPCs exprimieren iMKTPCs purinerge Rezeptoren, und Stimulation mit ATP erzeugte vergleichbare Erhöhungen von pro-inflammatorischen Zytokinleveln. Sie stellen daher ein vielversprechendes Mittel für tiefgreifendere Studien am purinergen System dar und sind ein translationales Modell für humane peritubuläre Zellen.

Die Ergebnisse der vorliegenden Arbeiten zeigen, dass unterschiedliche Teile des purinergen Systems im Hoden an verschiedenen Regulationsmechanismen der Hodenfunktion beteiligt sind. Ein Teil koordiniert Kontraktionsmechanismen von peritubulären Zellen im Rahmen des Spermientransports, ein anderer ist involviert in die Regulation von inflammatorischen Vorgängen. Sofern dies auf die *in vivo* Situation übertragbar ist, könnte eine pharmakologische Beeinflussung von Rezeptoren und Ektonukleotidasen dieses Systems neue Herangehensweisen bei der Behandlung von männlicher Unfruchtbarkeit repräsentieren.

1. INTRODUCTION

"Individuals and couples have the right to decide the number, timing and spacing of their children." (WHO 2020)

Sustaining a species requires successful reproduction. As testicular disorders and impaired fertility in men are constantly increasing, there is a growing need for basic research in the human testis. The wish for a child is an individual decision whereby fertility disorders can cause extreme misery.

The number of reproductive disorders in Western countries is rising steadily and the total fertility rate has significantly decreased in the last decades (Skakkebaek et al. 2016). Fertility in humans describes the ability to induce pregnancy, infertility occurs if vulnerable intercourse within one year does not result in a pregnancy (Nieschlag 2009). Worldwide, 48 million couples are affected by infertility (WHO 2020), in Germany, fertility problems concern one in eight couples. Men contribute to roughly half of the cases (Statistisches Bundesamt, 2021). About 30 - 45% of male infertility is due to not identified causes of abnormal semen quality, and described as 'idiopathic male infertility'. Likely environmental and genetic factors are involved (Pierik et al. 2000; Jungwirth et al. 2012).

The testis, as the site of sperm production, is one of the least investigated organs in the human body. Understanding molecular processes in the testicular tissue is the main basis of a better comprehension of male reproduction, to both recover and circumvent testicular disorders and therefore to eventually improve male fertility.

The reproductive performance of men can be impaired by a wide variety of factors. Abnormal semen quality, inadequate number of sperm, erectile disfunction and malfunction of the ductal system mirror only a small proportion of potential issues. There is an increasing evidence for a decline in sperm counts (Levine et al. 2017) and testosterone levels (Travison et al. 2007; Travison et al. 2009) of Western men, while the amount of testicular cancer (McGlynn et al. 2003; Skakkebaek et al. 2016) and prevalence of erectile disfunctions are rising (Capogrosso et al. 2019).

1.1 Normal and impaired testicular function

The typical healthy human testis is of solid consistency with a volume of 12 – 30 ml (on average 18 ml) (Nieschlag and Behre 2009). To be classified as normozoospermic according to recently updated decision limits, the ejaculate of men should have a volume of at least 1.5 ml with more than 48 million sperm cells per ml, a sperm motility over 63% and more than 12% of a normal sperm morphology (Kandil et al. 2021; WHO 2021).

Azoospermia is the absence of sperm in the ejaculate, involving 15% of infertile men and can be divided into two subgroups, obstructive azoospermia (OA) or non-obstructive azoospermia (NOA). About 40% of the cases are due to OA, as a consequence of physical blockades in the ductal system, from the *rete testis* to the ejaculatory ducts, but of normal spermatogenesis (Jow et al. 1993; Wosnitzer et al. 2014). NOA comprises 60% of azoospermia cases including testicular failures, resulting in disturbed spermatogenesis. Made accountable for this can be, for instance, hypogonadism, genetic abnormalities, toxin exposure, cryptorchidism, Sertoli cell only syndrome and germ cell arrest. However, the reasons in the majority of cases are still unknown (Wosnitzer et al. 2014; Chiba et al. 2016).
As 2 – 9% of all boys at birth suffer from cryptorchidism, this is one of the most common birth defects (Boisen et al. 2004) and the risk for cryptorchidism is increasing (Le Moal et al. 2021). The failure of the testis to descend to the bottom of the scrotum is associated with decreased fertility later in life, as well as increased risks for germ cell tumours and testicular torsion. If not surgically corrected within the first six months of life, about 10% of the patients will become infertile (Leslie et al. 2021). Sertoli cell only syndrome or germ cell aplasia concerns about 30% of infertile patients, due to low or absent spermatogenesis. It is an idiopathic condition of men, typically without sexual abnormality (Nieschlag et al. 2009; Ramphul and Mejias 2021). Germ cell arrest or spermatogenesis arrest interrupts the differentiation of germ cells at several steps of spermatogenesis, due to genetic or hormonal factors, impaired cell-cell interactions, or secondary external factors (Martin-du Pan and Campana 1993; Tsai et al. 2012).

1.2 Testicular physiology & infertility associated changes

Understanding testicular anatomy and physiology is the foundation to both maintain and recover male fertility. The main functions of the testis are the production of germ cells, as well as synthesis and secretion of male steroid hormones. The testis is enclosed by the *tunica albuginea* (Figure 1A) and divided into two major compartments, the tubular and the interstitial one, as well as a small peritubular one in between.

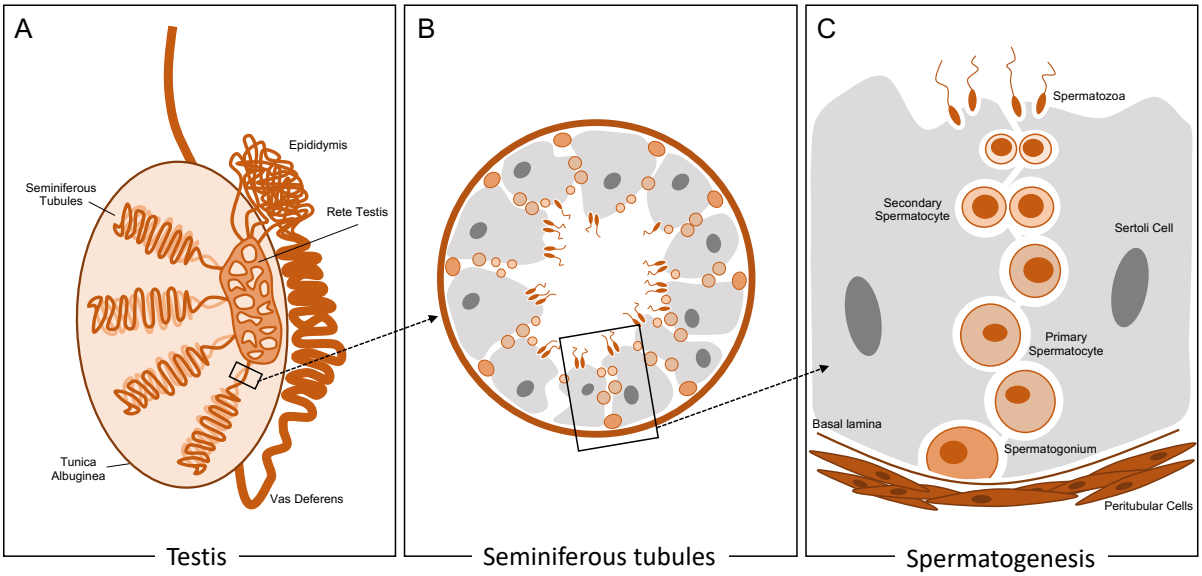

Figure 1. Schematic overview of the whole testis, seminiferous tubules and spermatogenesis in the human.

(A) Encased into the tunica albuginea, the testis contains sperm producing seminiferous tubules, and the tubules ends merge into the rete testis. Sperm cells in the rete testis migrate to the epididymis and leave the testis through the vas deferens. (B) Cross section of a seminiferous tubule. (C) Schematic representation of the cellular structure and germ cell differentiation of a seminiferous tubule. Surrounded by several layers of peritubular cells and a basal lamina, Sertoli cells build the scaffold of the tubules and the location of spermatogenesis. Different states of germ cells differentiate into spermatozoa, surrounded by Sertoli cells. Modified on the basis of Premanandan and Jennings (2017).

One main actor of the interstitial compartment is the testosterone producing Leydig cell, next to immune cells, blood vessels, nerve fibres, lymphatic vessels and loose connective tissue. Spermatogenesis takes place in the tubular compartment (Figure 1B). The shape of the seminiferous tubules is defined by Sertoli cells, enclosing

germ cell development (Figure 1C), and the tubules in men are surrounded by multiple layers of peritubular cells (Weinbauer et al. 2009).

1.2.1 The tubular, interstitial and peritubular compartments

Composed of germ cells and Sertoli cells, the tubular compartment forms 60 - 80% of the total testis volume. In total, one healthy human testis contains approximately 600 seminiferous tubules (Weinbauer et al. 2009). Elongated, thin and spindle-shaped peritubular cells build several layers of the wall of the seminiferous tubules, next to extracellular matrix (ECM) proteins (Anthony and Skinner 1989; Mayerhofer 2013). The ECM is composed of collagens, fibronectin, laminin, decorin and others (Albrecht et al. 2006; Adam et al. 2011; Adam et al. 2012), stabilizing the wall of the seminiferous tubules (Skinner et al. 1985). The inner part of the peritubular layer displays a smooth-muscle like phenotype, the outer layer the phenotype of connective tissue (Davidoff et al. 1990).

There is a huge variation in the anatomy and physiology of reproductive tracts and gonads between different species (Wildt et al. 2010). For example, in contrast to several layers in humans, the peritubular wall of rodents consists of a single layer of peritubular cells (Tung and Fritz 1990; Mayerhofer 2013). Further variations are the missing ECM in rodents in contrast to the peritubular wall of humans (Adam et al. 2011; Flenkenthaler et al. 2014).

In the orchestra of testicular cells, peritubular cells play an essential role. They are in direct contact to both germ cells and Sertoli cells on one side, and on the other side to interstitial cells, such as Leydig cells and immune cells (Spinnler et al. 2010; Oatley and Brinster 2012). Their strategic position and paracrine role in the testis indicate their impact on the whole testicular function (Welsh et al. 2012). They contribute to the stem cell niche, a special environment along the basement membrane, protecting spermatogonial stem cells and maintaining the stem cell pool by self-renewal and differentiation. Adjacent somatic cells supply required signalling molecules and growth factors (Spinnler et al. 2010; Goossens and Tournaye 2013).

A remodelling of this compartment is often seen in an infertile phenotype and defined as fibrosis. As a response to stress and injury, pathophysiological repair mechanisms induce an increased amount of ECM, a thickening of the basal lamina and abnormal arranged collagen fibers, leading to an overall thickening of the peritubular wall (Soderstrom 1986; Kisseleva and Brenner 2008). The major contribution to excessive production of ECM during fibrosis is described by collagens, fibronectin, decorin and biglycan (Adam et al. 2012; Bonnans et al. 2014; Mayer et al. 2016).

1.2.2 Sperm development / spermatogenesis

Spermatogenesis is the basis of male fertility. It takes place in the thin and coiled seminiferous tubules, bordered by the Sertoli cells, which stretch their highly polarized cellular bodies along the seminiferous tubule epithelium to nourish adjacent germ cells. Seminiferous tubules are arranged in lobules and surrounded by a basement membrane, extracellular matrix, and peritubular cells (Bustos-Obregon 1976). Sertoli cells have an enormous surface area, reaching from the basal lamina to the lumen, and each one is closely associated with about 30 germ cells in different stages (Weber et al. 1983; Mruk and Cheng 2004). Spermatogenesis consists of highly organized cycles, which are essential for continuous sperm production and depends on both intrinsic and extrinsic factors (Hess and Renato de Franca 2008).

A special peritubular environment, supporting germ cell development and movement and separating germ cells from the immune system, is created by the blood-testis barrier and formed by Sertoli cells, connected *via* tight junctions (Wong and Cheng 2005). During spermatogenesis, initially diploid spermatogonial stem cells (SSC) can be either self-renewed to restore the stem cell pool or divided into spermatogonia by mitosis. SSCs are imbedded in the cytoplasmic niches of Sertoli cells to get nourished by them. Starting with mitosis, spermatogonia are transformed and differentiated into spermatocytes, prior to a meiotic generation of haploid spermatids. The last step is the so called spermiogenesis, the maturation of spherical, haploid spermatids into highly condensed, elongated and mature spermatozoa (Hess and Renato de Franca 2008; Weinbauer et al. 2009; O'Donnell et al. 2011). The number of cell divisions during the expansion of spermatogonia into spermatocytes is characteristic for each species (Clermont 1972; Ehmcke et al. 2006; Hess and Renato de Franca 2008). Apoptosis of germ cells occurs in all mammals. This type of cell death controls the amount of sperm

output and is mediated among others by the tumour suppressor protein p53 (Russell et al. 2002).

1.2.3 Hormonal regulation of spermatogenesis

The main regulators of steroid synthesis and gametogenesis are the gonadotropins GnRH (gonadotropin releasing hormone), LH (luteinizing hormone) and FSH (follicle-stimulating hormone). In a neuro-endocrine network, GnRH is released from the hypothalamus and stimulates the pituitary to synthesize and secrete FSH and LH. Both hormones bind to G-protein coupled receptors. LH stimulates the secretion of testosterone and other androgens by Leydig cells. FSH targets Sertoli cells to promote the maturation of spermatogonia (Weinbauer et al. 2009; Schlatt and Ehmcke 2014; Yoon et al. 2019).

1.2.4 Contractile cells and sperm transport

Spermatogenesis is completed with the release of immature and immotile spermatozoa from the Sertoli cell environment into the tubular lumen. For the final maturation, cells have to reach the *rete testis* and epididymis, but how they are transported is still unclear (Hargrove et al. 1977; Romano et al. 2005). As human testicular peritubular cells in the wall of seminiferous tubules are able to contract and relax, they are thought to drive transport of immotile spermatozoa (Ross and Long 1966; Romano et al. 2005; Schell et al. 2010). They express the smooth muscle proteins SMA (smooth muscle actin, ACTA2), CNN1 (calponin), and MYH11 (myosin-heavy chain 11) (Mayerhofer 2013). MYH11 is one of the main actors of contractile mechanisms (Fernandez et al. 2008). Potent stimuli of smooth muscle contraction are TGF-β (transforming growth factor β), endothelin-1, oxytocin and angiotensin II (Tung and Fritz 1991; Harris and Nicholson 1998; Rossi et al. 2002). Endothelin can be secreted by Sertoli cells, acting on specific receptors on peritubular cells (Filippini et al. 1993; Maggi et al. 1995; Tripiciano et al. 1996; Romano et al. 2005). The hormone Angiotensin II causes contraction *via* binding to the AT1R receptor (Rossi et al. 2002; Welter et al. 2014).

Despite some evidence, a direct link between (impaired) contractility and male (in)fertility was still missing. In testes of infertile men, mast cells and macrophages multiply in a fibrotically remodelled peritubular wall and imply sterile inflammation events, which are linked to a reduction or even a loss of the contractile markers SMA and CNN1 (Schell et al. 2010; Welter et al. 2013). Structural changes and depositions of ECM proteins are indicators for fibrotic processes and can also be linked to inflammation in the peritubular wall. This might lead to a phenotypic switch of the peritubular wall and its cells, impaired sperm transport, and consequently infertility may result (Adam et al. 2011; Welter et al. 2013).

1.3 Cellular models of testicular peritubular cells

1.3.1 Patient-derived HTPCs

Human testicular peritubular cells are a unique human testicular cell culture model, which allows mechanistic studies. They can be isolated by a tissue explant culture of small patient-derived tissue fragments and are usable for up to twelve passages (Albrecht et al. 2006; Walenta et al. 2018). These smooth-muscle like cells express the androgen receptor (AR) (Mayer et al. 2018), produce two stem cell niche regulatory factors, the glial cell line-derived neutrophic factor (GDNF) (Spinnler et al. 2010) and C-X-C motif chemokine ligand 12 (CXCL12) (Flenkenthaler et al. 2014), extracellular matrix components like collagen, decorin and biglycan (Adam et al. 2012), and toll-like receptors (TLRs) (Mayer et al. 2016). Also, a plethora of pro-inflammatory cytokines was found to be released by HTPCs (Mayerhofer 2013; Welter et al. 2014; Walenta et al. 2018).

1.3.2 Differences in spermatogenesis among species

Species-dependent differences include both testicular structure and the spermatogonial stem cell system. The peritubular wall of rodents differs from the one of humans, as rodents have only a single layer of peritubular cells (Tung and Fritz 1990; Mayerhofer 2013). Consequently, mice have no ECM in the peritubular layer in contrast to humans (Adam et al. 2011; Flenkenthaler et al. 2014). Further, rodents have

an increased amount of germ cells linked to one Sertoli cell and therefore a higher density of germ cells compared to humans (Weinbauer et al. 2009). Also, spermatogonial stem cells differs in between species, as they can vary regarding their type, number and efficiency. While one spermatogonial stem cell of mice generates 1024 spermatocytes in theory, there are 32 spermatocytes in rhesus monkeys and more similar to the monkey, 4 generated spermatocytes in humans (Ehmcke et al. 2006).

1.3.3 A translational model for testicular peritubular cells

More similar to the human, and therefore suitable as translational model organisms, are non-human primates. One of those is the new world monkey common marmoset (*Callithrix jacchus*), a small monkey (200 – 600 g) with a high reproductive efficiency, originating from the South American rainforest (Orsi et al. 2011). A vast number of studies using the common marmoset monkey are known, including neuroscience (Okano et al. 2012; Shimogori et al. 2018; Schaeffer et al. 2019), multiple sclerosis (t Hart et al. 2000) or pharmacology and toxicology (Zuhlke and Weinbauer 2003). These monkeys are well established in reproductive research as they have similar testicular structures to the human regarding germ cell development and architecture of the tubular wall (Hearn et al. 1978; Holt and Moore 1984; Millar et al. 2000; Li et al. 2005; Albert et al. 2010).
A recent study investigated isolated peritubular cells from adult common marmosets and compared them to HTPCs. Isolated monkey testicular peritubular cells (MKTPCs) showed expression of all relevant peritubular markers and high similarities to HTPCs on the proteome level (Schmid et al. 2018).

1.4 Inflammatory processes in the testis

Inflammatory events in the genital tract of men can account for male infertility by several reasons, deceptively often without any physical discomfort. Inflammation in the testis can be either sterile or induced by viral or bacterial infections (Schuppe et al. 2010). Accountable reasons for sterile inflammation are mechanical traumas, testicular torsion or autoimmune disorders (Sarkar et al. 2011). Other possible consequences of

testicular inflammation are decreasing testosterone and LH levels, spermatogenic arrest, and perturbed sperm motility (Cutolo et al. 1991; O'Bryan et al. 2000).

Inflammation in the human testis can be both acute and chronic and caused by several reasons including oxidative stress or an imbalance of cytokines (Reddy et al. 2006). For instance, increased cytokine levels in the seminal plasma of men are associated with abnormal semen quality (Maegawa et al. 2002). Despite their potential danger, the availability of pro-inflammatory cytokines is crucial for most physiological functions in the testis, albeit dependent on their concentration levels.

1.4.1 Pro-inflammatory cytokines

Cytokines are a group of signalling molecules, secreted by various cells, affecting cellular interaction and communication. They mediate immunity and inflammation and can be on the one side soluble messenger factors, and on the other side integral membrane proteins (Dinarello 2007). Cytokines are classified by their functionality, and not by structural features, into molecule families. Three classes are known, tumour necrosis factors (TNFs), interleukins (IL) and chemokines (Holtmann and Resch 1995). Cells use cytokines as regulators against pathogens, as they can cause powerful paracrine or autocrine amplification mechanisms. Failures of this well-orchestrated system can result in dramatic consequences (Holtmann and Resch 1995).

1.4.2 Inflammatory cytokines in the testis

Cytokines have a direct regulatory effect on functionality and development of the testis. There are pro- and anti-inflammatory ones, based on their spectrum of actions. Especially an imbalance of pro-inflammatory cytokine levels can result in impaired male fertility (Naz and Evans 1998). One major and the prototypical pro-inflammatory cytokine is IL-1B. In the testis, it is essential to regulate spermatogenesis, but higher amounts can be cytotoxic to germ cells and can decrease the quality of semen, the amount of sperm and their motility (Gruschwitz et al. 1996; Kocak et al. 2002; Fraczek and Kurpisz 2007). Several testicular cells are described to produce the interleukin IL-6 (Boockfor et al. 1994; Syed et al. 1995). For instance, Sertoli cells release IL-6 to regulate

spermatogonial proliferation (Stephan et al. 1997; Okuma et al. 2005). However, increased levels of both IL-6 and IL-8 are correlated with disturbed fertility (Naz and Evans 1998; Seshadri et al. 2009).
TNF-α mediates cell-death signals (Hedger and Meinhardt 2003). In the testis this cytokine is involved in apoptosis of germ cells, binding of germ cells to Sertoli cells, steroidogenesis of Leydig cells and the production of testosterone (Hong et al. 2004; Xia et al. 2005). Increased levels were found in the semen of men with impaired fertility (Seshadri et al. 2009; Martinez-Prado and Camejo Bermudez 2010).

Previous publications described HTPCs as sources of pro-inflammatory cytokines including IL-1B, IL-6, IL-8, TNF-α and the monocyte chemotactic proteins (MCPs) MCP1 and MCP3 (Schell et al. 2008; Eubler et al. 2018; Walenta et al. 2018). The activation of the cation channel TRPV2 increased levels of *IL-6*, MCP1 and IL8 in HTPCs (Eubler et al. 2018), treatment of HTPCs with ATP led to an increase of *IL-1B*, *IL-6*, *MCP1* and *MCP3* levels (Walenta et al. 2018).

1.5 ATP is a key mediator in purinergic signalling

A wide range of biological events is mediated by extracellular nucleosides and nucleotides. ATP (Adenosine 5'triphosphate) is best known as the energy supplier for cellular processes. However, if released into the extracellular space it can also provoke inflammation (Allard et al. 2017). ATP and its metabolite adenosine were already described in 1929 as essential signalling actors in heart and coronary blood vessels (Drury and Szent-Gyorgyi). Later, ATP was detected as a co-transmitter of noradrenaline and acetylcholine in sympathetic and cholinergic nerves, the first time as an extracellular messenger molecule (Burnstock 1972, 2009).
Intracellular levels of ATP range from 1 – 10 mM, much higher than those in extracellular spaces (~10 nM) (Trautmann 2009; Zhao et al. 2017). In the testis, sources of extracellular ATP are thought to be Sertoli cells, mast cells, nerve fibers and continuously dying germ cells (Mayerhofer et al. 1999; Gelain et al. 2003; Xiong et al. 2009; Mayerhofer et al. 2018). As impaired spermatogenesis can cause higher innervation density and increased mast cell numbers, this can raise ATP levels in all testicular compartments (Mayerhofer et al. 1999; Meineke et al. 2000). However, even

though the testis contains multiple possible sources of ATP, insights in the roles of extracellular ATP regarding the testis are still rare (Burnstock 2014).

Extracellular ATP can be a local regulator of adjacent cells by the activation of purinergic receptors. Two types of purinergic receptors are known, one group is called P1 or adenosine receptors and is selective to adenosine, the other family is called P2 receptors and is activated by ATP and/or ADP (Adenosine 5'diphosphate) (Figure 2). P2 receptors are distinguished into two subgroups, defined as the ligand-gated ion channels P2X receptors and G protein-coupled P2Y receptors (Burnstock and Kennedy 1985; Abbracchio and Burnstock 1994). A recent publication demonstrated the expression of P2X4 and P2X7 in peritubular cells of the human testis, *in situ* and *in vitro*, and identified ATP as a contributor in the regulation of these cells (Walenta et al. 2018).

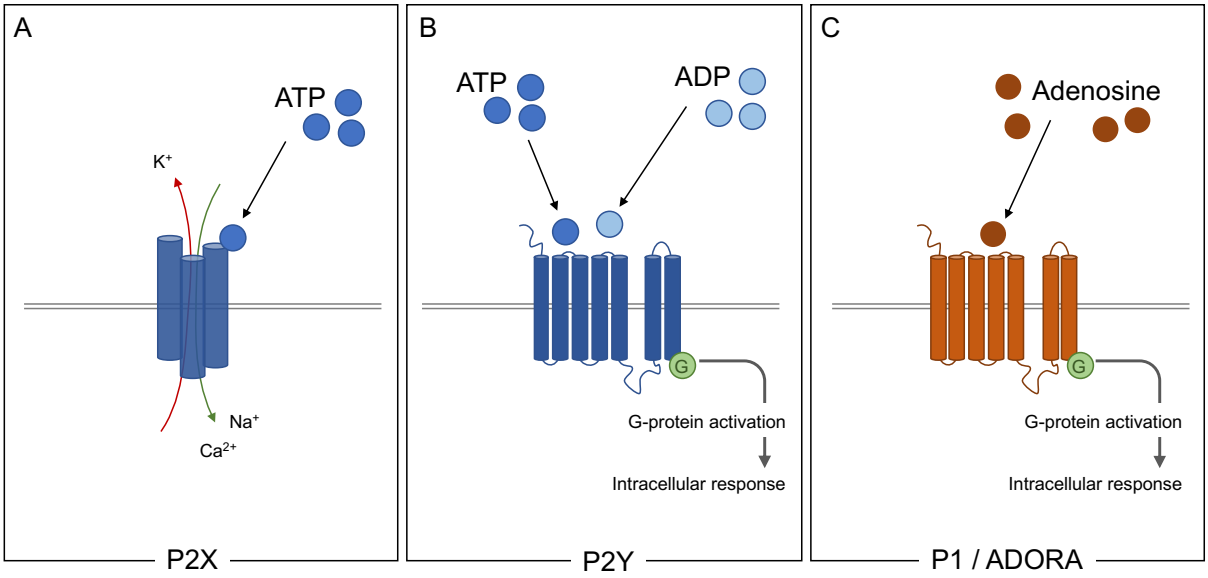

Figure 2. P receptors of the purinergic system.

(A) P2 receptors bind di- and triphosphate nucleotides and can be subdivided into the cation channels P2X and P2Y receptors. P2X receptors consist of three protein subunits and get activated by binding of ATP. (B) Both ATP and ADP bind to the seven transmembrane-spanning G protein-coupled P2Y receptors. (C) P1 receptors or adenosine receptors (also called ADORA receptors) are of similar structure as P2Y receptors, but selective for adenosine. Modified on the basis of Menzies et al. (2017).

1.5.1 The ATP-CD39-CD73-adenosine cascade

Ectonucleotidases are enzymes which hydrolyse phosphate groups, and thereby control the levels of different extracellular nucleotides. In the ATP-CD39-CD73-adenosine cascade, the ectonucleotidases CD39 (ectonucleoside triphosphate diphosphohydrolase-1; also called ENTPD1) and CD73 (ecto-5'-nucleotidase; also called NT5E) are responsible for the generation of adenosine out of extracellular ATP (Figure 3). CD39 is part of the E-NTPDase-family and the converter of ATP to both ADP and AMP (Adenosine 5'monophosphate), after ATP is released into the extracellular space (Zimmermann et al. 2012; Antonioli et al. 2013; Burnstock 2014). CD39 has an extracellular catalytic site and two transmembrane domains, serving as an anchor to the cell membrane. These domains interact with each other and are essential for the catalytic activity and specificity to the substrate (Grinthal and Guidotti 2006). CD73 can either exist as a cytosolic membrane-bound or in an extracellular membrane-bound form. Glycosyl phosphatidylinositol links the glycoprotein CD73 to the membrane. The extracellular one is part of the ATP cascade, hydrolysing AMP to adenosine (DePierre and Karnovsky 1974; Zimmermann 1992; Schetinger et al. 2007). Different from ENTPD-ases, 5'-nucleotidases solely dephosphorylate nucleoside mono-phosphates (Hunsucker et al. 2005).

In contrast to missing data in the human testis, expression of CD39 and CD73 was described in rodents. In mouse and rat testis, CD39 was found in blood vessels, peritubular cells, Sertoli cells and the interstitium (Martin-Satue et al. 2009). CD73 is expressed in peritubular cells, Sertoli cells and interstitial cells, but also in all germ cell stages, except spermatozoa (Martin-Satue et al. 2010). The first evidence for their functionality was an accumulation of extracellular adenosine when isolated peritubular cells of immature rats were exposed to ATP (Gelain et al. 2003).

Ectonucleotidases can be inhibited by pharmacological tools, to modulate the concentration of extracellular cytokines. The NTPDase inhibitors Polyoxometalates (POM) are negatively charged, composed of stable anionic complexes with the metal ions tungsten, molybdenum or vanadium and therefore simulate the nucleotides (Müller et al. 2006). They bind to the substrate-binding loop structure in an electrostatically way, inducing conformational changes in the enzymes and then

reduce their functionality (Zebisch et al. 2012). In addition, they are very stable at physiological pH levels (Lee et al. 2015). The family member POM-1 (Polyoxotungstate-1) is an effective blocker of the ATP breakdown by CD39. POM-1 was, for instance, a useful tool to detect specific roles of CD39 in renal and myocardial diseases, as it inhibited ischemic precondition *in situ* (Grenz et al. 2007; Kohler et al. 2007).

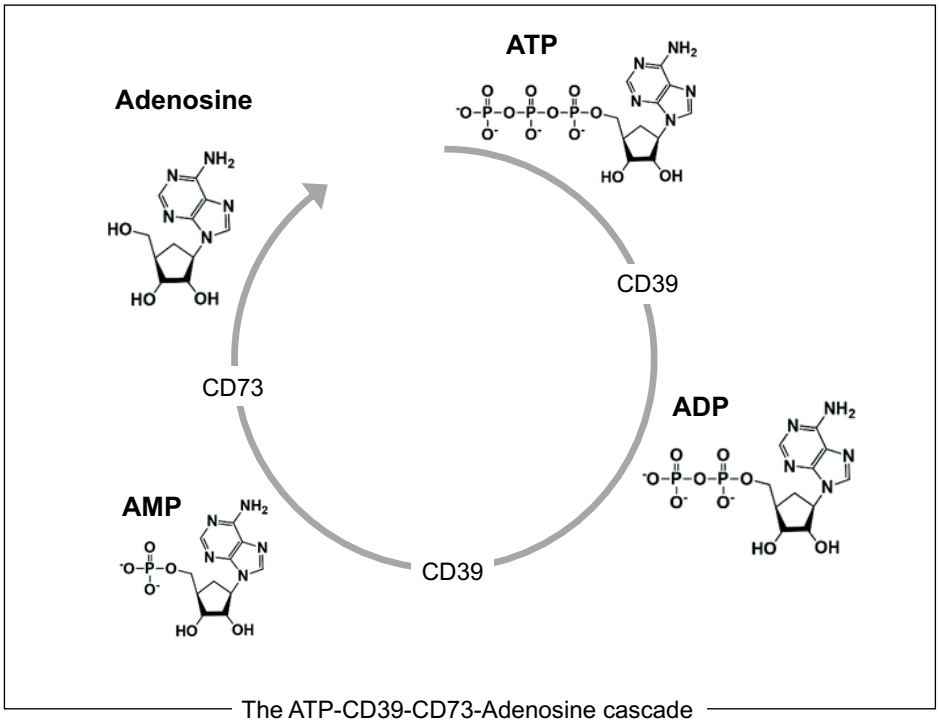

Figure 3. ATP and its metabolites.

Adenosine can be generated by the ectonucleotidases CD39 and CD73 in the extracellular space. CD39 hydrolyses ATP/ADP resulting in ADP/AMP, respectively. CD73 is responsible for the dephosphorylation step of AMP to adenosine. Modified on the basis of Li and Liu (2020).

Levels of extracellular adenosine are between 20 and 300 nM in normal physiological conditions and can rise due to extreme physiological conditions or pathological states up to 30 µM (Newby 1984). Like many other molecules, the location and local concentration of adenosine decides between boon or bane. On the one hand, adenosine has organ- and cytoprotective functions. It can inhibit inflammatory processes and support angiogenesis. On the other hand, adenosine can also accumulate in solid

tumours, stimulating tumour growth and angiogenesis and inhibiting cytokine production (Spychala 2000).

1.5.2 The adenosine receptors *ADORA*

Adenosine can bind with different affinities to adenosine receptors (gene name: *ADORA* (Fredholm et al. 2019)), a superfamily of (rhodopsin-like) G protein-coupled receptors, comprising A1, A2A, A2B and A3 (Fredholm et al. 1994; Hasko et al. 2008; Jacobson et al. 2012; Borea et al. 2018). Their distribution is described in a wide range of tissues and organs, concerning among others to vasodilation, neuromodulation, and inflammation (Ballesteros-Yanez et al. 2017). Due to their wide spectrum of expression, they are of great interest and an attractive target for potential drugs. Next to adenosine itself, an agonist of A2A is, for example, used to image coronary arteries or an antagonist to treat Parkinson's disease. A3 agonists are applied in autoimmune diseases and cancer (Borea et al. 2016).

All four adenosine receptors share homologue sequences of 80 - 95% and their core domains consist of seven transmembrane domains, which are linked by three intra- and three extracellular loops (Ramkumar et al. 1993; Fredholm et al. 2000). Adenosine receptors are able to act as homo- and heteromers (Ferre et al. 2008; Moriyama and Sitkovsky 2010; Smith and Milligan 2010) which enhance the complexity to address their specific roles in certain tissues. All four subtypes share their variety of functionality in inflammatory responses, dependent on the specific tissue. Both pro- and anti-inflammatory actions are described for all adenosine receptors. For example, A2A has pro-inflammatory actions in the central nervous system, but also anti-inflammatory ones in the peripheral system and is a strong inhibitor of cytokine production (Borea et al. 2016). A3 affects a wide range of inflammatory diseases and is expressed in almost all immune cells, however, potentially both pro- and anti-inflammatory (Borea et al. 2018).

To date, knowledge about expression and functionality of adenosine receptors in the testis is still very rare and missing in humans. Earlier studies in testis of 15-day old rats identified expression of A1 dominantly in Sertoli cells (Murphy and Snyder 1981;

Monaco and Conti 1986). Another study using adult rats identified A3 in germ cells, A1 in Sertoli cells and failed to detect A2 receptors (Rivkees 1994).

1.5.3 Further adenosine metabolism enzymes and nucleoside transporters

In resting conditions, there is a good balance of extra- and intracellular levels of adenosine (Figure 4). In certain circumstances, including inflammation, ischemia or hypoxia, adenosine can pass the cell membrane by transport through ENTs (equilibrative nucleoside transporters) and/or CNTs (cation-linked concentrative nucleoside transporters). Intracellular adenosine can be rapidly deaminated to inosine by the adenosine deaminase (ADA) or converted to AMP by the adenosine kinase (ADK) (Borea et al. 2018). In addition to the intracellular ADA, this deaminase is also present on the extracellular site, bound to the dipeptidyl peptidase CD26. Similar to ectonucleotidases and adenosine receptors, this part of the adenosine metabolism is largely unclear in the human testis. However, rat studies of Gelain et al. (2003) gave clear pharmacological evidence for ADA functionality in Sertoli cells, germ cells and peritubular cells.

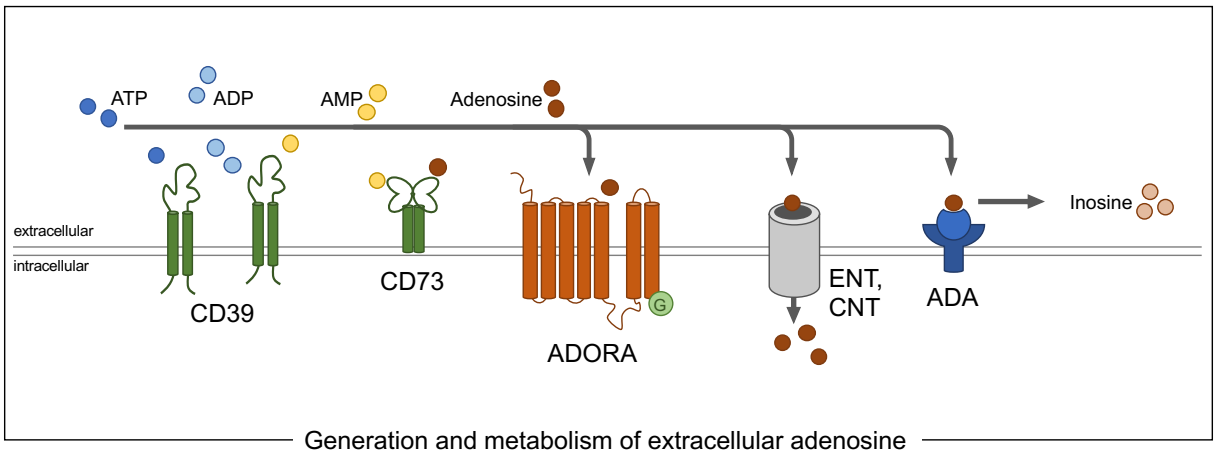

Figure 4. Components of the purinergic system.

The ectonucleotidases CD39 and CD73 hydrolyse extracellular ATP to its metabolites ADP, AMP and adenosine. Extracellular adenosine can activate the adenosine receptors ADORA, pass the membrane through the transporters ENT or CNT or can be converted by ADA to inosine. Modified on the basis of Junger (2011) and Zimmermann (2021).

1.6 Aims of the thesis

Purinergic signalling is a rather well described mechanism throughout the human body. However, it is poorly understood in the testis, especially in the human one. The goal of this work was to gain insights into this complex signalling system in the testis, with a focus on inflammatory events, contractile forces, and the impact on male (in)fertility. Three, closely related main topics are the basis of the present work.

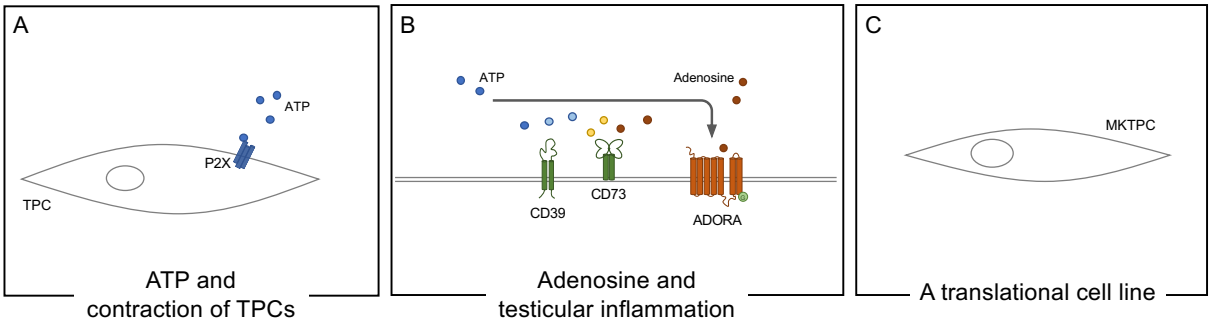

Figure 5. Schematic overview of the main projects.

A) Contractions of the seminiferous tubules in the testis are the only way to transport immotile spermatozoa to the *rete testis* and therefore to the epididymis. Still unclear are the mechanisms and potential trigger events of tubular contractions. A possible involvement of extracellular ATP was therefore investigated, employing the cellular model HTPC (Figure 5A). Contraction measurements in response to ATP were realized, both in a live-cell-imaging setting and with the use of collagen-gel lattices. Moreover, the results obtained in HTPCs were compared to an *in vivo* mouse model and *in vitro* mouse testicular peritubular cells (MTPCs).

B) ATP is a main player of the purinergic system, and was found to be a danger signal in HTPCs (Walenta et al. 2018). Still unclear was the role of ATP metabolites, the question whether adenosine is generated in the human testicular compartment by ectonucleotidases, and how adenosine interacts with other receptors of the purinergic system. The expression of ectonucleotidases and adenosine receptors and their roles in ATP and adenosine signalling was therefore assessed (Figure 5B). Beside HTPCs and MTPCs, an organotypic

mouse whole testis culture was exploited for better insights into intratesticular actions.

C) While HTPCs are the only human *in vitro* model for mechanistic studies in the human testis, their usability is limited due to their availability and patient origin. MKTPCs bypass most of the limitations. Nevertheless, *in vitro* in-depth mechanistic studies are restricted, because they exhibit replicative senescence. Therefore, MKTPCs were immortalized to receive a functional, stable and translational model for a better understanding of the role of peritubular cells. The newly generated cell line was characterized, compared to MKTPCs and tested for expression of the ATP-mediators P2X4 and P2X7 (Figure 5C).

2 RESULTS

2.1 Publication I (Fleck et al. 2021)

ATP activation of peritubular cells drives testicular sperm transport

David Fleck, Lina Kenzler, Nadine Mundt, Martin Strauch, Naofumi Uesaka, Robert Moosmann, Felicitas Bruentgens, **Annika Missel**, Artur Mayerhofer, Dorit Merhof, Jennifer Spehr & Marc Spehr

Elife, 10. doi:10.7554/eLife.62885

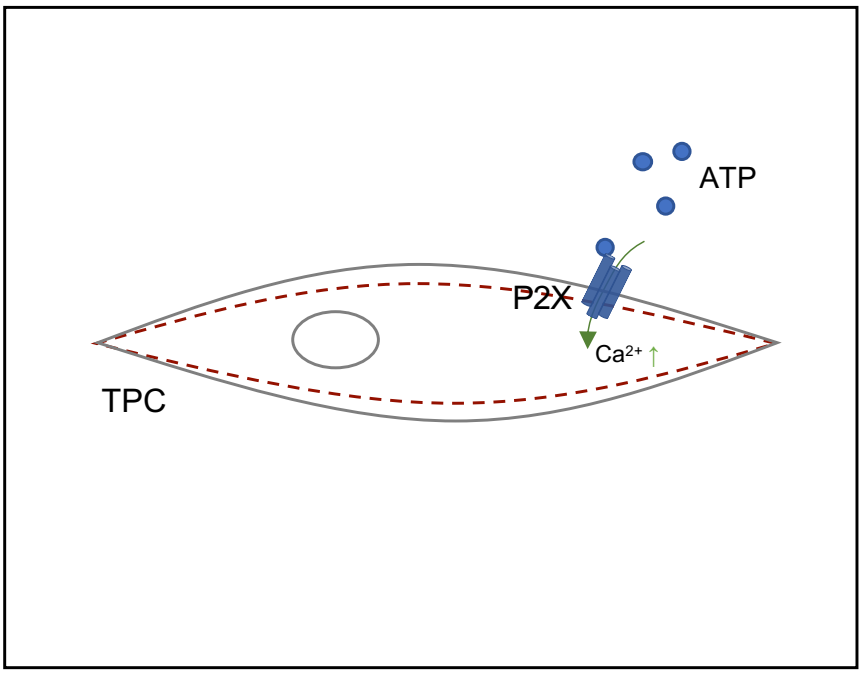

Figure 6. Graphical abstract of Fleck et al. (2021).

Extracellular ATP triggers contraction of peritubular cells, acting through P2 receptor-dependent pathways. The purinergic system is therefore involved in the regulation of contractile forces in the testis.

Copyright
This article is licensed under a Creative Commons Attribution 4.0 International License.

RESEARCH ARTICLE

ATP activation of peritubular cells drives testicular sperm transport

David Fleck[1†], Lina Kenzler[1†], Nadine Mundt[1,2], Martin Strauch[3], Naofumi Uesaka[1,4], Robert Moosmann[1], Felicitas Bruentgens[1‡], Annika Missel[5], Artur Mayerhofer[5], Dorit Merhof[3], Jennifer Spehr[1], Marc Spehr[1,2]*

[1]Department of Chemosensation, Institute for Biology II, RWTH Aachen University, Aachen, Germany; [2]Research Training Group 2416 MultiSenses – MultiScales, RWTH Aachen University, Aachen, Germany; [3]Institute of Imaging and Computer Vision, RWTH Aachen University, Aachen, Germany; [4]Department of Cognitive Neurobiology, Tokyo Medical and Dental University, Tokyo, Japan; [5]Biomedical Center Munich (BMC), Cell Biology, Anatomy III, Ludwig-Maximilians-Universität München, Planegg-Martinsried, Germany

Abstract Spermatogenesis, the complex process of male germ cell proliferation, differentiation, and maturation, is the basis of male fertility. In the seminiferous tubules of the testes, spermatozoa are constantly generated from spermatogonial stem cells through a stereotyped sequence of mitotic and meiotic divisions. The basic physiological principles, however, that control both maturation and luminal transport of the still immotile spermatozoa within the seminiferous tubules remain poorly, if at all, defined. Here, we show that coordinated contractions of smooth muscle-like testicular peritubular cells provide the propulsive force for luminal sperm transport toward the rete testis. Using a mouse model for in vivo imaging, we describe and quantify spontaneous tubular contractions and show a causal relationship between peritubular Ca^{2+} waves and peristaltic transport. Moreover, we identify P2 receptor-dependent purinergic signaling pathways as physiological triggers of tubular contractions both in vitro and in vivo. When challenged with extracellular ATP, transport of luminal content inside the seminiferous tubules displays stage-dependent directionality. We thus suggest that paracrine purinergic signaling coordinates peristaltic recurrent contractions of the mouse seminiferous tubules to propel immotile spermatozoa to the rete testis.

***For correspondence:** m.spehr@sensorik.rwth-aachen.de

[†]These authors contributed equally to this work

Present address: [‡] Charité-Universitätsmedizin Berlin, Neuroscience Research Center, Berlin, Germany

Competing interests: The authors declare that no competing interests exist.

Funding: See page 24

Received: 07 September 2020
Accepted: 16 December 2020
Published: 27 January 2021

Reviewing editor: Anna Akhmanova, Utrecht University, Netherlands

© Copyright Fleck et al. This article is distributed under the terms of the Creative Commons Attribution License, which permits unrestricted use and redistribution provided that the original author and source are credited.

Introduction

Spermatogenesis ranks among the most complex, yet least understood developmental processes in postnatal life. Inside the seminiferous tubules, which represent the functional units of the testis, this intricate course of mass cell proliferation and transformation events generates haploid spermatozoa from diploid spermatogonial stem cells. The seminiferous epithelium is composed of Sertoli cells, each intimately associated with ≥30 germ cells at different developmental stages (***Mruk and Cheng, 2004***). Sertoli cells provide the microenvironment critical for spermatogenesis by establishing the blood-testis barrier (***Cheng and Mruk, 2010***), forming the spermatogonial stem cell niche (***Oatley and Brinster, 2012***), and controlling epithelial cyclicity via auto-, para-, and endocrine feedback (***Heindel and Treinen, 1989***). Different types of spermatogonia (type A, intermediate, type B) are localized along the seminiferous tubule basement membrane (***Chiarini-Garcia and Russell, 2001***). Upon detachment, type B spermatogonia enter meiosis as preleptotene spermatocytes. During meiotic divisions and subsequent maturation steps, germ cells progress from primary to secondary spermatocytes and round to elongated spermatids.

eLife digest As sperm develop in the testis, the immature cells must make their way through a maze of small tubes known as seminiferous tubules. However, at this stage, the cells do not yet move the long tails that normally allow them to 'swim'; it is therefore unclear how they are able to move through the tubules.

Now, Fleck, Kenzler et al. have showed that, in mice, muscle-like cells within the walls of seminiferous tubules can create waves of contractions that push sperm along. Further experiments were then conducted on cells grown in the laboratory. This revealed that a signaling molecule called ATP orchestrates the moving process by activating a cascade of molecular events that result in contractions. Fleck, Kenzler et al. then harnessed an advanced microscopy technique to demonstrate that this mechanism occurs in living mice. Together, these results provide a better understanding of how sperm mature, which could potentially be relevant for both male infertility and birth control.

Accumulating evidence implicates purinergic signaling in testicular paracrine communication. While the general picture is still incomplete, cell- and stage-specific testicular expression of different purinoceptor isoforms has been reported in Leydig cells (***Antonio et al., 2009***; ***Foresta et al., 1996***), Sertoli cells (***Veitinger et al., 2011***), both pre- and postmeiotic germ cells (***Fleck et al., 2016***; ***Glass et al., 2001***), testicular peritubular cells (TPCs) (***Walenta et al., 2018***), as well as mature spermatozoa (***Navarro et al., 2011***), albeit with contradictory results. Functionally, several studies have suggested purinergic paracrine control of gonadotropin effects on Leydig and Sertoli cells (***Filippini et al., 1994***; ***Gelain et al., 2005***; ***Gelain et al., 2003***; ***Lalevée et al., 1999***; ***Meroni et al., 1998***; ***Poletto Chaves et al., 2006***), including steroidogenesis and testosterone/17β-estradiol secretion (***Foresta et al., 1996***; ***Rossato et al., 2001***).

Members of the P2 purinoceptor family are activated by extracellular ATP (***Burnstock, 1990***). P2 receptors subdivide into ionotropic P2X (***Bean, 1992***; ***Bean and Friel, 1990***) and metabotropic P2Y (***Barnard et al., 1994***) receptors, comprising seven (P2X) and eight (P2Y) isoforms, respectively (***Müller et al., 2020***). All P2X channels display substantial Ca^{2+} permeability and show distinct pharmacological profiles, ligand affinities, and desensitization kinetics (***Khakh and North, 2012***). G-protein-coupled P2Y receptors are sensitive to both ATP and UTP and they form two subgroups that either activate phospholipase C via $G_{\alpha q}/G_{\alpha 11}$ (P2Y1, 2, 4, 6, and 11) or couple to $G_{\alpha i/o}$ (P2Y12, 13, and 14) (***Müller et al., 2020***). Notably, several P2 receptor isoforms affect smooth muscle cell physiology, with P2X1, P2X2, P2X4, P2X7, P2Y1, and P2Y2 acting as the principle subunits (***Burnstock, 2014***). So far, the most prominent role for a specific subunit in reproductive physiology has been attributed to P2X1, which is critical for vas deferens smooth muscle contraction and male fertility (***Mulryan et al., 2000***).

In mice, stimulation-dependent ATP secretion from both Sertoli and germ cells was reported (***Gelain et al., 2005***; ***Gelain et al., 2003***) and may itself be under endocrine control (***Gelain et al., 2005***; ***Lalevée et al., 1999***). The mechanism(s) of cellular ATP release, however, remain subject to debate. ATP secretion via exocytotic release (***Bodin and Burnstock, 2001***; ***Zhang et al., 2007***) has been proposed. Alternative ATP release pathways include connexin/pannexin hemichannels (***Bao et al., 2004***; ***Cotrina et al., 1998***), transporters (***Lohman et al., 2012***), voltage-gated (***Taruno et al., 2013***) or large-conductance anion (***Bell et al., 2003***) channels, or even P2X7 receptors (***Pellegatti et al., 2005***; ***Suadicani et al., 2006***).

Along the seminiferous epithelium, spermatogenesis has been conceptualized by attribution of sequential cellular 'stages' (***Figure 1A***), which progress through coordinated cycles (***Hess and De Franca, 2008***; ***Russell, 1990***). First initiated in mice about 7 days postpartum (***Kolasa et al., 2012***), each spermatogenic cycle comprises 12 stages and lasts 8.7 days (***Hermo et al., 2010***). After approximately 39 days (4.5 cycle repetitions), spermatogenesis completes with the release of immotile spermatozoa from the seminiferous epithelium into the lumen of the tubule (spermiation). Once detached from the Sertoli cells, sperm must be transported to the *rete testis* and epididymis for final maturation. Precisely regulated tubular transport mechanisms are, thus, imperative for reproduction.

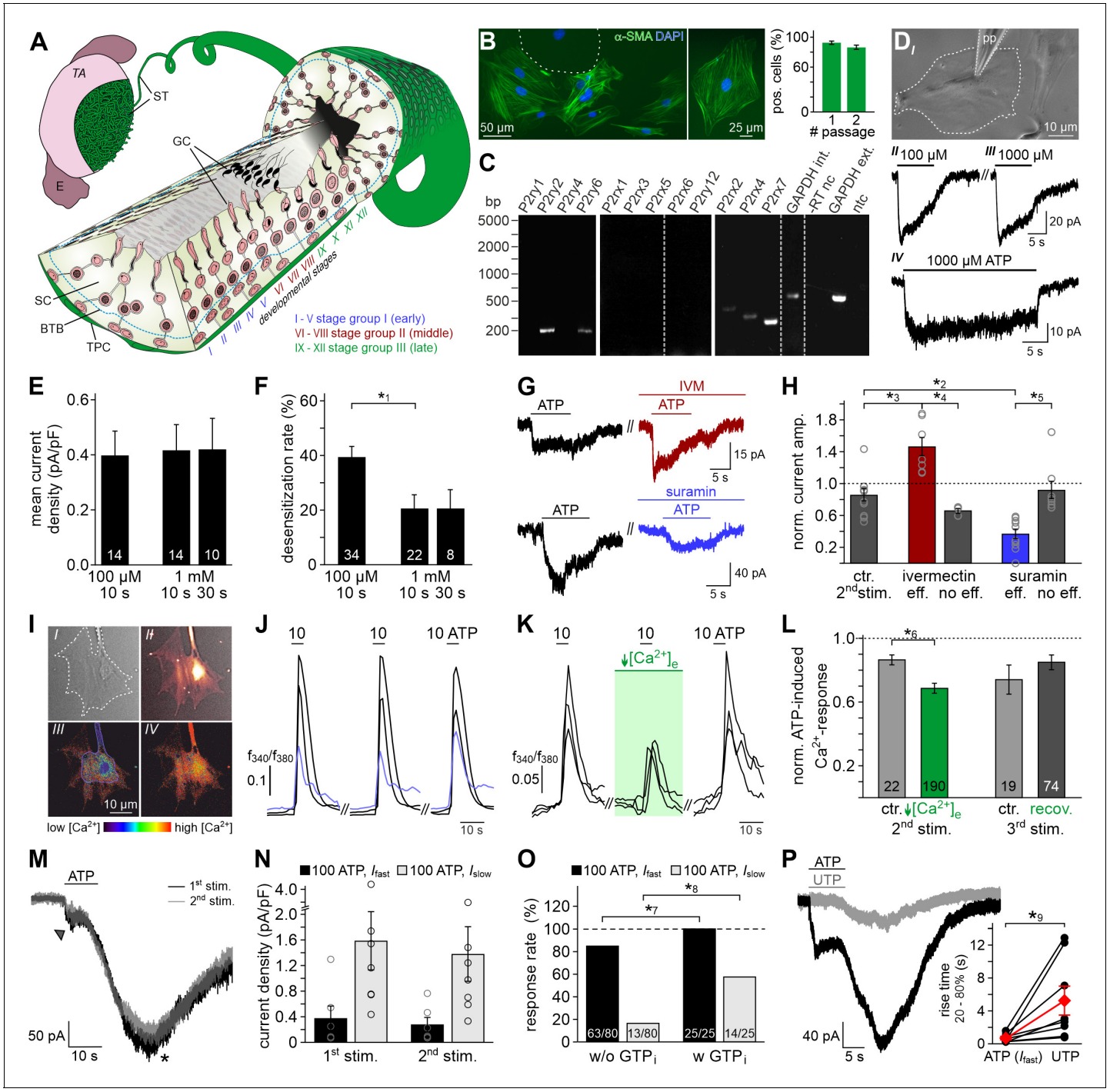

Figure 1. ATP is a potent TPC stimulus. (**A**) Schematic sketch of the mouse seminiferous tubule (ST) highlighting 12 stages (I – XII) of the spermatogenic cycle (***Hess and De Franca, 2008***; ***Russell, 1990***), which are arranged in consecutive order along the length of the tubule. A single layer of flat testicular peritubular cells (TPC; green) lines the tubular wall. Sertoli cells (SC) span the tubule from the basal lamina to the lumen. Developing germ cells (GC) are distributed between Sertoli cells. Spermatogonia are located near the basal membrane. Prophase spermatocytes move across the blood-testis barrier (BTB) to the adluminal compartment where they complete meiosis. The resulting haploid spherical cells (round spermatids) differentiate into elongated spermatids and, eventually, into highly condensed and compartmentalized spermatozoa (spermiogenesis). These mature, yet still immotile germ cells are then released into the lumen (spermiation). E, epididymis; TA, *tunica albuginea*; inspired by ***Hess and De Franca, 2008***. (**B**) Immunostaining against α-smooth muscle actin (α-SMA, green) marks TPCs in vitro (***Tung and Fritz, 1989***). Cell count is determined by nuclear staining (DAPI, blue). Cultures retain high TPC purity for at least two passages (92 ± 2%, n = 1102 (#1); 86 ± 3%, n = 542 (#2)). Dashed line delimits one of the few α-SMA-negative cells. (**C**) RT-PCR profiling of purinoceptor isoforms in TPC cultures reveals P2rx2, P2rx4, P2rx7, P2ry2, and P2ry6 transcripts. Dashed gray vertical lines indicate cuts in a given gel. (**D–H**) ATP exposure triggers TPC transmembrane currents. (**D$_I$**) Phase-contrast micrograph

Figure 1 continued on next page

Figure 1 continued

depicting a TPC (dashed line) targeted by a patch pipette (pp). (D_{II}-D_{IV}) Original whole-cell recordings illustrate representative currents in response to ATP stimulation (100 µM (D_{II}) vs. 1000 µM (D_{III}) and 10 s (D_{III}) vs. 30 s (D_{IV}), respectively). V_{hold} = −80 mV. (**E, F**) Quantification (bar charts; mean ± SEM; n as indicated) reveals saturation of peak current density at ≤100 µM ATP (**E**) and modest desensitization at a concentration-dependent rate (**F**). (**G**) Whole-cell voltage-clamp recordings show ATP-induced currents (100 µM; 10 s) that are potentiated by ivermectin (3 µM) and partially inhibited by suramin (100 µM), respectively (≥60 s preincubation). V_{hold} = −80 mV. (**H**) Quantification (bar charts; mean ± SEM; data normalized to initial control response) demonstrates dichotomy in drug sensitivity. Treatment was categorized as effective (eff) if current amplitudes deviate by ± SD from average control recordings (85 ± 24%, 2nd ATP stimulation). Note that each drug proved ineffective (no eff) in some cells. Gray circles depict data from individual cells. (**I–L**) ATP-dependent Ca^{2+} mobilization in cultured TPCs. Ca^{2+} transients in response to repetitive stimulation (10 µM, 10 s) are monitored by ratiometric (fura-2) fluorescence imaging. (**I**) Phase contrast (*I*) and merged fluorescence (f_{380}; *II*) images of a TPC in vitro. Bottom pseudocolor frames (rainbow 256 color map) illustrate relative cytosolic Ca^{2+} concentration ($[Ca^{2+}]_c$) before (*III*) and during (*IV*) ATP stimulation. (**J, K**) Representative original traces from time-lapse fluorescence ratio (f_{340}/f_{380}) recordings depict repetitive $[Ca^{2+}]_c$ elevations upon ATP exposure under control conditions ((**J**) blue traces correspond to the TPC in (**I**)) and during reduced extracellular Ca^{2+} concentration ((**K**) $[Ca^{2+}]_e$ = 100 nM; 60 s preincubation). (**L**) Bar chart depicting Ca^{2+} signal amplitudes (mean ± SEM; n as indicated) – normalized to the initial ATP response – under control conditions (gray) vs. low $[Ca^{2+}]_e$ (green). Asterisks denote statistically significant differences (*^{1}p=0.001; *^{2}p=0.002; *^{3}p=5.5e^{-5}; *^{4}p=0.0006; *^{5}p=0.02; *^{6}p=0.02; Student *t*-test (**F, L**), one-way ANOVA (**H**)). (**M**) Representative whole-cell voltage-clamp recordings (V_{hold} = −80 mV) of ATP-induced inward currents in cultured mouse TPCs. Two components – a fast relatively small current (arrow head) and a delayed lasting current (asterisk) – are triggered repeatedly by successive ATP exposure (100 µM; 90 s inter-stimulus interval). Notably, we never observed a delayed slow current without a fast response. (**N**) Bar chart quantifying peak densities (mean ± SEM, circles show individual values) of the fast (I_{fast}; black) and the delayed (I_{slow}; gray) ATP-induced current components (1st stimulation: I_{fast} 0.37 ± 0.2 pA/pF; I_{slow} 1.58 ± 0.5 pA/pF; 2nd stimulation I_{fast} 0.27 ± 0.1 pA/pF; I_{slow} 1.37 ± 0.4 pA/pF). (**O**) Bar graph illustrating the frequency of I_{fast} (black) and I_{slow} (gray) occurrence upon ATP (100 µM) stimulation in absence (w/o) and presence (w) of GTP (500 µM) in the pipette solution, respectively. Asterisks denote statistically significant differences (*^{7}p=0.008, *^{8}p=0.0003; Fisher's exact test); n as indicated in bars. (**P**) Representative whole-cell voltage-clamp recordings (V_{hold} = −80 mV) of inward currents induced by ATP (100 µM) and UTP (100 µM), respectively. Whenever ATP triggers both I_{fast} and I_{slow} (left), I_{slow} is also induced by UTP (right). UTP-dependent currents develop significantly slower than ATP-evoked I_{fast} (inset; *^{9}p=0.03; paired *t*-test).

The online version of this article includes the following figure supplement(s) for figure 1:

Figure supplement 1. Mouse TPCs in primary culture.

Figure supplement 2. ATP/UTP-dependent I_{slow} in cultured mouse TPCs is largely carried by Cl^-.

While bulk movement of luminal content has been anecdotally reported (***Cross, 1958***; ***Setchell et al., 1978***; ***Worley et al., 1985***), no quantitative data on sperm transport within the seminiferous tubules is available. Early in vitro observations of apparent minute undulating motions of seminiferous tubule segments (***Roosen-Runge, 1951***; ***Suvanto and Kormano, 1970***) suggested that smooth muscle-like TPCs (***Clermont, 1958***; ***Ross, 1967***) could mediate contractile tubule movements. This concept has gained widespread support from several, mostly indirect, in vitro studies (***Ailenberg et al., 1990***; ***Filippini et al., 1993***; ***Miyake et al., 1986***; ***Tripiciano et al., 1996***). However, quantitative direct (i.e. live cell) measurements of seminiferous tubule contractions are rare and controversial (***Ellis et al., 1978***; ***Harris and Nicholson, 1998***; ***Losinno et al., 2012***; ***Worley and Leendertz, 1988***). Moreover, mechanistic in vivo evidence is lacking. Here, we demonstrate that, by acting on ionotropic and metabotropic P2 receptors, extracellular ATP activates TPC contractions that trigger directional sperm movement within the mouse seminiferous tubules both in vitro and in vivo.

Results

ATP is a potent TPC stimulus

Accumulating data suggests that purinergic signaling constitutes a critical component of testicular paracrine communication (***Fleck et al., 2016***; ***Foresta et al., 1995***; ***Gelain et al., 2003***; ***Poletto Chaves et al., 2006***; ***Veitinger et al., 2011***; ***Walenta et al., 2018***), with Sertoli cells acting as a primary source of ATP secretion (***Gelain et al., 2005***). Therefore, we asked if mouse TPCs are sensitive to extracellular ATP. Primary TPC cultures retain high purity for ≥14 days in vitro (***Figure 1B***, and ***Figure 1—figure supplement 1A&B***) and cells express transcripts for several ionotropic (P2X2, P2X4, P2X7) and metabotropic (P2Y2, P2Y6) purinoceptors (***Figure 1C***). The specific biophysical and pharmacological profile of ATP-dependent transmembrane currents (***Figure 1D–H***) strongly suggests functional expression of P2X2 and/or P2X4, but not P2X7 receptors. As reported for both P2X2 and P2X4 (***North, 2002***), TPC currents are saturated at ≤100 µM ATP (***Figure 1D&E***),

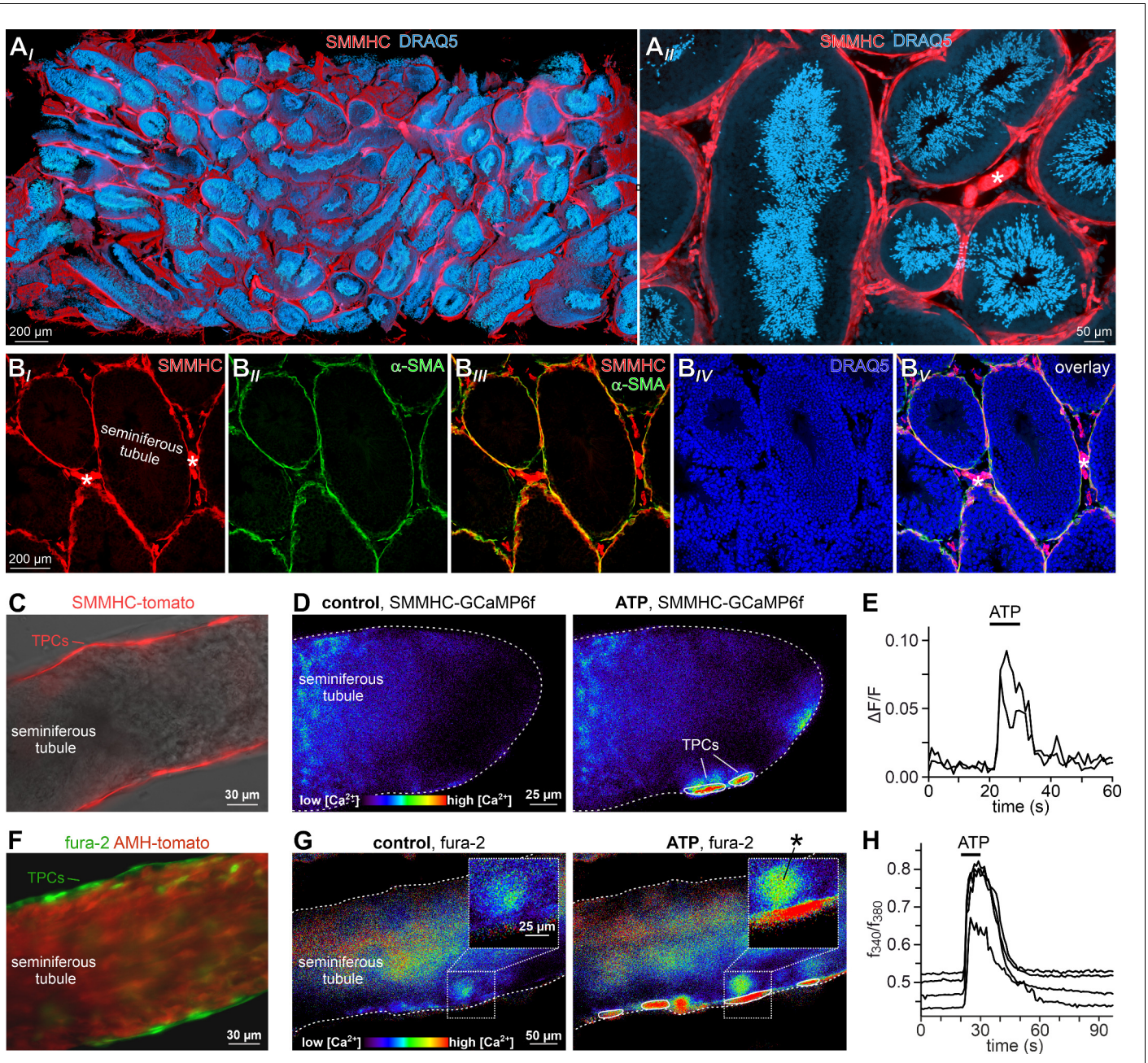

Figure 2. ATP triggers TPC Ca^{2+} signals in acute seminiferous tubule sections. (**A**) 3D reconstruction of an intact 6 × 3 × 1.5 mm testis sample from a SMMHC-CreER^{T2} x Ai14D mouse after tissue clearing (CLARITY ***Chung and Deisseroth, 2013***) reveals tdTomato expression (red) restricted to TPCs and vascular endothelial cells (asterisk in (**A**$_{II}$)). Nuclear staining (DRAQ5; blue) is most prominent in post-meiotic germ cells because of their high degree of DNA condensation. (**B**) SMMHC-CreER^{T2}-expressing cells in the tubule wall are TPCs. In testis cryosections from adult SMMHC-CreER^{T2} x Ai14D mice, Cre-driven tdTomato signals (**B**$_{I}$) and α-SMA immunostaining (**B**$_{II}$) colocalize at tubular margins (**B**$_{III}$). Nuclei are stained with DRAQ5 (blue (**B**$_{IV}$)). Note that endothelial vasculature in interstitial regions (asterisks) is α-SMA-negative (merged image (**B**$_{V}$)). (**C–H**) Both TPC-specific expression of a genetically encoded Ca^{2+} indicator (GCaMP6f) and bulk loading with a synthetic Ca^{2+} sensor (fura-2) allow for TPC-selective live cell Ca^{2+} imaging in acute seminiferous tubule sections. (**C**) Merged fluorescence and reflected light micrographs show the location of SMMHC-expressing TPCs (red) within the wall of an intact tubule. (**D–E**) Cre-dependent GCaMP6f expression in SMMHC-CreER^{T2} x Ai95D mice reveals Ca^{2+} transients in TPCs in response to ATP. Representative fluorescence images ((**D**) rainbow 256 color map) before and during ATP exposure (100 µM; 10 s), and corresponding traces (**E**) showing changes in GCaMP6f intensity (ΔF/F) over time. Traces from ROIs outlined in (**D**) (white solid lines). (**F**) Merged fluorescence image of an acute seminiferous tubule section from an AMH-Cre x Ai14D mouse after bulk loading with fura-2/AM (green). Anti-Müllerian hormone (AMH) dependent expression of tdTomato (red) specifically labels Sertoli cells that build the seminiferous epithelium. Note the narrow green band of marginal TPCs that are preferentially labeled by the Ca^{2+}-sensitive dye. (**G–H**) Ratiometric Ca^{2+} imaging in fura-2-loaded tubules enables semi-quantitative live-cell

Figure 2 continued on next page

Figure 2 continued

monitoring of TPC activity. Representative fluorescence images ((**G**) rainbow 256 color map) before and during ATP exposure (100 µM; 10 s). Corresponding traces (**H**) show the fluorescence intensity ratio (f_{340}/f_{380}) from four ROIs (in (**G**); white solid lines) over time. Inset (**G**) shows a putative TPC and an adjacent putative spermatogonium (asterisk) at higher magnification.

whereas P2X7 receptors display strongly reduced ATP sensitivity (***Donnelly-Roberts et al., 2009***). Moreover, currents recorded from TPCs showed modest but persistent desensitization (***Figure 1D&F***), which is similarly observed for recombinant P2X2 and P2X4, but not P2X7 receptors (***Coddou et al., 2011***). TPCs also displayed reduced BzATP sensitivity (data not shown), which is a potent activator of P2X7 receptors (***Donnelly-Roberts et al., 2009***). Ivermectin (***Figure 1G&H***), an agent selectively potentiating P2X4 receptor currents (***Khakh et al., 1999***; ***Silberberg et al., 2007***), increased ATP-induced currents in a subpopulation of TPCs (n = 7/12), whereas suramin (***Figure 1G&H***), a drug inhibiting P2X2, but not P2X4 receptors (***Evans et al., 1995***), inhibited a TPC subset (n = 10/18).

Notably, live-cell ratiometric Ca^{2+} imaging in cultured TPCs revealed robust and repetitive cytosolic Ca^{2+} transients upon ATP exposure (***Figure 1I&J***). We next reduced the extracellular Ca^{2+} concentration ($[Ca^{2+}]_e$) to 100 nM, a concentration approximately equimolar to cytosolic levels, by adding an appropriate chelator/ion concentration ratio (1 mM EGTA/0.5 mM $CaCl_2$). This treatment, which drastically diminishes the driving force for Ca^{2+} influx, did substantially reduce, but not abolish ATP response amplitudes (***Figure 1K&L***). The selective P2Y receptor agonist UTP (***Alexander et al., 2019b***) also triggered Ca^{2+} signals (data not shown), indicating a role for G protein-dependent Ca^{2+} release from internal storage organelles (***Müller et al., 2020***). Notably, ~46% of all ATP-sensitive TPCs additionally displayed a delayed, but long-lasting inward current that gradually developed over tens of seconds after ATP stimulation ended (***Figure 1M&N***). We hypothesized that this slower current could result from P2Y receptor-/G protein-dependent Ca^{2+} release, likely mediated by the P2Y2 isoform since P2Y6 receptors lack substantial ATP sensitivity (***Alexander et al., 2019a***; ***Jacobson et al., 2015***). Indeed, occurrence of the delayed current depends on presence of intracellular GTP (***Figure 1O***). Moreover, selective recruitment of G protein-coupled P2Y receptors with UTP (***Figure 1P***) exclusively triggered such slowly developing currents. Largely carried by Cl^- (***Figure 1—figure supplement 2***), this current likely results from P2Y receptor-mediated phosphoinositide turnover, Ca^{2+} release, and activation of Ca^{2+}-gated Cl^- channels. Together, these data suggest that mouse TPCs functionally express both ionotropic and metabotropic purinoceptors.

Next, we asked if TPCs also exhibit ATP sensitivity in their physiological setting. Therefore, we examined purinergic Ca^{2+} signals from mouse TPCs in acute seminiferous tubule sections (***Fleck et al., 2016***). In parallel approaches, we employed two different fluorescent Ca^{2+} reporters, a synthetic ratiometric Ca^{2+} sensor (fura-2) as well as a genetically encoded Ca^{2+} indicator (GCaMP6f). The dual excitation ratiometric indicator fura-2 allows semi-quantitative Ca^{2+} measurements (***Bootman et al., 2013***), but lacks cell type specificity as tubules are bulk-loaded with a membrane-permeable acetoxymethyl ester conjugate. By contrast, conditional gene targeting via the Cre/Lox system (***Smith, 2011***) allows TPC-specific expression of the single-wavelength indicator GCaMP6f. First, we confirmed inducible TPC-targeted testicular expression of fluorescent reporter proteins in SMMHC-$CreER^{T2}$ x Ai14D mice (***Figure 2A–C***, ***Video 1***). Tamoxifen-induced transgenic expression of $CreER^{T2}$ under control of the mouse smooth muscle myosin, heavy polypeptide 11 (a.k.a. SMMHC) promoter drives *Cre*-mediated recombination of *loxP*-flanked reporters (tdTomato (Ai14D mice) or GCaMP6f (Ai95D))

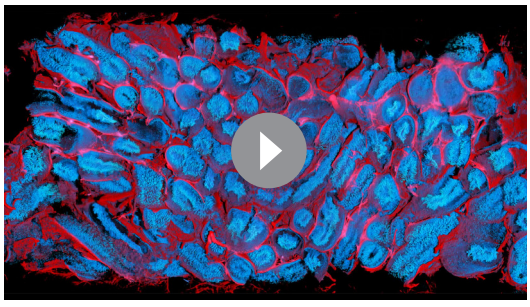

Video 1. SMMHC-$CreER^{T2}$ mice allow inducible TPC-specific expression of genetically encoded fluorescent reporter proteins. After tamoxifen injections, SMMHC-$CreER^{T2}$ x Ai14D male offspring express tdTomato (red) in both TPCs and vascular smooth muscle cells. Video shows the 3D reconstruction of an intact and cleared (CLARITY, ***Chung and Deisseroth, 2013***) 6 × 3 × 1.5 mm testis sample with nuclei labeled by DRAQ5 (blue).
https://elifesciences.org/articles/62885#video1

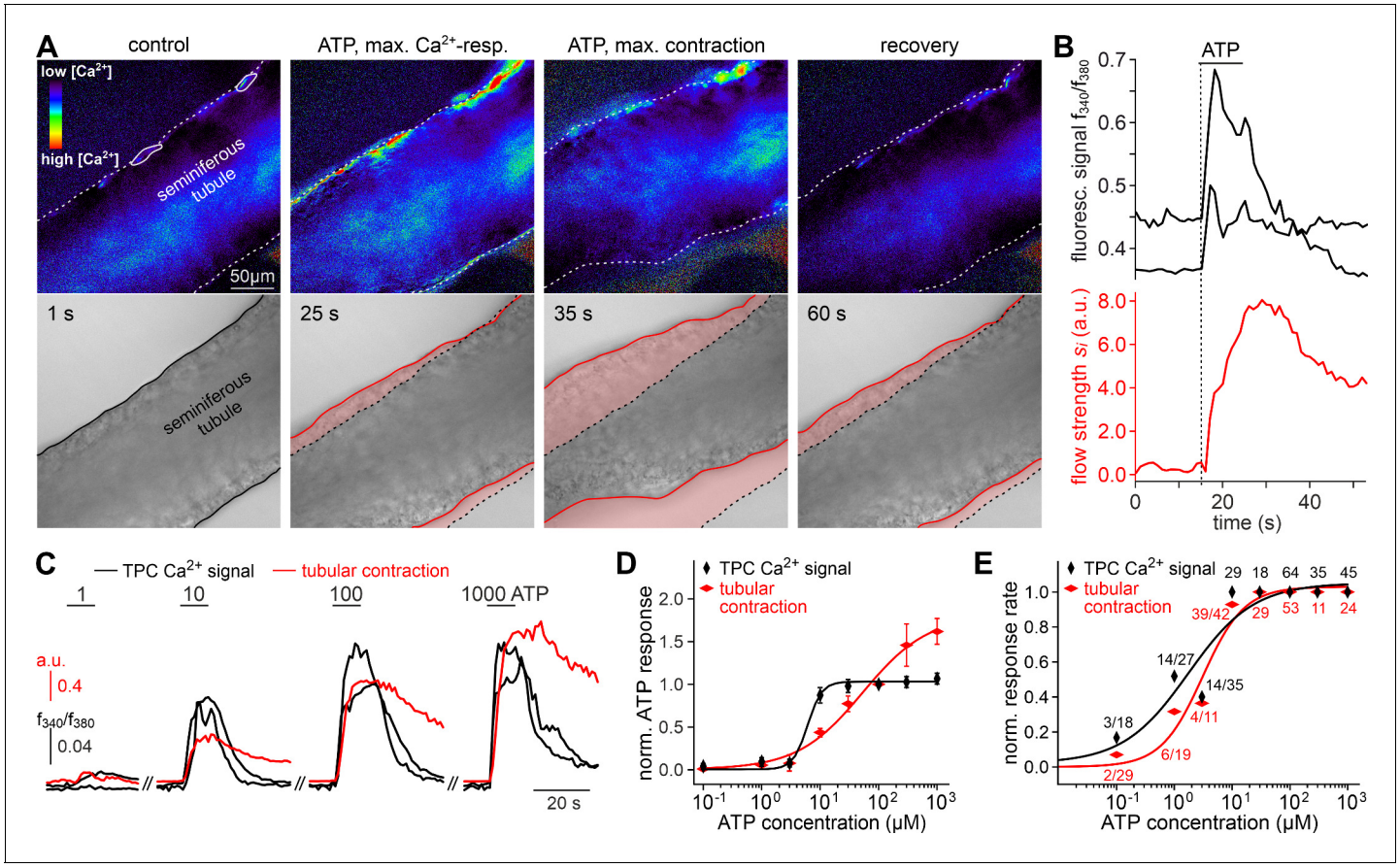

Figure 3. ATP triggers seminiferous tubule contractions. (**A**) Quasi-simultaneous imaging of $[Ca^{2+}]_c$-dependent fluorescence (top; f_{340}/f_{380}; rainbow 256 color map) and tubular position (bottom; reflected light microscopy). Focus adjusted to provide sharp images of the seminiferous tubule's edges. Individual frames correspond to the time points indicated, i.e. before, during, and after ATP exposure (see (**B**)). Dashed white lines (top) and corresponding solid black/red lines (bottom) depict the outline of the tubule in each image, respectively. Dotted black lines (bottom) show the contour at t = 1 s for comparison. Pink shades (bottom) accentuate areas that moved. (**B**) Fluorescence ratio (top; black traces correspond to regions-of-interest delimited by solid white lines in (**A**)) and integrated flow strength s_i – a measure of strength and direction of pixel displacement (bottom; red trace) – over time. ATP (100 µM) stimulation as indicated (horizontal bar). With the t = 0 s image as reference, flow strength s_i is calculated by custom code as the average whole tubule pixel shift vector (methods). Dashed vertical line marks the Ca^{2+} signal onset. (**C–E**) Ca^{2+} responses and tubular movement are dose-dependent. (**C**) Original traces depict $[Ca^{2+}]_c$ (black) and tubule movement (red) from a representative experiment. Data calculated as in (**B**). Brief (10 s) stimulations with increasing ATP concentrations (1–1000 µM) trigger dose-dependent Ca^{2+} transients and corresponding contractions. (**D, E**) Data quantification. Dose-response curves illustrate peak signals (**D**) and the percentage of responding putative TPCs (black)/tubules (red) (**E**). Data are normalized to responses to 100 µM ATP (n as indicated in (**E**)).

in smooth muscle cells and TPCs (***Wirth et al., 2008***). Second, TPC-specific GCaMP6f expression in SMMHC-CreER^{T2} x Ai95D mice revealed robust Ca^{2+} transients in cells of the tubular wall upon ATP exposure (***Figure 2D&E***). Third, fura-2/AM loading of acute seminiferous tubule sections preferentially labeled the outermost cell layer (***Figure 2F***), allowing semi-quantitative in situ imaging of ATP-dependent Ca^{2+} signals in mouse TPCs (***Figure 2G&H***). So far, our results thus demonstrate that challenging TPCs with extracellular ATP triggers robust Ca^{2+} signals both in vitro and in situ.

ATP triggers seminiferous tubule contractions

We hypothesized that ATP-induced Ca^{2+} signals in TPCs could mediate contractile motion of the seminiferous tubule. To address this, we established a fast, quasi-simultaneous image acquisition method that enables parallel recording of both peritubular Ca^{2+} responses and seminiferous tubule movement (methods). Brief ATP exposure resulted in a peripheral band of Ca^{2+} activity at the edge of the tubule. Such signals usually coincided with a pronounced contractile motion of the seminiferous tubule (***Figure 3A***, ***Video 2***). When movement is quantified as the time-lapse image flow field

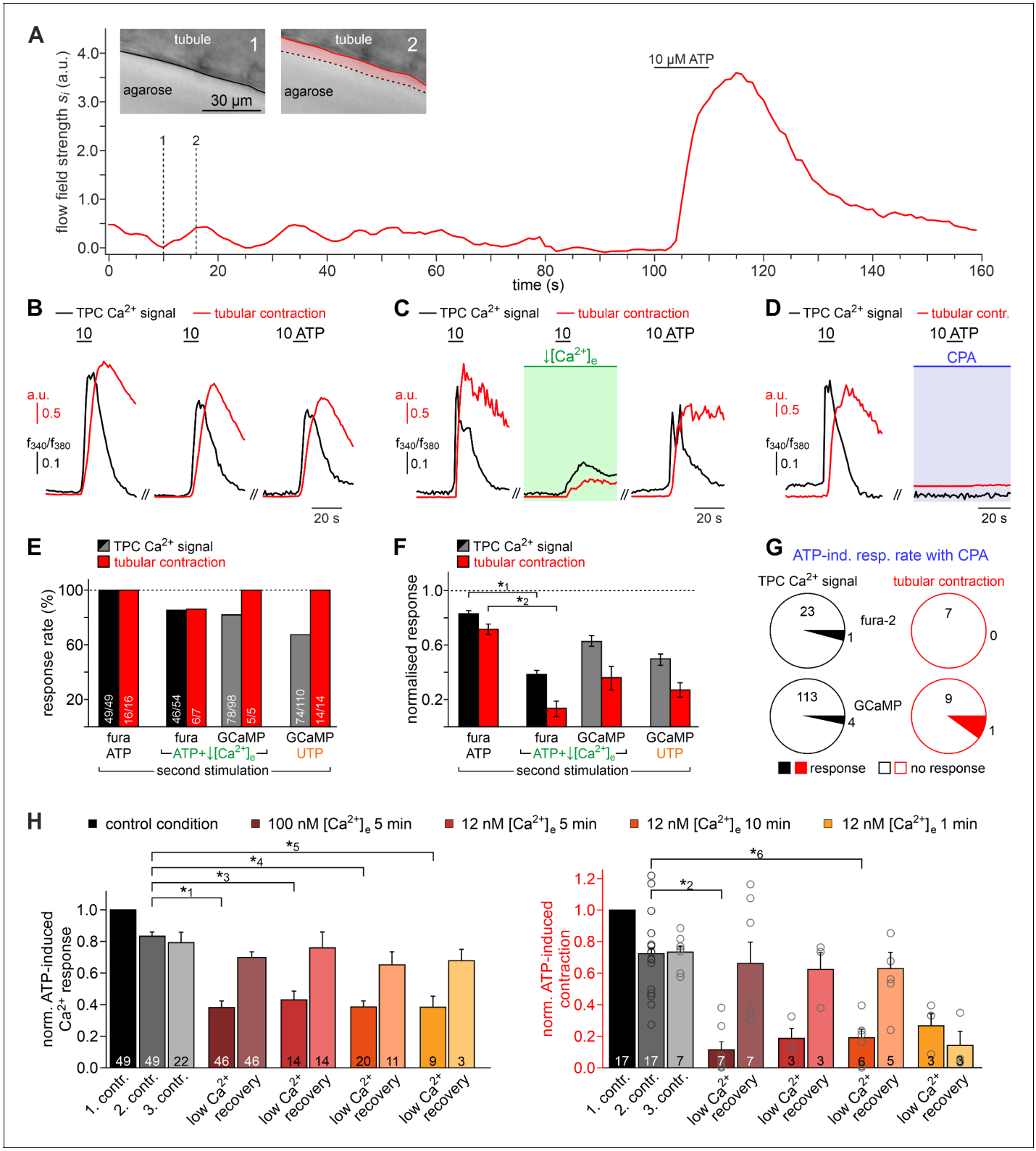

Figure 4. Both intra- and extracellular Ca^{2+} sources contribute to ATP-dependent TPC contractions. (**A**) In situ imaging identifies spontaneous low-amplitude 'vibratory' movements in acute seminiferous tubule slices. Representative trace illustrating flow field strength analysis of tubular motion under control conditions and upon ATP exposure (10 µM; 10 s). Note that spontaneous indentations share small amplitudes and are restricted to the tubule edge (inset). Black/red lines (inset) depict the outline of the tubule in each image, respectively. Dotted black lines show the contour at t = 1 for comparison. Pink shades accentuate areas that moved. (**B**) Repeated purinergic stimulation triggers robust Ca^{2+} elevations and concurring seminiferous

Figure 4 continued on next page

Figure 4 continued

tubule contractions with only minor response adaptation. Traces depict changes in fura-2 intensity ratio (f_{340}/f_{380}; black) or tubular movement (red) upon brief ATP exposure (10 s; 10 µM; 5 min intervals) under control conditions. (**C**) Reducing $[Ca^{2+}]_e$ (100 nM; 5 min incubation) strongly diminishes responses to ATP (10 s; 10 µM). (**D**) Depletion of internal Ca^{2+} stores (CPA ***Seidler et al., 1989***; 90 µM; 18.8 ± 9.3 min incubation) essentially abolishes both Ca^{2+} signals and tubule contractions. (**E–G**) Quantification of data exemplified in (**B–D**). (**E**) Bar chart depicting ATP sensitivity (response rate; %), independent of signal strength. Occurrence of Ca^{2+} elevations (black) and tubule contractions (red) are plotted for different experimental conditions [i.e. stimulation with ATP or UTP, regular or reduced $[Ca^{2+}]_e$ (1 mM or 100 nM, respectively), and Ca^{2+} indicator (fura-2 or GCaMP6f, respectively)]. Numbers of experiments are indicated in each bar. (**F**) Signal amplitudes (Ca^{2+}, black; contractions, red) of responding TPCs/tubules, quantified as a function of stimulus, treatment, and Ca^{2+} sensor. Data (mean ± SEM) are normalized to the respective initial responses to ATP (10 µM) under control conditions (dotted horizontal line; see first stimulations in **B** and **C**). Experimental conditions and numbers of experiments as in (**E**). Asterisks denote statistical significance ($*^1p=2.2e^{-19}$ and $*^2p=5.6e^{-8}$; *t*-test; note: tests only performed when n > 5 and only one variable was changed). (**G**) Pie charts illustrating the profoundly reduced ATP sensitivity of TPCs/tubules after depletion of Ca^{2+} storage organelles (CPA; 90 µM). Numbers within pies correspond the total count of cells/tubules that responded to ATP before treatment. (**H**) Effects of lowering $[Ca^{2+}]_e$ are comparable over both incubation periods and concentrations in the nanomolar range. Significantly reduced, though not abolished TPC Ca^{2+} signals (left) and seminiferous tubule contractions (right) are observed in presence of both 100 nM and 12 nM $[Ca^{2+}]_e$ as well as for variable incubation periods lasting between 1 and 10 min, respectively. Asterisks denote statistical significance ($*^3p=2.8e^{-10}$, $*^4p=7.8e^{-14}$, $*^5p=3.8e^{-9}$, $*^6p=1.0e^{-6}$; one-way ANOVA with *post-hoc* Tukey HSD test; note: tests only performed when $n \geq 5$).

The online version of this article includes the following figure supplement(s) for figure 4:

Figure supplement 1. Purinergic stimulation mediates contractions in cultured human TPCs.

strength (methods) tubular contraction follows the Ca^{2+} signal onset with minimal delay, outlasts the Ca^{2+} signal peak, and recovers slowly (***Figure 3B***). Both Ca^{2+} responses and tubular movement are dose-dependent and share an ATP threshold concentration of approximately 1 µM (***Figure 3C–E***, ***Video 3***). Contractile smooth muscle plasticity (***Tuna et al., 2012***) likely underlies the apparent difference in signal saturation (***Figure 3D***). Notably, in some tubules, we observed spontaneous low-

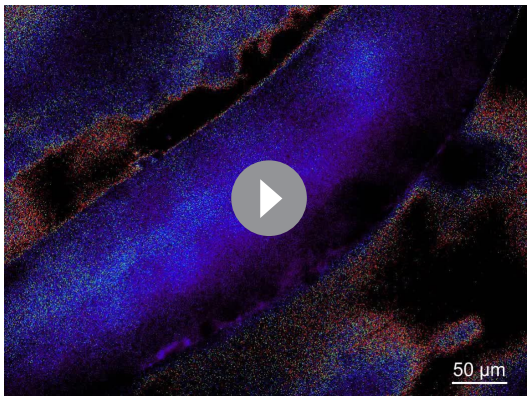

Video 2. Quasi-simultaneous recording of peritubular Ca^{2+} signals and seminiferous tubule movement. A representative seminiferous tubule section (250 µm) is stimulated with ATP (100 µM, 10 s). After fura-2 bulk loading, ratiometric fluorescence imaging (f_{340}/f_{380}) reveals relative changes in Ca^{2+} concentration (rainbow color map; blue, low Ca^{2+}; red, high Ca^{2+}) in a peripheral band of putative TPCs at the tubule's edge. Since each image acquisition cycle (1 Hz) captures two fluorescence ($Ex\lambda_{340}$; $Ex\lambda_{380}$) and one reflective light image (brightfield), time-lapse recordings allow parallel physiological phenotyping of both seminiferous tubule Ca^{2+} responses and movement (shown sequentially for clarity).
https://elifesciences.org/articles/62885#video2

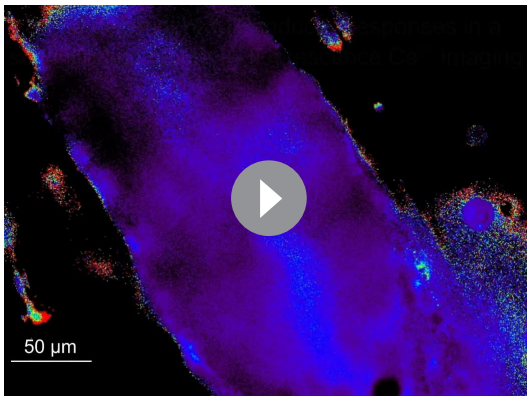

Video 3. Both ATP-induced seminiferous tubule Ca^{2+} responses and contractions are dose-dependent. A representative seminiferous tubule section (250 µm; fura-2 bulk loading) is stimulated with increasing ATP concentrations (1–1000 µM, 10 s). Ratiometric fluorescence imaging (f_{340}/f_{380}) reveals relative changes in Ca^{2+} concentration (rainbow color map; blue, low Ca^{2+}; red, high Ca^{2+}) in putative TPCs. Quasi-simultaneous time-lapse recording of fluorescence ($Ex\lambda_{340}$; $Ex\lambda_{380}$) and brightfield (reflective light) images illustrates that both seminiferous tubule Ca^{2+} signals and contractions (shown sequentially for clarity) are dose-dependent and share an ATP threshold concentration of approximately 1 µM.
https://elifesciences.org/articles/62885#video3

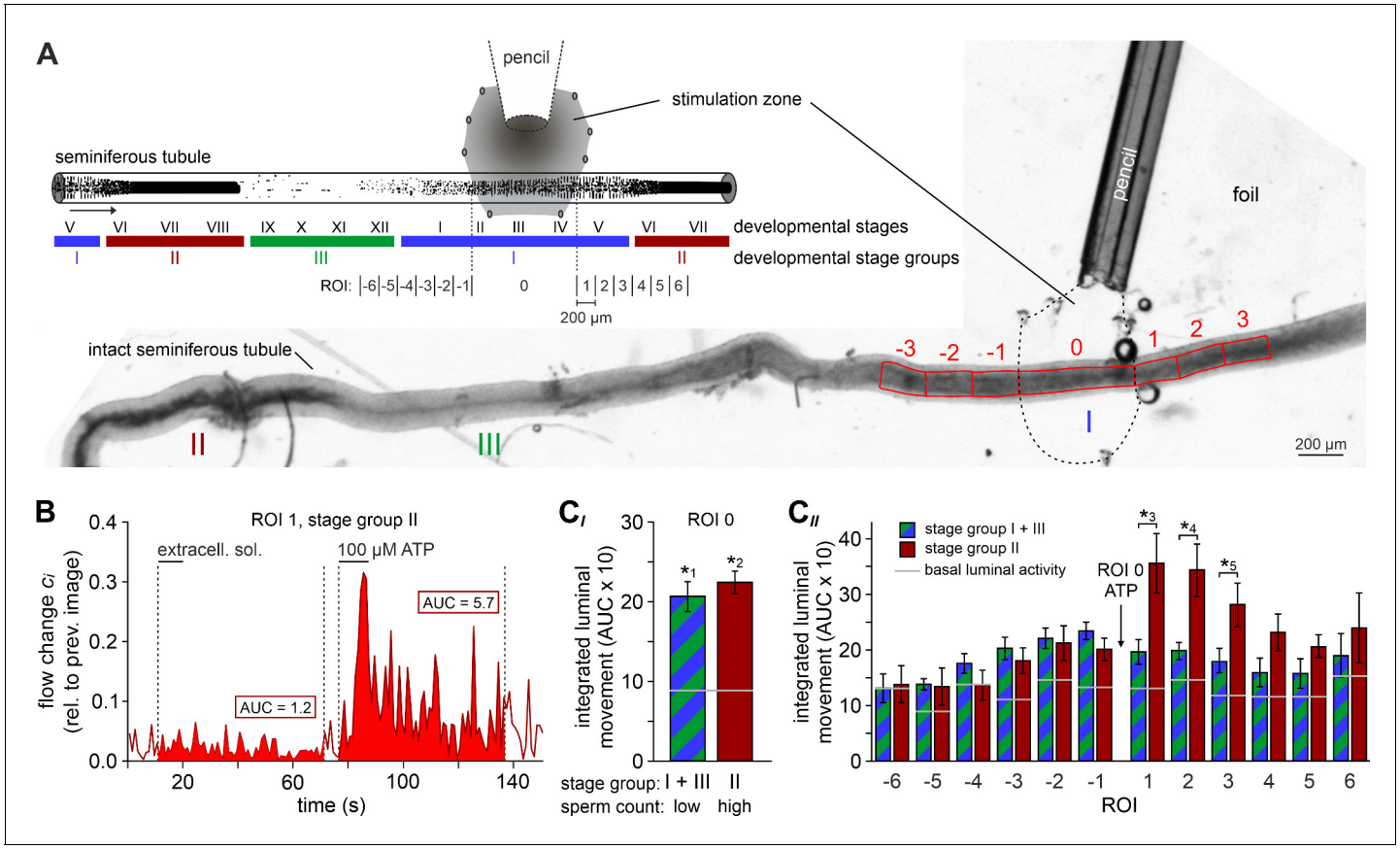

Figure 5. ATP drives directional luminal transport. (**A**) Schematic drawing (top) and original low-magnification image (bottom) of the experimental setup. Intact seminiferous tubules are placed on transparent foil in a custom-built macroscopic imaging chamber. The tubule is kept stationary by gentle suction through tiny holes punched in the foil and vacuum underneath. As previously suggested (***Hess and De Franca, 2008***), tubules are coarsely categorized into three stages (I–III; color code) according to luminal sperm content. Precise mapping of stimulated regions is feasible by positioning both tubule and perfusion pencil within an area delimited by several holes that outline a stimulation zone (methods). The tubule region directly exposed to ATP is designated as ROI 0, with adjacent equidistant sections numbered consecutively (up to ROI ±6; schematic). In the original image shown, only ROIs ± 3 are outlined for clarity. (**B**) Analysis of luminal content movement by calculation of flow change c_i relative to each previous image (methods) within a representative luminal ROI. Motion is quantified by measuring the area under curve (AUC; solid red) within 60 s after stimulation onset. Note that mechanical control stimulation (extracellular solution) does not affect basal luminal motion. (**C**) Bar charts depicting luminal content movement (means ± SEM) upon ATP stimulation (100 µM; 10 s) in either directly exposed regions (C_I; n = 17) or adjacent areas (C_{II}; n = 3–17). Green/blue (groups I and III) and red (group II) bars depict stages with a low vs. a high luminal sperm count, respectively. Horizontal gray lines mark the average basal luminal motion prior to stimulation. ATP induces significantly increased content movement in directly stimulated areas (ROI 0) independent of luminal sperm count/stage group (C_I). Note that in adjacent regions (C_{II}) unidirectional movement occurs exclusively in tubule sections with high luminal sperm density. Asterisks denote statistically significant differences ($*^1p=8.7e^{-5}$; $*^2p=6.7e^{-7}$; $*^3p=0.005$; $*^4p=0.002$; $*^5p=0.03$; unpaired two-tailed *t*-test).

amplitude 'vibratory' movements and local indentations (***Figure 4A***), reminiscent of the relatively high frequency rippling previously described (***Ellis et al., 1981***; ***Worley et al., 1985***).

We next investigated the Ca^{2+} signaling mechanism(s) underlying ATP-dependent TPC contractions. First, we asked whether influx of external Ca^{2+} is involved in TPC force generation. Similar to in vitro observations (***Figure 1K&L***), diminishing or even reversing the driving force for transmembrane Ca^{2+} flux by reducing $[Ca^{2+}]_e$ to 100 nM or 12 nM, respectively, for variable durations, significantly decreased both TPC Ca^{2+} signals and tubular contractions (***Figure 4B–H***). While, upon $[Ca^{2+}]_e$ reduction, ATP-dependent responses (both Ca^{2+} signals and contractions) were still detected in the vast majority of cells/experiments (***Figure 4E***), response strength was strongly diminished (***Figure 4F***). These effects were independent of both the extent (12 nM or 100 nM) and the duration (1–10 min) of $[Ca^{2+}]_e$ reduction and were fully reversible (***Figure 4H***). Second, we examined a potential role of ATP-induced Ca^{2+} release from internal storage organelles. Ca^{2+} depletion of the

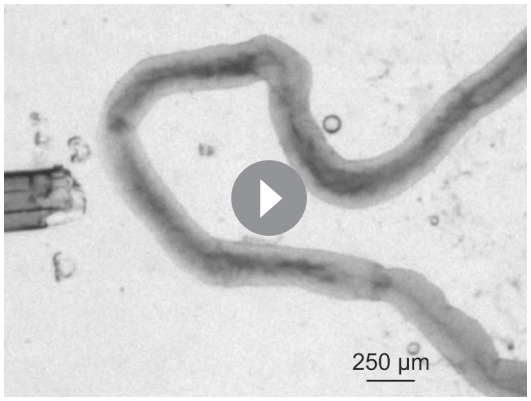

Video 4. ATP stimulation triggers movement of luminal content in intact seminiferous tubules. Brightfield time-lapse recording of an intact isolated seminiferous tubule (field of view shows cycle stages II and III) challenged by brief focal ATP perfusion (100 µM, 10 s). The spatial extent of the stimulation zone had been defined by prior perfusion with a dye solution (fast green).
https://elifesciences.org/articles/62885#video4

sarcoplasmic reticulum via pharmacological inhibition of the sarco/endoplasmic reticulum Ca^{2+}-ATPase by cyclopiazonic-acid (CPA) essentially abolished both ATP-dependent Ca^{2+} signals and contractions (***Figure 4D***), with very few cells/tubules retaining some residual ATP sensitivity during CPA treatment (***Figure 4G***). Importantly, all results from ratiometric fura-2 imaging were qualitatively indistinguishable from those obtained with genetically targeted GCaMP6f (***Figure 4E–G***), showing that both approaches to TPC Ca^{2+} measurement provide comparable results. Third, given the pronounced effect of pharmacological store depletion, we aimed to quantify the specific contribution of metabotropic purinoceptors to the overall ATP-mediated effect. The P2Y receptor-selective agonist UTP (***Coddou et al., 2011***) evoked both TPC Ca^{2+} signals and tubular contractions (***Figure 4E&F***). However, under control $[Ca^{2+}]_e$ conditions, UTP-evoked responses were substantially reduced compared to control ATP stimulations (***Figure 4F***). Notably, these UTP responses were statistically indistinguishable from the diminished ATP-dependent signals we observed under low $[Ca^{2+}]_e$ conditions (***Figure 4F***).

Together, these data strongly suggest that (i) extracellular ATP acts as a potent TPC stimulus that triggers seminiferous tubule contractions in situ, that (ii) P2X and P2Y receptors act in concert to mediate TPC responses to ATP exposure, that (iii), while P2X receptor-dependent external Ca^{2+} influx apparently boosts responses to ATP, P2Y receptor-mediated Ca^{2+} mobilization from the sarcoplasmic reticulum is necessary to evoke TPC responses, and consequently – since store depletion essentially abolishes ATP-dependent signals – that (iv) influx of external Ca^{2+} via ionotropic P2X receptors is not sufficient to drive TPC signals and evoke contractions. Notably, our general finding of ATP-induced mouse TPC contractions is likely transferable to human peritubular cells. When primary human TPC cultures (***Walenta et al., 2018***) were exposed to extracellular ATP, morphological changes were observed within seconds-to-minutes (***Figure 4—figure supplement 1A&B***). Moreover, embedding cells in collagen gel lattices revealed considerable contractile force in response to ATP (***Figure 4—figure supplement 1C&D***).

ATP drives directional luminal transport

We hypothesized that ATP-induced tubular contractions could impact the transport of luminal fluid and spermatozoa. To test this, we custom-built a whole-mount macroscopic imaging platform, designed to allow both widefield and fluorescence time-lapse imaging of intact seminiferous tubules (***Figure 5A***). In addition, this setup enables visual categorization of the spermatogenic cycle into three distinct stage groups following published protocols (***Hess and De Franca, 2008***) and allows precisely timed focal perfusion (methods). First, we asked if brief focal purinergic stimulation triggers seminiferous tubule contractions and, consequently, luminal content movement. Flow field change analysis reveals some basal luminal motion independent of mechanical stimulation (***Figure 5B***). However, ATP exposure triggered a strong increase in luminal flow that outlasted the presence of ATP for several tens of seconds (***Figure 5B***, ***Video 4***). Second, we analyzed if luminal movement depends on the tubule's cycle stage and, consequently, luminal sperm count. When we analyzed ATP-induced movement in directly stimulated luminal regions (each designated as region-of-interest (ROI) 0) and compared stage groups with a high (group II) vs. a relatively low (groups I and III) amount of luminal sperm, we observed no difference in stimulation-dependent motion (***Figure 5C$_I$***). Thus, direct ATP exposure triggers tubular contractions independent of cycle stage and luminal sperm count. Third, we investigated if luminal movement is restricted to the area of stimulation or, by contrast, if fluid

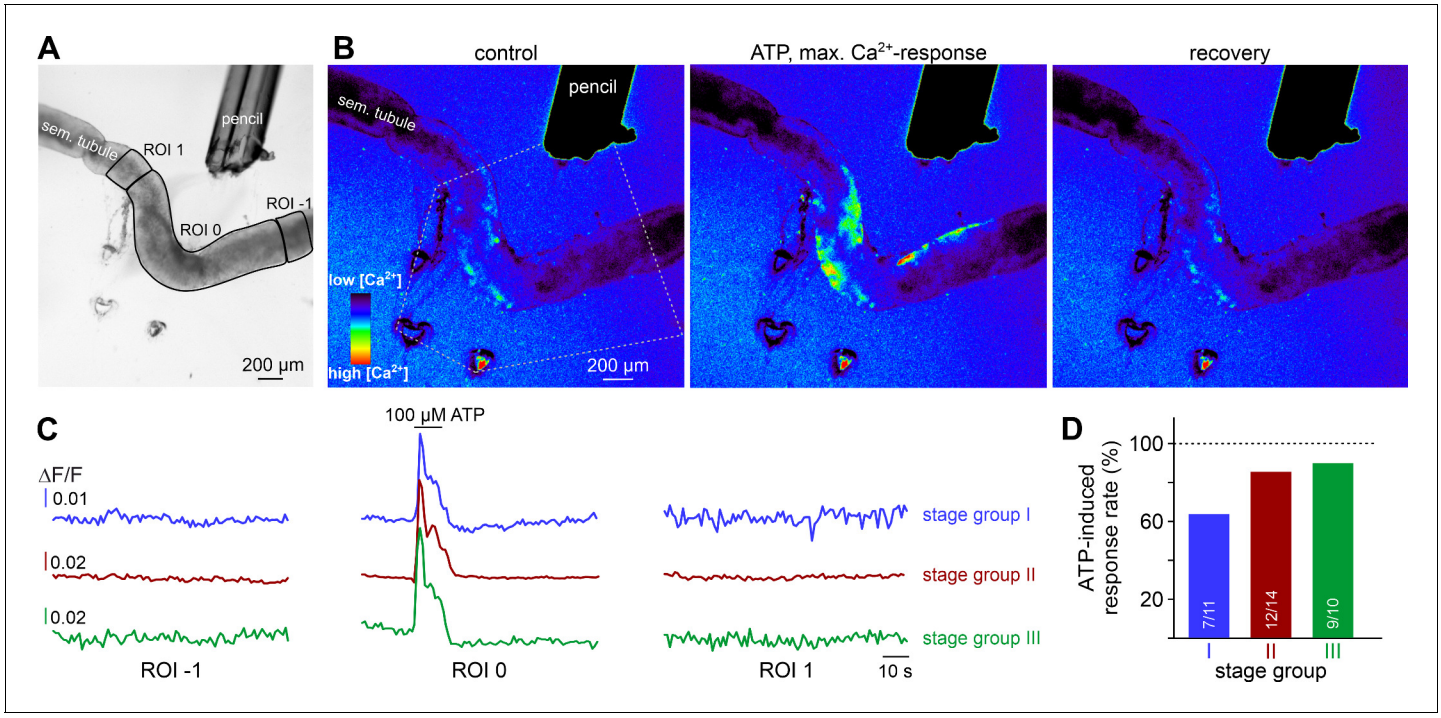

Figure 6. ATP causes Ca^{2+} elevations within a restricted paracrine radius. (**A**) Low-magnification brightfield image of an intact seminiferous tubule segment dissected from SMMHC-CreER^{T2} x Ai95D mice and positioned directly in front of the tip of a 250 µm diameter perfusion pencil. ROIs (black lines) are drawn to encompass the area that is directly exposed to fluid flow (ROI 0) as well as adjacent regions (ROIs 1 and −1), respectively. Suction produced by negative pressure (applied through holes in the elastic foil pad beneath the tubule) limits the area of perfusion. (**B**) Pseudocolor GCaMP6f fluorescence intensity images of the tubule shown in (**A**) reveals Ca^{2+} transients in TPCs in response to ATP. Representative images (rainbow 256 color map) correspond to time points before, during, and after focal ATP exposure (100 µM; 10 s). The area directly challenged with ATP is denoted by the white dotted lines. For clarity, autofluorescence of the perfusion pencil was removed. Note that Ca^{2+} elevations are limited to ROI 0. (**C**) Representative original recordings of changes in GCaMP6f intensity (ΔF/F) over time from tubule segments of the three different stage groups (I–III). Traces exemplify Ca^{2+} signals (or the lack thereof) in ROIs 0, –1, and 1, respectively. Independent of the epithelial cycle stage investigated, ATP-induced $[Ca^{2+}]_c$ elevations are restricted to directly exposed tissue segments. (**D**) Quantification of ATP sensitivity among tubule segments of different cycle stage. Bar charts illustrate that purinergic stimulation causes Ca^{2+} signals irrespective of stage and, thus, luminal sperm count. Numbers of experiments as indicated in bars.

flow propagates beyond the directly stimulated tubule section. When we analyzed luminal motion in equidistant tubule sections adjacent to the directly stimulated area ROI 0 (***Figure 5A***), we found a significant, though relatively small bidirectional wave of propagating movement in stage groups I and III, which exhibit a low luminal sperm count (***Figure 5C$_{II}$***). Strikingly, we observed strong unidirectional luminal movement upon ATP stimulation of stage group II tubule sections which show high luminal sperm density associated with spermiation (***Figure 5C$_{II}$***). In this stage group, luminal content is predominantly propelled toward areas of ascending spermatogenic cycle stages. These findings demonstrate directionality of sperm transport upon focal purinergic TPC stimulation in isolated seminiferous tubules.

As expected, ATP-induced tubule contractions also manifest as Ca^{2+} signals in TPCs (***Figure 6A&B***, ***Video 5***). However, these Ca^{2+} elevations appear to be limited to those areas directly exposed to ATP (ROI 0). We observed no such signals in adjacent tubule sections independent of the stimulated stage group or an ascending or descending stage direction (***Figure 6C&D***). This finding indicates that, in the isolated seminiferous tubule, ATP acts as a local messenger that, by itself, is not sufficient to trigger a signal that propagates in a regenerative wave-like fashion along a tubule's longitudinal axis. However, local contractions generate sufficient force to move luminal content beyond the directly stimulated area and, in turn, directionality of flow along short-to-medium distances (≤600 µm; ***Figure 5C$_{II}$***) is not critically dependent on peristaltic contractility.

Video 5. ATP stimulation triggers transient Ca^{2+} signals in TPCs of intact seminiferous tubules. Fluorescence time-lapse recording of an intact seminiferous tubule (field of view shows cycle stage II) isolated from a mouse selectively expressing GCaMP6f in TPCs (SMMHC-CreER^{T2} x Ai95D male offspring). Fluorescence imaging (ΔF/F) during brief focal ATP perfusion (100 µM, 10 s) – the spatial extent of the stimulation zone had been defined by prior perfusion with a dye solution (food color) – reveals relative changes in TPC Ca^{2+} concentration (rainbow color map; blue, low Ca^{2+}; red, high Ca^{2+}).
https://elifesciences.org/articles/62885#video5

ATP induces tubular contractions in vivo

To ultimately attribute a physiological role to ATP-dependent Ca^{2+} signals in TPCs, tubular contractions, and corresponding transport of luminal content, these phenomena must (i) occur spontaneously in living animals, and must (ii) be triggered experimentally by ATP exposure in vivo. Thus, to investigate any in vivo relevance of our findings, we designed a custom-built 3D printed in vivo imaging stage (***Figure 7—figure supplement 1***) that allows both widefield epi-fluorescence and multiphoton microscopy of the mouse testis.

Initially, we monitored spontaneous seminiferous tubule activity in SMMHC-CreER^{T2} x Ai95D mice. Multiphoton time-lapse imaging revealed spontaneous TPC Ca^{2+} signals that typically accompanied strong tubule contractions (***Figure 7A&B***, ***Video 6***). Several characteristics emerged from quantitative analysis of these observations. First, during sufficiently long recording periods (≤30 min), contractions occur in essentially all seminiferous tubules (***Figure 7—figure supplement 2A***). Second, contractions of individual tubules within the 2D confocal plane are not synchronized (***Figure 7B***). Third, periods of enhanced activity (≥2 contractions within 90 s) are interrupted by long episodes of quiescence (***Figure 7B***, ***Figure 7—figure supplement 2B***). Fourth, the durations of TPC Ca^{2+} signals and corresponding contractions are positively correlated (***Figure 7—figure supplement 2C***), confirming a causal relationship.

Next, we asked whether spontaneous in vivo contractions are coordinated along the longitudinal tubular axis. Low magnification incident light microscopy enabled simultaneous observation of several superficial seminiferous tubule segments (***Figure 7C***). Movement analysis along the length of digitally straightened tubules demonstrates wave-like unidirectional motions that propagate with high velocities (***Figure 7C&D***). These movements coincide with 'macroscopic' Ca^{2+} waves that travel at comparable speed and direction (***Figure 7—figure supplement 2D***). Notably, the observed coordinated contractile movements provide sufficient force to ensure luminal sperm transport (***Video 7***).

Finally, we examined if brief focal ATP stimulation also triggers peritubular Ca^{2+} signals and seminiferous tubule contractions in vivo. Therefore, we filled low resistance patch pipettes with fluorescently labeled ATP solution, penetrated the tunica albuginea, and targeted the interstitial space close to neighboring tubules (***Figure 7E***, ***Video 8***). Nanoliter puffs of ATP-containing test solution induced both Ca^{2+} transients in genetically labeled TPCs and strong tubule contractions in the majority of experiments (***Figure 7F&G***). By contrast, puffs of extracellular saline rarely stimulated any such response (***Figure 7—figure supplement 2E***). Taken together, in vivo recordings demonstrate that robust recurrent seminiferous tubule contractions (i) occur spontaneously, (ii) are driven by cytosolic Ca^{2+} elevations in TPCs that propagate in a wave-like fashion, and (iii) can be triggered experimentally by ATP exposure. Consequently, paracrine purinergic signaling in the mouse testis is a mediator of luminal sperm transport within the seminiferous tubule network.

Discussion

The molecular and cellular mechanisms that control paracrine testicular communication have to a large extent remained controversial, if not elusive (***Schlatt and Ehmcke, 2014***). For TPCs in particular, a contractile function under paracrine control and, consequently, a critical role in male infertility have long been proposed (***Albrecht et al., 2006***; ***Romano et al., 2005***), but direct experimental

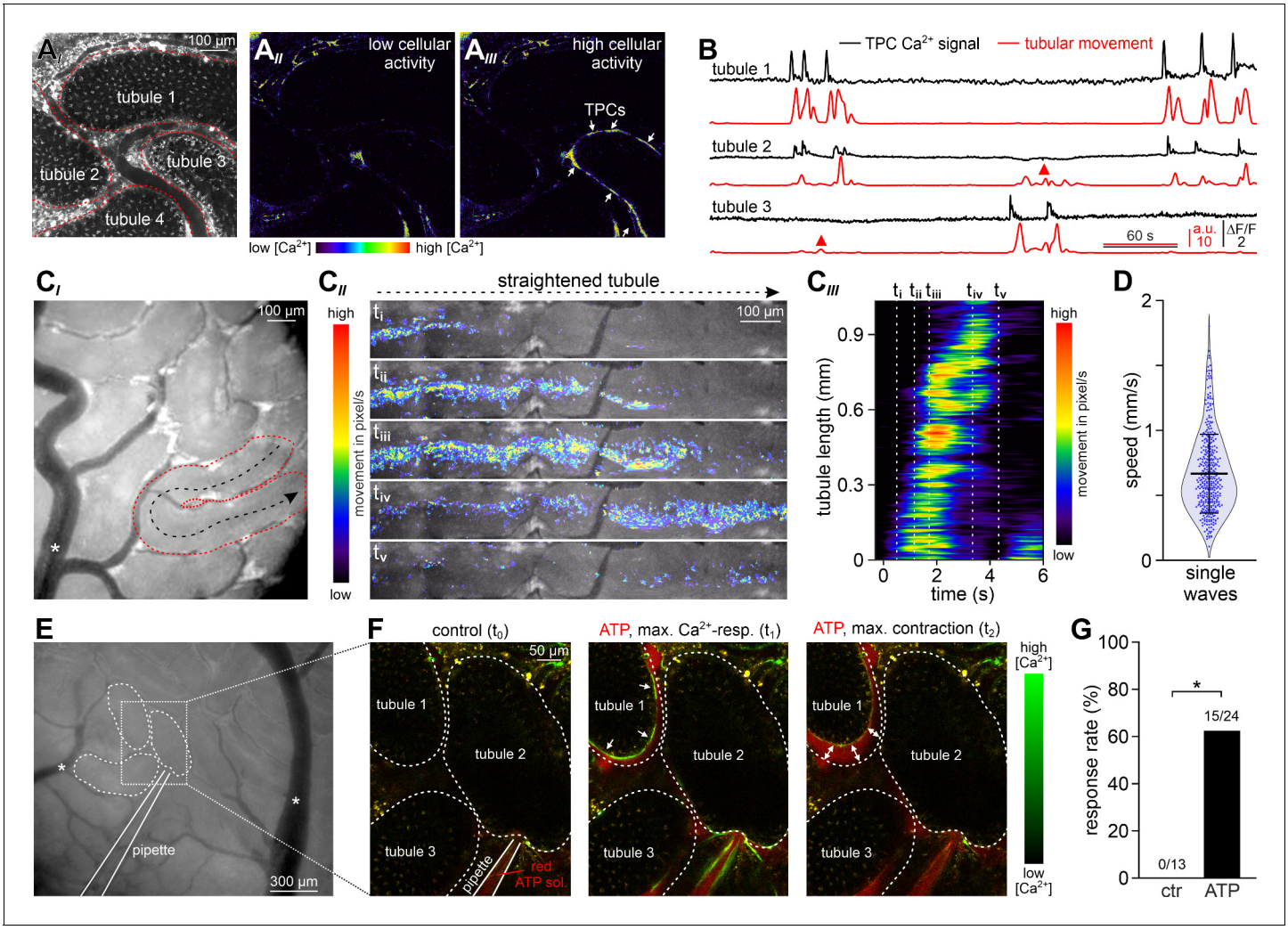

Figure 7. ATP induces tubular contractions in vivo. (**A**) Multiphoton in vivo fluorescence microscopy in SMMHC-CreER^{T2} x Ai95D mice enables time-lapse imaging of TPC activity. Maximum gray scale projection outlines segments from four seminiferous tubules (red dotted lines (**A**$_I$)). Pseudocolor images of GCaMP6f intensity indicate $[Ca^{2+}]_c$ changes in TPCs of tubule three during phases of low (**A**$_{II}$) vs. high (**A**$_{III}$) spontaneous activity (rainbow color map; white arrows in (**A**$_{III}$)). (**B**) Original traces depict simultaneous TPC Ca^{2+} signals (black; ΔF/F) and tubular contractions (red; calculated as flow change c_i relative to each previous image (methods) over time in tubules 1–3) (**A**). Red triangles mark passive movements, which occur upon contractions of adjacent tubules. Note the lack of a corresponding Ca^{2+} signal. (**C**) Analysis of spontaneous tubular motion in vivo. Low magnification incident light image of the mouse testis (**C**$_I$) shows several superficial seminiferous tubule segments, testicular blood vessels (white asterisk; note that unobstructed blood supply (i.e. visualizing erythrocyte flow) is checked routinely), and a specific segment outlined by red dotted lines. After time-lapse imaging, this segment is digitally straightened (**C**$_{II}$) and subjected to motion analysis. For different time points (i–v), pixel movement and its propagation are reflected by merged pseudocolor images. Directionality is indicated by the black arrow in (**C**$_I$). From a kymograph (**C**$_{III}$), the time–space relationship of tubular motion becomes apparent (time points i–v as indicated by dashed vertical lines). (**D**) Violin plot depicting the velocity of contractile movement in individual tubule segments (blue dots). (**E–G**) ATP-induced Ca^{2+} signals and contractions in vivo. (**E**) Low magnification epi-fluorescence image of several superficial seminiferous tubule segments and blood vessels (white asterisks). The boxed area includes three tubule segments (dotted black lines), which are targeted by a low resistance pipette filled with fluorescently labeled ATP solution. (**F**) Enlarged view of the area outlined in (**E**). Merged (red/green) multiphoton fluorescence images taken before and during/after brief stimulation with ATP. The middle and right frames correspond to the point of maximum Ca^{2+} signal (green) and contraction (double arrows) of tubule 1, respectively. (**G**) Bar chart quantification of contractions induced by nanoliter puffs of saline with or without ATP (1 mM). Asterisk denotes statistical significance (p=0.036; Fisher's Exact test).
The online version of this article includes the following figure supplement(s) for figure 7:

Figure supplement 1. A custom-built 3D printed microscope stage enables simultaneous in vivo multiphoton imaging of Ca^{2+} signals and contractions in mouse seminiferous tubules.

Figure supplement 2. In vivo imaging of tubular activity in SMMHC-CreER^{T2} x Ai95D mice.

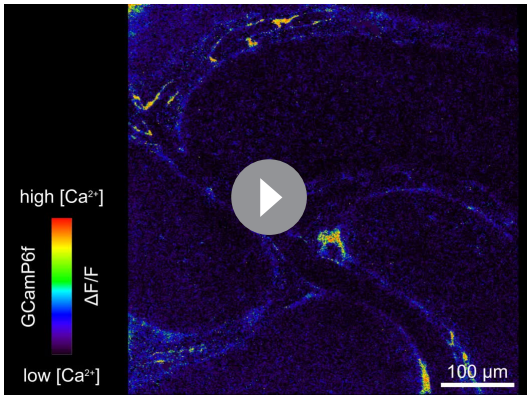

Video 6. In vivo multiphoton microscopy demonstrates spontaneous Ca^{2+} signals in mouse TPCs. Spontaneous seminiferous tubule in vivo activity monitored in SMMHC-CreER^{T2} x Ai95D mice. Intravital multiphoton fluorescence time-lapse imaging (ΔF/F, 2 Hz) reveals coordinated changes in TPC Ca^{2+} concentration (rainbow color map; blue, low Ca^{2+}; red, high Ca^{2+}) among one of three seminiferous tubules in the field of view (591 µm x 591 µm).
https://elifesciences.org/articles/62885#video6

release as well as the mechanism(s) that trigger ATP secretion in vivo currently remain elusive. The apparent absence of efferent nerve endings in the seminiferous tubules and interstitial tissue (***Tripiciano et al., 1996***) suggests that tubule contractility is under endo-/paracrine control. By evidence has been lacking (***Mayerhofer, 2013***). While several signaling molecules, including vasopressin (***Pickering et al., 1989***), oxytocin (***Worley et al., 1985***), prostaglandins (***Hargrove et al., 1975***), endothelin (***Filippini et al., 1993***), and others (***Albrecht et al., 2006***; ***Mayerhofer, 2013***), have been proposed to act on TPCs, a role of ATP in seminiferous tubule contractility has been explicitly ruled out early on (***Hovatta, 1972***). By contrast, our data reveal ATP is a strong stimulus that activates TPCs via both P2X and P2Y receptors, mediating coordinated tubule contractions and luminal sperm transport in situ and in vivo. Both spontaneous and ATP-dependent contractions trigger fast, stage-dependent, and directional transport of luminal content. It is thus tempting to speculate that seminiferous tubule contractility in general, and purinergic TPC signaling in particular, are promising targets for male infertility treatment and/or contraceptive development.

The site(s)/cellular origin of testicular ATP

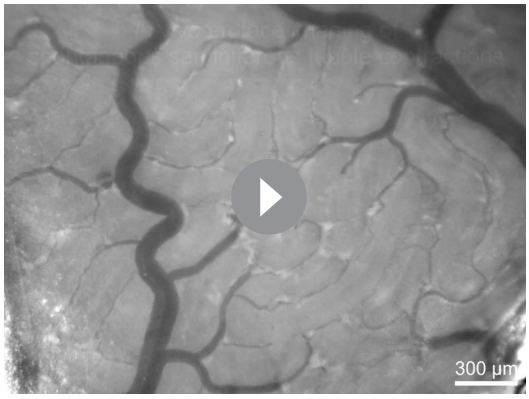

Video 7. Coordinated contractile movements ensure luminal sperm transport in vivo. Intravital en-face brightfield imaging illustrates spontaneous contractions and luminal movement in seminiferous tubules of adult mice. Low (1.5 x 1.4 mm field of view) and high-magnification time-lapse recordings reveal that contractions and luminal content propulsion are routinely observed in vivo. Note the unobstructed blood flow within testicular vessels.
https://elifesciences.org/articles/62885#video7

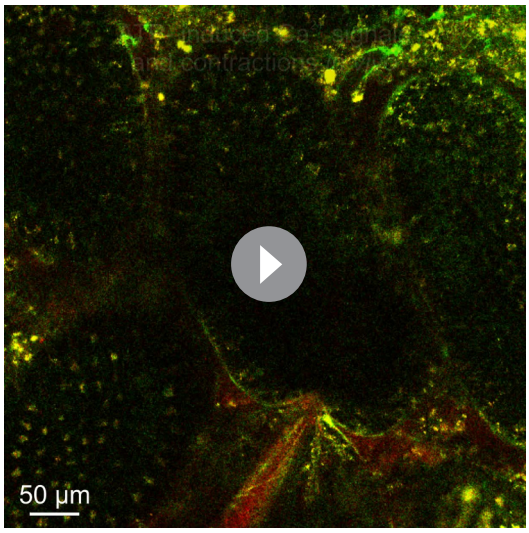

Video 8. Focal ATP stimulation triggers peritubular Ca^{2+} signals and seminiferous tubule contractions in vivo. Intravital multiphoton fluorescence time-lapse imaging in SMMHC-CreER^{T2} x Ai95D mice. Overlay of two detection channels (ΔF/F, GCaMP6f, green; Alexa Fluor 555, red). Stimulus solution (containing Alexa Fluor 555 (4 µM) and ATP (1 mM)) is puffed from a glass micropipette, which penetrated the *tunica albuginea* to target the interstitial space. Changes in TPC Ca^{2+} concentration are color-coded (black, low Ca^{2+}; green, high Ca^{2+}). Note that typically such contractions / Ca^{2+} signals do not occur when ATP is omitted from the 'puff' solution (data not shown).
https://elifesciences.org/articles/62885#video8

contrast, autonomic innervation of the testicular capsule mediates smooth muscle cell contraction of the *tunica albuginea*, using ATP as a (co)transmitter (**Banks et al., 2006**). Regulated ATP release has been reported for both Sertoli and germ cells (**Gelain et al., 2005**; **Gelain et al., 2003**). Moreover, TPCs express P2Y6 receptors (**Figure 1C**), which were reported to mediate ATP release upon activation (**Carneiro et al., 2014**). Thus, TPCs could themselves participate in regenerative nucleotide release.

During spermatogenesis, apoptosis is a vital process (**Print and Loveland, 2000**). In fact, up to 75% of germ cells undergo apoptosis under physiological conditions (**Huckins, 1978**). This substantial germ cell loss is called 'density-dependent regulation' (**Hess and De Franca, 2008**). Since ATP release from apoptotic cells is well documented (**Elliott et al., 2009**) it is likely that cell density-dependent waves of apoptosis could regularly generate local ATP surges. We have previously shown that one result of seminiferous extracellular ATP elevation is signal amplification by increased ATP release (**Fleck et al., 2016**), although the mechanistic basis of this positive feedback pathway is yet unknown. Given (i) the robust cytosolic Ca^{2+} transients observed in response to ATP exposure in various testicular cell types (**Fleck et al., 2016**; **Gelain et al., 2005**; **Liévano et al., 1996**; **Veitinger et al., 2011**; **Walenta et al., 2018**) and (ii) the usually millimolar ATP content in secretory vesicles (**Bodin and Burnstock, 2001**; **Zhang et al., 2007**), the most parsimonious explanation for ATP-induced ATP release would be an inevitable ATP 'co-secretion' upon any Ca^{2+}-dependent exocytosis event. In addition, ATP release has been observed in several cell types as a result of mechanical deformation, shear stress, stretch, or osmotic swelling (**Button et al., 2013**) adding another putative mechanism of regenerative signaling in purinergic contraction control.

Notably, extracellular ATP is rapidly degraded by ecto-nucleotidases (**Zimmermann et al., 2012**), rendering its interstitial half-life relatively short and, thus, narrowing its paracrine radius to a few hundred micrometers (**Fitz, 2007**). Combined with its fast diffusion – approximately 1 µm in less than 10 ms (**Khakh, 2001**) – extracellular ATP bears all characteristics of a fast paracrine agent in testicular communication (**Praetorius and Leipziger, 2009**).

Excitation–contraction coupling in TPCs is poorly described. Our results strongly suggest that a combination of P2X (isoforms 2 and/or 4) receptor-dependent Ca^{2+} influx and P2Y (likely isoform 2) receptor-activated phospholipase Cβ-dependent Ca^{2+} release from the sarcoplasmic reticulum – the latter being critical and resembling the recently reported mechanism of vascular smooth muscle cell contraction in small pulmonary veins (**Henriquez et al., 2018**) – provides the $[Ca^{2+}]_c$ elevation required for force generation (**Berridge, 2008**). P2X and P2Y receptors act on different time scales and display different ligand sensitivity, with EC_{50} values in the nanomolar (P2Y) vs. micromolar (P2X) range (**North, 2002**). It is possible that the co-activation of an ionotropic (P2X) and a metabotropic (P2Y) signaling pathway serves functions analogous to the concomitant exposure to both ATP and noradrenaline in mesenteric artery smooth muscle. Here, activation of P2X1 receptors generates a small initial contraction that is followed by larger noradrenaline-induced contraction (**Lamont et al., 2006**; **Lamont et al., 2003**). Regarding TPC $[Ca^{2+}]_c$ elevation, our data suggest that P2X receptor activation also targets Ca^{2+} release from internal stores, as their depletion inhibits excitation–contraction coupling entirely. Therefore, it is likely that P2X receptors act as signal boosters that mediate Ca^{2+}-induced Ca^{2+} release, possibly via activation of ryanodine receptors (**Berridge, 2008**). This way, the combined action of P2X and P2Y receptors might equip TPCs with a broader 'two-step' stimulus integration range.

Whole-mount imaging of isolated seminiferous tubules reveals propagation of luminal content that extends beyond the confines of the stimulated/contracted area and displays stage-dependent directionality. While peristaltic contractions are driven by propagating wave-like Ca^{2+} signals in vivo, focal ATP stimulation appears insufficient to trigger a regenerative Ca^{2+} wave in isolated tubules. We, thus, conclude that the observed directionality results from other, likely structural characteristics, for example anatomical features of stage group II and III tubules that favor a specific flow direction (increased tubule diameter and reduced luminal resistance along the stage II-to-III transition zone). We cannot, however, rule out that the use of large field-of-view/low numerical aperture objectives for 'macroscopic' imaging simply prevents the detection of low-amplitude Ca^{2+} signal spread.

Translation of our findings from the mouse model to humans awaits further in-depth investigation. We have recently reported that ATP activates Ca^{2+} signals in human TPCs in vitro (**Walenta et al., 2018**). Moreover, our present findings reveal ATP-induced contractions in cultured human TPCs. There are, however, notable differences between the human and the mouse tubular walls. While a

single layer of TPCs surrounds the mouse seminiferous tubules, the human tubular wall architecture is more complex, containing several TPC layers, substantial amounts of extracellular matrix proteins, and immune cells (**Mayerhofer, 2013**). Impaired spermatogenesis in sub-/infertile men typically coincides with tubular wall remodeling and a partial loss of TPC contractility proteins has been reported in infertile men (**Welter et al., 2013**). Accordingly, interference with TPC contractility had been proposed as a promising strategy for human male contraception (**Romano et al., 2005**). However, a causal relationship between contractility (or the lack thereof) and male (in)fertility has never been established. In fact, seminiferous tubule contractions had, so far, never been observed in vivo and most in vitro reports were based on indirect and non-quantitative evidence, for example from *post-hoc* fluorescence or scanning electron microscopy (**Barone et al., 2002**; **Fernández et al., 2008**; **Losinno et al., 2016**; **Losinno et al., 2012**; **Tripiciano et al., 1999**; **Tripiciano et al., 1997**; **Tripiciano et al., 1996**), morphometry of single cells in culture (**Rossi et al., 2002**; **Santiemma et al., 2001**; **Santiemma et al., 1996**; **Tripiciano et al., 1996**), or intraluminal pressure analysis (**Miyake et al., 1986**; **Yamamoto et al., 1989**). The fact that expression of TPC contractility proteins initiates with puberty under androgen control and that selective androgen receptor knockout in TPCs renders mice infertile (**Welsh et al., 2009**) underscores a potential role of TPC contractions in male fertility. Accordingly, pharmacological targeting of purinergic signaling pathways to (re) gain control of TPC contractility represents an attractive approach for male infertility treatment or contraceptive development.

Among several remaining questions, future experimental efforts will have to address (i) whether TPCs are coupled by gap junctions to display coordinated activity; (ii) whether and, if so, how the final ATP metabolite adenosine affects seminiferous tubule physiology; (iii) whether Rho/Rho kinase signaling pathways modulate TPC contractility as frequently observed in other smooth muscle cells (**Somlyo and Somlyo, 2003**); (iv) what, if any, role is played by P2X receptor-dependent changes in membrane potential; (v) which function is served by the sustained Ca^{2+}-gated Cl^- current (**Figure 1—figure supplement 2**); (vi) why periods of enhanced contractile activity are interrupted by longer quiescent episodes (**Figure 7—figure supplement 2B**); (vii) which additional or complementary roles in TPC physiology are played by previously proposed activators, including vasopressin, oxytocin, prostaglandins, and endothelin (**Albrecht et al., 2006**; **Mayerhofer, 2013**); (viii) whether an additional cytosolic and/or membrane Ca^{2+} oscillator (**Berridge, 2008**) provides an endogenous pacemaker mechanism that acts independent of purinergic stimulation; and (ix) whether, similar to vascular smooth muscle cells, some specific tone is maintained between contractions by spatial averaging of asynchronous oscillations (**Berridge, 2008**), a mechanism that could explain the occurrence of spontaneous low-amplitude 'vibratory' movements and local indentations that we (**Figure 4A**) and others (**Ellis et al., 1981**; **Worley et al., 1985**) have observed.

Materials and methods

Key resources table

Reagent type (species) or resource	Designation	Source or reference	Identifiers	Additional information
Strain, strain background (*M. musculus*)	C57BL/6J	Charles River Laboratories	Jax # 000664, RRID:IMSR_JAX:000664	
Strain, strain background (*M. musculus*)	SMMHC-CreERT2	Jackson Laboratories	Jax # 019079, RRID:IMSR_JAX:019079	
Strain, strain background (*M. musculus*)	129S.FVB-Tg(Amh-cre) 8815Reb/J	Jackson Laboratories	Jax # 007915, RRID:IMSR_JAX:007915	
Strain, strain background (*M. musculus*)	Ai95D	Jackson Laboratories	Jax # 028865, RRID:IMSR_JAX:028865	Cre-dependent GCaMP6f expression
Strain, strain background (*M. musculus*)	Ai14D	Jackson Laboratories	Jax # 007914, RRID:IMSR_JAX:007914	Cre-dependent tdTomato expression

Continued on next page

Continued

Reagent type (species) or resource	Designation	Source or reference	Identifiers	Additional information
primary cells (*M. musculus*)	testicular peritubular cells (TPC)	this paper		early passage number, Spehr laboratory (see: **TPC culture**)
primary cells (*Homo sapiens*)	testicular peritubular cells (TPC)	this paper		early passage number ***Albrecht et al., 2006***, Mayerhofer laboratory
Biological sample (*M. musculus*)	seminiferous tubules	this paper		freshly isolated from *Mus musculus*, Spehr laboratory (see: **Slice preparation**)
Antibody	anti-actin, α-smooth muscle - FITC antibody (α-SMA-FITC); mouse, monoclonal	Millipore Sigma	cat # F3777, RRID:AB_476977	(1:500)
Sequence-based reagent	P2 receptors	this paper	PCR primers	table in methods section (see: **Gene expression analysis**), Spehr laboratory
Commercial assay, kit	RevertAid H Minus kit	Thermo Fisher	cat # K1632	
Chemical compound, drug	soybean trypsin inhibitor (SBTI)	Sigma Aldrich	cat # T6522	(100 µg/ml)
Chemical compound, drug	fura-2/AM	Thermo Fisher Scientific	cat # F-1201	(cell culture: 5 µM, tissue slices: 30 µM)
Chemical compound, drug	ivermectin	Sigma Aldrich	cat # I8898	(3 µM)
Chemical compound, drug	suramin	Sigma Aldrich	cat # S2671	(100 µM)
Chemical compound, drug	cyclopiazonic-acid (CPA)	Tocris Bioscience	cat # 1235	(90 µM)
Software, algorithm	Imaris 8	Bitplane	RRID:SCR_007370	microscopy image analysis software
Software, algorithm	custom-written MATLAB code	this paper	https://github.com/rwth-lfb/Fleck_Kenzler_et_al; ***Fleck, 2021***; copy archived at swh:1:rev:88c8792860ddf09fd7da969fef6bf86c40441135	contraction and Ca^{2+} signal analysis, Merhof laboratory (see: **Data analysis**)
Other	DAPI stain	Thermo Fisher Scientific	cat # D1306, RRID:AB_2629482	(5 µg/ml)
Other	DRAQ5 stain	Thermo Fisher Scientific	cat # 65-0880-96, RRID:AB_2869620	(IH: 1:500 CLARITY: 1:1000)

Animals

All animal procedures were approved by local authorities and in compliance with both European Union legislation (Directive 2010/63/EU) and recommendations by the Federation of European Laboratory Animal Science Associations (FELASA). When possible, mice were housed in littermate groups of both sexes (room temperature (RT); 12:12 hr light-dark cycle; food and water available ad libitum). If not stated otherwise, experiments used adult (>12 weeks) males. Mice were killed by CO_2 asphyxiation and decapitation using sharp surgical scissors. We used C57BL/6J mice (Charles River Laboratories, Sulzfeld, Germany) as well as offspring from crossing either SMMHC-CreER^{T2} (JAX #019079) (***Wirth et al., 2008***) or 129S.FVB-Tg(Amh-cre)8815Reb/J (JAX #007915) (***Holdcraft and Braun, 2004***) mice with either Ai95D (JAX #028865) (***Madisen et al., 2015***) or Ai14D (JAX #007914) (***Madisen et al., 2010***) mice, respectively.

Chemicals and solutions

The following solutions were used:

(**S_1**) 4-(2-Hydroxyethyl)piperazine-1-ethanesulfonic acid (HEPES) buffered extracellular solution containing (in mM) 145 NaCl, 5 KCl, 1 $CaCl_2$, 0.5 $MgCl_2$, 10 HEPES; pH = 7.3 (adjusted with NaOH); osmolarity = 300 mOsm (adjusted with glucose).

(**S_2**) Oxygenated (95% O_2, 5% CO_2) extracellular solution containing (in mM) 120 NaCl, 25 $NaHCO_3$, 5 KCl, 1 $CaCl_2$, 0.5 $MgCl_2$, 5 N,N-bis(2-hydroxyethyl)−2-aminoethanesulfonic acid (BES); pH = 7.3; 300 mOsm (glucose).

(**S_3**) Extracellular low Ca^{2+} solution containing (in mM) 145 NaCl, 5 KCl, 0.5 $MgCl_2$, 10 HEPES; pH = 7.3 (NaOH); osmolarity = 300 mOsm (glucose); $[Ca^{2+}]_{free}$ = ~110 nM (1 mM EGTA, 0.5 mM $CaCl_2$) or ~12 nM (1 mM EGTA, 0.1 mM $CaCl_2$).

(**S_4**) Oxygenated (95% O_2, 5% CO_2) extracellular solution containing (in mM) 120 NaCl, 25 $NaHCO_3$, 5 KCl, 0.5 $MgCl_2$, 5 BES; pH = 7.3; 300 mOsm (glucose); $[Ca^{2+}]_{free}$ = ~110 nM (1 mM EGTA, 0.5 mM $CaCl_2$) or ~12 nM (1 mM EGTA, 0.1 mM $CaCl_2$).

(**S_5**) Gluconate-based extracellular solution containing (in mM) 122.4 Na gluconate, 22.6 NaCl, 5 KCl, 1 $CaCl_2$, 0.5 $MgCl_2$, 10 HEPES; pH = 7.3 (adjusted with NaOH); osmolarity = 300 mOsm (glucose).

(**S_6**) Standard pipette solution containing (in mM) 143 KCl, 2 KOH, 1 EGTA, 0.3 $CaCl_2$, 10 HEPES ($[Ca^{2+}]_{free}$ = ~110 nM); pH = 7.1 (adjusted with KOH); osmolarity = 290 mOsm (glucose).

(**S_7**) Gluconate-based pipette solution containing (in mM) 110 Cs gluconate, 30 CsCl, 2 CsOH, 1 EGTA, 0.3 $CaCl_2$, 10 HEPES ($[Ca^{2+}]_{free}$ = ~110 nM); pH = 7.1 (adjusted with CsOH); osmolarity = 290 mOsm (glucose).

In some experiments Na-GTP (0.5 mM) was added to the pipette solution. Free Ca^{2+} concentrations were calculated using WEBMAXCLITE v1.15 (RRID:SCR_000459). If not stated otherwise, chemicals were purchased from Sigma (Schnelldorf, Germany). Cyclopiazonic-acid (CPA) and 2'(3')-O-(4-Benzoylbenzoyl)adenosine-5'-triphosphate (BzATP) triethylammonium salt was purchased from Tocris Bioscience (Bristol, UK). Fura-2/AM was purchased from Thermo Fisher Scientific (Waltham, MA). Final solvent concentrations were $\leq$0.1%. When high ATP concentrations ($\geq$1 mM) were used, pH was readjusted.

Stimulation

For focal stimulation, solutions and agents were applied from air pressure-driven reservoirs via an 8-in-1 multi-barrel 'perfusion pencil' (AutoMate Scientific; Berkeley, CA). Changes in focal superfusion (***Veitinger et al., 2011***) were software-controlled and, if required, synchronized with data acquisition by TTL input to 12V DC solenoid valves using a TIB 14S digital output trigger interface (HEKA Elektronik, Lambrecht/Pfalz, Germany). For focal stimulation during in vivo recordings, ATP was puffed from pulled glass pipettes using a microinjection dispense system (Picospritzer III; Parker Hannifin, Hollis, NH).

Low $[Ca^{2+}]_e$ solutions (**S_3 and S_4**) were applied via both the bath and perfusion pencil. To ensure depletion of Ca^{2+} stores by CPA we monitored intracellular Ca^{2+} levels during drug treatment (0.05 Hz frame rate). Transient CPA-dependent Ca^{2+} elevations lasted 10–40 min. After baseline Ca^{2+} levels were restored, cells/slices were again challenged with ATP. Control recordings, omitting CPA, were performed under the same conditions.

Slice preparation

Acute seminiferous tubule slices were prepared as previously described (***Fleck et al., 2016***) with minor modifications. Briefly, seminiferous tubules from young adults were isolated after *tunica albuginea* removal, embedded in 4% low-gelling temperature agarose (VWR, Erlangen, Germany), and 250 µm slices were cut with a VT1000S vibratome (RRID:SCR_016495; Leica Biosystems, Nussloch, Germany). Acute slices were stored in a submerged, oxygenated storage container (**S_2**; RT). When using testicular tissue from Ai95D mice, slices were protected from light during storage to avoid GCaMP6f bleaching.

TPC culture

After mouse testis isolation and removal of the *tunica albuginea,* the seminiferous tubules were placed in Dulbecco's Modified Eagle Medium/Nutrient Mixture F-12 (DMEM/F-12; Invitrogen) containing 1 mg ml^{-1} collagenase A and 6 µg ml^{-1} DNase (10 min; 34˚C; shaking water bath (60 cycles

min^{-1})). Three times, the samples were washed (DMEM/F-12; 5 ml), allowed to settle for 5 min, and the supernatant was discarded. Next, tubules were incubated DMEM/F-12 containing 1 mg ml^{-1} trypsin and 20 µg ml^{-1} DNase (20 min; 34˚C; shaking water bath (60 cycles min^{-1})). Digestion was stopped by addition of 100 µg ml^{-1} soybean trypsin inhibitor (SBTI) and 20 µg ml^{-1} DNase in phosphate-buffered saline (D-PBS). Then, samples were allowed to settle for 5 min and the supernatant was collected. After two more cycles of washing (DMEM/F-12), settling (5 min), and supernatant collection, the collected cell suspension was centrifuged (10 min; 400 g) and the supernatant discarded. The pellet was resuspended in DMEM containing FBS (10%) and penicillin G/streptomycin (1%), filtered (cell strainer (100 µm)), and cells were plated in 75 cm^2 cell culture flask (T75; Invitrogen) and placed in a humidified incubator (37˚C; 5% CO_2). Approximately $^1/_3$ of medium volume was replaced every 3 days. Cells usually reached 100% confluence after 7 days in vitro (DIV). Then, cells were washed twice (DPBS$^{-/-}$; 5 min; 37˚C) and incubated in 0.05% trypsin/EDTA (5 min; 37˚C). Detachment of cells was checked visually and, if necessary, facilitated mechanically. The cell suspension was centrifuged (3 min; 800 g) and the supernatant discarded. The pellet was resuspended in DMEM at cell densities of ~10^5 cells ml^{-1} and plated again either in culture flasks or on glass coverslips in 35 mm dishes for experimental use. Again, $^1/_3$ of medium volume was replaced every 3 days. Experiments were performed for ≤5 days after passage.

Human TPCs were isolated from small testicular tissue fragments derived from consenting donors with obstructive azoospermia and normal spermatogenesis as described (***Albrecht et al., 2006***; ***Walenta et al., 2018***). The study was approved by the local ethical committee (Ethikkommission, School of Medicine, TU Munich, project 169/18S).

Gene expression analysis

Total RNA was isolated and purified from cultured mouse TPCs (passage 1) with Trizol followed by complementary DNA synthesis with RevertAid H Minus kit (#K1632 Thermo Fisher) according to the manufacturer's instructions. Controls in which the reverse transcriptase was omitted were routinely performed. PCR amplification was performed during 30 thermal cycles (95˚C, 20 s; 58˚C, 20 s; 72˚C, 20 s). The following specific primer pairs were used for PCR amplification:

Target	Forward primer 5´–3´	Reverse primer 5´–3´
P2X1	CCGAAGCCTTGCTGAGAA	GGTTTGCAGTGCCGTACAT
P2X2	GACCTCCATCGGGGTGGGCT	TGGGGTCCGTGGATGTGGAGT
P2X3	CTGCCTAACCTCACCGACAAG	AATACCCAGAACGCCACCC
P2X4	CCCTTTGCCTGCCCAGATAT	CCGTACGCCTTGGTGAGTGT
P2X5	GCTGCCTCCCACTGCAACCC	AAGCCCCAGCACCCATGAGC
P2X6	CCCAGAGCATCCTTCTGTTCC	GGCACCAGCTCCAGATCTCA
P2X7	CCCAGATGGACTTCTCCGAC	GGACTTAGGGGCCACCTCTT
P2Y1	CGACAGGGTTTATGCCACTT	TCGTGTCTCCATTCTGCTTG
P2Y2	CGTGCTCTACTTCGTCACCA	GACCTCCTGTGGTCCCATAA
P2Y4	ACTGGCTTCTGCAAGTTCGT	AGGCAGCCAGCTACTACCAA
P2Y6	CATTAGCTTCCAGCGCTACC	GCTCAGGTCGTAGCACACAG
P2Y12	CATTGCTGTACACCGTCCTG	AACTTGGCACACCAAGGTTC
GAPDH	CAAGGTCATCCATGACAACTTTG	GTCCACCACCCTGTTGCTGTAG

Immunochemistry and tissue clearing

For immunochemistry of testicular cryosections, testes were fixed with 4% (w/v) paraformaldehyde (PFA) in PBS$^{-/-}$ (10 mM, pH 7.4; ≥12 hr; 4˚C) and subsequently cryoprotected in PBS$^{-/-}$ containing 30% sucrose (≥24 hr; 4˚C). Samples were then embedded in Tissue Freezing Medium (Leica Biosystems), sectioned at 20 µm on a Leica CM1950 cryostat (RRID:SCR_018061; Leica Biosystems), and mounted on Superfrost Plus slides (Menzel, Braunschweig, Germany). For immunostaining of cultured mouse TPCs, cells were washed (3x; PBS$^{-/-}$), fixed with ice-cold 4% PFA in PBS$^{-/-}$ (20 min; RT),

and washed again (3x; $PBS^{-/-}$). For blocking, sections/cells were incubated in $PBS^{-/-}$ containing Tween-20 (0.1%)/BSA (3%) solution (1 hr; RT). After washing ($PBS^{-/-}$; 2 × 5 min), sections/cells were incubated FITC-conjugated monoclonal anti-actin, α-smooth muscle (α-SMA-FITC, cat # F3777, MilliporeSigma) antibody (1:500 in 3% BSA; 1 hr; RT). Excess antibodies were removed by washing (2 × 5 min $PBS^{-/-}$). For nuclear counterstaining, sections/cells were then incubated in $PBS^{-/-}$ containing either DAPI (5 µg ml^{-1}; 10 min; RT; Thermo Fisher Scientific) or DRAQ5 (1:500; 5 min; RT; Thermo Fisher Scientific).

Fluorescent images were taken using either an inverted microscope (Leica DMI4000B, Leica Microsystems) or an upright fixed stage scanning confocal microscope (TCS SP5 DM6000 CFS; Leica Microsystems) equipped with a 20 × 1.0 NA water immersion objective (HCX APO L; Leica Microsystems). To control for non-specific staining, experiments in which the primary antibody was omitted were performed in parallel with each procedure. Digital images were uniformly adjusted for brightness and contrast using Adobe Photoshop CS6 (Adobe Systems, San Jose, CA, USA).

For testicular tissue clearing we adopted the CLARITY method (***Chung et al., 2013***) with minor modifications (***Gretenkord et al., 2019***). Briefly, testes from adult mice were fixed overnight at 4˚C in hydrogel fixation solution containing 4% acrylamide, 0.05% bis-acrylamide, 0.25% VA-044 Initiator, 4% PFA in $PBS^{-/-}$ to maintain structural integrity. After hydrogel polymerization, lipids were removed by incubation in 4% sodium dodecyl phosphate (SDS) solution with 200 mM boric acid (pH 8.5) over periods of two months. Solutions were changed bi-weekly. During the final incubation period, the nuclear marker DRAQ5 (1:1000) was added. After washing (2 d) with PBST (0.1% TritonX), samples were incubated for 24 hr in RIMS80 containing 80 g Nycodenz, 20 mM PS, 0.1% Tween 20, and 0.01% sodium acid. Cleared samples were imaged using a Leica TCS SP8 DLS confocal microscope, equipped with a digital light-sheet module, 552 nm and 633 nm diode lasers, a HC PL FLUOTAR 5x/0.15 IMM DLS objective (observation), a L 1.6x/0.05 DLS objective (illumination), a DLS TwinFlect 7.8 mm Gly mirror cap, and a DFC9000 sCMOS camera. Rendering and three-dimensional reconstruction of fluorescence images was performed using Imaris 8 microscopy image analysis software (Bitplane, Zurich, Switzerland).

Electrophysiology

Whole-cell patch-clamp recordings were performed as described (***Fleck et al., 2016***; ***Veitinger et al., 2011***). Briefly, mouse TPCs were transferred to the stage of an inverse microscope (DMI 4000B, Leica Microsystems), equipped with phase contrast objectives and a cooled CCD camera (DFC365FX, Leica Microsystems). Cells were continuously superfused with solution $\mathbf{S_1}$ (~3 ml min^{-1}; gravity flow;~23˚C). Patch pipettes (~5 MΩ) were pulled from borosilicate glass capillaries with filament (1.50 mm OD/0.86 mm ID; Science Products) on a PC-10 vertical two-step micropipette puller (Narishige Instruments, Tokyo, Japan), fire-polished (MF-830 Microforge; Narishige Instruments) and filled with $\mathbf{S_6}$. An agar bridge (150 mM KCl) connected reference electrode and bath solution. An EPC-10 amplifier (RRID:SCR_018399) controlled by Patchmaster 2.9 software (RRID:SCR_000034; HEKA Elektronik) was used for data acquisition. We monitored and compensated pipette and membrane capacitance (C_{mem}) as well as series resistance (R_{series}). C_{mem} values served as a proxy for the cell surface area and, thus, for normalization of current amplitudes (i.e. current density). Cells displaying unstable R_{series} values were not considered for further analysis. Liquid junction potentials were calculated using JPCalcW software (***Barry, 1994***) and corrected online. Signals were low-pass filtered [analog 3- and 4-pole Bessel filters (–3 dB); adjusted to $^1/_3$ - $^1/_5$ of the sampling rate (10 kHz)]. If not stated otherwise, holding potential (V_{hold}) was –60 mV.

Fluorescence Ca^{2+} imaging

Cultured mouse TPCs were imaged as described (***Veitinger et al., 2011***). Briefly, cells were loaded with fura-2/AM in the dark (5 µM; 30 min; RT; $\mathbf{S_1}$) and imaged with an upright microscope (Leica DMI6000FS, Leica Microsystems) equipped for ratiometric live-cell imaging with a 150 W xenon arc lamp, a motorized fast-change filter wheel illumination system for multi-wavelength excitation, a CCD camera (DFC365 FX, Leica), and Leica LAS X imaging software. Ten to thirty cells in randomly selected fields of view were viewed at 20x magnification and illuminated sequentially at 340 nm and 380 nm (cycle time 2 s). The average pixel intensity at 510 nm emission within user-selected ROIs was digitized and calculated as the f_{340}/f_{380} intensity ratio.

For parallel recordings of intracellular Ca^{2+} signals and tubular contractions, acute seminiferous tubule slices were bulk-loaded with fura-2/AM in the dark (30 µM; 30 min; RT). After washing (3x; **S_1**), slices were transferred to a recording chamber and imaged with an upright microscope (Leica DMI6000FS, see above). We installed a custom-built reflective shield beneath the recording chamber for parallel monitoring of fluorescence and reflected light. At 1 Hz imaging cycles, we thus recorded two 510 nm fluorescence images (340/380 nm excitation) and a 'pseudo-brightfield' reflected light image that allowed quasi simultaneous analysis of intracellular Ca^{2+} and tubular movement.

To ensure effective store depletion by CPA treatment, we recorded intracellular Ca^{2+} levels during CPA incubation at low frequency to monitor Ca^{2+} release from the ER, but also prevent phototoxicity. Experiments were only conducted if (i) we detected a substantial gradual rise in intracellular Ca^{2+} upon CPA treatment, and if (ii) functional Ca^{2+} extrusion mechanisms ensured that Ca^{2+}-dependent fluorescence signals returned to base level. The time-course of this Ca^{2+} release – Ca^{2+} extrusion process varied between samples and ranged between 5.3 and 44.0 min (18.8 ± 9.3 min; mean ± SD).

Whole-mount seminiferous tubule imaging

Isolated tubules (>1 cm length) were placed onto a membrane within a custom-built 3D printed two-compartment recording chamber that was constantly superfused with **S_1**. Small membrane holes under the tubules and around a defined stimulation area allowed for (i) gentle fixation of the tubules and (ii) focal ATP perfusion of selected tubular regions by vacuum-generated negative pressure (80–180 mmHg) in the submembraneous chamber compartment and continuous suction of **S_1** from the top compartment. After visual determination of tubular stages (**I – III**) (***Parvinen, 1982***), the perfusion pencil was positioned to selectively stimulate an area of known and homogeneous stage. Focal stimulation in the desired area was routinely confirmed by transient dye perfusion (Fast Green) prior to ATP exposure. ATP stimulations (100 µM; 10 s) and corresponding negative controls were compared to determine ATP-dependent Ca^{2+} signals (offspring from crossing SMMHC-CreER^{T2} and Ai95D mice) or tubular contractions and sperm transport. For low-magnification brightfield or fluorescence imaging, we used a MacroFluo Z16 APO A system (Leica Microsystems) equipped with either a DFC450C camera and a PLANAPO 1.0x/WD 97 mm objective (brightfield) or with a monochrome DFC365FX camera and a 5.0x/0.50 LWD PLANAPO objective (fluorescence). Images were acquired at 1 Hz.

In vivo imaging

We administered tamoxifen (75 mg tamoxifen kg^{-1} body weight) to double-positive adult male offspring (SMMHC-CreER^{T2} x Ai95D) via daily intraperitoneal injections for five consecutive days. Mice were closely monitored for any adverse reactions to the treatment. Experiments were performed 2–5 weeks after the first injection. For surgery, mice were anesthetized with ketamine-xylazine-buprenorphine (100, 10, 0.05–0.1 mg kg^{-1}, respectively; Reckitt Benckiser Healthcare, UK). First, we made an incision next to the *linea alba* in the hypogastric region, followed by a 5 mm incision into the peritoneum. One testis was gently lifted from the abdominal cavity. Its *gubernaculum* was cut and the testis – with the spermatic cord, its blood vessels and *vas deferens* still intact – was transferred to a temperature-controlled imaging chamber filled with extracellular solution (**S_1**; 35˚C), mounted on a custom-designed 3D printed in vivo stage (***Figure 7—figure supplement 1***). Throughout each experiment, vital signs (heartbeat, blood oxygen level, breathing rhythm) were constantly monitored and recorded (breathing). Moreover, we routinely checked unobstructed blood flow within testicular vessels during experiments. To avoid movement artifacts, the tunica was glued to two holding strings using Histoacryl tissue adhesive. After surgery, anesthesia was maintained by constant isoflurane inhalation (1–1.5% in air). Time-lapse intravital imaging was performed using a Leica TCS SP8 MP microscope. For incident light illumination/reflected light widefield recordings (5–10 Hz), we used N PLAN 5x/0.12 or HC APO L10x/0.30 W DLS objectives with large fields of view. Multiphoton time-lapse images were acquired at ~2 Hz frame rates using external hybrid detectors and the HCX IRAPO L25x/0.95 W objective at 930 nm excitation wavelength. Individual recording duration varied between 13 and 30 min (mean = 25 min). For in vivo stimulation experiments, we used a Picospritzer III (Parker Hannifin, Pine Brook, NJ) to puff nanoliter volumes of control saline (**S_1**; containing Alexa

Fluor 555 (4 µM)) or stimulus solution (S_1; containing Alexa Fluor 555 (4 µM) and ATP (1 mM)), respectively, from beveled glass micropipettes onto the surface of seminiferous tubules.

Data analysis

All data were obtained from independent experiments performed on at least three days. Individual numbers of cells/tubules/experiments (n) are denoted in the respective figures and/or legends. If not stated otherwise, results are presented as means ± SEM. Statistical analyses were performed using paired or unpaired *t*-tests, one-way ANOVA with Tukey's HSD *post hoc* test or the Fisher Exact test (as dictated by data distribution and experimental design). Tests and corresponding *p*-values that report statistical significance ($\leq$0.05) are individually specified in the legends. Data were analyzed offline using FitMaster 2.9 (HEKA Elektronik), IGOR Pro 8 (RRID:SCR_000325; WaveMetrics), Excel 2016 (Microsoft, Seattle, WA), and Leica LAS X (RRID:SCR_013673; Leica Microsystems) software. Dose-response curves were fitted by the Hill-equation. Time-lapse live-cell imaging data displaying both Ca^{2+} signals and tubular contractions were analyzed using custom-written code in MATLAB (RRID:SCR_001622; The MathWorks, Natick, MA).

For quantitative image analysis, images from both reflected light and fluorescence time-lapse recordings were registered to their respective first image frame at time point t_0, using the registration algorithm from ***Liu et al., 2015*** (implementation in ***Evangelidis, 2013***), resulting in stabilized recordings without movement. For fura-2 fluorescence recordings, we first performed a single registration on the combined image (f_{340} + f_{380}) and then applied the displacement vector field, computed by the registration algorithm, to both images (f_{340} and f_{380}) separately. ROIs were defined manually at t_0 and superimposed onto all subsequent images of the stabilized recording. At each time point t_i, the fluorescence signal F was computed as the mean f_{340}/f_{380} ratio of all pixels within a given ROI. When measuring Ca^{2+}-dependent changes in GCaMP6f intensity, the fluorescence signal F was normalized with respect to a baseline before stimulation, computing the intensity change for the i^{th} time point as $\frac{F_i - F_{\text{baseline}}}{F_i}$. For clarity, linear baseline shifts were corrected in some example traces.

Seminiferous tubule contractions and transport of luminal content were visualized by reflected light microscopy of acute slices or whole-mount macroscopic tubule imaging, respectively. Data from both types of time-lapse recordings were analyzed and quantified as either flow strength or flow change (see below). For each frame at a given time point t_i, the registration algorithm computed a flow or displacement vector field $V_i = \begin{pmatrix} \mathbf{v}_{1,1} & \cdots & \mathbf{v}_{1,n} \\ \vdots & \ddots & \vdots \\ \mathbf{v}_{m,1} & \cdots & \mathbf{v}_{m,n} \end{pmatrix}$, where $\mathbf{v}_{1,1} = (x, y)$ is a vector indicating strength and direction of the displacement of pixel $(1, 1)$ between time points t_0 and t_i. The average norm $|V_i| = \frac{1}{mn}\sum_{p,q}\|\mathbf{v}_{p,q}\|$ is a measure for the effort that is necessary to register the image at t_0 to the image at t_i. The flow field strength quantified by this measure is interpreted as the amount of visible changes that, dependent on the experiment, result from tubule contraction and / or luminal content movement. For analysis of contractions in acute seminiferous tubule slices (Figures 3, 4, 7), we quantified the *flow strength* s_i within an ROI as the average norm $|V_i|$ computed only for the $\mathbf{v}_{p,q}$ corresponding to pixels within the ROI defined at t_0. For whole-mount macroscopic imaging of luminal content movement in intact tubule segments (***Figure 5***), we quantified the *flow change* $c_i = s_i - s_{i-1}$ as the change of flow strength between two consecutive time points / frames. Here, s_i values were preprocessed by smoothing with a moving average filter. Results are reported as the AUC, that is, the area under the c_i curve.

For analysis of in vivo data, we employed a custom set of ImageJ macros utilizing build-in functions of Fiji-ImageJ (RRID:SCR_002285) (***Rueden et al., 2017***; ***Schindelin et al., 2012***). Widefield imaging data was first corrected for brightness fluctuation caused by a 50 Hz AC power supply. Here, we used the *bleach correction* plugin in histogram matching mode (***Miura et al., 2014***). Next, we applied Gaussian filter functions (*GausBlur* (five px radius) and *Gaussian Blur3D* (x = 0, y = 0, z = 5)). We calculated flow change via the *Gaussian Window MSE* function (sigma = 1; max distance = 3). Tubule selection used the polyline tool (line width adjusted to tubule diameter). Selected tubules ranged from 200 µm to 3.4 mm length. Next, flow fields of individual tubules were straightened. Average movement intensity was calculated from transversal line profiles (perpendicular to the

straightened longitudinal axis of each tubule) and plotted as kymographs (space-time plots) to measure movement progression speed from linear regressions.

Multiphoton time-lapse imaging data was recorded in dual-channel mode, with (i) a target channel recording GCaMP6f fluorescence and some background signal (525\50 nm), and (ii) a background channel mainly recording autofluorescence (585\40 nm), allowing for background correction of the GCaMP6f signal using a dye separation routine. Slow constant movement in both channels was registered and removed to correct for steady drift. After Gaussian filtering (*GausBlur* (five px radius); *Gaussian Blur3D* (x = 0, y = 0, z = 5)), flow fields were calculated from the background signal. Again, flow change was calculated via the *Gaussian Window MSE* function (sigma = 1; max distance = 3). Time-lapse epifluorescence in vivo recordings were processed to isolate transient fluorescence signals from static background noise using custom ImageJ code with Fiji's build-in functions (see **Data and materials availability**).

Acknowledgements

We thank Corinna Engelhardt, Jessica von Bongartz, and Stefanie Kurth (RWTH Aachen University) for assistance, Andreas Meinhardt and Jörg Klug (Justus-Liebig-University Giessen) for kindly providing detailed information about the mouse TPC cell culture protocol, Andrea Mietens and Ralf Middendorff (Justus-Liebig-University Giessen) for comments and suggestions, J Ullrich Schwarzer (Andrology-Center, Munich) and Frank-Michael Köhn (Andrologicum, Munich) for providing human samples, and all members of the Spehr laboratory for discussions.

Additional information

Funding

Funder	Grant reference number	Author
Deutsche Forschungsgemeinschaft	368482240/GRK2416	Marc Spehr Nadine Mundt
Deutsche Forschungsgemeinschaft	412888997	David Fleck
Deutsche Forschungsgemeinschaft	245169951	Marc Spehr Artur Mayerhofer
Volkswagen Foundation	I/83533	Marc Spehr
Deutsche Forschungsgemeinschaft	233509121	Dorit Merhof

The funders had no role in study design, data collection and interpretation, or the decision to submit the work for publication.

Author contributions

David Fleck, Conceptualization, Formal analysis, Funding acquisition, Validation, Investigation, Visualization, Methodology, Writing - review and editing; Lina Kenzler, Nadine Mundt, Formal analysis, Validation, Investigation, Visualization, Writing - review and editing; Martin Strauch, Software, Validation, Methodology, Writing - review and editing; Naofumi Uesaka, Investigation, Methodology, Writing - review and editing; Robert Moosmann, Formal analysis, Investigation; Felicitas Bruentgens, Formal analysis, Investigation, Methodology, Writing - review and editing; Annika Missel, Formal analysis, Investigation, Writing - review and editing; Artur Mayerhofer, Supervision, Funding acquisition, Methodology, Writing - review and editing; Dorit Merhof, Supervision, Methodology, Writing - review and editing; Jennifer Spehr, Conceptualization, Formal analysis, Supervision, Validation, Visualization, Methodology, Writing - review and editing; Marc Spehr, Conceptualization, Resources, Data curation, Supervision, Funding acquisition, Visualization, Methodology, Writing - original draft, Project administration

Author ORCIDs

David Fleck https://orcid.org/0000-0002-6692-2388
Lina Kenzler https://orcid.org/0000-0002-6738-2221
Nadine Mundt https://orcid.org/0000-0003-3370-2933
Robert Moosmann https://orcid.org/0000-0003-2321-7213
Felicitas Bruentgens https://orcid.org/0000-0001-7754-1313
Artur Mayerhofer https://orcid.org/0000-0002-9388-4639
Dorit Merhof https://orcid.org/0000-0002-1672-2185
Marc Spehr https://orcid.org/0000-0001-6616-4196

Ethics

Animal experimentation: Mice were maintained and sacrificed according to European Union legislation (Directive 2010/63/EU) and recommendations by the Federation of European Laboratory Animal Science Associations (FELASA). All experimental procedures were approved by the State Agency for Nature, Environment and Consumer Protection (LANUV; protocol number / AZ 84-02.04.2016. A371).

Decision letter and Author response

Decision letter https://doi.org/10.7554/eLife.62885.sa1
Author response https://doi.org/10.7554/eLife.62885.sa2

Additional files

Supplementary files

- Transparent reporting form

Data availability

All data is available in the main text or the supplementary materials. Previously unpublished source code for data analysis (quantification of tubular contractions, flow strength/change, Ca2+ signals) is available at: https://github.com/rwth-lfb/Fleck_Kenzler_et_al Copy archived at https://archive.softwareheritage.org/swh:1:rev:88c8792860ddf09fd7da969fef6bf86c40441135/ and https://doi.org/10.5281/zenodo.4280752.

The following dataset was generated:

Author(s)	Year	Dataset title	Dataset URL	Database and Identifier
Fleck D	2020	Transient Signal Enhancer for Fiji ImageJ	https://doi.org/10.5281/zenodo.4280752	Zenodo, 10.5281/zenodo.4280752

References

Ailenberg M, Tung PS, Fritz IB. 1990. Transforming growth factor-beta elicits shape changes and increases contractility of testicular peritubular cells. *Biology of Reproduction* **42**:499–509. DOI: https://doi.org/10.1095/biolreprod42.3.499, PMID: 2160295

Albrecht M, Rämsch R, Köhn FM, Schwarzer JU, Mayerhofer A. 2006. Isolation and cultivation of human testicular peritubular cells: a new model for the investigation of fibrotic processes in the human testis and male infertility. *The Journal of Clinical Endocrinology & Metabolism* **91**:1956–1960. DOI: https://doi.org/10.1210/jc.2005-2169, PMID: 16478819

Alexander SPH, Christopoulos A, Davenport AP, Kelly E, Mathie A, Peters JA, Veale EL, Armstrong JF, Faccenda E, Harding SD, Pawson AJ, Sharman JL, Southan C, Davies JA, CGTP Collaborators. 2019a. The concise guide to pharmacology 2019/20: g protein-coupled receptors. *British Journal of Pharmacology* **176**:S21–S141. DOI: https://doi.org/10.1111/bph.14748, PMID: 31710717

Alexander SPH, Mathie A, Peters JA, Veale EL, Striessnig J, Kelly E, Armstrong JF, Faccenda E, Harding SD, Pawson AJ, Sharman JL, Southan C, Davies JA, CGTP Collaborators. 2019b. The concise guide to pharmacology 2019/20: ion channels. *British Journal of Pharmacology* **176**:S142–S228. DOI: https://doi.org/10.1111/bph.14749, PMID: 31710715

Antonio LS, Costa RR, Gomes MD, Varanda WA. 2009. Mouse Leydig cells express multiple P2X receptor subunits. *Purinergic Signalling* **5**:277–287. DOI: https://doi.org/10.1007/s11302-008-9128-9
Banks FC, Knight GE, Calvert RC, Turmaine M, Thompson CS, Mikhailidis DP, Morgan RJ, Burnstock G. 2006. Smooth muscle and purinergic contraction of the human, rabbit, rat, and mouse testicular capsule. *Biology of Reproduction* **74**:473–480. DOI: https://doi.org/10.1095/biolreprod.105.044602, PMID: 16280417
Bao L, Locovei S, Dahl G. 2004. Pannexin membrane channels are mechanosensitive conduits for ATP. *FEBS Letters* **572**:65–68. DOI: https://doi.org/10.1016/j.febslet.2004.07.009, PMID: 15304325
Barnard EA, Burnstock G, Webb TE. 1994. G protein-coupled receptors for ATP and other nucleotides: a new receptor family. *Trends in Pharmacological Sciences* **15**:67–70. DOI: https://doi.org/10.1016/0165-6147(94)90280-1, PMID: 8184488
Barone F, Genazzani AA, Conti A, Churchill GC, Palombi F, Ziparo E, Sorrentino V, Galione A, Filippini A. 2002. A pivotal role for cADPR-mediated $^{Ca2+}$ signaling: regulation of endothelin-induced contraction in peritubular smooth muscle cells. *The FASEB Journal* **16**:697–705. DOI: https://doi.org/10.1096/fj.01-0749com, PMID: 11978734
Barry PH. 1994. JPCalc, a software package for calculating liquid junction potential corrections in patch-clamp, intracellular, epithelial and bilayer measurements and for correcting junction potential measurements. *Journal of Neuroscience Methods* **51**:107–116. DOI: https://doi.org/10.1016/0165-0270(94)90031-0
Bean BP. 1992. Pharmacology and electrophysiology of ATP-activated ion channels. *Trends in Pharmacological Sciences* **13**:87–90. DOI: https://doi.org/10.1016/0165-6147(92)90032-2
Bean BP, Friel DD. 1990. ATP-activated channels in excitable cells. *Ion Channels* **2**:169–203. DOI: https://doi.org/10.1007/978-1-4615-7305-0_5, PMID: 1715204
Bell PD, Lapointe J-Y, Sabirov R, Hayashi S, Peti-Peterdi J, Manabe K-i, Kovacs G, Okada Y. 2003. Macula densa cell signaling involves ATP release through a maxi anion channel. *PNAS* **100**:4322–4327. DOI: https://doi.org/10.1073/pnas.0736323100
Berridge MJ. 2008. Smooth muscle cell calcium activation mechanisms. *The Journal of Physiology* **586**:5047–5061. DOI: https://doi.org/10.1113/jphysiol.2008.160440
Bodin P, Burnstock G. 2001. Evidence that release of adenosine triphosphate from endothelial cells during increased shear stress is vesicular. *Journal of Cardiovascular Pharmacology* **38**:900–908. DOI: https://doi.org/10.1097/00005344-200112000-00012, PMID: 11707694
Bootman MD, Rietdorf K, Collins T, Walker S, Sanderson M. 2013. Ca2+-sensitive fluorescent dyes and intracellular Ca2+ imaging. *Cold Spring Harbor Protocols* **2013**:pdb.top066050.066099. DOI: https://doi.org/10.1101/pdb.top066050, PMID: 23378644
Burnstock G. 1990. Overview purinergic mechanisms. *Annals of the New York Academy of Sciences* **603**:1–17. DOI: https://doi.org/10.1111/j.1749-6632.1990.tb37657.x, PMID: 1981306
Burnstock G. 2014. Purinergic signalling: from discovery to current developments. *Experimental Physiology* **99**:16–34. DOI: https://doi.org/10.1113/expphysiol.2013.071951
Button B, Okada SF, Frederick CB, Thelin WR, Boucher RC. 2013. Mechanosensitive ATP release maintains proper mucus hydration of airways. *Science Signaling* **6**:ra46. DOI: https://doi.org/10.1126/scisignal.2003755, PMID: 23757023
Carneiro I, Timóteo MA, Silva I, Vieira C, Baldaia C, Ferreirinha F, Silva-Ramos M, Correia-de-Sá P. 2014. Activation of P2Y6 receptors increases the voiding frequency in anaesthetized rats by releasing ATP from the bladder urothelium. *British Journal of Pharmacology* **171**:3404–3419. DOI: https://doi.org/10.1111/bph.12711, PMID: 24697602
Cheng CY, Mruk DD. 2010. A local autocrine axis in the testes that regulates spermatogenesis. *Nature Reviews Endocrinology* **6**:380–395. DOI: https://doi.org/10.1038/nrendo.2010.71
Chiarini-Garcia H, Russell LD. 2001. High-resolution light microscopic characterization of mouse spermatogonia. *Biology of Reproduction* **65**:1170–1178. DOI: https://doi.org/10.1095/biolreprod65.4.1170, PMID: 11566740
Chung K, Wallace J, Kim S-Y, Kalyanasundaram S, Andalman AS, Davidson TJ, Mirzabekov JJ, Zalocusky KA, Mattis J, Denisin AK, Pak S, Bernstein H, Ramakrishnan C, Grosenick L, Gradinaru V, Deisseroth K. 2013. Structural and molecular interrogation of intact biological systems. *Nature* **497**:332–337. DOI: https://doi.org/10.1038/nature12107
Chung K, Deisseroth K. 2013. CLARITY for mapping the nervous system. *Nature Methods* **10**:508–513. DOI: https://doi.org/10.1038/nmeth.2481, PMID: 23722210
Clermont Y. 1958. Contractile elements in the limiting membrane of the seminiferous tubules of the rat. *Experimental Cell Research* **15**:438–440. DOI: https://doi.org/10.1016/0014-4827(58)90052-1
Coddou C, Yan Z, Obsil T, Huidobro-Toro JP, Stojilkovic SS. 2011. Activation and Regulation of Purinergic P2X Receptor Channels. *Pharmacological Reviews* **63**:641–683. DOI: https://doi.org/10.1124/pr.110.003129
Cotrina ML, Lin JH, Alves-Rodrigues A, Liu S, Li J, Azmi-Ghadimi H, Kang J, Naus CC, Nedergaard M. 1998. Connexins regulate calcium signaling by controlling ATP release. *PNAS* **95**:15735–15740. DOI: https://doi.org/10.1073/pnas.95.26.15735, PMID: 9861039
Cross BA. 1958. Hypothalamic Influences on Sperm Transport in the Male and Female Genital Tract. In: Lloyd C. W (Ed). *Recent Progress in the Endocrinology of Reproduction*. Academic Press. p. 167–176.
Donnelly-Roberts DL, Namovic MT, Han P, Jarvis MF. 2009. Mammalian P2X7 receptor pharmacology: comparison of recombinant mouse, rat and human P2X7 receptors. *British Journal of Pharmacology* **157**:1203–1214. DOI: https://doi.org/10.1111/j.1476-5381.2009.00233.x, PMID: 19558545
Elliott MR, Chekeni FB, Trampont PC, Lazarowski ER, Kadl A, Walk SF, Park D, Woodson RI, Ostankovich M, Sharma P, Lysiak JJ, Harden TK, Leitinger N, Ravichandran KS. 2009. Nucleotides released by apoptotic cells

act as a find-me signal to promote phagocytic clearance. *Nature* **461**:282–286. DOI: https://doi.org/10.1038/nature08296, PMID: 19741708

Ellis LC, Buhrley LE, Hargrove JL. 1978. Species differences in contractility of seminiferous tubules and Tunica albuginea as related to sperm transport through the testis. *Archives of Andrology* **1**:139–146. DOI: https://doi.org/10.3109/01485017808988330, PMID: 736669

Ellis LC, Groesbeck MD, Farr CH, Tesi RJ. 1981. Contractility of seminiferous tubules as related to sperm transport in the male. *Archives of Andrology* **6**:283–294. DOI: https://doi.org/10.3109/01485018108987539, PMID: 6113819

Evangelidis G. 2013. *Iat: a matlab toolbox for image alignment*. https://sites.google.com/site/imagealignment/download

Evans RJ, Lewis C, Buell G, Valera S, North RA, Surprenant A. 1995. Pharmacological characterization of heterologously expressed ATP-gated cation channels (P2x purinoceptors). *Molecular Pharmacology* **48**:178–183. PMID: 7544432

Fernández D, Bertoldi MV, Gómez L, Morales A, Callegari E, Lopez LA. 2008. Identification and Characterization of Myosin from Rat Testicular Peritubular Myoid Cells1. *Biology of Reproduction* **79**:1210–1218. DOI: https://doi.org/10.1095/biolreprod.107.066472

Filippini A, Tripiciano A, Palombi F, Teti A, Paniccia R, Stefanini M, Ziparo E. 1993. Rat testicular myoid cells respond to endothelin: characterization of binding and signal transduction pathway. *Endocrinology* **133**:1789–1796. DOI: https://doi.org/10.1210/endo.133.4.8404621

Filippini A, Riccioli A, De Cesaris P, Paniccia R, Teti A, Stefanini M, Conti M, Ziparo E. 1994. Activation of inositol phospholipid turnover and calcium signaling in rat sertoli cells by P2-purinergic receptors: modulation of follicle-stimulating hormone responses. *Endocrinology* **134**:1537–1545. DOI: https://doi.org/10.1210/endo.134.3.8119196, PMID: 8119196

Fitz JG. 2007. Regulation of cellular ATP release. *Transactions of the American Clinical and Climatological Association* **118**:199–208. PMID: 18528503

Fleck D, Mundt N, Bruentgens F, Geilenkirchen P, Machado PA, Veitinger T, Veitinger S, Lipartowski SM, Engelhardt CH, Oldiges M, Spehr J, Spehr M. 2016. Distinct purinergic signaling pathways in prepubescent mouse spermatogonia. *Journal of General Physiology* **148**:253–271. DOI: https://doi.org/10.1085/jgp.201611636

Fleck D. 2021. Fleck_Kenzler_et_al. *Software Heritage*. swh:1:rev:88c8792860ddf09fd7da969fef6bf86c40441135. https://archive.softwareheritage.org/swh:1:dir:f28da11872de51e80b8926ab879ef0f7d6d7fe2d;origin=https://github.com/rwth-lfb/Fleck_Kenzler_et_al;visit=swh:1:snp:11d407d1f92ff4e0de77fb20e3798ef90c5fd1b5;anchor=swh:1:rev:88c8792860ddf09fd7da969fef6bf86c40441135/

Foresta C, Rossato M, Bordon P, Di Virgilio F. 1995. Extracellular ATP activates different signalling pathways in rat Sertoli cells. *Biochemical Journal* **311**:269–274. DOI: https://doi.org/10.1042/bj3110269

Foresta C, Rossato M, Nogara A, Gottardello F, Bordon P, Di Virgilio F. 1996. Role of P2-purinergic receptors in rat Leydig cell steroidogenesis. *Biochemical Journal* **320**:499–504. DOI: https://doi.org/10.1042/bj3200499

Gelain DP, de Souza LF, Bernard EA. 2003. Extracellular purines from cells of seminiferous tubules. *Molecular and Cellular Biochemistry* **245**:1–9. DOI: https://doi.org/10.1023/A:1022857608849

Gelain DP, Casali EA, de Oliveira RB, de Souza LF, Barreto F, Dal-Pizzol F, Moreira JC. 2005. Effects of follicle-stimulating hormone and vitamin A upon purinergic secretion by rat sertoli cells. *Molecular and Cellular Biochemistry* **278**:185–194. DOI: https://doi.org/10.1007/s11010-005-7500-4, PMID: 16180104

Glass R, Bardini M, Robson T, Burnstock G. 2001. Expression of nucleotide P2X receptor subtypes during spermatogenesis in the adult rat testis. *Cells Tissues Organs* **169**:377–387. DOI: https://doi.org/10.1159/000047905, PMID: 11490117

Gretenkord S, Kostka JK, Hartung H, Watznauer K, Fleck D, Minier-Toribio A, Spehr M, Hanganu-Opatz IL. 2019. Coordinated electrical activity in the olfactory bulb gates the oscillatory entrainment of entorhinal networks in neonatal mice. *PLOS Biology* **17**:e2006994. DOI: https://doi.org/10.1371/journal.pbio.2006994

Hargrove JL, Seeley RR, Ellis LC. 1975. Rabbit testicular contractions: bimodal interaction of prostaglandin E1 with other agonists. *American Journal of Physiology-Legacy Content* **228**:810–814. DOI: https://doi.org/10.1152/ajplegacy.1975.228.3.810

Harris GC, Nicholson HD. 1998. Stage-related differences in rat seminiferous tubule contractility in vitro and their response to oxytocin. *Journal of Endocrinology* **157**:251–257. DOI: https://doi.org/10.1677/joe.0.1570251

Heindel JJ, Treinen KA. 1989. Physiology of the male reproductive system: endocrine, paracrine and autocrine regulation. *Toxicologic Pathology* **17**:411–445. DOI: https://doi.org/10.1177/019262338901700219, PMID: 2675292

Henriquez M, Fonseca M, Perez-Zoghbi JF. 2018. Purinergic receptor stimulation induces calcium oscillations and smooth muscle contraction in small pulmonary veins. *The Journal of Physiology* **596**:2491–2506. DOI: https://doi.org/10.1113/JP274731

Hermo L, Pelletier R-M, Cyr DG, Smith CE. 2010. Surfing the wave, cycle, life history, and genes/proteins expressed by testicular germ cells Part 1: Background to spermatogenesis, spermatogonia, and spermatocytes. *Microscopy Research and Technique* **73**:241–278. DOI: https://doi.org/10.1002/jemt.20783

Hess RA, De Franca LR. 2008. Spermatogenesis and cycle of the seminiferous epithelium. In: Cheng C. Y (Ed). *Molecular Mechanisms in Spermatogenesis*. Springer p. 1–15.

Holdcraft RW, Braun RE. 2004. Androgen receptor function is required in Sertoli cells for the terminal differentiation of haploid spermatids. *Development* **131**:459–467. DOI: https://doi.org/10.1242/dev.00957

Hovatta O. 1972. Contractility and structure of adult rat seminiferous tubules in organ culture. *Zeitschrift FUR Zellforschung Und Mikroskopische Anatomie* **130**:171–179. DOI: https://doi.org/10.1007/BF00306955
Huckins C. 1978. The morphology and kinetics of spermatogonial degeneration in normal adult rats: An analysis using a simplified classification of the germinal epithelium. *The Anatomical Record* **190**:905–926. DOI: https://doi.org/10.1002/ar.1091900410
Jacobson KA, Paoletta S, Katritch V, Wu B, Gao ZG, Zhao Q, Stevens RC, Kiselev E. 2015. Nucleotides acting at P2Y receptors: connecting structure and function. *Molecular Pharmacology* **88**:220–230. DOI: https://doi.org/10.1124/mol.114.095711, PMID: 25837834
Khakh BS, Proctor WR, Dunwiddie TV, Labarca C, Lester HA. 1999. Allosteric control of gating and kinetics at P2X(4) receptor channels. *The Journal of Neuroscience* **19**:7289–7299. PMID: 10460235
Khakh BS. 2001. Molecular physiology of p2x receptors and atp signalling at synapses. *Nature Reviews Neuroscience* **2**:165–174. DOI: https://doi.org/10.1038/35058521
Khakh BS, North RA. 2012. Neuromodulation by extracellular ATP and P2X receptors in the CNS. *Neuron* **76**:51–69. DOI: https://doi.org/10.1016/j.neuron.2012.09.024, PMID: 23040806
Kolasa A, Misiakiewicz K, Marchlewicz M, Wiszniewska B. 2012. The generation of spermatogonial stem cells and spermatogonia in mammals. *Reproductive Biology* **12**:5–23. DOI: https://doi.org/10.1016/S1642-431X(12)60074-6, PMID: 22472937
Lalevée N, Rogier C, Becq F, Joffre M. 1999. Acute effects of Adenosine triphosphates, cyclic 3',5'-adenosine Monophosphates, and follicle-stimulating hormone on cytosolic calcium level in cultured immature rat ssertoli cells. *Biology of Reproduction* **61**:343–352. DOI: https://doi.org/10.1095/biolreprod61.2.343, PMID: 10411510
Lamont C, Vainorius E, Wier WG. 2003. Purinergic and adrenergic Ca2+ transients during neurogenic contractions of rat mesenteric small arteries. *The Journal of Physiology* **549**:801–808. DOI: https://doi.org/10.1113/jphysiol.2003.043380, PMID: 12740429
Lamont C, Vial C, Evans RJ, Wier WG. 2006. P2X1 receptors mediate sympathetic postjunctional ca2+ transients in mesenteric small arteries. *American Journal of Physiology. Heart and Circulatory Physiology* **291**:H3106–H3113. DOI: https://doi.org/10.1152/ajpheart.00466.2006
Liévano A, Santi CM, Serrano CJ, Treviño CL, Bellvé AR, Hernández-Cruz A, Darszon A. 1996. T-type Ca2+ channels and alpha1E expression in spermatogenic cells, and their possible relevance to the sperm acrosome reaction. *FEBS Letters* **388**:150–154. DOI: https://doi.org/10.1016/0014-5793(96)00515-7, PMID: 8690075
Liu C, Yuen J, Torralba A. 2015. Sift flow: dense correspondence across scenes and its applications. In: Hassner T (Ed). *Dense Image Correspondences for Computer Vision*. Springer. p. 15–49. DOI: https://doi.org/10.1007/978-3-319-23048-1_2
Lohman AW, Billaud M, Isakson BE. 2012. Mechanisms of ATP release and signalling in the blood vessel wall. *Cardiovascular Research* **95**:269–280. DOI: https://doi.org/10.1093/cvr/cvs187, PMID: 22678409
Losinno AD, Morales A, Fernández D, Lopez LA. 2012. Peritubular myoid cells from rat seminiferous tubules contain actin and myosin filaments distributed in two independent Layers1. *Biology of Reproduction* **86**:1–8. DOI: https://doi.org/10.1095/biolreprod.111.095158
Losinno AD, Sorrivas V, Ezquer M, Ezquer F, López LA, Morales A. 2016. Changes of myoid and endothelial cells in the peritubular wall during contraction of the seminiferous tubule. *Cell and Tissue Research* **365**:425–435. DOI: https://doi.org/10.1007/s00441-016-2386-x
Madisen L, Zwingman TA, Sunkin SM, Oh SW, Zariwala HA, Gu H, Ng LL, Palmiter RD, Hawrylycz MJ, Jones AR, Lein ES, Zeng H. 2010. A robust and high-throughput Cre reporting and characterization system for the whole mouse brain. *Nature Neuroscience* **13**:133–140. DOI: https://doi.org/10.1038/nn.2467
Madisen L, Garner AR, Shimaoka D, Chuong AS, Klapoetke NC, Li L, van der Bourg A, Niino Y, Egolf L, Monetti C, Gu H, Mills M, Cheng A, Tasic B, Nguyen TN, Sunkin SM, Benucci A, Nagy A, Miyawaki A, Helmchen F, et al. 2015. Transgenic mice for intersectional targeting of neural sensors and effectors with high specificity and performance. *Neuron* **85**:942–958. DOI: https://doi.org/10.1016/j.neuron.2015.02.022, PMID: 25741722
Mayerhofer A. 2013. Human testicular peritubular cells: more than meets the eye. *Reproduction* **145**:R107–R116. DOI: https://doi.org/10.1530/REP-12-0497, PMID: 23431272
Meroni SB, Canepa DF, Pellizzari EH, Schteingart HF, Cigorraga SB. 1998. Effects of purinergic agonists on aromatase and gamma-glutamyl transpeptidase activities and on transferrin secretion in cultured sertoli cells. *Journal of Endocrinology* **157**:275–283. DOI: https://doi.org/10.1677/joe.0.1570275
Miura K, Rueden C, Hiner M, Schindelin J, Rietdorf J. 2014. *ImageJ Plugin CorrectBleach V2.0.2*.
Miyake K, Yamamoto M, Narita H, Hashimoto J, Mitsuya H. 1986. Evidence for contractility of the human seminiferous tubule confirmed by its response to noradrenaline and acetylcholine. *Fertility and Sterility* **46**:734–737. DOI: https://doi.org/10.1016/S0015-0282(16)49663-9, PMID: 3758398
Mruk DD, Cheng CY. 2004. Sertoli-Sertoli and Sertoli-germ cell interactions and their significance in germ cell movement in the seminiferous epithelium during spermatogenesis. *Endocrine Reviews* **25**:747–806. DOI: https://doi.org/10.1210/er.2003-0022, PMID: 15466940
Müller CE, Baqi Y, Namasivayam V. 2020. Agonists and antagonists for purinergic receptors. In: Pelegrín P (Ed). *Purinergic Signaling: Methods and Protocols, Methods in Molecular Biology*. New York, NY: Springer Science +Business Media, LLC. p. 45–64.
Mulryan K, Gitterman DP, Lewis CJ, Vial C, Leckie BJ, Cobb AL, Brown JE, Conley EC, Buell G, Pritchard CA, Evans RJ. 2000. Reduced vas deferens contraction and male infertility in mice lacking P2X1 receptors. *Nature* **403**:86–89. DOI: https://doi.org/10.1038/47495, PMID: 10638758
Navarro B, Miki K, Clapham DE. 2011. ATP-activated P2X2 current in mouse spermatozoa. *PNAS* **108**:14342–14347. DOI: https://doi.org/10.1073/pnas.1111695108, PMID: 21831833

North RA. 2002. Molecular physiology of P2X receptors. *Physiological Reviews* **82**:1013–1067. DOI: https://doi.org/10.1152/physrev.00015.2002, PMID: 12270951

Oatley JM, Brinster RL. 2012. The germline stem cell niche unit in mammalian testes. *Physiological Reviews* **92**: 577–595. DOI: https://doi.org/10.1152/physrev.00025.2011, PMID: 22535892

Parvinen M. 1982. Regulation of the Seminiferous Epithelium*. *Endocrine Reviews* **3**:404–417. DOI: https://doi.org/10.1210/edrv-3-4-404

Pellegatti P, Falzoni S, Pinton P, Rizzuto R, Di Virgilio F. 2005. A novel recombinant plasma membrane-targeted luciferase reveals a new pathway for ATP secretion. *Molecular Biology of the Cell* **16**:3659–3665. DOI: https://doi.org/10.1091/mbc.e05-03-0222, PMID: 15944221

Pickering BT, Birkett SD, Guldenaar SE, Nicholson HD, Worley RT, Yavachev L. 1989. Oxytocin in the testis: what, where, and why? *Annals of the New York Academy of Sciences* **564**:198–209. DOI: https://doi.org/10.1111/j.1749-6632.1989.tb25898.x, PMID: 2549833

Poletto Chaves LA, Pontelli EP, Varanda WA. 2006. P2X receptors in mouse leydig cells. *American Journal of Physiology-Cell Physiology* **290**:C1009–C1017. DOI: https://doi.org/10.1152/ajpcell.00506.2005, PMID: 16291815

Praetorius HA, Leipziger J. 2009. ATP release from non-excitable cells. *Purinergic Signalling* **5**:433–446. DOI: https://doi.org/10.1007/s11302-009-9146-2

Print CG, Loveland KL. 2000. Germ cell suicide: new insights into apoptosis during spermatogenesis. *BioEssays* **22**:423–430. DOI: https://doi.org/10.1002/(SICI)1521-1878(200005)22:5<423::AID-BIES4>3.0.CO;2-0

Romano F, Tripiciano A, Muciaccia B, De Cesaris P, Ziparo E, Palombi F, Filippini A. 2005. The contractile phenotype of peritubular smooth muscle cells is locally controlled: possible implications in male fertility. *Contraception* **72**:294–297. DOI: https://doi.org/10.1016/j.contraception.2005.03.009

Roosen-Runge EC. 1951. Motions of the seminiferous tubules of rat and dog. *The Anatomical Record* **109**:413.

Ross MH. 1967. The fine structure and development of the peritubular contractile cell component in the seminiferous tubules of the mouse. *American Journal of Anatomy* **121**:523–557. DOI: https://doi.org/10.1002/aja.1001210307

Rossato M, Merico M, Bettella A, Bordon P, Foresta C. 2001. Extracellular ATP stimulates estradiol secretion in rat Sertoli cells in vitro: modulation by external sodium. *Molecular and Cellular Endocrinology* **178**:181–187. DOI: https://doi.org/10.1016/S0303-7207(01)00426-9

Rossi F, Ferraresi A, Romagni P, Silvestroni L, Santiemma V. 2002. Angiotensin II stimulates contraction and growth of testicular peritubular myoid cells in vitro. *Endocrinology* **143**:3096–3104. DOI: https://doi.org/10.1210/endo.143.8.8955, PMID: 12130575

Rueden CT, Schindelin J, Hiner MC, DeZonia BE, Walter AE, Arena ET, Eliceiri KW. 2017. ImageJ2: ImageJ for the next generation of scientific image data. *BMC Bioinformatics* **18**:529. DOI: https://doi.org/10.1186/s12859-017-1934-z

Russell LD. 1990. *Histological and Histopathological Evaluation of the Testis*. Vienna: Cache River Press.

Santiemma V, Beligotti F, Magnanti M, Palleschi S, Silvestroni L, Fabbrini A. 1996. Endothelin-1 stimulates deoxyribonucleic acid synthesis and contraction in testicular peritubular myoid cells. *Biology of Reproduction* **54**:583–590. DOI: https://doi.org/10.1095/biolreprod54.3.583, PMID: 8835379

Santiemma V, Rossi F, Guerrini L, Markouizou A, Pasimeni G, Palleschi S, Fabbrini A. 2001. Adrenomedullin inhibits the contraction of cultured rat testicular peritubular myoid cells induced by endothelin-1. *Biology of Reproduction* **64**:619–624. DOI: https://doi.org/10.1095/biolreprod64.2.619, PMID: 11159365

Schindelin J, Arganda-Carreras I, Frise E, Kaynig V, Longair M, Pietzsch T, Preibisch S, Rueden C, Saalfeld S, Schmid B, Tinevez JY, White DJ, Hartenstein V, Eliceiri K, Tomancak P, Cardona A. 2012. Fiji: an open-source platform for biological-image analysis. *Nature Methods* **9**:676–682. DOI: https://doi.org/10.1038/nmeth.2019, PMID: 22743772

Schlatt S, Ehmcke J. 2014. Regulation of spermatogenesis: an evolutionary biologist's perspective. *Seminars in Cell & Developmental Biology* **29**:2–16. DOI: https://doi.org/10.1016/j.semcdb.2014.03.007, PMID: 24685618

Seidler NW, Jona I, Vegh M, Martonosi A. 1989. Cyclopiazonic acid is a specific inhibitor of the Ca2+-ATPase of sarcoplasmic reticulum. *The Journal of Biological Chemistry* **264**:17816–17823. PMID: 2530215

Setchell BP, Davies RV, Gladwell RT, Hinton BT, Main SJ, Pilsworth L, Waites GMH. 1978. The movement of fluid in the seminiferous tubules and rete testis. *Annales De Biologie Animale Biochimie Biophysique* **18**:623–632. DOI: https://doi.org/10.1051/rnd:19780336

Silberberg SD, Li M, Swartz KJ. 2007. Ivermectin interaction with transmembrane helices reveals widespread rearrangements during opening of P2X receptor channels. *Neuron* **54**:263–274. DOI: https://doi.org/10.1016/j.neuron.2007.03.020, PMID: 17442247

Smith L. 2011. Good planning and serendipity: exploiting the cre/Lox system in the testis. *Reproduction* **141**: 151–161. DOI: https://doi.org/10.1530/REP-10-0404, PMID: 21084571

Somlyo AP, Somlyo AV. 2003. Ca2+ sensitivity of smooth muscle and nonmuscle myosin II: modulated by G proteins, kinases, and myosin phosphatase. *Physiological Reviews* **83**:1325–1358. DOI: https://doi.org/10.1152/physrev.00023.2003, PMID: 14506307

Suadicani SO, Brosnan CF, Scemes E. 2006. P2X7 receptors mediate ATP release and amplification of astrocytic intercellular Ca2+ signaling. *Journal of Neuroscience* **26**:1378–1385. DOI: https://doi.org/10.1523/JNEUROSCI.3902-05.2006, PMID: 16452661

Suvanto O, Kormano M. 1970. The relation between in vitro contractions of the rat seminiferous tubules and the cyclic stage of the seminiferous epithelium. *Reproduction* **21**:227–232. DOI: https://doi.org/10.1530/jrf.0.0210227

Taruno A, Vingtdeux V, Ohmoto M, Ma Z, Dvoryanchikov G, Li A, Adrien L, Zhao H, Leung S, Abernethy M, Koppel J, Davies P, Civan MM, Chaudhari N, Matsumoto I, Hellekant G, Tordoff MG, Marambaud P, Foskett JK. 2013. CALHM1 ion channel mediates purinergic neurotransmission of sweet, bitter and umami tastes. *Nature* **495**:223–226. DOI: https://doi.org/10.1038/nature11906, PMID: 23467090

Tripiciano A, Filippini A, Giustiniani Q, Palombi F. 1996. Direct visualization of rat peritubular myoid cell contraction in response to endothelin. *Biology of Reproduction* **55**:25–31. DOI: https://doi.org/10.1095/biolreprod55.1.25, PMID: 8793054

Tripiciano A, Palombi F, Ziparo E, Filippini A. 1997. Dual control of seminiferous tubule contractility mediated by ETA and ETB endothelin receptor subtypes. *FASEB Journal: Official Publication of the Federation of American Societies for Experimental Biology* **11**:276–286. DOI: https://doi.org/10.1096/fasebj.11.4.9068617, PMID: 9068617

Tripiciano A, Peluso C, Morena AR, Palombi F, Stefanini M, Ziparo E, Yanagisawa M, Filippini A. 1999. Cyclic expression of Endothelin-converting Enzyme-1 mediates the functional regulation of seminiferous tubule contraction. *Journal of Cell Biology* **145**:1027–1038. DOI: https://doi.org/10.1083/jcb.145.5.1027

Tuna BG, Bakker EN, VanBavel E. 2012. Smooth muscle biomechanics and plasticity: relevance for vascular calibre and remodelling. *Basic & Clinical Pharmacology & Toxicology* **110**:35–41. DOI: https://doi.org/10.1111/j.1742-7843.2011.00794.x, PMID: 21902815

Tung PS, Fritz IB. 1987. Morphogenetic restructuring and formation of basement membranes by Sertoli cells and testis peritubular cells in co-culture: Inhibition of the morphogenetic cascade by cyclic AMP derivatives and by blocking direct cell contact. *Developmental Biology* **120**:139–153. DOI: https://doi.org/10.1016/0012-1606(87)90112-6

Tung PS, Fritz IB. 1989. Characterization of rat testicular peritubular myoid cells in culture: α-smooth muscle isoactin is a specific differentiation Marker1. *Biology of Reproduction* **42**:351–365. DOI: https://doi.org/10.1095/biolreprod42.2.351

Veitinger S, Veitinger T, Cainarca S, Fluegge D, Engelhardt CH, Lohmer S, Hatt H, Corazza S, Spehr J, Neuhaus EM, Spehr M. 2011. Purinergic signalling mobilizes mitochondrial Ca^{2+} in mouse sertoli cells. *The Journal of Physiology* **589**:5033–5055. DOI: https://doi.org/10.1113/jphysiol.2011.216309, PMID: 21859825

Walenta L, Fleck D, Fröhlich T, von Eysmondt H, Arnold GJ, Spehr J, Schwarzer JU, Köhn FM, Spehr M, Mayerhofer A. 2018. ATP-mediated events in peritubular cells contribute to sterile testicular inflammation. *Scientific Reports* **8**:1431. DOI: https://doi.org/10.1038/s41598-018-19624-3, PMID: 29362497

Welsh M, Saunders PTK, Atanassova N, Sharpe RM, Smith LB. 2009. Androgen action *via* testicular peritubular myoid cells is essential for male fertility. *The FASEB Journal* **23**:4218–4230. DOI: https://doi.org/10.1096/fj.09-138347

Welter H, Kampfer C, Lauf S, Feil R, Schwarzer JU, Köhn FM, Mayerhofer A. 2013. Partial loss of contractile marker proteins in human testicular peritubular cells in infertility patients. *Andrology* **1**:318–324. DOI: https://doi.org/10.1111/j.2047-2927.2012.00030.x, PMID: 23413143

Wirth A, Benyó Z, Lukasova M, Leutgeb B, Wettschureck N, Gorbey S, Orsy P, Horváth B, Maser-Gluth C, Greiner E, Lemmer B, Schütz G, Gutkind JS, Offermanns S. 2008. G12-G13-LARG-mediated signaling in vascular smooth muscle is required for salt-induced hypertension. *Nature Medicine* **14**:64–68. DOI: https://doi.org/10.1038/nm1666, PMID: 18084302

Worley RTS, Nicholson HD, Pickering BT. 1985. Testicular oxytocin: an initiator of seminiferous tubule movement? . Recent Progress in Cellular Endocrinology of the Testis.

Worley RT, Leendertz JA. 1988. A videomicrographic low-frequency movement analyser (VLMA) and perifusion chamber for recording and analysis of the physical behaviour of seminiferous tubules and other contractile tissues in vitro. *Journal of Microscopy* **151**:61–69. DOI: https://doi.org/10.1111/j.1365-2818.1988.tb04613.x, PMID: 3193459

Yamamoto M, Nagai T, Takaba H, Hashimoto J, Miyake K. 1989. In-vitro contractility of human seminiferous tubules in response to testosterone, dihydrotestosterone and estradiol. *Urological Research* **17**:265–268. DOI: https://doi.org/10.1007/BF00262608, PMID: 2773191

Zhang Z, Chen G, Zhou W, Song A, Xu T, Luo Q, Wang W, Gu XS, Duan S. 2007. Regulated ATP release from astrocytes through lysosome exocytosis. *Nature Cell Biology* **9**:945–953. DOI: https://doi.org/10.1038/ncb1620, PMID: 17618272

Zimmermann H, Zebisch M, Sträter N. 2012. Cellular function and molecular structure of ecto-nucleotidases. *Purinergic Signalling* **8**:437–502. DOI: https://doi.org/10.1007/s11302-012-9309-4, PMID: 22555564

2.1.1 Supplementary information of publication I

Figure 1—figure supplement 1

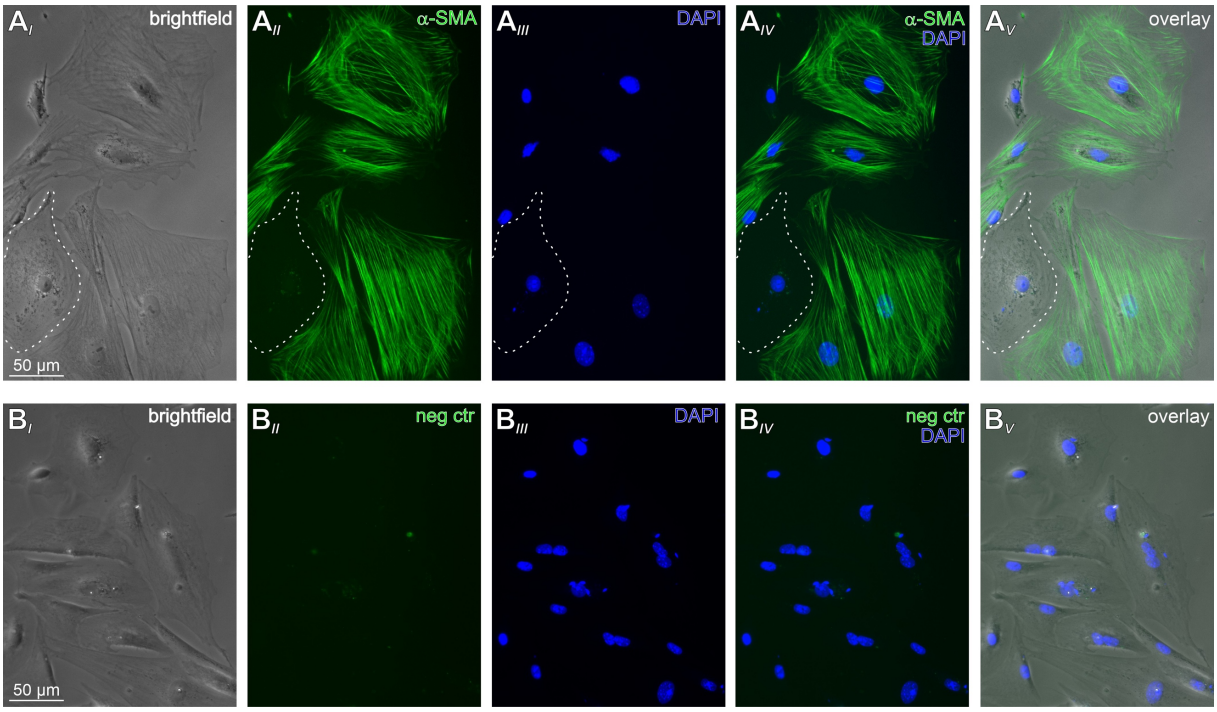

Mouse TPCs in primary culture.

(**A**) Representative phase contrast (**AI**) and epi-fluorescence images of TPCs *in vitro*. The vast majority of cultured cells are immunopositive for the TPC marker α-smooth muscle actin (α-SMA; green (**AII**)). The dotted white line delimits one of the few α-SMA-negative cells. Cell count was based on nuclear staining (DAPI, blue (**AIII**)). Merged images (**AIV-V**) allow categorization. (**B**) Corresponding control images taken after the primary α-SMA antibody was omitted.

Figure 4 – figure supplement 1

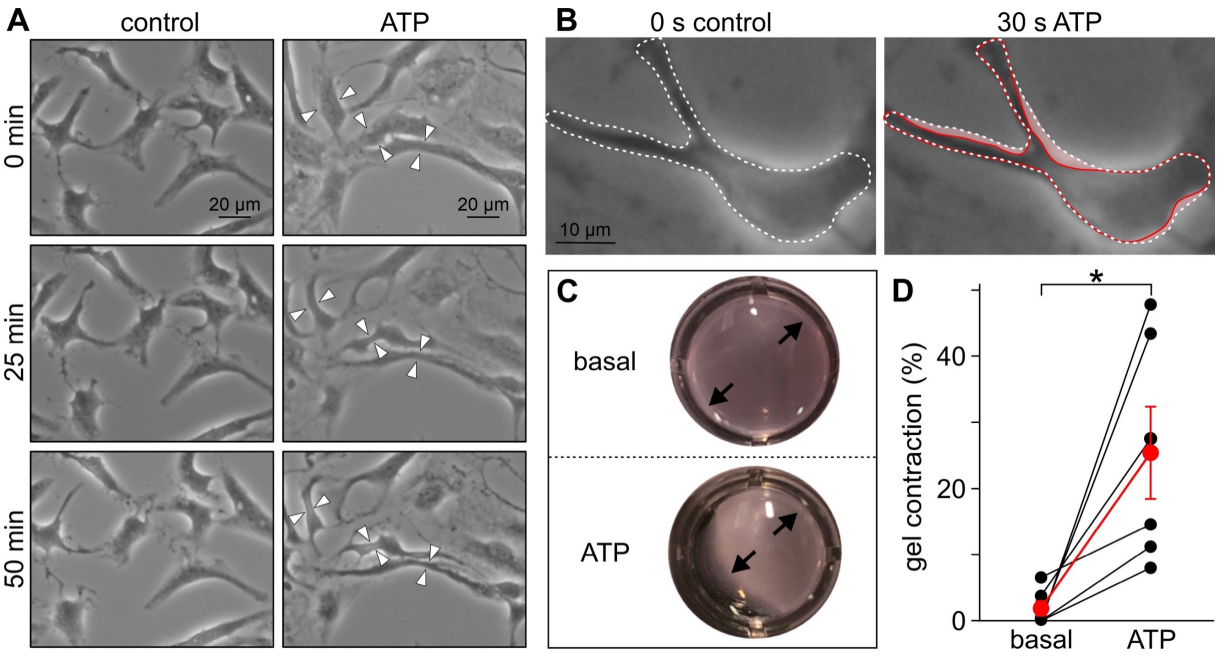

Purinergic stimulation mediates contractions in cultured human TPCs.

(**A**) Phase contrast micrographs of human TPC in primary culture (Walenta et al. 2018) that were monitored (50 min) under either control conditions (left) or during treatment with ATP (right; 1 mM). White arrow heads denote regions where a substantial reduction in cell surface area upon ATP exposure becomes readily apparent. (**B**) Some TPCs already 'shrink' within 30 s of treatment. Cell contour is indicated before (dashed white line) and during (solid red line) ATP exposure (red 'shadow' illustrates the putative contraction). (**C, D**) 24 hr collagen gel contraction assays (Tung and Fritz 1987; Ailenberg et al. 1990) allow quantification of human TPC contractility *in vitro*. As exemplified in (**C**) and quantified in (**D**) ATP (1 mM) incubation of human TPCs that are embedded in collagen lattices mediates a massive reduction in gel area (ATP; 25.5 ± 7.0%, mean ± SEM; human TPCs from n = 3 patients, measured in duplicates). By contrast, gel size remains essentially unchanged under control conditions (basal). Asterisk denotes statistical significance (p=0.003; unpaired *t*-test).

Figure 7—figure supplement 1

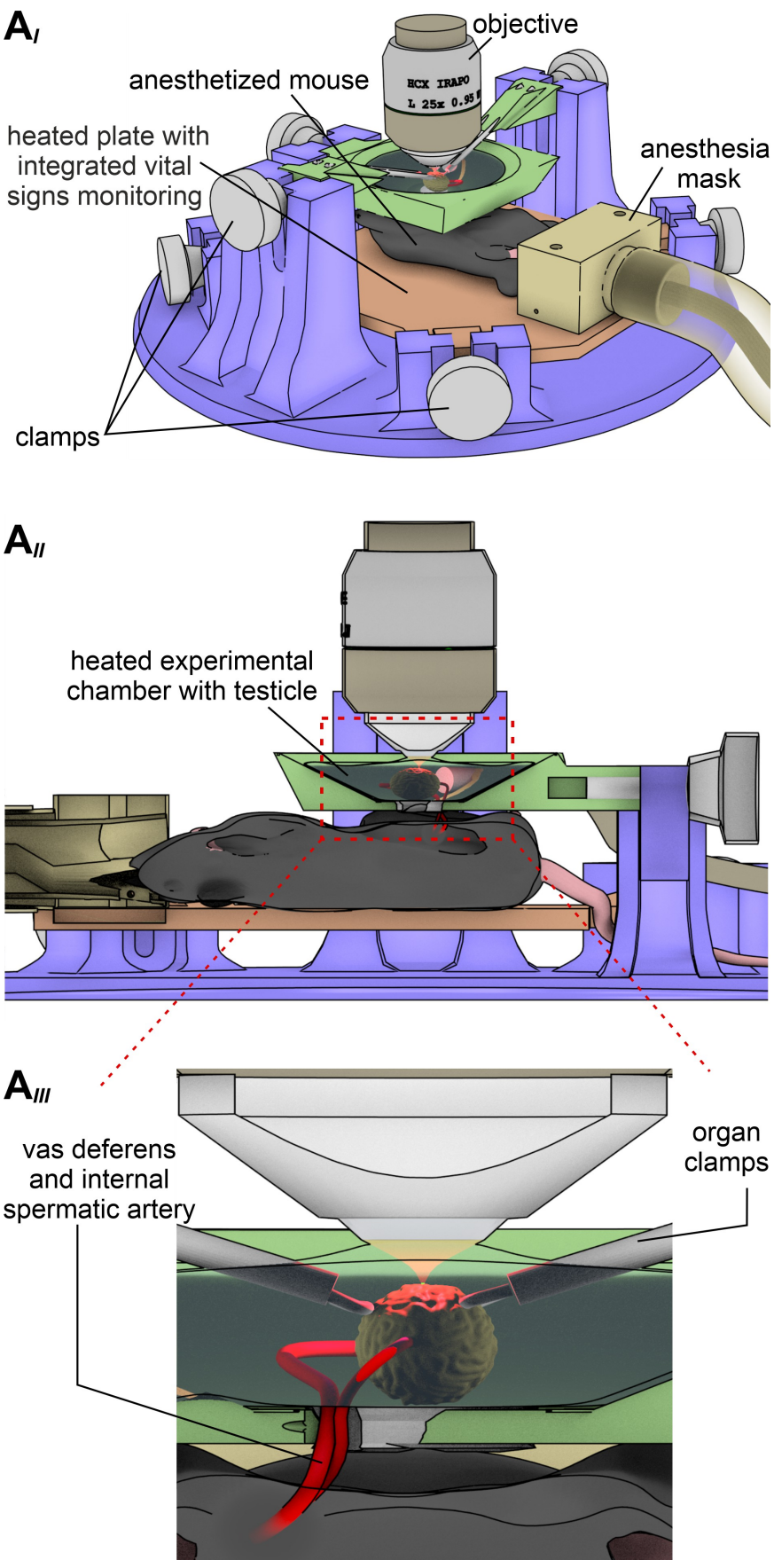

A custom-built 3D printed microscope stage enables simultaneous *in vivo* multiphoton imaging of Ca^{2+} signals and contractions in mouse seminiferous tubules.

(**A**) Schematic drawing that illustrates the custom-built intravital imaging stage designed for *in vivo* recordings testicular activity. Three different views depict design details from different perspectives. A top view of the apparatus (**A***i*) shows that several adjustable clamps allow exact positioning of the anesthetized animal on a heated plate equipped for online vital sign monitoring. After centering one testicle in a heated (35°C) and saline-filled recording chamber (**A***ii*) within the microscope's optical axis, a large working distance (~3 mm) infrared-optimized water-immersion objective (25x; 0.95 NA) enables multiphoton deep tissue imaging. A close-up cartoon of the recording chamber (**A***iii*) illustrates that two micromanipulator-based moveable organ clamps enable precise (re)positioning of the testis as well as effective movement cancellation. Note that the *vas deferens* and internal spermatic arteries are kept intact to assure blood supply and fluid transport.

Figure 7—figure supplement 2

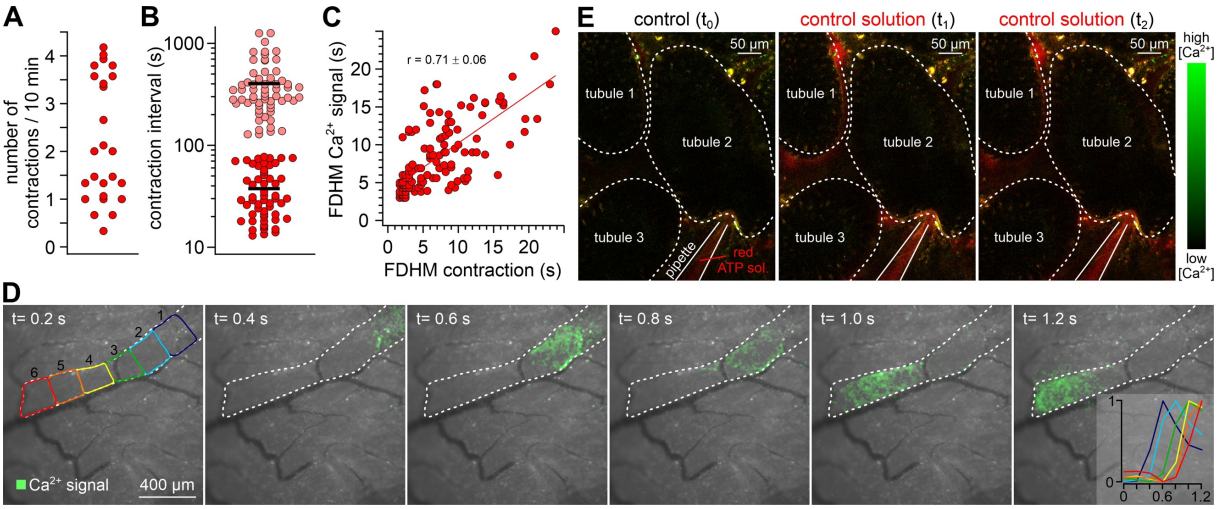

***In vivo* imaging of tubular activity in SMMHC-CreERT2 x Ai95D mice.**

(**A–C**) Quantitative analysis of spontaneous seminiferous tubule contractions *in vivo*. Dot plots depict (**A**) the number of contractions observed in a given tubule segment per 10 min during variable windows of observation (13–30 min; mean = 25 min; n = 28;

four mice), and (**B**) the intervals between two consecutive contractions. Note that two distinct types of either relatively short (<80 s; red; 38 ± 21 s; mean ± SD) and long (>2 min; magenta; 403 ± 250 s; mean ± SD) intervals become apparent. Moreover, we never observed tubules that lacked contractions. (**C**) 2D dot plot shows positive correlation (Pearson correlation coefficient r = 0.71) between TPC Ca^{2+} signal durations (full duration at half-maximum; FDHM) and corresponding tubule contractions. (**D**) Representative epifluorescence *in vivo* recording of a Ca^{2+} wave propagating along the longitudinal axis of a seminiferous tubule in a SMMHC-CreERT2 x Ai95D mouse (n = 3 animals). Individual consecutive frames indicate fluorescence intensity in pseudocolor (green; time as indicated; frames merged with corresponding brightfield image). Dashed white line denotes tubule dimensions. Inset (right) shows the color-coded Ca^{2+} signal onset (min/max normalization) in six adjacent tubule regions of comparable size (left). (**E**) Example experiment that controls for pressure-dependent signal artifacts when seminiferous tubules are exposed to 'puffs' of solution. Three fluorescence images show outlines of three seminiferous tubule segments (white dotted lines) at different time points (t0 – t2). Aside the addition of a red fluorescent dye to the solution in the pipette, compositions of bath and pipette solution match. Note that puffs of stained solution (t1 and t2) cause neither contractions, nor Ca^{2+} signals.

2.2 Publication II (Missel et al. 2021)

Testicular adenosine acts as a pro-inflammatory molecule: role of testicular peritubular cells

Annika Missel, Lena Walenta, Katja Eubler, Nadine Mundt, Hanna Heikelä, Ulrich Pickl, Matthias Trottmann, Bastian Popper, Matti Poutanen, Leena Strauss, Frank-Michael Köhn, Lars Kunz, Marc Spehr & Artur Mayerhofer

Mol Hum Reprod. doi:10.1093/molehr/gaab037

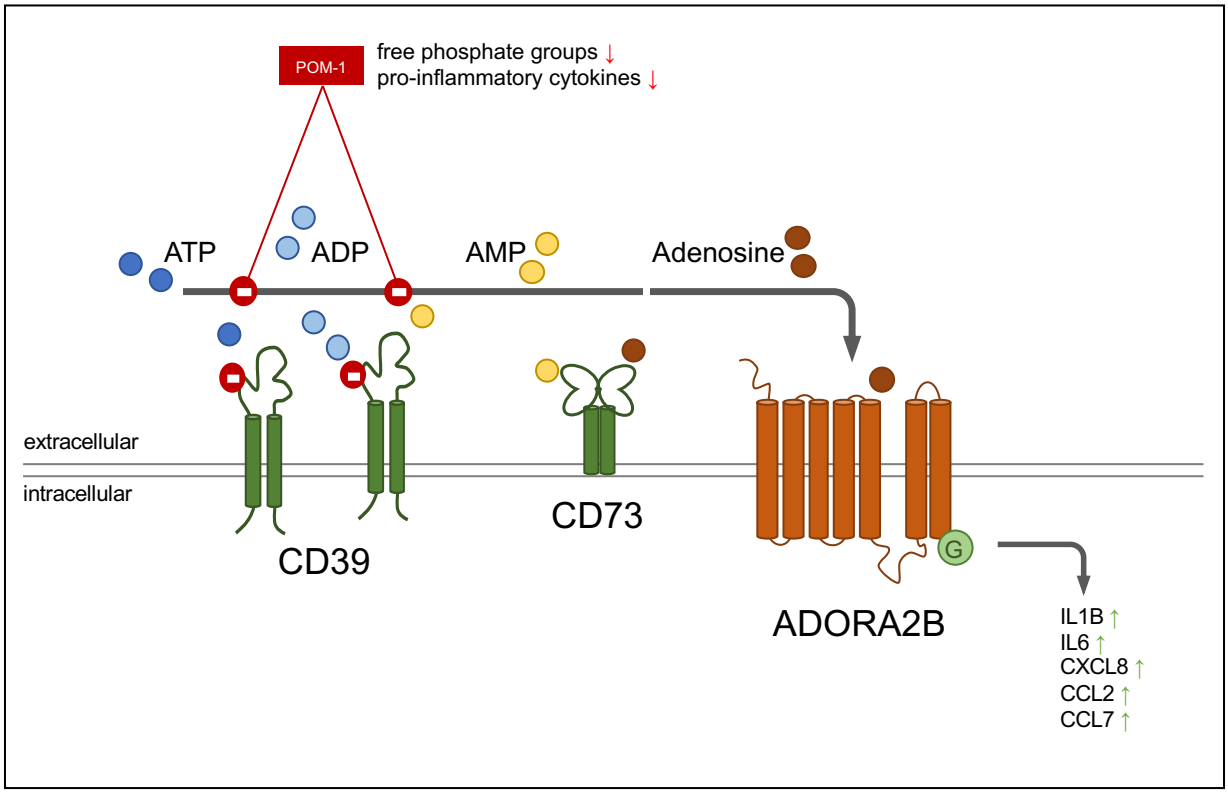

Figure 7. Graphical abstract of Missel et al. (2021).

Adenosine is the final metabolite of ATP, generated by the ectonucleotidases CD39 and CD73. Both are present in peritubular cells in situ and in vitro, and their functionality was indicated by malachite green assay and pharmacological inhibition of CD39. The inhibitor POM-1 reduced the formation of extracellular phosphate and pro-inflammatory cytokine levels, which were evoked upon ATP. Adenosine exposure resulted in elevated pro-inflammatory cytokines and A2B was identified as the main mediator.

Copyright

This article is printed with permission from Oxford University Press (License number: 5173070755649).

Molecular Human Reproduction, Vol.0, No.0, pp. 1–13, 2021
doi:10.1093/molehr/gaab037

molecular human reproduction

ORIGINAL RESEARCH

Testicular adenosine acts as a pro-inflammatory molecule: role of testicular peritubular cells

Annika Missel[1], Lena Walenta[1], Katja Eubler[1], Nadine Mundt[2,3], Hanna Heikelä[4], Ulrich Pickl[5], Matthias Trottmann[5], Bastian Popper[6], Matti Poutanen[4], Leena Strauss[4], Frank-Michael Köhn[7], Lars Kunz[8], Marc Spehr[2,3], and Artur Mayerhofer [1]*

[1]Cell Biology-Anatomy III, Faculty of Medicine, Biomedical Center (BMC), Ludwig-Maximilians-University Munich, Martinsried, Germany [2]Institute of Biology II/Department of Chemosensation, RWTH Aachen University, Aachen, Germany [3]Research Training Group 2416, MultiSenses—MultiScales, RWTH Aachen University, Aachen, Germany [4]Institute of Biomedicine, Research Center for Integrative Physiology and Pharmacology, Turku Center for Disease Modeling, University of Turku, Turku, Finland [5]Urologie und Andrologie, Munich, Germany [6]Biomedical Center (BMC), Core Facility Animal Models, Faculty of Medicine, Ludwig-Maximilians-University Munich, Martinsried, Germany [7]Andrologicum, Munich, Germany [8]Division of Neurobiology, Department of Biology II, Ludwig-Maximilians-University Munich, Martinsried, Germany

*Correspondence address. Biomedical Center (BMC), Cell Biology- Anatomy III, Faculty of Medicine, Ludwig-Maximilians-UniversityMunich, 82152 Martinsried, Germany. Tel: +49-89-2180-75859; E-mail: Mayerhofer@bmc.med.uni-muenchen.de
https://orcid.org/0000-0002-9388-4639

Submitted on February 15, 2021; resubmitted on April 27, 2021; editorial decision on May 12, 2021

ABSTRACT: Extracellular ATP has been described to be involved in inflammatory cytokine production by human testicular peritubular cells (HTPCs). The ectonucleotidases ENTPD1 and NT5E degrade ATP and have been reported in rodent testicular peritubular cells. We hypothesized that if a similar situation exists in human testis, ATP metabolites may contribute to cytokine production. Indeed, ENTPD1 and NT5E were found *in situ* and *in vitro* in HTPCs. Malachite green assays confirmed enzyme activities in HTPCs. Pharmacological inhibition of ENTPD1 (by POM-1) significantly reduced pro-inflammatory cytokines evoked by ATP treatment, suggesting that metabolites of ATP, including adenosine, are likely involved. We focused on adenosine and detected three of the four known adenosine receptors in HTPCs. One, A2B, was also found *in situ* in peritubular cells of human testicular sections. The A2B agonist BAY60-6583 significantly elevated levels of IL6 and CXCL8, a result also obtained with adenosine and its analogue NECA. Results of siRNA-mediated A2B down-regulation support a role of this receptor. In mouse peritubular cells, in contrast to HTPCs, all four of the known adenosine receptors were detected; when challenged with adenosine, cytokine expression levels significantly increased. Organotypic short-term testis cultures yielded comparable results and indicate an overall pro-inflammatory action of adenosine in the mouse testis. If transferable to the *in vivo* situation, our results may implicate that interference with the generation of ATP metabolites or interference with adenosine receptors could reduce inflammatory events in the testis. These novel insights may provide new avenues for treatment of sterile inflammation in male subfertility and infertility.

Key words: adenosine / testis / peritubular cells / ADORA / A2B / inflammation / ENTPD1 / NT5E / CD39 / CD73

Introduction

It is now well accepted that extracellular ATP can act as a signaling molecule and has a variety of roles in different tissues of the body (Corriden and Insel, 2010; Venereau *et al.*, 2015; Le *et al.*, 2019; Linden *et al.*, 2019). However, with regard to the testis, in particular human testis, insights in such roles are scarce (Burnstock, 2014). There is an obvious lack of knowledge about the components of the purinergic system in the male gonad and its specific roles in the testis.

Extracellular ATP can be released from dying cells including germ cells (Baum *et al.*, 2005; Xiong *et al.*, 2009), from Sertoli cells of the tubular compartment, as well as from nerve fibers and mast cells,

© The Author(s) 2021. Published by Oxford University Press on behalf of European Society of Human Reproduction and Embryology. All rights reserved.
For permissions, please email: journals.permissions@oup.com

Downloaded from https://academic.oup.com/molehr/article/27/7/gaab037/6276438 by Universitaetsbibliothek Muenchen user on 28 October 2021

which exist in the interstitial and peritubular areas of the testis (Mayerhofer et al., 1999; Gelain et al., 2003; Xiong et al., 2009; Mayerhofer et al., 2018). Hence, extracellular ATP is likely available in all testicular compartments. Innervation density and mast cell numbers increase specifically in the peritubular compartment in men with impaired spermatogenesis (Mayerhofer et al., 1999; Meineke et al., 2000), implying that, consequently, the levels of extracellular ATP also increase in these cases specifically within this testicular compartment.

The human testis is not readily accessible for investigation, yet the cells composing the peritubular compartment can be isolated and examined *in vitro* (Albrecht et al., 2006). These HTPCs are smooth muscle-like cells (myoid cells), which together with extracellular matrix form a small compartment surrounding the seminiferous tubule. They are thought to transport sperm due to their contractile activity (Hargrove et al., 1977; Romano et al., 2005) and a recent study confirmed this important function (Fleck et al., 2021). Furthermore, recent studies showed that isolated HTPCs produce extracellular matrix components, some of which (such as decorin and biglycan) interfere with growth factor signaling (Adam et al., 2012). Importantly, they also produce glial cell line-derived neutrophic factor (GDNF) (Spinnler et al., 2010), which is required for spermatogonial stem cell renewal. HTPCs also have immunological roles and produce cytokines (Mayerhofer, 2013; Welter et al., 2014; Walenta et al., 2018). Hence, they likely contribute in various ways to testis function and consequently to male fertility/infertility.

How peritubular cells are regulated is not well known. Yet, they express receptors for hormones, namely androgen receptors (Mayer et al., 2018) and glucocorticoid receptors (Welter et al., 2020), and their smooth muscle-like cellular phenotype has been shown to be regulated by these hormones. In addition to systemic regulation, there is evidence for local regulation of peritubular cells. For example, a recent study described that HTPCs possess P2X receptors, *in situ* and *in vitro*, and, thus, ATP was implicated in the regulation of HTPC functions (Walenta et al., 2018). Application of ATP to HTPCs increased pro-inflammatory cytokine expression and secretion within 24 h (Walenta et al., 2018). The study concluded that ATP may promote a pro-inflammatory environment, which likely contributes to sterile inflammation associated with male infertility. Of note, a follow-up study showed that ATP acutely induced contraction of HTPCs. This, together with parallel studies performed in rodent models, indicated a role in sperm transport (Fleck et al., 2021).

Actions of extracellular ATP are locally confined because of its rapid degradation. ATP is dephosphorylated by two specific hydrolyzing enzymes (Fig. 2d), named ENTPD1 (ectonucleoside triphosphate diphosphohydrolase; CD39) and NT5E (ecto-5'-nucleotidase; CD73) (Zimmermann, 1992; Colgan et al., 2006; Grinthal and Guidotti, 2006; Allard et al., 2017). In mice, ENTPD1, which generates ADP and AMP, and NT5E, the generator of adenosine, are expressed by testicular peritubular cells (Zimmermann, 1992; Grinthal and Guidotti, 2006). Whether ENTPD1 or NT5E are also present in the human testis was not known. We reasoned that if expressed and active, extracellular ATP could give rise to its metabolites, which then may act via their respective receptors and may further influence testicular functions. This view is based on growing insights that for example extracellular adenosine can act as a ubiquitous endogenous signaling mediator in numerous physiological and pathophysiological processes (Gelain et al., 2003). It binds, with different affinities, to four ADORA receptors, A1, A2A, A2B and A3. They are linked to modulatory effects of adenosine in inflammatory environments and belong to the class A (rhodopsin-like) G-protein-coupled receptor superfamily (Fredholm et al., 1994; Hasko et al., 2008; Jacobson et al., 2012; Borea et al., 2018). Interactions and dimerization between the receptors can occur (Moriyama and Sitkovsky, 2010; Smith and Milligan, 2010), which make it difficult to assess their specific impact. Little is known about the roles of the ADORAs in the human testis, but previous studies already identified A1 receptors in the rat testis (Murphy and Snyder, 1981). Monaco and Conti (1986) detected binding of radioactive cyclohexyladenosine, indicative of the presence of ADORA receptors, mainly in rat Sertoli cells. Of note, the scope of this study was limited to immature 15-day old animals.

In the present study, we examined whether the ectonucleotidases ENTPD1 and NT5E are present and functional in HTPCs. Moreover, we investigated whether ATP-metabolites, especially adenosine, are involved in cytokine production in the testis.

Materials and methods

Ethical approval

For isolation of human testicular peritubular cells (HTPCs) and immunohistochemical staining small fragments of patient-derived human testicular biopsies were used. Tissues were either derived from patients (age range 28–56) undergoing reconstructive surgery of the *vas deferens* or (mainly) from patients undergoing testicular sperm extraction (TESE) (Albrecht et al., 2006; Schell et al., 2008). Patients granted written informed consent and the ethical committee (Technical University of Munich, Department of Medicine, project number 169/18S) approved the scientific use of the cells.

Peritubular cell isolation, culture and treatment

HTPCs were obtained by explant culture from testicular donor tissues. Identity and purity of cells was assessed as described previously (Walenta et al., 2018). Cells were cultured in DMEM High Glucose (Gibco, Paisley, UK) including 10% fetal bovine serum (FBS, Capricorn Scientific, Ebsdorfergrund, Germany) and 1% penicillin/streptomycin (Biochrom, Berlin, Germany) at standard conditions (37°C, 5% CO_2). Cells (Passages 4–12) were deprived of FBS supplementation 24 h prior to treatment. Cells were treated in serum-free media for 24 h (unless indicated otherwise) before using following reagents: Adenosine, AMP, ADP, ATP, inosine (all 1 mM; all from Sigma, Steinheim, Germany), NECA (10 mM), CCPA (0.5 nM–1 mM), CGS 21680 (100 nM–10 µM), BAY60-6583 (10 µM) and POM-1 (5 µM; all from Tocris, Bristol, UK). In the case of NECA, CCPA, BAY60-6583 and CGS, DMSO (≤ 1:1000, Sigma) was used as a solvent and added to all controls.

qPCR

Total RNA from cells was isolated using the RNeasy Plus Micro Kit (Qiagen, Hilden, Germany), and RNA from testes with normal spermatogenesis was isolated using the RNeasy Plus Universal Kit

Downloaded from https://academic.oup.com/molehr/article/27/7/gaab037/6276438 by Universitaetsbibliothek Muenchen user on 28 October 2021

(Qiagen), according to the manufacturer's instructions. SuperScriptII (Invitrogen, Darmstadt, Germany) and random 15mer primers were used for reverse transcription. For qPCR studies the QuantiFast SYBR Green PCR Kit (Qiagen) was applied using the following protocol in a LightCycler® 96 System (Roche Diagnostics, Penzberg, Germany): pre-incubation (95°C, 5 min), 40–43 cycles denaturation (95°C, 10 s) and annealing/extension (annealing temperature, 30 s) followed by melting (65–97°C) and cooling (37°C, 30 s). Oligonucleotide primers for amplification and corresponding annealing temperatures can be found in Table I. Samples were analyzed in duplicates and amplicon identity was

Table I Information about oligonucleotide primers used for PCR.

Gene	Species	Nucleotide sequence	Amplicon size	Annealing temperature
ACTA2	Human	5'-ACA ATG AGC TTC GTG TTG CC-3' 5'-GAG TCA TTT TCT CCC GGT TGG-3'	90 bp	59°C
ADORA1	Human	5'-AGA CCT ACT TCC ACA CCT GC-3' 5'-CCG CAC TCAG ATT GTT CCA G-3'	234 bp	60°C
Adora1	Mouse	5'-GCG ATG CTA CCT TCT GCT TC-3' 5'-CAA TAG CAA GCA GAG CCA GG-3'	183 bp	60°C
ADORA2A	Human	5'-CGC CAT TGA CCG CTA CAT TG-3' 5'-TGG TTC TTG CCC TCC TTT GG-3'	171 bp	60°C
Adora2a	Mouse	5'-CCA TTC GCC ATC ACC ATC AG-3' 5'-CAA GCC ATT GTA CCG GAG TG-3'	165 bp	59°C
ADORA2B	Human	5'-CTT CTA CGG CTG CCT CTT CC-3' 5'-GAG TCA ATC CGA TGC CAA AGG-3'	197 bp	60°C
Adora2b	Mouse	5'-GTG AAA GAC AGC TGC ACC TC-3' 5'-TCA ATT CAA GCT GCC ACC AC-3'	170 bp	60°C
ADORA3	Human	5'-TTT ACC CAC GCC TCC ATC AT-3' 5'-AAT GAC ACC AGC CAG CAA AG-3'	140 bp	60°C
Adora3	Mouse	5'-ATC TGG GTG GTC AAG CTG AA-3' 5'-GCA GCA CAC AGG ACA TGA AA-3'	172 bp	60°C
AR	Human	5'-AGC CTC AAT GAA CTG GGA GA-3' 5'-TCC TGG AGT TGA CAT TGG TG-3'	175 bp	62°C
CCL2	Human	5'-CAG CCA GAT GCA ATC AAT GCC-3' 5'-TGG AAT CCT GAA CCC ACT TCT-3'	190 bp	58°C
Ccl2	Mouse	5'-GGC TCA GCC AGA TGC AGT TAA-3' 5'-CCA GCC TAC TCA TTG GGA TCA-3'	80 bp	60°C
CCL7	Human	5'-TGG AGA GCT ACA GAA GGA CCA-3' 5'-GTG GGG TCA GCA CAG ATC TC-3'	94 bp	58°C
Ccl7	Mouse	5'-ATC TCT GCC ACG CTT CTG T-3' 5'-TAT AGC CTC CTC GAC CCA CT-3'	249 bp	60°C
COL1A1	Human	5'-CAC ACG TCT CGG TCA TGG TA-3' 5'-AAG AGG AAG GCC AAG TCG AG-3'	91 bp	58°C
Cxcl1	Mouse	5'-AGT TCC AGC ACT CCA GAC TC-3' 5'-AGT GTG GCT ATG ACT TCG GT-3'	246 bp	60°C
CXCL8	Human	5'-TCT TGG CAG CCT TCC TGA-3' 5'-GAA TTC TCA GCC CTC TTC-3'	190 bp	58°C
Cyp11a1	Mouse	5'-GCA CAC AAC TTG AAG GTA CAG GAG-3' 5'-CAG CCA AAG CCC AAG TAC CGG AAG-3'	344 bp	60°C
DCN	Human	5'-GGA ATT GAA AAT GGG GCT TT-3' 5'-GCC ATT GTC AAC AGC AGA GA-3'	221 bp	59°C
ENTPD1	Human	5'-GGT TCT GGA TGT GGT GGA GA-3' 5'-GGG ACT ATG CTG AAC CAC CT-3'	159 bp	60°C
Entpd1	Mouse	5'-AAA CCT TTG GCG CTT TGG AT-3' 5'-GCC ACC ACT TGA AAC CTG AA-3'	209 bp	60°C
Fshr	Mouse	5'-TCG TCT GCC TTT TAG AGC CA-3' 5'-TTC CTC AGC CAG CTT CAT CA-3'	159 bp	59°C
GDNF	Human	5'-GCA GAC CCA TCG CCT TTG AT-3' 5'-ATC CAC ACC TTT TAG CGG AAT G-3'	93 bp	60°C

(continued)

Downloaded from https://academic.oup.com/molehr/article/27/7/gaab037/6276438 by Universitaetsbibliothek Muenchen user on 28 October 2021

HPRT	Human	5'-CCT GGC GTC GTG ATT AGT GA-3' 5'-GGC CTC CCA TCT CCT TCA TC-3'	163 bp	60°C
Hprt	Mouse	5'-TGG ATA CAG GCC AGA CTT TGT T-3' 5'-CAG ATT CAA CTT GCG CTC ATC-3'	163 bp	60°C
IL1B	Human	5'-CTT GGT GAT GTC TGG TCC ATA TG-3' 5'-GGC CAC AGG TAT TTT GTC ATT AC-3'	127 bp	60°C
Il1b	Mouse	5'-TGA AGT TGA CGG ACC CCA AA-3' 5'-TGA TGT GCT GCT GCG AGA TT-3'	101 bp	59°C
IL6	Human	5'-AAC CTG AAC CTT CCA AAG ATG G-3' 5'-TCT GGC TTG TTC CTC ACT ACT-3'	159 bp	62°C
Il6	Mouse	5'-TTG GGA CTG ATG CTG GTG AC-3' 5'-CAG GTC TGT TGG GAG TGG TAT-3'	91 bp	59°C
Lhr	Mouse	5'-ATG CAT TCA ATG GGA CGA CG-3' 5'-GCC TGC AAT TTG GTG GAA GA-3'	133 bp	61°C
NT5E	Human	5'-CTC CTC TCA ATC ATG CCG CT-3' 5'-TGG ATT CCA TTG TTG CGT TCA-3'	174 bp	60°C
Nt5e	Mouse	5'-AGG TTG TGG GGA TTG TTG GA-3' 5'-CCC CAG GGC GAT GAT CTT AT-3'	152 bp	59°C
RPL19	Human	5'-AGG CAC ATG GGC ATA GGT AA-3' 5'-CCA TGA GAA TCC GCT TGT TT-3'	199 bp	60°C
Rpl19	Mouse	5'-AGG CAT ATG GGC ATA GGG AA-3' 5'-CCA TGA GGA TGC GCT TGT TT-3'	199 bp	60°C
Star	Mouse	5'-CAG GGA GAG GTG GCT ATG CA-3' 5'-CCG TGT CTT TTC CAA TCC TCT G-3'	262 bp	62°C

confirmed by agarose gel electrophoresis and sequence analysis (GATC, Konstanz, Germany). Quantitative results were calculated according to the $2^{-\Delta\Delta Cq}$ method and normalized to *RPL19* and *HPRT* as reference genes.

Malachite green assay

A total of 100000 cells per well were grown on 6-well plates in DMEM High Glucose (10% FBS; 1% penicillin/streptomycin; 37°C, 5% CO_2). Cells were washed with standard extracellular solution comprising 140 mM NaCl, 3 mM KCl, 10 mM HEPES and 10 mM glucose (pH 7.4 adjusted by using NaOH) as described previously (Eubler *et al.*, 2018), to get rid of FBS and the same solution was added to the dishes 2 h prior to stimulation. Treatment was performed for 24 h and supernatant was collected for extracellular phosphate detection using the malachite green assay (MAK307, Sigma) according to manufacturer's instructions. Absorbance was detected at 612 nm in a fluorometer (FLUOstar Omega, BMG LABTECH, Ortenberg, Germany).

ELISA

The commercially available ELISA Kits Human CCL7/MCP-3 Quantikine ELISA Kit (R&D systems, Minneapolis, MN, USA), Human IL-6 Platinum ELISA (eBioscience/Bender MedSystems, Vienna, Austria) and Human IL-8 ELISA Kit (Invitrogen/Bender MedSystems, Vienna, Austria) were used according to the manufacturer's instructions. Cell culture supernatants after 24 h of treatment were measured, normalized to sample protein content and compared to untreated control levels.

Immunohistochemistry

Samples of human testicular tissues were fixed in Bouin's solution, embedded in paraffin and sectioned. Immunohistochemical staining was performed as previously described (Walenta *et al.*, 2018) using primary antibodies ENTPD1 (1:100, #223843, Abcam, Cambridge, UK), NT5E (1:1000, #HPA917357, Sigma) and A2B (1:1000, #222901, Abcam). Negative controls consisted of omission of the primary antibody and incubation with non-immune serum. Sections were counterstained with hematoxylin. Pictures were taken using a Zeiss Axioplan microscope with a Plan-Neofluar 20× or 40×/0.75 objective (Carl Zeiss Microscopy, Jena, Germany) and a Jenoptik camera (Progres Gryphax Arktur; Jenoptik, Jena, Germany).

siRNA

HTPCs were seeded into P60 plates and transfected at a confluency of ~50%. Cells were serum starved for 30 min in DMEM including 1% FBS, prior to transfection with siRNA A2B (18 h, 10 µM, Santa Cruz Biotechnology, DAL, TX, USA) using RNAiMAX (#13778075, Thermo Fisher Scientific, Darmstadt, Germany), diluted in OPTI-MEM (#31985070, Thermo Fisher Scientific) according to the manufacturer's protocol. A scrambled non-targeting siRNA (5 nM, Silencer Select Negative Control #1, Thermo Fisher Scientific) was used as a control. After transfection, medium was replaced for additional 30 h. At 48 h after transfection initiation, cells were treated with 1 mM adenosine for 24 h. Silencing efficiency was verified by western blot, as described previously (Walenta *et al.*, 2018), using the A2B antibody (1:1000, #222901, Abcam) and β-actin (1:10,000, #A5441, Sigma) as references.

Downloaded from https://academic.oup.com/molehr/article/27/7/gaab037/6276438 by Universitaetsbibliothek Muenchen user on 28 October 2021

Animals

All animals had free access to soy-free food pellets (FVB/N mice: SDS, Witham, Essex, England; C57BL/6J mice: 1314P, Altromin, Netherlands) and tap water. Room temperature and relative humidity ranged from 20 to 22°C and 45–55%, respectively. The light cycle was adjusted to 12 h light:12 h dark period. Mice used in the present study were killed by CO_2 asphyxiation and cervical dislocation before tissue removal. *FVB/N mice*: The animals were handled in accordance with the institutional animal care policies of the University of Turku (Turku, Finland). The number of the animal license is KEK/2018-0608-Strauss. *C57BL/6J mice*: Housing of laboratory mice was in accordance with European and German animal welfare legislations (5.1-231 5682/LMU/BMC/CAM 2019-0007). The mice were housed in individually ventilated cages (TypII long, Tecniplast, Germany) under specified-pathogen-free conditions. Hygiene monitoring was performed every three months based on the recommendations of the FELASA-14 working group.

Mouse testicular peritubular cell isolation

Mouse testicular peritubular cells were isolated from the testes of five adult wildtype C57BL/6J mice, as described (Fleck *et al.*, 2021). In brief, the tunica albuginea was removed and testes were placed in collagenase A-DNase solution Sigma; 1 mg/ml collagenase A; 6 µg/ml DNase; in DMEM/F12) for 10 min (34°C; shaking at 60 cycles/min). The supernatant was then removed, the suspension resuspended in DMEM/F12, incubated for 5 min and this procedure was repeated three times. Remaining tubules were dissolved in trypsin-DNase solution (1 mg/ml trypsin; 0.02 mg/ml DNase; in DMEM/F12; 20 min; 34°C; shaking at 60 cycles/min) and the reaction was stopped in soybean trypsin inhibitor (SBTI; Sigma)-DNase solution (0.1 mg/ml SBTI; 0.02 mg/ml DNase; in PBS). After 5 min of settling down, the supernatant was collected and the tissue was washed two times with DMEM/F12 (5 min each). Each time, the supernatant was collected. Collected cells were centrifuged (400 *g*; 10 min; RT), then the supernatant was discarded, the cell pellet was resuspended in DMEM containing 10% FBS and 1% penicillin/streptomycin, filtered in a 100 µm cell strainer, plated in 75 cm^2 cell culture flask (T75; Invitrogen) and incubated in standard conditions (5% CO_2; 37°C). When cells reached 90–100% cell confluence, they were passaged and seeded onto P35 dishes. Cells were serum starved 24 h prior to stimulation with ATP and adenosine (both 1 mM, 24 h). For each condition, five dishes were used and pooled after RNA isolation. RNA was isolated as described above. RevertAid H Minus Kit (Thermo Fisher Scientific) was used for cDNA synthesis.

Organotypic tissue culture of mouse testes

This method was used to preserve cellular interactions and tissue structure of the mouse testis sample during stimulation. Whole testes of 11 wildtype FVB/N mice (2–7 months old) were decapsulated, cut in four equal pieces and each piece was placed in a 24-well plate containing DMEM/F12.

Testes of wildtype C57BL/6J mice (Charles River, Germany) were used for the establishment of the method. Samples were treated with ATP, ADP, AMP, adenosine (6 h; all 1 mM) and POM-1 (1 h + 6 h; 5 µM) and incubated on a plate shaker at cell culture standard conditions (37°C, 5% CO_2). After treatment, sample pieces were shock frozen in liquid nitrogen and RNA was isolated using the RNeasy Plus Universal Kit (Qiagen) according to manufacturer's instructions.

Statistical analyses

Raw data of qPCR, ELISA and malachite green assays were analyzed using Microsoft Excel (2018, Microsoft, Redmond, WA, USA), statistical analyses were obtained using Prism 6.0 (GraphPad Software Inc., San Diego, CA, USA). qPCR ($-\Delta\Delta$Cq values) and ELISA (unnormalized values) data were analyzed using one-sample *t*-tests or by one-way ANOVA followed by Tukey's post-test. Malachite green assay values were analyzed by one-way ANOVA and Tukey's post-test. Individual numbers (n) of experiments are stated in the figure legends. All results are depicted in means + SEM. $P < 0.05$ was considered statistically significant.

Results

HTPCs express the ectonucleotidases ENTPD1 and NT5E, which degrade ATP

Immunohistochemical staining of human testis samples showed ENTPD1 in peritubular cells, surrounding the seminiferous tubules, and in interstitial blood vessel. In contrast, NT5E expression was associated with a number of testicular cells. It was located in peritubular cells, in cells of the seminiferous epithelium and Sertoli cells, as well as in some interstitial cells (Fig. 1a). A comparable, ubiquitous staining pattern is also depicted by the images provided in the Human Protein Atlas (HPA; https://www.proteinatlas.org). All controls were negative.

ENTPD1 and *NT5E* were readily detected in whole human testis of patients with normal spermatogenesis and in cultured HTPCs (Fig. 1b). When cultured HTPCs, derived from nine individual patients, were examined by qPCR (Fig. 1c), we found a strong, robust *NT5E* expression in all samples and a somewhat more variable expression profile of *ENTPD1*.

Ectonucleotidase activity in HTPCs was indicated by the results of malachite green assays. Significantly increased extracellular phosphate levels, indicative of enzymatic activity, were detected after 24 h in the supernatant when ATP or ADP (both at 1 mM) were added, compared to unchanged levels after adenosine treatment (1 mM) and under control conditions. The strongest elevation was recorded upon addition of AMP (1 mM; Fig. 1d). Hence, the results indicate that while both ectonucleotidase are active, NT5E (degrading AMP and generating adenosine) may be the more active one.

Purines regulate cytokines in HTPCs

As expected (Walenta *et al.*, 2018), transcript levels of several pro-inflammatory cytokines were consistently upregulated in HTPCs after treatment with ATP (1 mM) within 24 h. They were, however, also elevated upon addition of adenosine (1 mM, 24 h; Fig. 2a). Levels of

Downloaded from https://academic.oup.com/molehr/article/27/7/gaab037/6276438 by Universitaetsbibliothek Muenchen user on 28 October 2021

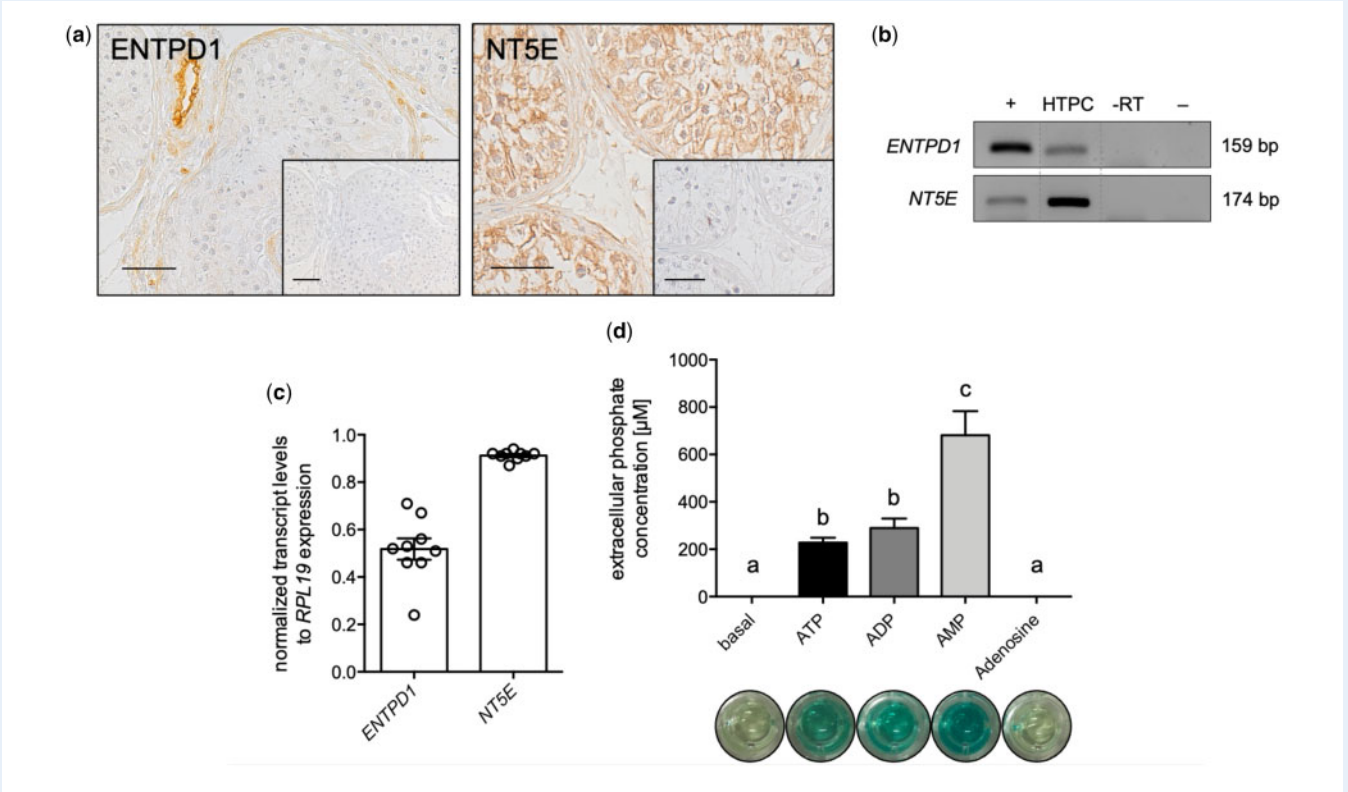

Figure 1. Expression and functionality of ENTPD1 and NT5E in HTPCs. (**a**) Immunohistochemical staining of human testis samples indicates expression of ENTPD1 in peritubular cells and blood vessels in the interstitial areas, while NT5E is expressed not only in peritubular cells, but also cells of the tubular compartment and interstitial cells. Insets: negative controls (omission of first antibody); scale bars = 50 µm. (**b**) Expression of *ENTPD1* and *NT5E* in pooled cDNA of three individual patient-derived HTPCs and human whole testis samples (+). Negative controls: -RT, non-reverse transcription control; – = non-template control. (**c**) Comparison of mRNA expression levels of nine individual patient-derived HTPCs normalized to *RPL19* mRNA expression. *ENTPD1* expression is lower and more variable compared to consistently high levels of *NT5E*. (**d**) Increasing extracellular phosphate concentration (indicated by a green color change) was detected 24 h after treatment with ATP (n = 9), ADP (n = 9) and AMP (each at 1 mM; n = 6). Control conditions and adenosine treatment (1 mM; n = 7) of HTPCs did not result in release of extracellular phosphate levels, as expected. Bars with different letters indicate that results are significantly different from each other according to Tukey's multiple comparison test ($P < 0.05$) and one-way ANOVA.

interleukins *IL1B, IL6* and *CXCL8* were comparably elevated by both stimulants. There was also a trend to increased *CCL7* and *IL1B* levels after the addition of adenosine as compared to ATP (Fig. 2a). The actions of adenosine were concentration-dependent (Fig. 2b). Addition of the structurally related adenosine metabolite inosine (at different concentrations) did not result in changes of pro-inflammatory cytokines (Fig. 2c and Supplementary Fig. S1a). When exposed to the non-selective adenosine receptor agonist NECA (10 µM, 24 h), results were comparable to that evoked by adenosine (1 mM, 24 h; Fig. 2c and Supplementary Fig. S1c).

The specific ENTPD1 inhibitor POM-1 was employed next and its ability to block ectonucleotidase activity was examined by malachite green assay. When POM-1 (5 µM) was added 1 h prior to ATP or ADP (both 1 mM), the results (monitored after 24 h) showed significantly reduced levels of extracellular phosphate for POM-1/ADP versus ADP and a trend to reduced levels for POM-1/ATP versus ATP (Fig. 2e). Additionally, we observed decreased expression levels of some of pro-inflammatory cytokines in HTPCs (POM-1, 1 h; ATP, 24 h), as compared to ATP alone. Specifically, *IL1B* and *CCL7* were significantly reduced by POM-1, whereas *IL6*, *CCL2* and *CXCL8* showed no significant reduction (Fig. 2f).

Pro-inflammatory actions of HTPCs mediated by ADORA2B

Expression of the ADORA receptors *A1*, *A2A* and *A2B* was demonstrated at the transcript level in nine individual donor-derived HTPC samples (Fig. 3a) and whole human testes (Fig. 3b). Attempts to immunostain human testicular sections, employing several commercial antibodies directed against the receptors A1 and A2A, yielded only non-specific staining (not shown). When we used an antibody against A2B, three of the six different histological samples, which we examined, showed specific signals, while in the others non-specific staining prevailed. Expression of A2B was detected in peritubular cells and blood vessels, as well as in cells of the tubular compartment.

Downloaded from https://academic.oup.com/molehr/article/27/7/gaab037/6276438 by Universitaetsbibliothek Muenchen user on 28 October 2021

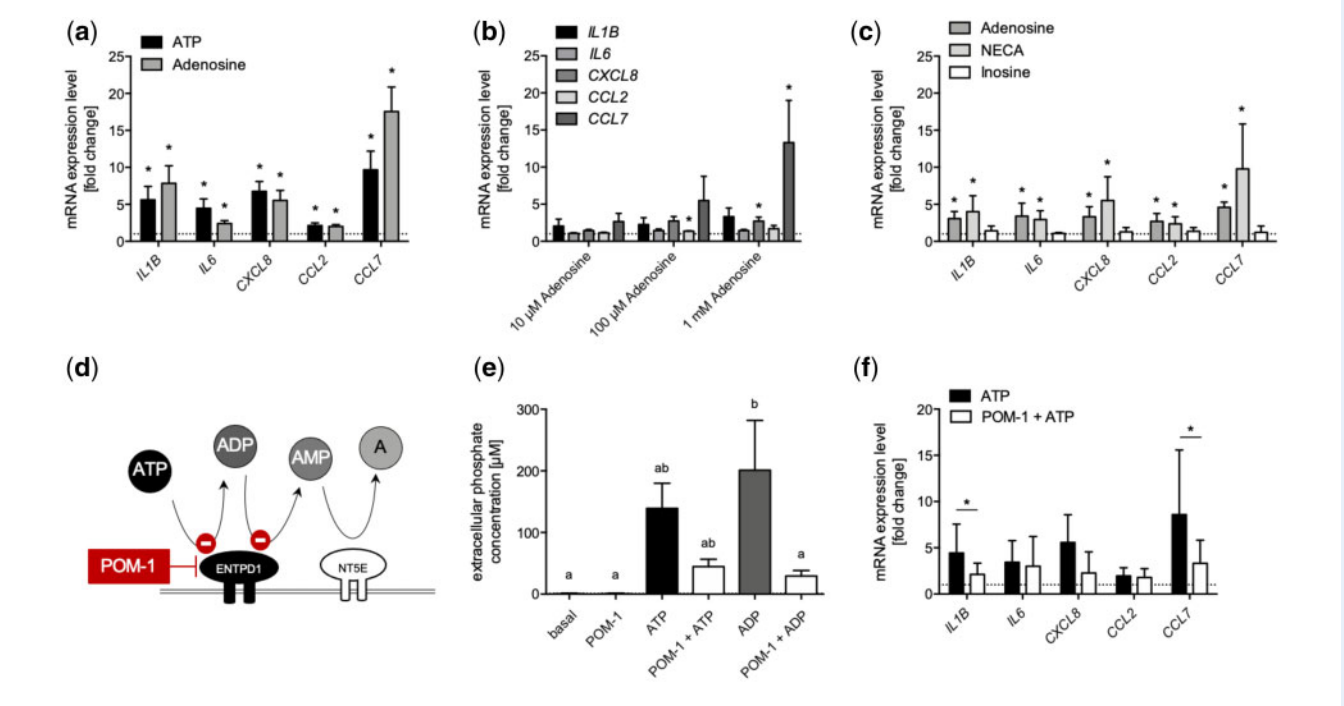

Figure 2. Regulation of pro-inflammatory cytokines in HTPCs. (**a**) Treatment of HTPCs with ATP (n = 7) and adenosine (both 1 mM, 24 h; n = 10) caused a weak to moderate increase of the inflammation-associated markers *IL1B, IL6*, *CCL2* and *CXCL8* and a strong increase of *CCL7* levels. (**b**) Adenosine increased inflammatory cytokines in a dose-dependent manner (n = 3). (**c**) Non-selective adenosine receptor agonist NECA (10 µM; n = 4) increased pro-inflammatory cytokine levels similar to adenosine (1 mM; n = 4), in contrast to inosine treatment (1 mM; n = 3) after 24 h. (**d**) Scheme of the ectonucleotidases ENTPD1 and NT5E, their role in the generation of ATP metabolites, and the action of POM-1. (**e**) Release of extracellular phosphates can be reduced by treatment with ENTPD1 inhibitor POM-1 (5 µM) 1 h before stimulation of HTPCs with ATP or ADP (both 1 mM, 24 h; n = 6). (**f**) HTPCs were pre-treated with the specific ENTPD1 inhibitor POM-1 (5 µM) 1 h prior to ATP exposure (1 mM, 24 h; n = 5). As a result, mRNA levels of *IL1B* and *CCL7* were significantly lowered. Data are means + SEM normalized to control conditions. (a, b, c and f) asterisks denote statistical significance ($P < 0.05$) of one-sample *t*-test. (e) Bars with different letters indicate that results are significantly different from each other according to Tukey's multiple comparison test ($P < 0.05$) and one-way ANOVA.

Peritubular cell staining appeared most distinct in thickened walls of tubules with signs of impaired spermatogenesis (Fig. 3c).

Employing the partial A2B agonist BAY60-6583 (10 µM, 24 h), we attempted to activate A2B receptors in HTPCs. This resulted in elevated transcript and protein levels of IL6 and CXCL8, i.e. results similar to the ones evoked by adenosine and NECA. However, levels of CCL7 were not elevated after treatment with BAY60-6583, when used at this concentration (10 µM), a result contrasting with the elevated CCL7 levels following adenosine and NECA stimulation in HTPCs (Fig. 3d). Of note, lower concentrations of BAY60-6583 (e.g. 1 µM) resulted in a small (2-fold) increase (Supplementary Fig. S1e), which, however, did not reach statistical significance. HTPCs were also treated with an A1 agonist (CCPA) and an A2A agonist (CGS 21680; both for 24 h) at different concentrations, and this resulted in no, or minimal, increases (2-fold) of pro-inflammatory cytokines (Supplementary Fig. S1b and d).

To obtain further insights in the assumed involvement of A2B in HTPC adenosine signaling, cells were transfected with siRNA targeting A2B. A scrambled non-targeting siRNA was used as a control. As expected, pro-inflammatory cytokines were increased by adenosine in non-targeting siRNA controls. In contrast, elevations were reduced upon siRNA treatment (Fig. 3e). The reduction level reflects the effectiveness of siRNA-knockdown, which led to a 45% reduction in A2B protein (Fig. 3f).

Adenosine has no influence on characteristic markers of HTPCs

HTPC treatment with 1 mM adenosine (24 h) did not change the mRNA levels of smooth muscle marker *ACTA2*, extracellular matrix factors (*COL1A1, DCN*) or the spermatogonial stem-cell regulatory factor *GDNF*. Only a slight increase of androgen receptor (*AR*) was detectable (Supplementary Fig. S2a). Moreover, adenosine treatment (1 mM; 24 h) did not influence total protein concentration (Supplementary Fig. S2b).

Downloaded from https://academic.oup.com/molehr/article/27/7/gaab037/6276438 by Universitaetsbibliothek Muenchen user on 28 October 2021

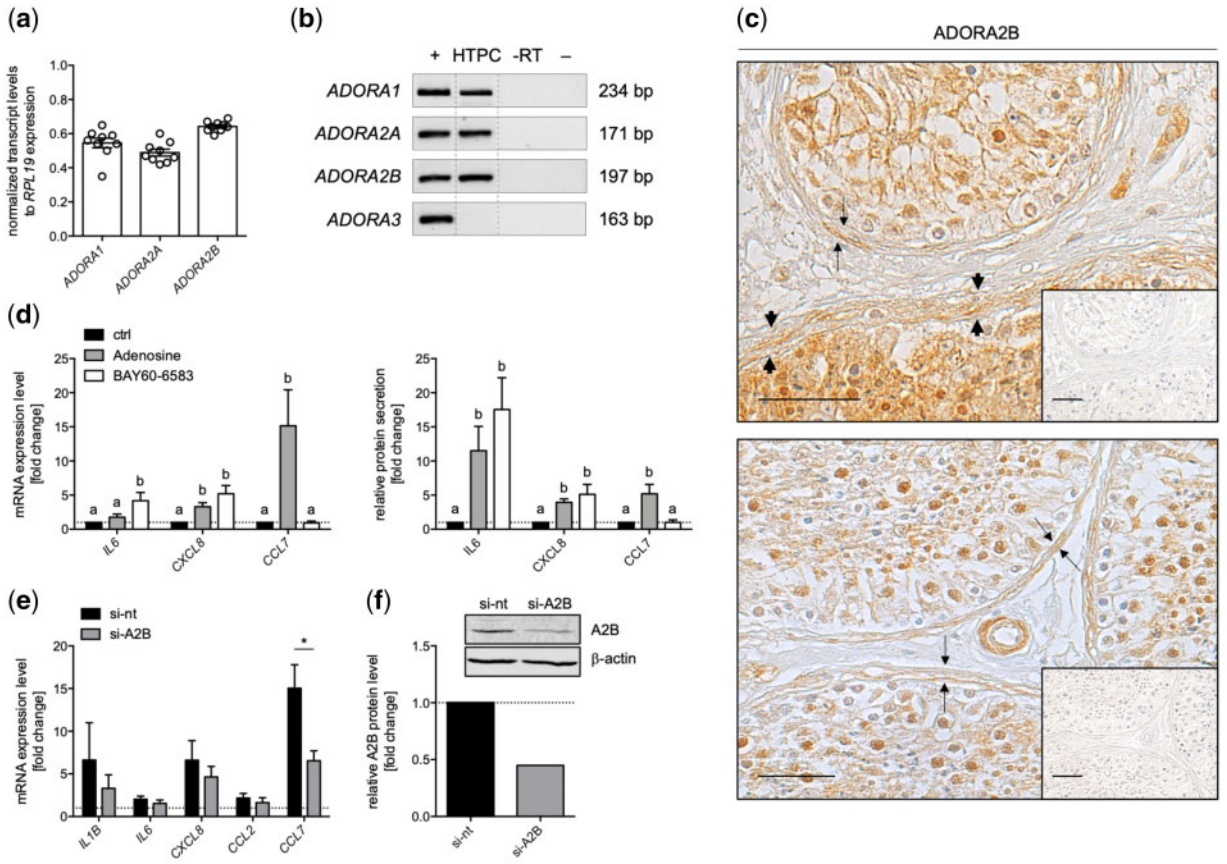

Figure 3. Adenosine receptor A2B is involved in pro-inflammatory signaling of adenosine in HTPCs. (**a**) Consistent expression of the ADORA receptors *A1*, *A2A* and *A2B* was revealed by PCR of 9 individual patient-derived HTPCs, normalized to *RPL19* mRNA expression. (**b**) *A3* expression was only detectable in the human whole testis lysate (+). Negative controls: -RT, non-reverse transcription control; – = non-template control. (**c**) Immunohistochemical staining of human testis samples shows A2B in the tubular compartment, comprising Sertoli cells and germ cells, the peritubular wall of the tubules (arrows) and in endothelial cells of the interstitial area. Peritubular staining was most obvious in thickened walls (arrowheads). Scale bars = 50 µm. (**d**) Treatment of HTPCs with partial A2B agonist BAY60-6583 (10 µM, 24 h) resulted in a similar significant upregulation of IL6 and CXCL8 transcript (qPCR; n = 6) and protein (ELISA; n = 4) levels. No change of CCL7 was detectable upon BAY60-6583 treatment, contrary to a severe significant increase after adenosine treatment (1 mM, 24 h). (**e**) Transfection of HTPCs with a A2B-siRNA (48 h) prior to adenosine treatment (1 mM, 24 h; n = 4) reduced inflammatory effects. The pro-inflammatory cytokines *IL1B, IL6, CXCL8 and CCL2* were decreased notably but not significantly after adenosine treatment compared to transfection with a scrambled non-targeting control siRNA. *CCL7* levels were decreased significantly after adenosine and si-A2B treatment compared to control conditions. (**f**) Transfection reduced A2B protein level (western blot) 72 h after siRNA treatment. Uncropped blots are provided in the Supplementary Fig. S3. Data are means + SEM normalized to control conditions. (d) Bars with different letters indicate that results are significantly different from each other according to Tukey's multiple comparison test ($P < 0.05$) and one-way ANOVA. (e) Asterisks denote statistical significance ($P < 0.05$) of unpaired *t*-test.

Ectonucleotidases, adenosine receptors and pro-inflammatory actions of adenosine in both mouse TPCs and organotypic testis cultures

Both mouse whole testes and isolated mouse testicular peritubular cells (MTPCs) express the ectonucleotidases *Entpd1* and *Nt5e*, as well as the four Adora receptors *A1*, *A2a*, *A2b* and *A3* (Fig. 4a and b). To explore intratesticular actions of adenosine, we employed organotypic, short-term cultures, lasting for 6 h, of mouse testis fragments. Treatment with adenosine (1 mM) resulted in consistent and significantly upregulated pro-inflammatory cytokine expression levels (*Il1b, Il6, Cxcl1, Ccl2, Ccl7*). Of note, ATP (1 mM, 6 h) did not elevate any of the pro-inflammatory cytokines, but rather slightly, yet statistically significantly decreased the mRNA levels of *Ccl2 and Ccl7* (Fig. 4d). Leydig cell markers (*Star, Cyp11a1, Lhr*) and a Sertoli cell marker (*Fshr*) remained unchanged (Fig. 4e). Based on our pilot studies, the culture periods for organotypic testes cultures cannot readily be extended beyond 6 h due to onset of cell death.

When isolated MTPCs were exposed to adenosine (1 mM) for 24 h, to mirror experiments performed with HTPCs, pro-inflammatory actions became evident, similar to that in HTPCs. They are indicated

Downloaded from https://academic.oup.com/molehr/article/27/7/gaab037/6276438 by Universitaetsbibliothek Muenchen user on 28 October 2021

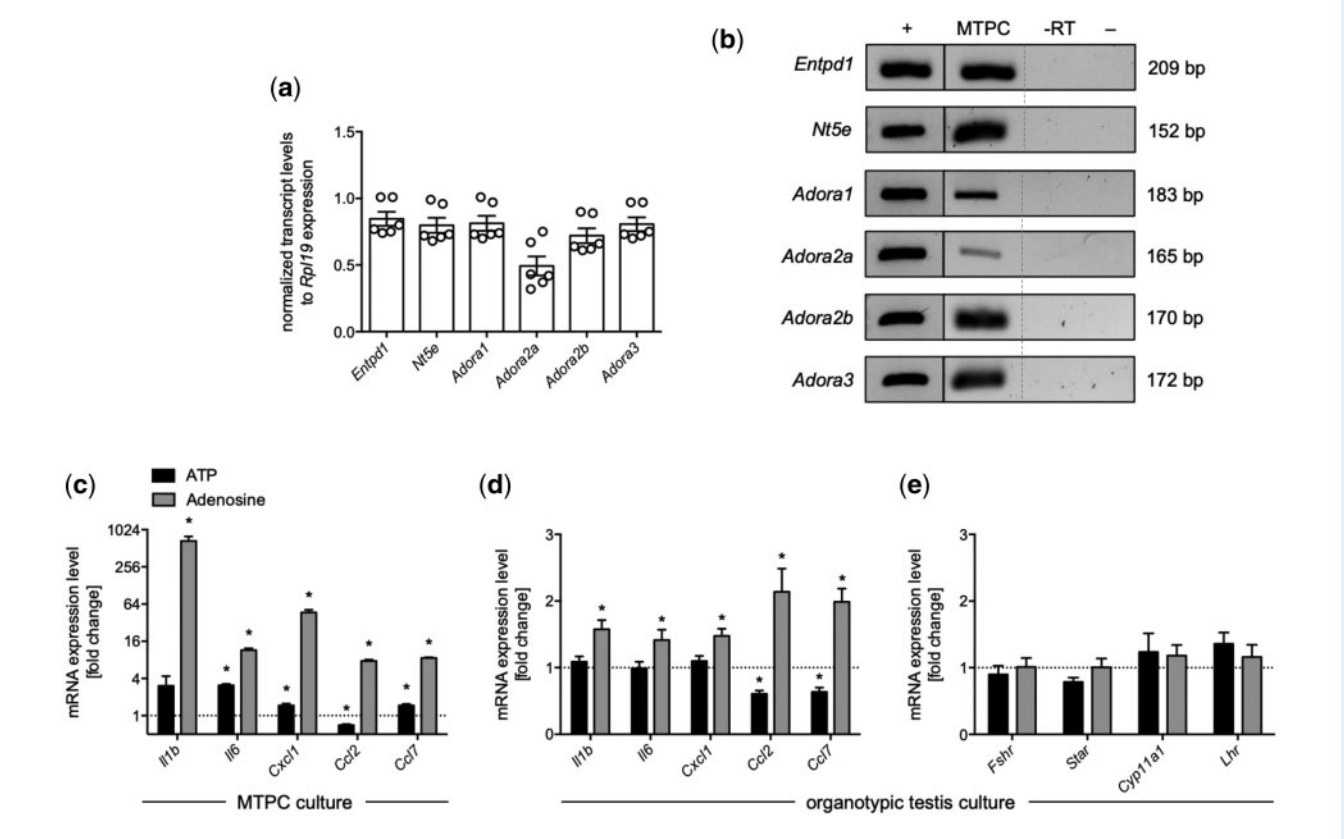

Figure 4. Purinergic signaling in mouse whole testis samples and MTPCs. (**a**) Comparison of mRNA expression levels of the ectonucleotidases *Entpd1* and *Nt5e* as well as all four Adora receptors in mouse whole testis samples, relative to *Rpl19* mRNA expression (n = 6). (**b**) MTPCs also express both ectonucleotidases *Entpd1*, *Nt5e* and the four *Adora* receptors. Positive control: whole testis (+); negative controls: -RT, non-reverse transcription control; – = non template control. (**c**) Treatment of MTPCs with ATP (1 mM, 24 h; n = 3) induced significant increases in mRNA levels of the pro-inflammatory cytokines *Il6, Cxcl1* and *Ccl7*, a significant decrease in *Ccl2* and a distinct increase in *Il1b*. Adenosine exposure (1 mM, 24 h; n = 3) of MTPCs caused strong significant increase of the cytokines *Il6, Cxcl1, Ccl2, Ccl7* and was most intensive in *Il1b* mRNA levels. (**d**) Organotypic tissue culture of mouse whole testis samples (n = 11) treated with ATP (1 mM) for 6 h led to stable mRNA levels of *Il1b, Il6* and *Cxcl1*. *Ccl2* and *Ccl7* mRNA levels were significantly down-regulated after ATP treatment. In contrast, adenosine treatment (1 mM, 6 h) caused significantly up-regulated levels of the pro-inflammatory cytokines *Il1b, Il6, Cxcl1, Ccl2* and *Ccl7*. (**e**) Sertoli (*Fshr*) and Leydig (*Star, Cyp11a1, Lhr*) cell markers remained unchanged after treatment with ATP or adenosine (n = 5). Data are means + SEM normalized to control conditions **(**c, d and e), asterisks denote statistical significance ($P < 0.05$) of one-sample *t*-test.

by strongly increased levels of *Il1b, Il6, Cxcl1, Ccl2* and *Ccl7*. ATP treatment (1 mM, 24 h) caused a moderate increase in most cytokines, but also a reduction of *Ccl2* (Fig. 4c).

Discussion

This study provides new insights into still poorly examined purinergic signaling mechanisms in the testis. We focused on the human testis by using a unique cellular model, HTPCs, and complemented our investigation with studies in mouse peritubular cells and in organotypic testes cultures.

Purinergic signaling is dependent on extracellular ATP and sources of this molecule in the testis are physically close to peritubular cells. They include dying germ cells, Sertoli cells, mast cells and nerve fibers (Mayerhofer *et al.*, 1999; Meineke *et al.*, 2000; Baum *et al.*, 2005; Gelain *et al.*, 2005; Xiong *et al.*, 2009). We found that HTPCs, like rodent peritubular cells (Martin-Satue *et al.*, 2009; Martin-Satue *et al.*, 2010), express the ectonucleotidases ENTPD1 and NT5E. This implies that breakdown of extracellular ATP can occur *in vitro* and *in situ*, specifically, but not exclusively, in the peritubular compartment. The peritubular compartment possesses a unique localization, possessing borders with both the tubular and the interstitial areas. Thus, it is conceivable that purines affect cells in both compartments. Despite some evidence for ATP actions in Sertoli, Leydig and germ cells (Casali *et al.*, 2001; Zamoner *et al.*, 2006; Veitinger *et al.*, 2011; Fleck *et al.*, 2016), actions within the peritubular compartment have, to the best of our knowledge, not been reported before. Indeed, an older study in rat (Monaco and Conti, 1986) did not find binding of a labelled adenosine-derivative in cultured rodent peritubular cells, and, hence,

Downloaded from https://academic.oup.com/molehr/article/27/7/gaab037/6276438 by Universitaetsbibliothek Muenchen user on 28 October 2021

concluded that they may not express associated receptors. However, the cells examined were from immature animals and, thus, most likely do not reflect the situation in the adult testis.

In contrast to the mentioned rat study, we identified adenosine receptors in both human and mouse adult testes and derived HTPCs and MTPCs, respectively. In HTPCs, we found A1, A2A and A2B, but not A3, whereas all four receptors were detected in MTPCs. We attempted to localize them *in situ* using commercial antibodies and paraffin-embedded human testes samples. We succeeded, however, only in case of A2B, while all other tested commercial antibodies yielded non-specific results. A2B staining appeared most striking in cells of thickened, remodeled peritubular walls of those seminiferous tubules, in which spermatogenesis was impaired. This may indicate a role for A2B in such cases, but this issue requires additional studies. Such a role would, however, be in line with previous observations. In testes of men with impaired spermatogenesis, signs of sterile inflammatory events are observed, including increased numbers of immune cells, namely mast cells and macrophages (Meineke *et al.*, 2000; Welter *et al.*, 2011; Abdel-Hamid *et al.*, 2018; Mayerhofer *et al.*, 2018). Previous studies showed that increased numbers of mast cells and macrophages accumulate specifically in the peritubular wall compartment. The mentioned studies also identified HTPCs as a cytokine source, which may be directly involved in sterile inflammatory events but also in attracting immune cells to this region (Welter *et al.*, 2011; Fraczek and Kurpisz, 2015; Syriou *et al.*, 2018).

Furthermore, previous cellular studies indicated that ATP raises cytokine production in HTPCs and suggested that P2X receptors are, at least in part, involved in this action (Walenta *et al.*, 2018). Here, the authors observed elevated cytokines 24 h after the addition of ATP. In the present study, results of the malachite green assay indicate that breakdown of ATP in HTPCs clearly occurs during that time period. Therefore, effects of other purines are to be considered, as well. When we tested ATP and its metabolites in parallel, we found indeed that ADP, AMP (data not shown), and specifically adenosine (but not the adenosine metabolite inosine) increased cytokine levels. Hence, actions of purine metabolites appear to be involved in inflammatory events.

The use of NECA, an analogue of adenosine (Bruns *et al.*, 1986), and the use of BAY60-6583, a partial agonist of the A2B receptor (Hinz *et al.*, 2014), allowed us to narrow down the main receptor involved in adenosine signaling and pinpointed A2B as a main player. Studies with siRNA supported involvement of A2B and showed a down-regulation of pro-inflammatory signaling after A2B silencing.

In general, consequences of A2B activation appear to depend on the cellular context. For example, receptor activation was reported to mediate inflammatory responses in the lung (Feoktistov and Biaggioni, 1995; Zhong *et al.*, 2004) or to coordinate mucosal inflammation in the gut (Aherne *et al.*, 2018). While our functional data identified A2B as the main mediator of peritubular cell adenosine signaling, we are aware that other receptors and/or receptor heterodimers may also be involved. Other receptors may include A1 and A2A, as activators of A1 (CCPA) and A2A (CGS 21680) had a weak effect on some pro-inflammatory cytokines.

The actions of BAY60-6583, a partial agonist at A2B, are of note. Like adenosine and NECA, it strongly elevated *IL6* and *CXCL8* but, as we found, the identical concentration of BAY60-6583 had no effect with respect to *CCL7*. Yet, a trend to weak actions became visible, when used at lower concentrations. While it is possible that the signaling cascades required for induction of *IL6* and *CXCL8* differ from the one of *CCL7*, this result may also be related to the specific properties of BAY60-6583 and/or possible formation of receptor heterodimers. BAY60-6583 is described as a partial agonist at A2B (Hinz *et al.*, 2014). Partial activity is documented by studies, in which cAMP accumulation and calcium mobilization assays were employed and in which BAY60-6583 was significantly less efficacious than adenosine or NECA (Hinz *et al.*, 2014). Furthermore, the mentioned study showed that at higher concentrations, BAY60-6583 acts rather as an antagonist at A2B receptors. This may explain, in part, our observation that BAY60-6583 failed to increase CCL7 at a concentration of 10 µM, while when used at lower concentrations a small effect became visible. In addition, it is known that G-protein coupled receptors and ADORAs can form dimers/heterodimers (Moriyama and Sitkovsky, 2010; Smith and Milligan, 2010). Such a possibility may play a role, as well, but remains to be examined in HTPCs. The sum of our results, obtained with adenosine, NECA, siRNA downregulation of A2B and a set of pharmacological tools, implicate A2B in the induction of the majority of inflammatory factors.

We also explored whether adenosine may influence characteristic functions of HTPCs and focused on typical markers (Ungefroren *et al.*, 1995; Maekawa *et al.*, 1996; Mayerhofer, 2013). We found that levels of *GDNF*, the extracellular matrix factors *COL1A1* and *DCN*, as well as *ACTA2* were unchanged. It remains to be shown, whether the minimal (<1.5-fold) elevation of *AR* is of biological relevance. Whether adenosine may be able to influence other aspects of HTPCs also awaits additional studies.

Given the strategic position of TPCs, diffusion of locally generated adenosine should influence both the interstitial and tubular compartment. Indeed, in rodents, receptors and actions were described in Sertoli and Leydig cells (Monaco and Conti, 1986; Bjelobaba *et al.*, 2015). For further insights into intratesticular actions, we turned to the mouse testis and employed organotypic short-term cultures of mouse testis fragments. Results of qPCR indicated that adenosine did not affect Leydig or Sertoli cell markers, but clearly elevated cytokine levels after 6 h. This supports the notion that adenosine is not only active in HTPCs but is a pro-inflammatory molecule in the whole testis.

Of note, in these organotypic short-term cultures of mouse testis fragments, parallel ATP treatment, which was also performed for 6 h, resulted in unchanged or lower cytokine levels. Organotypic testis short-term cultures were performed for 6 h only to ensure viability of testes fragments. This time period may have been too short for effective conversion of ATP to adenosine by the testicular ectonucleotidases. In line with this assumption, a previous cell culture study performed in HTPCs, showed a time-dependency of ATP actions. ATP induced weak actions after 6 h but strong pro-inflammatory actions after 24 h (Walenta *et al.*, 2018). Furthermore, temporarily high levels of ATP most likely exert actions primarily via other receptors (e.g. P2X4/7 in HTPCs; Walenta *et al.*, 2018; Fleck *et al.*, 2021). Whether such actions may include anti-inflammatory effects (suggested by somewhat lower mRNA levels of *Cd2*) awaits further studies. Indeed, to decipher the complex purinergic signaling system of multiple receptors in the testis requires a series of additional studies.

Here we only attempted to explore the possible contribution of peritubular cells to cytokines also in the mouse, and hence we studied isolated MTPCs. In this set of experiments performed, like in HTPCs

Downloaded from https://academic.oup.com/molehr/article/27/7/gaab037/6276438 by Universitaetsbibliothek Muenchen user on 28 October 2021

for 24 h, we found strong pro-inflammatory actions of adenosine. A lower, yet in general, with one exception, comparable activity after addition of ATP also became apparent and suggests that ATP-metabolites including adenosine were generated during 24 h and may be responsible. Taken together, although multiple cells, including immune cells, present in the testis may be involved in cytokine production, and despite species differences (e.g. A3 was found only in MTPCs), we conclude from these studies that adenosine is a pro-inflammatory molecule in the testis and that TPCs are involved in the production of a pro-inflammatory environment via adenosine action.

The results of this study, if transferable to the *in vivo* situation in humans, may be of relevance for male (in)fertility. Sterile inflammation is by now being recognized as a part of idiopathic infertility (Pelliccione *et al.*, 2011; Milardi *et al.*, 2017; Pilatz *et al.*, 2019). Hence, targeted pharmacological inhibition of processes, which fuel inflammatory events may be novel treatment approaches. Inhibition of ENTPD1 by POM-1 may represent such an approach. Indeed POM-1 is being tested for other conditions (Reutershan *et al.*, 2009; d'Almeida *et al.*, 2016; Pimenta-Dos-Reis *et al.*, 2017; Yang *et al.*, 2020). Further, A2B appears to be the major receptor involved and therefore receptor blockers and/or therapeutic antibodies directed against A2B (Wendell *et al.*, 2020) might also be suitable to impair the pro-inflammatory environment.

Supplementary data

Supplementary data are available at *Molecular Human Reproduction* online.

Acknowledgements

The authors thank Kim Dietrich, Astrid Tiefenbacher, Nina Schmid and Carola Herrmann for skilful technical assistance. The authors thank Prof. Dr. Schwarzer (Munich) for providing some of the human testis samples. This work was done in partial fulfilment of the requirements of a Dr. rer. nat. degree (of A.Mi.) at LMU Munich.

Author's roles

A.Mi. performed the majority of the experiments, subsequent analyses and interpretation of the results. A.Ma. conceived of the study. A.Mi, L.W., L.K., M.S. and A.Ma. contributed substantially to the implementation of this study. L.W., K.E., N.M. and H.H. participated in sample generation and analysis. U.P., M.T., F-M.K., B.P., L.S. and M.P. provided biopsies of human testes or mouse testes samples, respectively. A.Mi. and A.Ma. drafted the manuscript. All authors contributed to the writing of the final version and approved it.

Data availability

All data included in this study are available in the main text and the supplementary information. Raw data will be provided upon reasonable request from the corresponding author.

Funding

This study was supported by DFG (Project nos. 245169951/MA1080/23-2 and 368482240/GRK2416), DAAD (Deutscher Akademischer Austauschdienst) and the Academy of Finland.

Conflict of interest

The authors declare no conflict of interest.

References

Abdel-Hamid AAM, Atef H, Zalata KR, Abdel-Latif A. Correlation between testicular mast cell count and spermatogenic epithelium in non-obstructive azoospermia. *Int J Exp Path* 2018;**99**:22–28.

Adam M, Urbanski HF, Garyfallou VT, Welsch U, Kohn FM, Ullrich Schwarzer J, Strauss L, Poutanen M, Mayerhofer A. High levels of the extracellular matrix proteoglycan decorin are associated with inhibition of testicular function. *Int J Androl* 2012;**35**:550–561.

Aherne CM, Collins CB, Rapp CR, Olli KE, Perrenoud L, Jedlicka P, Bowser JL, Mills TW, Karmouty-Quintana H, Blackburn MR. *et al.* Coordination of ENT2-dependent adenosine transport and signaling dampens mucosal inflammation. *JCI Insight* 2018;**3**:e121521.

Albrecht M, Ramsch R, Kohn FM, Schwarzer JU, Mayerhofer A. Isolation and cultivation of human testicular peritubular cells: a new model for the investigation of fibrotic processes in the human testis and male infertility. *J Clin Endocrinol Metab* 2006;**91**:1956–1960.

Allard B, Longhi MS, Robson SC, Stagg J. The ectonucleotidases CD39 and CD73: Novel checkpoint inhibitor targets. *Immunol Rev* 2017;**276**:121–144.

Baum JS, St George JP, McCall K. Programmed cell death in the germline. *Semin Cell Dev Biol* 2005;**16**:245–259.

Bjelobaba I, Janjic MM, Stojilkovic SS. Purinergic signaling pathways in endocrine system. *Auton Neurosci* 2015;**191**:102–116.

Borea PA, Gessi S, Merighi S, Vincenzi F, Varani K. Pharmacology of adenosine receptors: the state of the art. *Physiol Rev* 2018;**98**:1591–1625.

Bruns RF, Lu GH, Pugsley TA. Characterization of the A2 adenosine receptor labeled by [3H]NECA in rat striatal membranes. *Mol Pharmacol* 1986;**29**:331–346.

Burnstock G. Purinergic signalling in endocrine organs. *Purinergic Signal* 2014;**10**:189–231.

Casali EA, da Silva TR, Gelain DP, Kaiser GR, Battastini AM, Sarkis JJ, Bernard EA. Ectonucleotidase activities in Sertoli cells from immature rats. *Braz J Med Biol Res* 2001;**34**:1247–1256.

Colgan SP, Eltzschig HK, Eckle T, Thompson LF. Physiological roles for ecto-5'-nucleotidase (CD73). *Purinergic Signal* 2006;**2**:351–360.

Corriden R, Insel PA. Basal release of ATP: an autocrine-paracrine mechanism for cell regulation. *Sci Signal* 2010;**3**:re1.

d'Almeida SM, Kauffenstein G, Roy C, Basset L, Papargyris L, Henrion D, Catros V, Ifrah N, Descamps P, Croue A. *et al.* The ecto-ATPDase CD39 is involved in the acquisition of the immunoregulatory phenotype by M-CSF-macrophages and ovarian cancer tumor-associated macrophages: regulatory role of IL-27. *Oncoimmunology* 2016;**5**:e1178025.

Downloaded from https://academic.oup.com/molehr/article/27/7/gaab037/6276438 by Universitaetsbibliothek Muenchen user on 28 October 2021

Eubler K, Herrmann C, Tiefenbacher A, Kohn FM, Schwarzer JU, Kunz L, Artur M. Ca(2+) signaling and IL-8 secretion in human testicular peritubular cells involve the cation channel TRPV2. *Int J Mol Sci* 2018;**19**:2829.

Feoktistov I, Biaggioni I. Adenosine A2b receptors evoke interleukin-8 secretion in human mast cells. An enprofylline-sensitive mechanism with implications for asthma. *J Clin Invest* 1995;**96**: 1979–1986.

Fleck D, Kenzler L, Mundt N, Strauch M, Uesaka N, Moosmann R, Bruentgens F, Missel A, Mayerhofer A, Merhof D. *et al.* ATP activation of peritubular cells drives testicular sperm transport. *Elife* 2021;**10**:10.

Fleck D, Mundt N, Bruentgens F, Geilenkirchen P, Machado PA, Veitinger T, Veitinger S, Lipartowski SM, Engelhardt CH, Oldiges M. *et al.* Distinct purinergic signaling pathways in prepubescent mouse spermatogonia. *J Gen Physiol* 2016;**148**; 253–271.

Fraczek M, Kurpisz M. Cytokines in the male reproductive tract and their role in infertility disorders. *J Reprod Immunol* 2015;**108**: 98–104.

Fredholm BB, Abbracchio MP, Burnstock G, Daly JW, Harden TK, Jacobson KA, Leff P, Williams M. Nomenclature and classification of purinoceptors. *Pharmacol Rev* 1994;**46**:143–156.

Gelain DP, Casali EA, de Oliveira RB, de Souza LF, Barreto F, Dal-Pizzol F, Moreira JC. Effects of follicle-stimulating hormone and vitamin A upon purinergic secretion by rat Sertoli cells. *Mol Cell Biochem* 2005;**278**:185–194.

Gelain DP, de Souza LF, Bernard EA. Extracellular purines from cells of seminiferous tubules. *Mol Cell Biochem* 2003;**245**:1–9.

Grinthal A, Guidotti G. CD39, NTPDase 1, is attached to the plasma membrane by two transmembrane domains. Why? *Purinergic Signal* 2006;**2**:391–398.

Hargrove JL, MacIndoe JH, Ellis LC. Testicular contractile cells and sperm transport. *Fertil Steril* 1977;**28**:1146–1157.

Hasko G, Linden J, Cronstein B, Pacher P. Adenosine receptors: therapeutic aspects for inflammatory and immune diseases. *Nat Rev Drug Discov* 2008;**7**:759–770.

Hinz S, Lacher SK, Seibt BF, Muller CE. BAY60-6583 acts as a partial agonist at adenosine A2B receptors. *J Pharmacol Exp Ther* 2014; **349**:427–436.

Jacobson KA, Balasubramanian R, Deflorian F, Gao ZG. G protein-coupled adenosine (P1) and P2Y receptors: ligand design and receptor interactions. *Purinergic Signal* 2012;**8**:419–436.

Le TT, Berg NK, Harting MT, Li X, Eltzschig HK, Yuan X. Purinergic signaling in pulmonary inflammation. *Front Immunol* 2019;**10**:1633.

Linden J, Koch-Nolte F, Dahl G. Purine release, metabolism, and signaling in the inflammatory response. *Annu Rev Immunol* 2019;**37**: 325–347.

Maekawa M, Kamimura K, Nagano T. Peritubular myoid cells in the testis: their structure and function. *Arch Histol Cytol* 1996;**59**:1–13.

Martin-Satue M, Lavoie EG, Fausther M, Lecka J, Aliagas E, Kukulski F, Sevigny J. High expression and activity of ecto-5'-nucleotidase/CD73 in the male murine reproductive tract. *Histochem Cell Biol* 2010;**133**:659–668.

Martin-Satue M, Lavoie EG, Pelletier J, Fausther M, Csizmadia E, Guckelberger O, Robson SC, Sevigny J. Localization of plasma membrane bound NTPDases in the murine reproductive tract. *Histochem Cell Biol* 2009;**131**:615–628.

Mayer C, Adam M, Walenta L, Schmid N, Heikela H, Schubert K, Flenkenthaler F, Dietrich KG, Gruschka S, Arnold GJ. *et al.* Insights into the role of androgen receptor in human testicular peritubular cells. *Andrology* 2018;**6**:756–765.

Mayerhofer A. Human testicular peritubular cells: more than meets the eye. *Reproduction* 2013;**145**:R107–116.

Mayerhofer A, Frungieri MB, Fritz S, Bulling A, Jessberger B, Vogt HJ. Evidence for catecholaminergic, neuronlike cells in the adult human testis: changes associated with testicular pathologies. *J Androl* 1999; **20**:341–347.

Mayerhofer A, Walenta L, Mayer C, Eubler K, Welter H. Human testicular peritubular cells, mast cells and testicular inflammation. *Andrologia* 2018;**50**:e13055.

Meineke V, Frungieri MB, Jessberger B, Vogt H, Mayerhofer A. Human testicular mast cells contain tryptase: increased mast cell number and altered distribution in the testes of infertile men. *Fertil Steril* 2000;**74**:239–244.

Milardi D, Luca G, Grande G, Ghezzi M, Caretta N, Brusco G, De Filpo G, Marana R, Pontecorvi A, Calafiore R. *et al.* Prednisone treatment in infertile patients with oligozoospermia and accessory gland inflammatory alterations. *Andrology* 2017;**5**:268–273.

Monaco L, Conti M. Localization of adenosine receptors in rat testicular cells. *Biol Reprod* 1986;**35**:258–266.

Moriyama K, Sitkovsky MV. Adenosine A2A receptor is involved in cell surface expression of A2B receptor. *J Biol Chem* 2010;**285**: 39271–39288.

Murphy KM, Snyder SH. Adenosine receptors in rat testes: labeling with 3H-cyclohexyladenosine. *Life Sci* 1981;**28**:917–920.

Pelliccione F, d'Angeli A, Cinque B, Falone S, Micillo A, Francavilla F, Amicarelli F, Gandini L, Francavilla S. Activation of the immune system and sperm DNA fragmentation are associated with idiopathic oligoasthenoteratospermia in men with couple subfertility. *Fertil Steril* 2011;**95**:2676–2679– e2671-2673.

Pilatz A, Kilb J, Kaplan H, Fietz D, Hossain H, Schuttler CG, Diemer T, Bergmann M, Domann E, Weidner W. *et al.* High prevalence of urogenital infection/inflammation in patients with azoospermia does not impede surgical sperm retrieval. *Andrologia* 2019;**51**: e13401.

Pimenta-Dos-Reis G, Torres EJL, Quintana PG, Vidal LO, Dos Santos BAF, Lin CS, Heise N, Persechini PM, Schachter J. POM-1 inhibits P2 receptors and exhibits anti-inflammatory effects in macrophages. *Purinergic Signal* 2017;**13**:611–627.

Reutershan J, Vollmer I, Stark S, Wagner R, Ngamsri KC, Eltzschig HK. Adenosine and inflammation: CD39 and CD73 are critical mediators in LPS-induced PMN trafficking into the lungs. *Faseb J* 2009;**23**:473–482.

Romano F, Tripiciano A, Muciaccia B, De Cesaris P, Ziparo E, Palombi F, Filippini A. The contractile phenotype of peritubular smooth muscle cells is locally controlled: possible implications in male fertility. *Contraception* 2005;**72**:294–297.

Schell C, Albrecht M, Mayer C, Schwarzer JU, Frungieri MB, Mayerhofer A. Exploring human testicular peritubular cells: identification of secretory products and regulation by tumor necrosis factor-alpha. *Endocrinology* 2008;**149**:1678–1686.

Smith NJ, Milligan G. Allostery at G protein-coupled receptor homo- and heteromers: uncharted pharmacological landscapes. *Pharmacol Rev* 2010;**62**:701–725.

Downloaded from https://academic.oup.com/molehr/article/27/7/gaab037/6276438 by Universitaetsbibliothek Muenchen user on 28 October 2021

Spinnler K, Kohn FM, Schwarzer U, Mayerhofer A. Glial cell line-derived neurotrophic factor is constitutively produced by human testicular peritubular cells and may contribute to the spermatogonial stem cell niche in man. *Hum Reprod* 2010;**25**:2181–2187.

Syriou V, Papanikolaou D, Kozyraki A, Goulis DG. Cytokines and male infertility. *Eur Cytokine Netw* 2018;**29**:73–82.

Ungefroren H, Ergun S, Krull NB, Holstein AF. Expression of the small proteoglycans biglycan and decorin in the adult human testis. *Biol Reprod* 1995;**52**:1095–1105.

Veitinger S, Veitinger T, Cainarca S, Fluegge D, Engelhardt CH, Lohmer S, Hatt H, Corazza S, Spehr J, Neuhaus EM. *et al.* Purinergic signalling mobilizes mitochondrial Ca(2)(+) in mouse Sertoli cells. *J Physiol* 2011;**589**:5033–5055.

Venereau E, Ceriotti C, Bianchi ME. DAMPs from cell death to new life. *Front Immunol* 2015;**6**:422.

Walenta L, Fleck D, Frohlich T, von Eysmondt H, Arnold GJ, Spehr J, Schwarzer JU, Kohn FM, Spehr M, Mayerhofer A. ATP-mediated events in peritubular cells contribute to sterile testicular inflammation. *Sci Rep* 2018;**8**:1431.

Welter H, Herrmann C, Dellweg N, Missel A, Thanisch C, Urbanski HF, Kohn FM, Schwarzer JU, Muller-Taubenberger A, Mayerhofer A. The glucocorticoid receptor NR3C1 in testicular peritubular cells is developmentally regulated and linked to the smooth muscle-like cellular phenotype. *J Clin Med* 2020;**9**:

Welter H, Huber A, Lauf S, Einwang D, Mayer C, Schwarzer JU, Kohn FM, Mayerhofer A. Angiotensin II regulates testicular peritubular cell function via AT1 receptor: a specific situation in male infertility. *Mol Cell Endocrinol* 2014;**393**:171–178.

Welter H, Kohn FM, Mayerhofer A. Mast cells in human testicular biopsies from patients with mixed atrophy: increased numbers, heterogeneity, and expression of cyclooxygenase 2 and prostaglandin D2 synthase. *Fertil Steril* 2011;**96**:309–313.

Wendell SG, Fan H, Zhang C. G Protein-coupled receptors in asthma therapy: pharmacology and drug action. *Pharmacol Rev* 2020;**72**:1–49.

Xiong W, Wang H, Wu H, Chen Y, Han D. Apoptotic spermatogenic cells can be energy sources for Sertoli cells. *Reproduction* 2009;**137**:469–479.

Yang R, Elsaadi S, Misund K, Abdollahi P, Vandsemb EN, Moen SH, Kusnierczyk A, Slupphaug G, Standal T, Waage A. *et al.* Conversion of ATP to adenosine by CD39 and CD73 in multiple myeloma can be successfully targeted together with adenosine receptor A2A blockade. *J Immunother Cancer* 2020;**8**:e000610.

Zamoner A, Bruno AN, Casali EA, Corbelini PF, Diniz GP, Barreto-Chaves ML, Silva FR, Sarkis JJ, Pessoa-Pureur R. Genomic-independent action of thyroid hormones on NTPDase activities in Sertoli cell cultures from congenital hypothyroid rats. *Life Sci* 2006;**80**:51–58.

Zhong H, Belardinelli L, Maa T, Feoktistov I, Biaggioni I, Zeng D. A(2B) adenosine receptors increase cytokine release by bronchial smooth muscle cells. *Am J Respir Cell Mol Biol* 2004;**30**:118–125.

Zimmermann H. 5'-Nucleotidase: molecular structure and functional aspects. *Biochem J* 1992;**285**:345–365.

Downloaded from https://academic.oup.com/molehr/article/27/7/gaab037/6276438 by Universitaetsbibliothek Muenchen user on 28 October 2021

2.2.1 Supplementary information of publication II

Testicular adenosine acts as a pro-inflammatory molecule: role of testicular peritubular cells: Supplementary Information

Annika Missel[a], Lena Walenta[a], Katja Eubler[a], Nadine Mundt[b,c], Hanna Heikelä[f], Ulrich Pickl[d], Matthias Trottmann[d], Bastian Popper[e], Matti Poutanen[f], Leena Strauss[f], Frank-Michael Köhn[g], Lars Kunz[h], Marc Spehr[b,c] and Artur Mayerhofer[a,*]

Contents:

Supplementary Figure 1
Dose-response studies of inosine and ADORA receptor agonists. mRNA levels of the inflammatory cytokines *IL1B, IL6, CXCL8, CCL2 and CCL7* after (**a**) inosine (10, 100, 1000 µM; 24 h; n = 3), (**b**) ADORA agonist CCPA (0.1, 1, 10 µM; 24 h; n = 3), (**c**) A1 agonist NECA (0.5 nM, 1 nM, n = 2; 10 nM, n = 5; 100 nM, 1000 nM, n = 3; 24 h), (**d**) A2A agonist CGS 2680 (100, 500 nM, 10 µM; 24 h; n = 2) and (**e**) A2B agonist BAY60-6583 (0.1, 1, 10 µM; 24 h; n = 3) treatment of HTPCs. Data are means + SEM normalised to control conditions. Asterisks denote statistical significance ($p < 0.05$) of one-sample t-test.

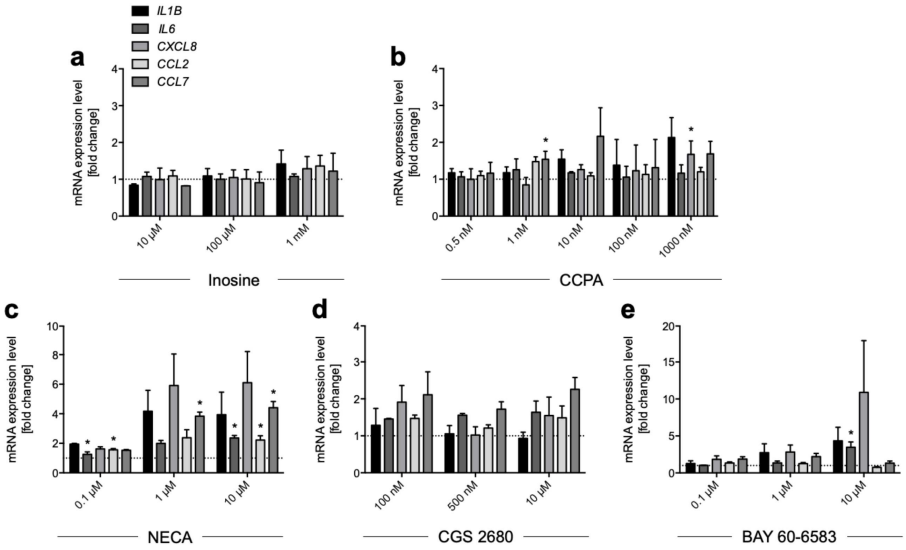

Supplementary Figure 2

Typical HTPC markers are not affected by adenosine. (a) Adenosine treatment (1 mM, 24 h; n = 7) of HTPCs did not affect mRNA levels of typical extracellular matrix markers, COL1A1 and DCN, GDNF or ACTA2. A minimal increase of AR was statistically significant. (b) Furthermore, adenosine treatment (1 mM, 24 h) did not alter protein concentrations in stimulated HTPCs (n = 5) indicating no effect of cell proliferation or cell death. (c) mRNA expression levels of ENTPD1, NT5E and ADORA2B, normalised to RPL19 mRNA expression, remain constant between young (1-3) and advanced (8-18) passages of HTPCs (n = 3).

a,b: Data are means + SEM normalised to control conditions. Asterisks denote statistical significance ($p < 0.05$) of one-sample t-test.

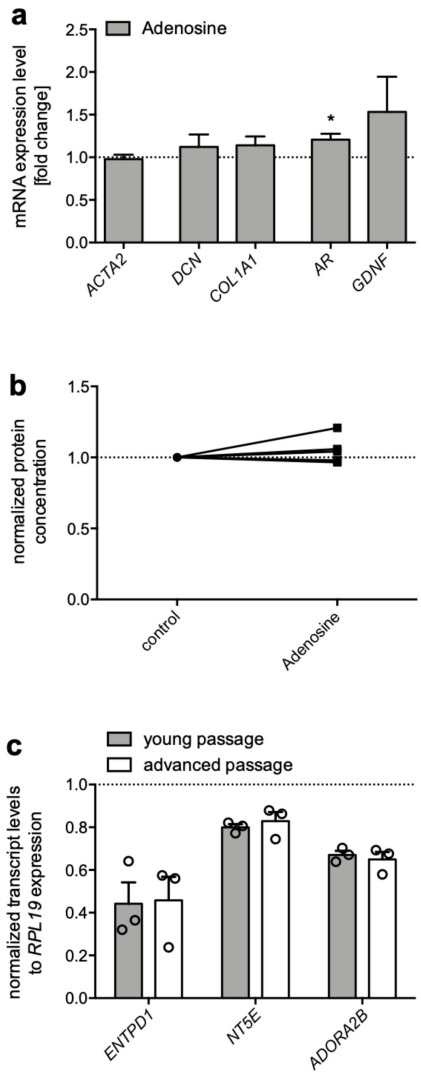

Supplementary Figure 3
Uncropped Western blots and Agarose gels of the Figures 1b, 3b, 3f, 4b.

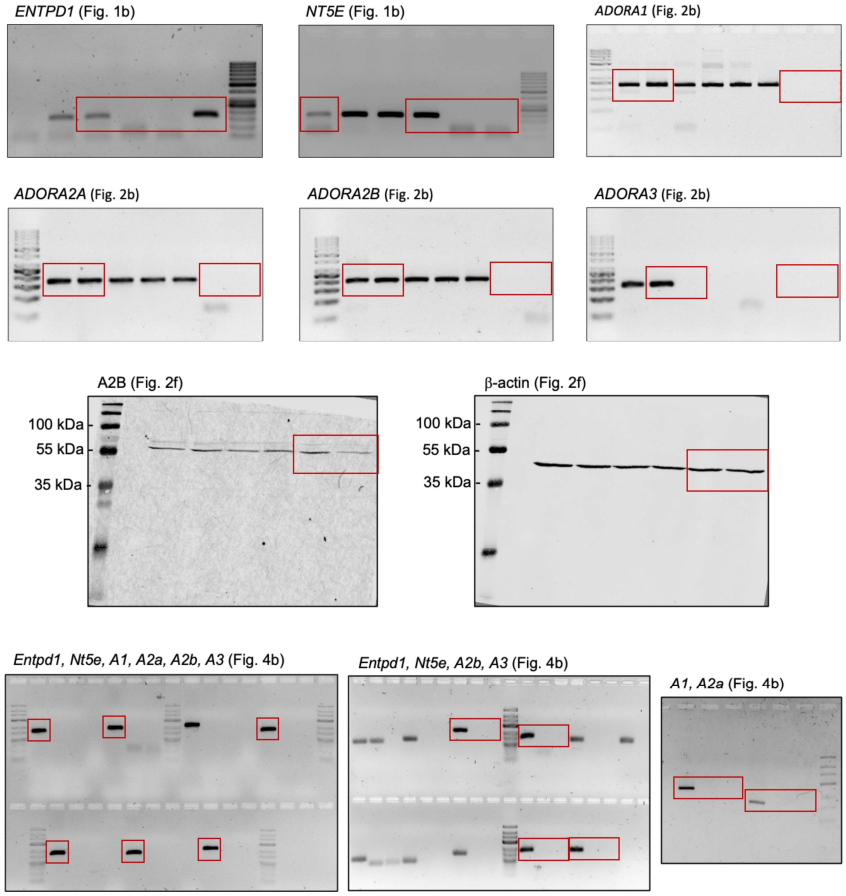

2.3 Publication III (Schmid et al. 2020)

A translational cellular model for the study of peritubular cells of the testis

Nina Schmid*, **Annika Missel***, Stoyan Petkov*, Jan Bernd Stöckl, Florian Flenkenthaler, Georg J. Arnold, Thomas Fröhlich, Rüdiger Behr* & Artur Mayerhofer* (*shared first/last authorship)

Reproduction, 160(2), 259-268. doi:10.1530/REP-20-0100

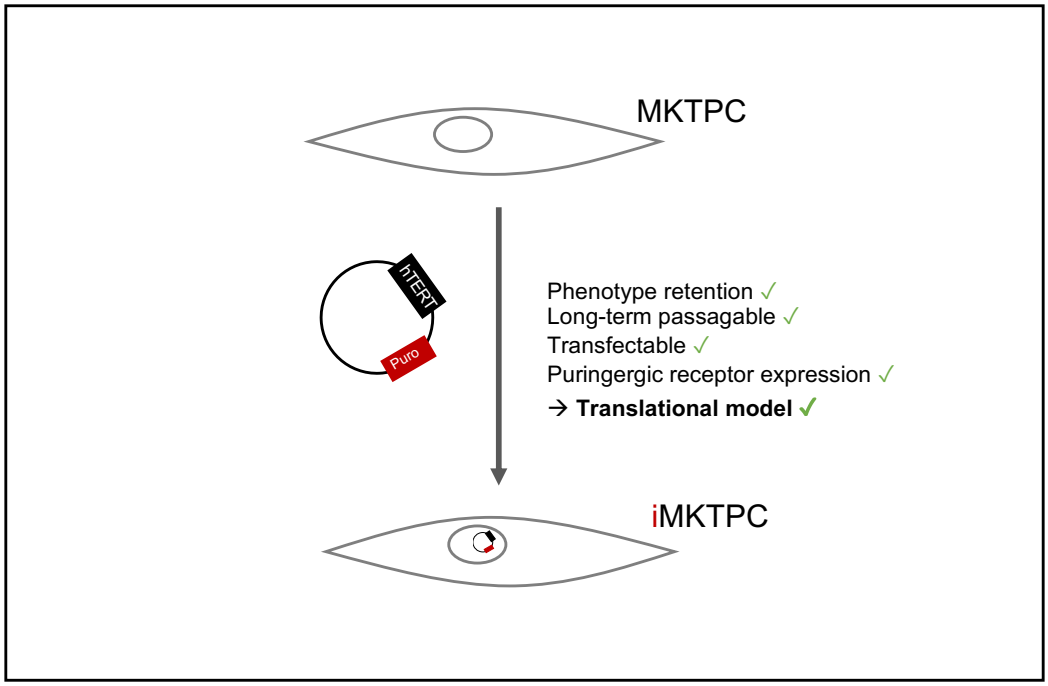

Figure 8. Graphical abstract of Schmid et al. (2020).

MKTPCs were immortalized with a piggyBac transposon containing the human telomerase hTERT. After immortalization, iMKTPCs retained their phenotype and grew continuously without discernable changes in cell culture. They express receptors of the purinergic system and revealed similar upregulation of pro-inflammatory cytokines after ATP exposure, as HTPCs did. Therefore, iMKTPCs are a translational model for human peritubular cells and promising for in-depth studies, as they have the ability for efficient transfection.

Copyright

This article is printed with permission of Bioscentifica Limited (License number: 1155700-1); permission conveyed through Copyright Clearance Center, Inc.

REPRODUCTION
RESEARCH

A translational cellular model for the study of peritubular cells of the testis

Nina Schmid[1,*], Annika Missel[1,*], Stoyan Petkov[2,3,*], Jan B Stöckl[4], Florian Flenkenthaler[4], Georg J Arnold[4], Thomas Fröhlich[4,†], Rüdiger Behr[2,3,†] and Artur Mayerhofer[1,†]

[1]LMU München, Biomedical Center (BMC), Anatomy III – Cell Biology, Martinsried, Germany, [2]Platform Degenerative Diseases, German Primate Center, Göttingen, Germany, [3]DZHK (German Center for Cardiovascular Research), Partner Site Göttingen, Göttingen, Germany and [4]Laboratory for Functional Genome Analysis LAFUGA, Gene Center, LMU München, München, Germany

Correspondence should be addressed to A Mayerhofer; Email: mayerhofer@bmc.med.lmu.de

*(N Schmid, A Missel and S Petkov are joint first authors)

†(T Frohlich, R Behr and A Mayerhofer are joint senior authors)

Abstract

Testicular peritubular cells (TPCs) are smooth muscle-like cells, which form a compartment surrounding the seminiferous tubules. Previous studies employing isolated human testicular peritubular cells (HTPCs) indicated that their roles in the testis go beyond sperm transport and include paracrine and immunological contributions. Peritubular cells from a non-human primate (MKTPCs), the common marmoset monkey, *Callithrix jacchus*, share a high degree of homology with HTPCs. However, like their human counterparts these cells age in vitro and replicative senescence limits in-depth functional or mechanistic studies. Therefore, a stable cellular model was established. MKTPCs of a young adult animal were immortalized by *piggyBac* transposition of human telomerase (*hTERT*), that is, without the expression of viral oncogenes. Immortalized MKTPCs (iMKTPCs) grew without discernable changes for more than 50 passages. An initial characterization revealed typical genes expressed by peritubular cells (androgen receptor (*AR*), smooth-muscle actin (*ACTA2*), calponin (*CNN1*)). A proteome analysis of the primary MKTPCs and the derived immortalized cell line confirmed that the cells almost completely retained their phenotype. To test whether they respond in a similar way as HTPCs, iMKTPCs were challenged with forskolin (FSK) and ATP. As HTPCs, they showed increased expression level of the StAR protein (*StAR*) after FSK stimulation, indicating steroidogenic capacity. ATP increased the expression of pro-inflammatory factors (e.g. *IL1B*; *CCL7*), as it is the case in HTPCs. Finally, we confirmed that iMKTPCs can efficiently be transfected. Therefore, they represent a highly relevant translational model, which allows mechanistic studies for further exploration of the roles of testicular peritubular cells.

Reproduction (2020) **160** 259–268

Introduction

The seminiferous tubules of the mammalian testis are surrounded by smooth muscle-like peritubular, myoid cells (Maekawa *et al.* 1996, Zhou *et al.* 2019), which in man form several layers, in contrast to rodents, which possess only a single layer (Mayerhofer 2013). The transport of sperm is an established function of these cells, they can contract and relax and thereby move sperm to the *rete testis*.

Further insights into the functional roles of peritubular cells have emerged from studies employing a cellular model, human testicular peritubular cells (HTPCs), as well as from mouse models (Chen *et al.* 2014, 2016). According to these results, peritubular cells secrete a great number of factors, by which they can affect the functioning of the testis (Spinnler *et al.* 2010, Mayer *et al.* 2016, 2018).

There are, however, differences between mouse testicular peritubular cells and HTPCs. For example, unlike in mouse (Chen *et al.* 2014), in which testosterone stimulated glial cell line-derived neurotrophic factor (GNDF), this was not found in HTPCs. Instead in men, prostaglandin E2 (PGE_2) stimulated GDNF production (Mayerhofer *et al.* 2018, Rey-Ares *et al.* 2018). Furthermore, HTPCs, but not their mouse counterparts, secrete vast amounts of extracellular matrix (ECM) proteins, which are deposited between the layers in the peritubular wall (Adam *et al.* 2011, Flenkenthaler *et al.* 2014). Some of these, namely decorin (DCN) and biglycan (BGN), are not or only barely detectable in rodent testes. Besides structural functions, DCN and BGN have additional roles and interfere with growth factor-signaling and Toll-like receptor-signaling (Adam *et al.* 2011, Mayer *et al.* 2016). In men, enhanced deposits of

© 2020 Society for Reproduction and Fertility
ISSN 1470–1626 (paper) 1741–7899 (online)
https://doi.org/10.1530/REP-20-0100
Online version via https://rep.bioscientifica.com
Downloaded from Bioscientifica.com at 10/28/2021 11:40:44AM
via Ludwig-Maximilians-University Munchen

ECM components, containing DCN and BGN, can be observed in most cases of male infertility due to impaired spermatogenesis. In these fibrotic-remodeled peritubular walls also mast cells are abundant (Meineke *et al.* 2000). As mast cells are almost absent in rodent testes, this is rather specific for man. Further, testicular mast cells, *via* tryptase, stimulate the production of decorin, which may be involved in fibrotic events within the testis (Adam *et al.* 2011). An increased number of mast cells in human testes may be related to the fact that HTPCs are immunologically active and produce a plethora of growth factors and cytokines (Mayerhofer 2013).

The few examples outlined show that the situation in mouse testes does not completely reflect the human situation and consequently, studies in mice cannot elucidate the full spectrum of peritubular cell functions in human testicular biology. Indeed, a recent gene expression study revealed that testis and liver showed the largest differences of individual genes between mouse and human compared to all other organs (Cardoso-Moreira *et al.* 2019). Therefore, studies employing adequate models for the human situation are required.

HTPCs can be generated by tissue explant culture from individual patients (Albrecht *et al.* 2006) and passaged up to approximately 12 times without substantial noticeable changes. However, as shown recently (Schmid *et al.* 2019), they eventually stop proliferating and show a number of typical senescence-associated changes, like increased cell size, elevated expression of senescence-associated β-galactosidase and telomere shortening. While this may provide insights into aspects of human testicular ageing, this fact limits the use of HTPCs.

Patient-derived cells are heterogenous in several aspects, including levels of secreted products, for example, steroids and cytokines (Landreh *et al.* 2014, Welter *et al.* 2014, Mayer *et al.* 2016). The observed heterogeneity of HTPCs, presumably due to age and patient history, was the primary reason to search for a suitable model organism for in-depth studies of testicular peritubular cells. We characterized testicular peritubular cells from a non-human primate species, *Callithrix jacchus* (Schmid *et al.* 2018). The comparison of HTPCs with these monkey testicular peritubular cells (MKTPCs) clearly indicated that they are an apt model for the human. However, both MKTPCs and HTPCs can only be studied for a limited number of passages, as both age and stop proliferation.

To circumvent the need for constant generation and characterization of MKTPCs, we attempted to generate a cellular model by immortalization of MKTPCs, using the human telomerase transcriptase (*hTERT*) (Masutomi *et al.* 2003, Bocker *et al.* 2008). This approach recently yielded immortalized *Callithrix jacchus* fibroblasts (Petkov *et al.* 2018). Here we describe successful immortalization of primary MKTPCs with a *piggyBac* transposon containing *hTERT*, provide a characterization of the modified cells and document that they are suitable for in-depth mechanistic studies.

Materials and methods

Animal

In the framework of a previous study (Schmid *et al.* 2018), MKTPCs were isolated from the testis of a young adult, sexually mature, three year old, healthy marmoset monkey (*Callithrix jacchus*) (Li *et al.* 2005). Early passages of these cells were examined and characterized previously (Schmid *et al.* 2018). Furthermore, cells from early passages were used for immortalization and subsequent characterization. As described (Schmid *et al.* 2018), the animal mentioned was obtained from the self-sustaining colony of the German Primate Center (Deutsches Primatenzentrum; DPZ, Göttingen). The animal was killed for scientific purposes unrelated to the study. Experienced veterinarians performed the killing. Organ retrieval from *Callithrix jacchus* was carried out in accordance with relevant institutional guidelines and legal regulations, namely the German Animal Protection Act. The collection of tissue samples after killing of non-treated animals requires only documentation and a retrospective report, and a separate permission for organ collection after killing, as well as an ethics statement are not required according to the German Animal Protection Act (§ 7 Abs. 2 Nr. 3, Tierschutzgesetz). Parts of the testis were fixed in Bouin's fixative and embedded in paraffin, sectioned and stained (HE).

Culture of MKTPCs

MKTPCs isolated in the previous study (Schmid *et al.* 2018) were cultured on 0.1% gelatin-coated cell-culture dishes and incubated at 37°C/5% CO_2 in Dulbecco's modified Eagle's medium (DMEM) high glucose (Gibco) with supplementary 10% fetal calf serum (Capricom Scientific GmbH, Ebersdorfergrund, Germany) and 1% penicillin/streptomycin (Life Technologies). Cells grew and were passaged until growth slowed and ceased (around passage (P) 16).

Immortalization of MKTPCs with hTERT-*expressing* piggyBac *transposon vector and culture of iMKTPCs*

The generation of the *piggyBac* transposon plasmid for overexpression of *hTERT* (pTT-PB-hTERT-Puro) was published recently (Petkov *et al.* 2018). The construction of the *piggyBac* transposase expression vector (pcA3-PBase-Tomato) was described earlier (Debowski *et al.* 2015). It encodes for a hyperactive, codon-optimized *piggyBac* transposase that efficiently catalyzes the genomic integration of the *hTERT* expression cassette (present in the co-transfected plasmid pTT-PB-hTERT-Puro), which is flanked by the 5′- and the 3′-terminal repeats of the transposon. The PBase open reading frame (ORF) is followed by an internal ribosomal entry site (IRES) and the ORF for the fluorescent protein tdTomato. In preparation for nucleofection, the MKTPCs (P6–P7) were split twice on gelatin-coated tissue culture dishes to improve attachment and proliferation. MKTPCs (termed DPZ_cjTPC

Downloaded from Bioscientifica.com at 10/28/2021 11:40:44AM
via Ludwig-Maximilians-University Munchen

for archival purpose at the DPZ) at P9–P10 were nucleofected using Amaxa™ 4D-Nucleofector™ (Lonza, Basel, Switzerland) according to the manufacturer's instructions. Briefly, 3.5 µg pTT-PB-hTERT-Puro and 2.8 µg pcA3-PBase-Tomato plasmids were added to 1×10^6 cells suspended in 100 µL P2 buffer (Lonza). The suspension was mixed, transferred to an electroporation cuvette (Lonza), and nucleofected using program CA-137. The cells with stable integration of the *piggyBac* transposon were selected for 2 weeks with 1 µg/mL puromycin (Sigma) starting at 48 h post nucleofection. Thereafter, the puromycin concentration was reduced to 0.3 µg/mL and maintained during long-term culture (>P50). All other culture conditions were otherwise identical to the ones of primary MKTPCs. For all experiments iMKTPCs from P21 up to P50 were used, as indicated in the following.

Functional studies

Treatment of iMKTPCs (P23–P50) was performed with FSK (10 µM, #F6886) or ATP (1 mM, #A6419). Both chemicals were purchased from Sigma-Aldrich. Defined cell numbers were seeded in DMEM containing 10% FCS. The medium was changed to serum-free medium 24 h before the treatment. The substances and respective solvents (FSK: ethanol; ATP: serum free DMEM) were added to the cells and transcript levels were evaluated after 24 h of stimulation. Results are normalized to control conditions.

Immunofluorescence

Prior to fixation with 3.7% formaldehyde (Sigma) for 10 min, iMKTPCs (P26) were seeded onto cover slips overnight. Washing, permeabilization, staining and mounting steps, as well as controls, were performed as described previously (Schmid *et al.* 2018). Antibodies were diluted in 0.1% Triton X-100/PBS + 5% goat normal serum (CNN1 1:100, Epitomics, Cambridge, UK; ACTA2 1:200, Sigma).

RNA isolation and qPCR

Cultured iMKTPCs (P23–P50) and MKTPCs (P4) were washed with PBS and total RNA was isolated according to the manufacturer's instructions of the Qiagen RNeasy Plus Micro Kit (Qiagen). Next, 1 µg of the isolated RNA was transcribed to cDNA using random 15-mer primers and reverse transcriptase (SuperScript II, 200 U/µL, Invitrogen GmbH). Real-time qPCR was performed in duplicates using the Roche LightCycler 96 System (Roche Diagnostics) and the Quantifast SYBR Green PCR Kit (Qiagen). After a 95°C preincubation step (300 s), 40 cycles of PCR amplification were performed using intron-spanning primer pairs (synthesized by Metabion, Munich, Germany). The protocol included the following: 95°C for 10 s, annealing and extension (60–72°C) for 15 s and a melting step (65–97°C) for 60 s. Detailed primer information is available in Table 1. Products were also visualized with Midori Green staining in agarose gels (*ACTA2*, *AR*, *CNN1*, *hTERT*, *P2RX4*, *P2RX7*). C_q values of treated cells were calculated using *RPL19* as an endogenous reference (*CCL2*, *CCL7*, *CXCL8*, *IL1B*, *IL6*, *StAR*). *RPL19* was used because of stable expression in both, MKTPCs and iMKTPCs, indicated by constant C_q values. The proof of amplicon identity was performed by sequence analysis (GATC, Konstanz, Germany). Data analysis was carried out using the one-sample *t*-test of $-\Delta\Delta C_q$ values.

Table 1 Oligonucleotide primer for qPCR studies.

Gene	Gene name	Reference ID	Nucleotide sequence	Amplicon size, bp
ACTA2	Actin alpha 2, smooth muscle	NM_001613.2	5′-ACCCAGTGTGGAGCAGCCC-3′ 5′-TTGTCACACACCAAGGCAGT-3′	100
AR	Androgen receptor	XM_008989422.2	5′-GCCCCTGATCTGGTTTTCAA-3′ 5′-CCACTGGAATAATGCTGAAGAGT-3′	163
CCL2	C-C motif chemokine ligand 2	XM_002748333.4	5′-GCAGCAAGTGTCCCAAAGAA-3′ 5′-TGGGGTTATGGAGTGAGTGT-3′	154
CCL7	C-C motif chemokine ligand 7	XM_002748371	5′-AGAAGAATCACCACCAGCCA-3′ 5′-GGCTTGGTTTCAGTTCAGTCA-3′	175
CNN1	Calponin 1	XM_017026289.1	5′-CGAAGACGAAAGGAAACAAGGT-3′ 5′-GCTTGGGGTCGTAGAGGTG-3′	183
CXCL8	C-X-C motif chemokine ligand 8	XM_002745733.3	5′-ACAAGAGCCAGCAAGAAACG-3′ 5′-CAGTGTGGTCCCCTCTCAAT-3′	233
hTERT	Human telomerase reverse transcriptase	NM_198253.3	5′-CTGGACGATATCCACAGG-3′ 5′-AAGTTCACCACGCAGCCATA-3′	653
IL1B	Interleukin 1 beta	XM_002757505.4	5'-GGTTGTCGTGGCTATGGAGA-3′ 5'-TTTTGTTGTGCATCCCGGAG-3′	189
IL6	Interleukin 6	XM_017975106.1	5′-AAGAGGTAGCTGCCCCAAAT-3′ 5′-AGTGCCTCTTTGCTGCTTTC-3′	145
P2RX4	Purinergic receptor P2X 4	NM_001256796.2	5′-GATCCCTTCTGCCCCATATT-3′ 5′-AGGTTGCAGTCCCAGTTGAC-3′	119
P2RX7	Purinergic receptor P2X 7	NM_002562.6	5′-CCACGAGAAACATCTTGACA-3′ 5′-CTGTATTTGGGACGGCAGTG-3′	211
RPL19	Ribosomal protein L19	NM_001330200.1	5′-AGGCACATGGGCATAGGTAA-3′ 5′-CCATGAGAATCCGCTTGTTT-3′	199
StAR	Steroidogenic acute regulatory protein	NM_000349	5′-ACGTGGATTAACCAGGTTCG-3′ 5′-CAGCCCTCTTGGTTGCTAAG-3′	149

Downloaded from Bioscientifica.com at 10/28/2021 11:40:44AM
via Ludwig-Maximilians-University Munchen

β-Galactosidase staining

As previously described, cells from both early and advanced passages of MKTPCs (P8; P16) and iMKTPCs (P28; P38; P48) were seeded onto coverslips in a 24-well plate (Schmid *et al.* 2018). Staining with β-galactosidase was carried out according to manufacturer's instructions using a commercial kit (Senescence β-Galactosidase Staining Kit, Cell Signaling Technology #9860, Danvers, MA, USA). Pictures were taken using the Zeiss Axiovert microscope (Zeiss GmbH).

Transfection studies

iMKTPCs (1.4×10^6 cells per reaction) from advanced passage (P23–P50) were mixed with pmaxGFP™ vector (Lonza, 2 µg/reaction) and transfected *via* electroporation using the Amaxa™ Nucleofector™ Technology (Lonza). After electroporation, iMKTPCs were immediately transferred to cell culture media (37°C), plated on cell culture dishes and incubated for 24 h at 37°C/5% CO_2. Transfection efficiency was evaluated by counting GFP-positive cells in all viable, adherent growing cells. Cell size and cell viability were measured using the CASY® Cell Counter on the principle of variations in electrical resistance (Schärfe Systems, Reutlingen, Germany), as described before (Schell *et al.* 2010).

Proteome analysis of MKTPCs and iMKTPCs

Cell pellets (primary MKTPCs: P2; iMKTPCs: P 21–25) were lysed in 8 M urea and 50 mM ammonium bicarbonate, protein content was quantified with a Pierce 660 nm protein assay (Thermo Fisher Scientific). Proteins were reduced (4 mM dithiothreitol/2mM + Tris(2-carboxyethyl)phosphine final concentrations) and alkylated (8 mM iodoacetamide final concentration), followed by digestion with Lys-C (enzyme/total protein: 1/100, Wako) for 4 h and trypsin (enzyme/total protein: 1/50, Promega) overnight at 37°C. LC-MS/MS was performed with an Ultimate 3000 RSLC instrument coupled to an Q Exactive HF-X mass spectrometer. About 2.5 µg peptides were separated on an EASY-Spray column (50 cm, 2 µm, C18, Thermo Fisher Scientific) with a two-step gradient from 3% B (0.1% formic acid in acetonitrile) to 25% in 160 min followed by a ramp to 40% in 10 min. Samples were acquired in three technical replicates. The data was processed using MaxQuant (v. 1.6.1.0) (Tyanova *et al.* 2016) with the UniProt subset for *Callithrix jacchus* (retrieval date: 04/29/2019) supplemented by the built-in contaminant database of MaxQuant. For protein quantification the MaxQuant label-free quantification (LFQ) strategy was used. The LFQ values are based on mass spectrometry intensity values of peptides and reflect the amounts of the proteins within a sample. For more details please refer to Cox *et al.* (2014). Further data analysis including statistical evaluation was done with Perseus (1.6.5.0) and R (3.6.1) software. Gene ontology (GO) analysis was performed with the Panther online tool (http://pantherdb.org) and the GO 'biological process' and 'molecular function' databases.

Results

Replicative senescence in MKTPCs and immortalization of MKTPCs by the insertion of hTERT

Primary MKTPCs were isolated from testicular tissue of a healthy, young, adult marmoset monkey with normal spermatogenesis (Fig. 1A). After serial passaging of MKTPCs, signs of replicative senescence appeared, as expected and previously observed in HTPCs (Schmid *et al.* 2019). This was indicated by prominent senescence-associated β-galactosidase (SA-β-gal) staining of MKTPCs in advanced passages (P16; Fig. 1B). Further, the cells stopped growing and cell size increased (mean diameter of trypsinized MKTPCs at P2: 20.71 µm and at P12: 24.33 µm; more than 1 million cells evaluated using CASY). In contrast, the cell size of iMKTPCs did not change in advanced passages (mean diameter of trypsinized iMKTPCs P24: 21.35 µm and P48: 21.41 µm; more than 1 million cells evaluated using CASY).

The insertion of *hTERT* using a *piggyBac* transposon (Petkov *et al.* 2018) was recently described for fibroblasts from *Callithrix jacchus*. An identical approach was chosen for MKTPCs. While mRNA expression of *hTERT* was found in the immortalized cell line, called iMKTPCs, whole testis samples and primary MKTPCs lacked *hTERT* expression (Fig. 1C). The iMKTPCs grew for more than 50 passages, without discernable morphological changes. Importantly, as seen in phase-contrast images of iMKTPCs in different advanced passages (P28; P38; P48), they lacked senescence-associated β-galactosidase expression (Fig. 1D).

Characteristic markers for testicular peritubular cells in iMKTPCs

In an initial step immunofluorescence staining for characteristic markers of TPCs was implemented to examine iMKTPCs. We observed, as expected and documented for MKTPCs (Schmid *et al.* 2018), positive staining for the smooth-muscle markers ACTA2 and CNN1 (Fig. 2A and B). Likewise, mRNA expression of both markers was detected. In addition, *AR* was readily detected (Fig. 2C). The expression of these markers was similar to the primary MKTPCs, prior to immortalization, implying that iMKTPCs keep their typical phenotype, in general.

Proteome analysis of iMKTPCs vs MKTPCs

In order to further investigate, how the protein pattern of MKTPCs is affected by the immortalization procedure, we performed a holistic proteome analysis of the primary MKTPCs (P2) and of iMKTPCs (P21–25). In MKTPCs and iMKTPCs we were able to identify 4033 and 4271 proteins, respectively. The entire list of identified proteins can be found in Supplementary Table 1

Downloaded from Bioscientifica.com at 10/28/2021 11:40:44AM
via Ludwig-Maximilians-University Munchen

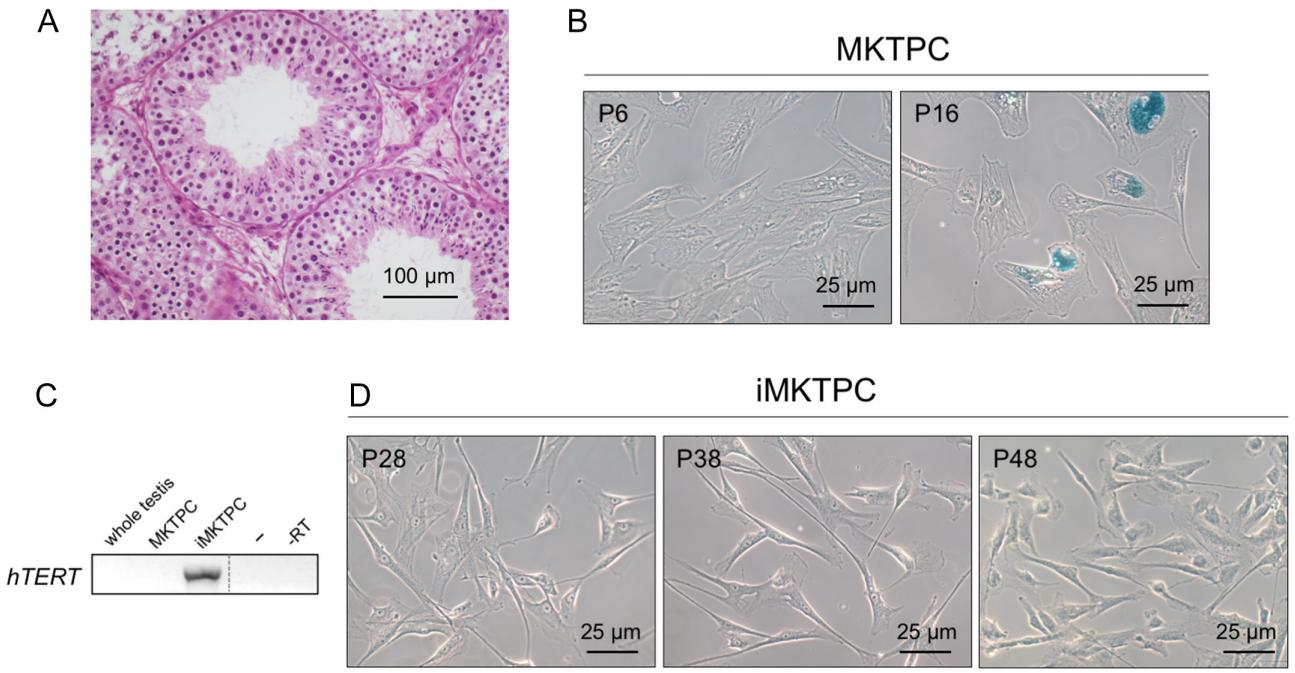

Figure 1 Immortalization of MKTPCs. (A) Morphology (H.E. staining) of the testis from the donor animal used for MKTPC isolation. (B) Senescence-associated β-galactosidase staining of primary MKTPCs in an early passage (P6) and an advanced passage (P16). (C) Expression of *hTERT* in immortalized cells (P31), but not in primary cells (P4) or whole testis (-: no template control; -RT: no reverse transcription control). (D) Absence of senescence-associated β-galactosidase staining of iMKTPCs in advanced passages (P28; P38; P48).

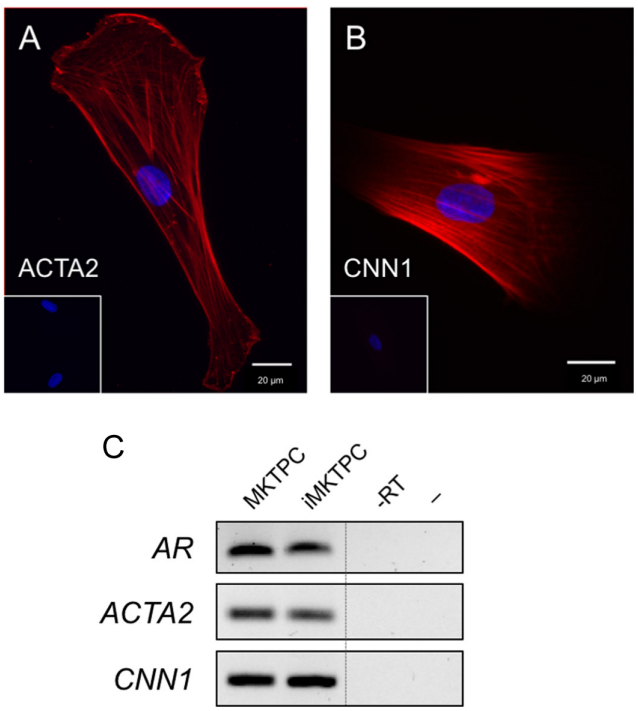

Figure 2 Initial characterization of iMKTPCs. (A) Immunofluorescence of smooth-muscle actin (ACTA2) and (B) calponin (CNN1) in iMKTPCs (P26). Inserts: controls (omission of primary antibody). (C) Expression analysis of androgen receptor (*AR*), *ACTA2* and *CNN1* in MKTPCs (P4) and iMKTPCs (P31) (-: no template control; -RT: no reverse transcription control).

(see section on supplementary materials given at the end of this article). Almost 90% of the identified proteins were found in both iMKTPCs and MKTPCs, indicating a high similarity of both proteomes. Of note, not only the expression of smooth muscle proteins, such as ACTA2 and CNN1, remains but also proteins relevant for further functions of peritubular cells, like DCN and BGN, were found in MKTPCs, as well as in iMKTPCs. In the next step, we performed a quantitative comparison of iMKTPCs vs MKTPCs proteomes. Hierarchical clustering separates iMKTPCs and MKTPCs indicating alterations in the proteome of iMKTPCs due to the transfection with *piggyBac* transposon plasmid (Fig. 3A). However, the scatter plot of protein intensity values (MaxQuant LFQ values) showed a high correlation coefficient of 0.96 (Fig. 3B) between MKTPCs and iMKTPCs. Proteins ranked by LFQ intensity values revealed similar S-shaped distributions over a dynamic range of four orders of magnitude of MS signals in the two cell types (Fig. 3C). To further investigate if the most abundant proteins in MKTPCs are also highly abundant in iMKTPCs, the 25 most abundant iMKTPC proteins were sorted according to their median intensity and compared to their abundance rank in MKTPCs. In all cases the proteins are contained in the top 50 list of most abundant MKTPC proteins (Table 2). This result reflects that immortalization affects the abundance of very high abundant MKTPC proteins. This is not surprising, since cell immortalization is a significant intervention into a

Downloaded from Bioscientifica.com at 10/28/2021 11:40:44AM
via Ludwig-Maximilians-University Munchen

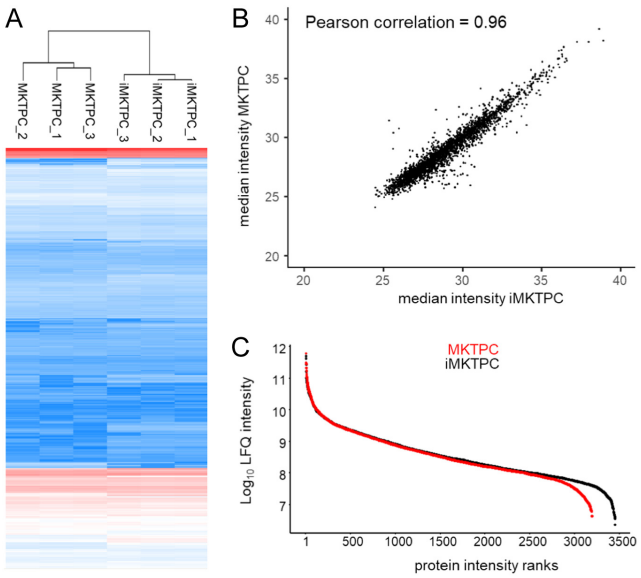

Figure 3 Quantitative proteome analysis of MKTPCs and iMKTPCs. Protein abundance was determined by MaxQuant label-free quantification (LFQ). (A) Hierarchical clustering analysis and (B) scatter plot of median log2 LFQ protein intensities from MKTPCs and iMKTPCs samples. The Pearson correlation coefficient is depicted in the left upper corner. (C) Dynamic range of the identified MKTPC and iMKTPC proteins. Proteins were ranked by their intensity values. Log10 intensities for each protein were plotted vs their rank. Dots represent single proteins.

complex biological system. Nevertheless, the 25 most abundant iMKTPC proteins (out of 4271 identified) were also very highly abundant in MKTPCs (among the 50 most abundant out of 4033 identified MKTPC proteins), indicating that the phenotype remains preserved to a high degree. To analyze the similarity between MKTPCs and iMKTPCs at the level of protein function, identified proteins were subjected to the PANTHER analysis tool. For both 'Biological Process' and 'Molecular Function' the proportion of Gene Ontology terms is very similar (Fig. 4).

Functional studies in iMKTPCs

A recent study described extracellular ATP as a mediator of danger-signaling in HTPCs by increasing expression of pro-inflammatory cytokines (Walenta *et al.* 2018). ATP, among others, may be derived from mast cells in human testes (Gelain *et al.* 2003, Junger 2011). Cell culture treatments of iMKTPCs (P23–P50) revealed similar results when examined by qPCR, showing upregulation of the inflammation-associated genes *IL1B*, *IL6*, *CXCL8*, *CCL2* and *CCL7* upon ATP treatment (Fig. 5A). Expression of the purinoceptor subtypes *P2RX4* and *P2RX7*, which in HTPCs appear to mediate these actions (Walenta *et al.* 2018), was found in cultured MKTPCs and iMKTPCs, as well (Fig. 5B). Further, stimulation of iMKTPCs (P23–P50) with FSK resulted in

Table 2 The top 25 most abundant iMKTPC proteins and their respective abundance rank in the MKTPC proteome.

Gene name	Protein name	Rank	
		iMKTPC	MKTPC
VIM	Vimentin	1	2
ACTG1	Actin, cytoplasmic 2	2	1
MYH9	Myosin-9	3	3
FLNA	Filamin-A	4	4
LGALS1	Galectin-1	5	14
TUBB4B	Tubulin beta-4B chain	6	11
ANXA2	Annexin A2	7	16
TPM1	Tropomyosin alpha-1 chain	8	5
ACTN1	Alpha-actinin-1	9	9
CALD1	Caldesmon	10	8
TAGLN	Transgelin	11	6
PKM	Pyruvate kinase PKM	12	20
ACTC1	Actin, alpha cardiac muscle 1	13	10
ACTA2	Actin, aortic smooth muscle	14	7
ENO1	Alpha-enolase	15	12
TUBA1B	Tubulin alpha-1B chain	16	17
PPIA	Peptidyl-prolyl cis-trans isomerase A	17	13
PRDX1	Peroxiredoxin-1	18	41
GAPDH	Glyceraldehyde-3-phosphate dehydrogenase	19	21
AHNAK	Neuroblast differentiation-associated protein AHNAK (Desmoyokin)	20	25
P4HB	Protein disulfide-isomerase A3	21	36
ACTN4	Alpha-actinin-4	22	18
HSPA8	Heat shock cognate 71 kDa protein	23	24
ANXA5	Annexin A5	24	19
PDIA3	Protein disulfide-isomerase A3	25	48

elevated mRNA levels of *StAR*, as described earlier for their human equivalent, HTPCs (Landreh *et al.* 2014), indicating their steroidogenic capacity (Fig. 5C). Finally, iMKTPCs (P23–P50) were efficiently transfected with a pmaxGFP™ vector by electroporation. GFP expression was observed in 76.1% of the viable, adherent growing cells after electroporation (Fig. 5D).

Discussion

Rodent models are often used in biomedical research. Yet, results of a recent gene expression study showed that among the organs examined the testis, together with liver, shows the largest differences in the expression of individual genes between mouse and human (Cardoso-Moreira *et al.* 2019). This emphasizes that in order to understand the human situation adequate models for the testis are required.

We previously identified *Callithrix jacchus* as a possible model, because testicular structures of marmosets are comparable with the ones in humans, including characteristics of germ cell development and function and the multilayered peritubular wall (Michel & Mahouy 1990, Millar *et al.* 2000, Mansfield 2003, Zuhlke & Weinbauer 2003). In addition, the whole genome of *Callithrix jacchus* is known (Sato *et al.* 2015),

Downloaded from Bioscientifica.com at 10/28/2021 11:40:44AM
via Ludwig-Maximilians-University Munchen

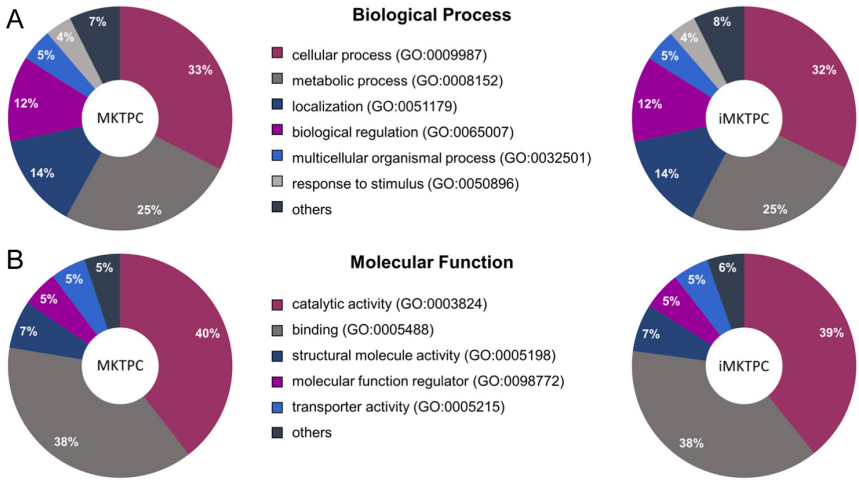

Figure 4 Functional annotation of identified MKTPC and iMKTPC proteins. PANTHER analysis using the (A) 'biological process' and (B) 'molecular function' Gene Ontology databases for MKTPC (left) and iMKTPC (right) proteomes.

enabling further investigations on the genomic and proteomic level.

Previously, MKTPCs from six different healthy, young marmoset monkeys, with normal spermatogenesis (raised under controlled conditions) were analyzed and the results confirmed that they very closely resemble patient-derived HTPCs (Schmid *et al.* 2018). The analysis of the proteome and the correlation analysis with HTPCs revealed conformity between MKTPCs and HTPCs at the level of protein expression patterns and a high degree of inter-individual reproducibility of MKTPCs. However, the use of MKTPCs for mechanistic studies has limits, as they age in cell culture, change their phenotype and stop proliferation. Signs of replicative senescence are observed after 10–16 passages in MKTPCs (Fig. 1B). Similar changes were seen in HTPCs after around 12 passages (Schmid *et al.* 2019). While this allows one to study the specific senescence-associated changes, which may then allow conclusions to testicular ageing (Schmid *et al.* 2019), the cessation of cell proliferation rules out additional experiments.

Therefore, MKTPCs derived from a young adult animal exhibiting normal spermatogenesis and testicular morphology (Fig. 1A), previously characterized together with further MKTPCs from other individuals (Schmid *et al.* 2018), were immortalized by insertion of a *piggyBac* transposon with *hTERT*. Such an approach has previously yielded immortalized fibroblasts (Petkov *et al.* 2018). This method does not need viral oncogenes, which could also contribute to the preservation of peritubular phenotype of iMKTPCs. The immortalized MKTPCs (termed DPZ_cjTPC1) grew without recognizable change for more than 50 passages in the meantime in our lab. No evidence for cellular senescence, indicated by senescence-associated β-galactosidase activity was observed (up to P48), but occurred in the original, primary cells in advanced passages, in which cell proliferation also slowed and eventually stopped.

Beside stability during cell culture experiments, the similarity to the primary cell is important for a cell culture model. Therefore, we investigated the molecular profiles of the primary and the immortalized MKTPCs at the highly relevant level of the proteome. Despite alterations induced by the immortalization procedure, the scatter plot of MKTPCs vs iMKTPCs protein intensity values showed a Pearson correlation coefficient of >0.95 clearly demonstrating a high degree of similarity between the abundance patterns of the primary MKTPC and the derived iMKTPC proteomes. Moreover, the preservation of the smooth muscle-like phenotype is reflected by the high abundance of characteristic proteins in iMKTPCs. Using a label-free quantification approach, we could show that the 25 most abundant MKTPC protein groups remain highly expressed in iMKTPCs. Also, a functional GO analysis of identified MKTPC and iMKTPC proteins lead to nearly identical results indicating that the iMKTPCs almost completely retain their phenotype after immortalization.

As the primary goal was to generate an adequate model for HTPCs, we next examined whether the response of iMKTPCs to FSK is comparable to the one described in HTPCs previously. HTPCs when challenged with FSK, increased level of *StAR* transcripts (Landreh *et al.* 2014). The primary MKTPCs and the derived iMKTPCs express *StAR*, like HTPCs, iMKTPCs responded to FSK stimulation by increased level of *StAR*, which indicates their steroidogenic capacity and thus may allow additional studies (Chemes *et al.* 1985, Haider 2004). HTPCs produce pro-inflammatory factors (e.g. *IL1B*, *CCL7*), which increased upon stimulation with ATP (Walenta *et al.* 2018). This was also found in iMKTPCs. Both primary MKTPCs and iMKTPCs express possible mediators of ATP signaling, the purinoceptors P2XR4 and P2RX7.

We evaluated the potential for mechanistic studies involving transfection in iMKTPCs. A transfection approach of iMKTPCs using the pmaxGFP® vector

Downloaded from Bioscientifica.com at 10/28/2021 11:40:44AM
via Ludwig-Maximilians-University Munchen

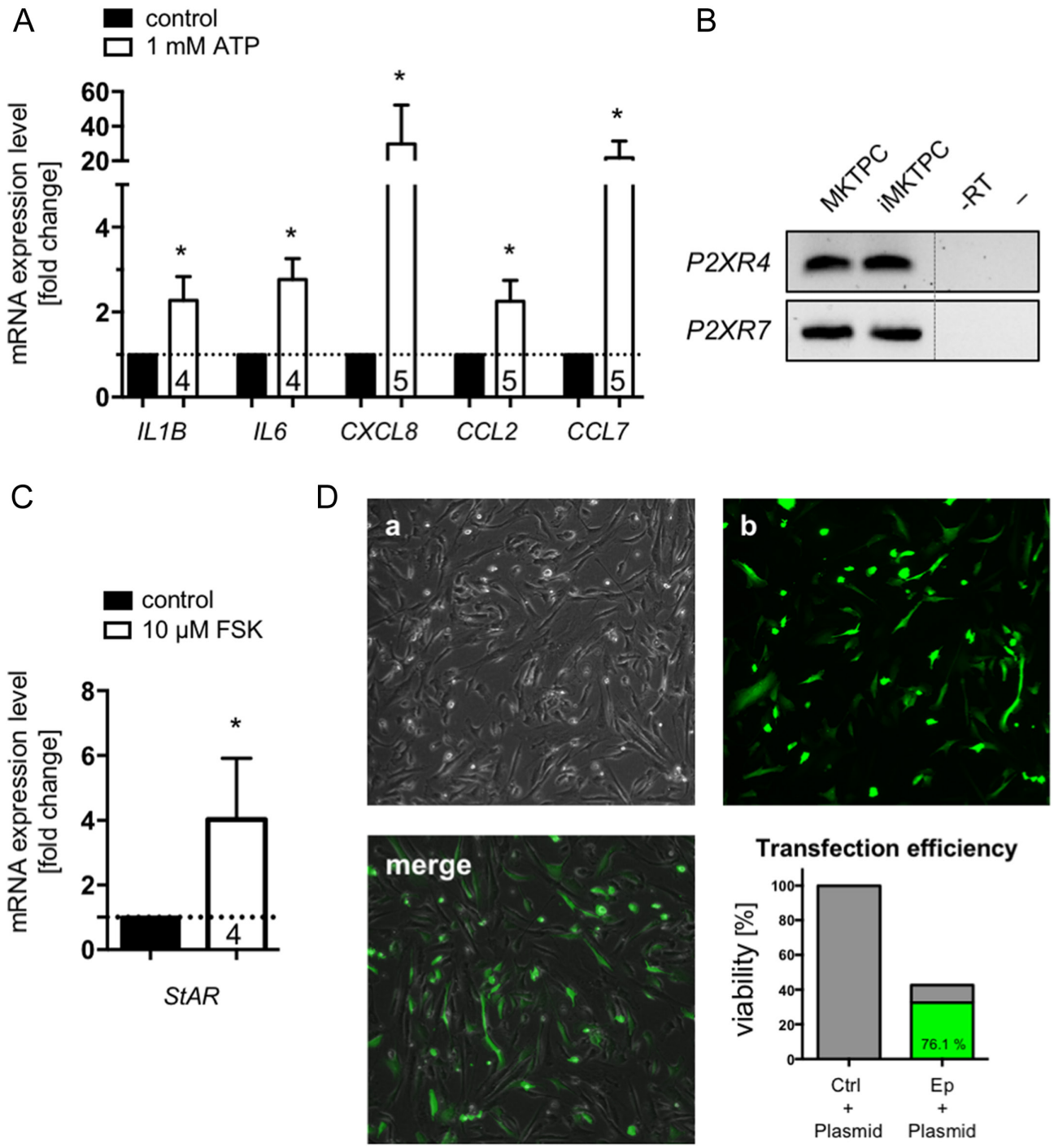

Figure 5 Cell culture treatment of iMKTPCs. (A) Treatment of iMKTPCs with ATP (1 mM, 24 h) significantly increased expression of pro-inflammatory factors (*IL1B*, *IL6*, *CXCL8*, *CCL2*, *CCL7*). (B) *P2XR4* and *P2XR7* expression in MKTPCs (P4) and iMKTPCs (P31) (-: no template control; -RT: no reverse transcription control). (C) Summary of qPCR analyses of *StAR* levels after FSK (10 µM, 24 h) treatment of iMKTPCs. For the qPCR studies iMKTPCs from four to five different passages (P23–P50) were used. qPCR data are means + S.D., normalized to the respective untreated controls. Asterisks denote statistical significance, $*P < 0.05$ (one-sample *t*-test). (D) Transfection *via* electroporation (Ep) of iMKTPCs with pmaxGFP™ showed 76.1% efficiency of the viable, adherent growing cells.

Downloaded from Bioscientifica.com at 10/28/2021 11:40:44AM
via Ludwig-Maximilians-University Munchen

and electroporation revealed that a high transfection efficiency can be reached. This allows, for instance, gene activation or inactivation studies, for example, using CRISPR/Cas9 technology, or overexpression of various proteins aimed at the development of potential treatments for infertility, in a stable cellular environment.

In conclusion, the results of this study indicate that iMKTPCs, derived from a healthy non-human primate, raised under controlled conditions, are a highly relevant translational model and a surrogate for HTPCs, which in contrast stem from patients and show high inter-individual variability. iMKTPCs will allow mechanistic studies to further explore the roles of peritubular cells of the testis, without the need of additional animals. We anticipate that the use of these cells may lead to a better understanding of the roles of peritubular cells in male (in)fertility.

Supplementary materials

This is linked to the online version of the paper at https://doi.org/10.1530/REP-20-0100.

Declaration of interest

The authors declare that there is no conflict of interest that could be perceived as prejudicing the impartiality of the research reported.

Funding

This work was supported by DFG grants (MA 1080/27-1; AR 362/9-1; BE 2296/8-1 and in part MA1080/23-2).

Author contribution statement

N S and A Mi performed the majority of the cellular experiments. S P and R B designed the immortalization experiments and S P conducted them. J B S, F F, T F, G J A, performed proteomic studies and evaluated the results. A Ma conceived of the study, directed the work and supervised the experiments. N S, A Mi and A Ma drafted the manuscript. All authors contributed to the manuscript and approved the final version.

Acknowledgements

The authors thank Kim-Gwendolyn Dietrich, Carola Herrmann and Astrid Tiefenbacher for skillful technical assistance.

References

Adam M, Schwarzer JU, Kohn FM, Strauss L, Poutanen M & Mayerhofer A 2011 Mast cell tryptase stimulates production of decorin by human testicular peritubular cells: possible role of decorin in male infertility by interfering with growth factor signaling. *Human Reproduction* **26** 2613–2625. (https://doi.org/10.1093/humrep/der245)

Albrecht M, Ramsch R, Kohn FM, Schwarzer JU & Mayerhofer A 2006 Isolation and cultivation of human testicular peritubular cells: a new model for the investigation of fibrotic processes in the human testis and male infertility. *Journal of Clinical Endocrinology and Metabolism* **91** 1956–1960. (https://doi.org/10.1210/jc.2005-2169)

Bocker W, Yin Z, Drosse I, Haasters F, Rossmann O, Wierer M, Popov C, Locher M, Mutschler W, Docheva D *et al.* 2008 Introducing a single-cell-derived human mesenchymal stem cell line expressing hTERT after lentiviral gene transfer. *Journal of Cellular and Molecular Medicine* **12** 1347–1359. (https://doi.org/10.1111/j.1582-4934.2008.00299.x)

Cardoso-Moreira M, Halbert J, Valloton D, Velten B, Chen C, Shao Y, Liechti A, Ascencao K, Rummel C, Ovchinnikova S *et al.* 2019 Gene expression across mammalian organ development. *Nature* **571** 505–509. (https://doi.org/10.1038/s41586-019-1338-5)

Chemes HE, Gottlieb SE, Pasqualini T, Domenichini E, Rivarola MA & Bergada C 1985 Response to acute hCG stimulation and steroidogenic potential of Leydig cell fibroblastic precursors in humans. *Journal of Andrology* **6** 102–112. (https://doi.org/10.1002/j.1939-4640.1985.tb00824.x)

Chen LY, Brown PR, Willis WB & Eddy EM 2014 Peritubular myoid cells participate in male mouse spermatogonial stem cell maintenance. *Endocrinology* **155** 4964–4974. (https://doi.org/10.1210/en.2014-1406)

Chen LY, Willis WD & Eddy EM 2016 Targeting the Gdnf Gene in peritubular myoid cells disrupts undifferentiated spermatogonial cell development. *PNAS* **113** 1829–1834. (https://doi.org/10.1073/pnas.1517994113)

Cox J, Hein MY, Luber CA, Paron I, Nagaraj N & Mann M 2014 Accurate proteome-wide label-free quantification by delayed normalization and maximal peptide ratio extraction, termed MaxLFQ. *Molecular and Cellular Proteomics* **13** 2513–2526. (https://doi.org/10.1074/mcp.M113.031591)

Debowski K, Warthemann R, Lentes J, Salinas-Riester G, Dressel R, Langenstroth D, Gromoll J, Sasaki E & Behr R 2015 Non-viral generation of marmoset monkey iPS cells by a six-factor-in-one-vector approach. *PLoS ONE* **10** e0118424. (https://doi.org/10.1371/journal.pone.0118424)

Flenkenthaler F, Windschuttl S, Frohlich T, Schwarzer JU, Mayerhofer A & Arnold GJ 2014 Secretome analysis of testicular peritubular cells: a window into the human testicular microenvironment and the spermatogonial stem cell niche in man. *Journal of Proteome Research* **13** 1259–1269. (https://doi.org/10.1021/pr400769z)

Gelain DP, de Souza LF & Bernard EA 2003 Extracellular purines from cells of seminiferous tubules. *Molecular and Cellular Biochemistry* **245** 1–9. (https://doi.org/10.1023/a:1022857608849)

Haider SG 2004 Cell biology of Leydig cells in the testis. *International Review of Cytology* **233** 181–241. (https://doi.org/10.1016/S0074-7696(04)33005-6)

Junger WG 2011 Immune cell regulation by autocrine purinergic signalling. *Nature Reviews: Immunology* **11** 201–212. (https://doi.org/10.1038/nri2938)

Landreh L, Spinnler K, Schubert K, Hakkinen MR, Auriola S, Poutanen M, Soder O, Svechnikov K & Mayerhofer A 2014 Human testicular peritubular cells host putative stem Leydig cells with steroidogenic capacity. *Journal of Clinical Endocrinology and Metabolism* **99** E1227–E1235. (https://doi.org/10.1210/jc.2013-4199)

Li LH, Donald JM & Golub MS 2005 Review on testicular development, structure, function, and regulation in common marmoset. *Birth Defects Research: Part B, Developmental and Reproductive Toxicology* **74** 450–469. (https://doi.org/10.1002/bdrb.20057)

Maekawa M, Kamimura K & Nagano T 1996 Peritubular myoid cells in the testis: their structure and function. *Archives of Histology and Cytology* **59** 1–13. (https://doi.org/10.1679/aohc.59.1)

Mansfield K 2003 Marmoset models commonly used in biomedical research. *Comparative Medicine* **53** 383–392.

Masutomi K, Yu EY, Khurts S, Ben-Porath I, Currier JL, Metz GB, Brooks MW, Kaneko S, Murakami S, DeCaprio JA *et al.* 2003 Telomerase maintains telomere structure in normal human cells. *Cell* **114** 241–253. (https://doi.org/10.1016/s0092-8674(03)00550-6)

Mayer C, Adam M, Glashauser L, Dietrich K, Schwarzer JU, Kohn FM, Strauss L, Welter H, Poutanen M & Mayerhofer A 2016 Sterile inflammation as a factor in human male infertility: involvement of Toll like receptor 2, biglycan and peritubular cells. *Scientific Reports* **6** 37128. (https://doi.org/10.1038/srep37128)

Downloaded from Bioscientifica.com at 10/28/2021 11:40:44AM
via Ludwig-Maximilians-University Munchen

Mayer C, Adam M, Walenta L, Schmid N, Heikela H, Schubert K, Flenkenthaler F, Dietrich KG, Gruschka S, Arnold GJ *et al.* 2018 Insights into the role of androgen receptor in human testicular peritubular cells. *Andrology* **6** 756–765. (https://doi.org/10.1111/andr.12509)

Mayerhofer A 2013 Human testicular peritubular cells: more than meets the eye. *Reproduction* **145** R107–R116. (https://doi.org/10.1530/REP-12-0497)

Mayerhofer A, Walenta L, Mayer C, Eubler K & Welter H 2018 Human testicular peritubular cells, mast cells and testicular inflammation. *Andrologia* **50** e13055. (https://doi.org/10.1111/and.13055)

Meineke V, Frungieri MB, Jessberger B, Vogt H & Mayerhofer A 2000 Human testicular mast cells contain tryptase: increased mast cell number and altered distribution in the testes of infertile men. *Fertility and Sterility* **74** 239–244. (https://doi.org/10.1016/s0015-0282(00)00626-9)

Michel JB & Mahouy G 1990 The marmoset in biomedical research. Value of this primate model for cardiovascular studies. *Pathologie-Biologie* **38** 197–204.

Millar MR, Sharpe RM, Weinbauer GF, Fraser HM & Saunders PT 2000 Marmoset spermatogenesis: organizational similarities to the human. *International Journal of Andrology* **23** 266–277. (https://doi.org/10.1046/j.1365-2605.2000.00236.x)

Petkov S, Kahland T, Shomroni O, Lingner T, Salinas G, Fuchs S, Debowski K & Behr R 2018 Immortalization of common marmoset monkey fibroblasts by piggyBac transposition of hTERT. *PLoS ONE* **13** e0204580. (https://doi.org/10.1371/journal.pone.0204580)

Rey-Ares V, Rossi SP, Dietrich KG, Kohn FM, Schwarzer JU, Welter H, Frungieri MB & Mayerhofer A 2018 Prostaglandin E2 (PGE2) is a testicular peritubular cell-derived factor involved in human testicular homeostasis. *Molecular and Cellular Endocrinology* **473** 217–224. (https://doi.org/10.1016/j.mce.2018.01.022)

Sato K, Kuroki Y, Kumita W, Fujiyama A, Toyoda A, Kawai J, Iriki A, Sasaki E, Okano H & Sakakibara Y 2015 Resequencing of the common marmoset genome improves genome assemblies and gene-coding sequence analysis. *Scientific Reports* **5** 16894. (https://doi.org/10.1038/srep16894)

Schell C, Albrecht M, Spillner S, Mayer C, Kunz L, Kohn FM, Schwarzer U & Mayerhofer A 2010 15-Deoxy-delta 12–14-prostaglandin-J2 induces hypertrophy and loss of contractility in human testicular peritubular cells: implications for human male fertility. *Endocrinology* **151** 1257–1268. (https://doi.org/10.1210/en.2009-1325)

Schmid N, Stockl JB, Flenkenthaler F, Dietrich KG, Schwarzer JU, Kohn FM, Drummer C, Frohlich T, Arnold GJ, Behr R *et al.* 2018 Characterization of a non-human primate model for the study of testicular peritubular cells-comparison with human testicular peritubular cells. *Molecular Human Reproduction* **24** 401–410. (https://doi.org/10.1093/molehr/gay025)

Schmid N, Flenkenthaler F, Stockl JB, Dietrich KG, Kohn FM, Schwarzer JU, Kunz L, Luckner M, Wanner G, Arnold GJ *et al.* 2019 Insights into replicative senescence of human testicular peritubular cells. *Scientific Reports* **9** 15052. (https://doi.org/10.1038/s41598-019-51380-w)

Spinnler K, Kohn FM, Schwarzer U & Mayerhofer A 2010 Glial cell line-derived neurotrophic factor is constitutively produced by human testicular peritubular cells and may contribute to the spermatogonial stem cell niche in man. *Human Reproduction* **25** 2181–2187. (https://doi.org/10.1093/humrep/deq170)

Tyanova S, Temu T & Cox J 2016 The MaxQuant computational platform for mass spectrometry-based shotgun proteomics. *Nature Protocols* **11** 2301–2319. (https://doi.org/10.1038/nprot.2016.136)

Walenta L, Fleck D, Frohlich T, von Eysmondt H, Arnold GJ, Spehr J, Schwarzer JU, Kohn FM, Spehr M & Mayerhofer A 2018 ATP-mediated events in peritubular cells contribute to sterile testicular inflammation. *Scientific Reports* **8** 1431. (https://doi.org/10.1038/s41598-018-19624-3)

Welter H, Huber A, Lauf S, Einwang D, Mayer C, Schwarzer JU, Kohn FM & Mayerhofer A 2014 Angiotensin II regulates testicular peritubular cell function via AT1 receptor: a specific situation in male infertility. *Molecular and Cellular Endocrinology* **393** 171–178. (https://doi.org/10.1016/j.mce.2014.06.011)

Zhou R, Wu J, Liu B, Jiang Y, Chen W, Li J, He Q & He Z 2019 The roles and mechanisms of Leydig cells and myoid cells in regulating spermatogenesis. *Cellular and Molecular Life Sciences* **76** 2681–2695. (https://doi.org/10.1007/s00018-019-03101-9)

Zuhlke U & Weinbauer G 2003 The common marmoset (Callithrix jacchus) as a model in toxicology. *Toxicologic Pathology* Supplement 123–127 **31** 123–127. (https://doi.org/10.1080/01926230390175002)

Received 21 February 2020
First decision 26 March 2020
Revised manuscript received 15 May 2020
Accepted 21 may 2020

Downloaded from Bioscientifica.com at 10/28/2021 11:40:44AM
via Ludwig-Maximilians-University Munchen

2.3.1 Supplementary information of publication III

Supplementary table 1

Entire list of identified proteins of the proteome analysis of iMKTPCs and MKTPCs (available at https://rep.bioscientifica.com/view/journals/rep/160/2/REP-20-0100.xml).

3 DISCUSSION

Fifty years ago, Geoffrey Burnstock established the concept of purinergic signalling (1972). Over the years, numerous studies investigated the role of the purinergic system, revealing functional and structural properties. However, in the human testis this signalling system is still poorly examined.

The present work aimed to explore the purinergic system in the human testis. The main focus was on the role of the nucleotide ATP (Figure 9A) and its metabolites, ectonucleotidases, adenosine receptors and specifically their role in contractile and inflammatory responses (Figure 9B). Testicular peritubular cells (TPCs) were used as an applicable cell culture model. Next to the patient-derived HTPCs, TPCs of mice were used as well. Furthermore, a translational cellular model for TPCs, using peritubular cells of the marmoset monkey *Callithrix jacchus*, was established and compared to HTPCs (Figure 9C).

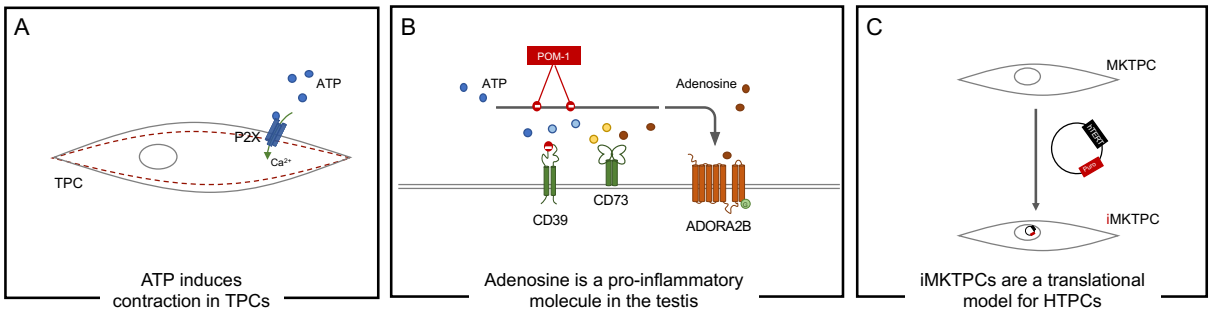

Figure 9. Overview of the main results.

(A) Fleck et al. (2021), (B) Missel et al. (2021) and (C) Schmid et al. (2020).

3.1 Contraction of peritubular cells by ATP and sperm transport

Seminiferous tubules of the human testis are the site of sperm production, which meant to be transported to the *rete testis* and epididymis. Sertoli cells surround germ cells during spermatogenesis, prior to detachment of immotile spermatozoa and their release into the lumen of the seminiferous tubules. The mechanisms of sperm transport through the seminiferous tubules remain unclear (Hargrove et al. 1977; Romano et al.

2005). Efferent nerve endings are missing in the testis, therefore contractile forces were already suggested to be regulated by endocrine and/or paracrine factors (Tripiciano et al. 1996; Romano et al. 2005; Albrecht et al. 2006). However, involvement of the purinergic system was not yet evaluated, or even considered as unlikely in older rat studies (Hovatta 1972; Kormano and Hovatta 1972).

Purinergic receptors mediate the actions of extracellular ATP, and the physiology of smooth muscle cells can be affected by P2 receptors. The ligand-gated ion channels P2X are activated by ATP and are permeable for Ca^{2+}. Smooth muscle cells of the *tunica albuginea* express the receptors P2X1 and P2X2, and contractions in this area were found to be mediated by autonomic innervation, which uses ATP as a (co)transmitter (Banks et al. 2006b). Also, the smooth muscle-mediated contraction of the *vas deferens* is regulated by P2X1. Its total absence leads to infertility in transgenic mice (Mulryan et al. 2000; Banks et al. 2006a).

Peritubular cells of both human and mouse express several P2X and P2Y receptors (Walenta et al. 2018; Fleck et al. 2021). This raised the question, whether extracellular ATP is a possible activator of TPC contractions and initiator of sperm transport through the seminiferous tubules towards the *rete testis*. The study of Fleck et al. (2021) is the first one that describes ATP as an activator of peritubular cells by P2 receptors, leading to coordinated tubule contractions. Seminiferous tubules in mice, *in situ* and *in vivo,* showed ATP-triggered luminal sperm transport. Spontaneous contractions, which were measured by a novel *in vivo* setting, and ATP-triggered contractions resembled in their velocity and direction in transporting luminal content through the tubules. Contractions were measured in acute seminiferous tubule sections (Fleck et al. 2016), as well as in isolated TPCs of mice and men. Measurements in mouse TPCs, *in vivo* and *in vitro*, exposed robust Ca^{2+}-signals in reaction to extracellular ATP. Peripheral Ca^{2+}-activity after short-term ATP exposure occurred coinciding to minimal delayed contractile motions of seminiferous tubules. Therefore, parallel recordings indicated a clear coherence due to the reaction's chronology. These responses in TPCs are jointly mediated by P2X and P2Y receptors, whereby P2X receptors react to ATP exposure in supporting Ca^{2+}-transport and trigger P2Y receptors to mediate intracellular Ca^{2+}-mobilization in TPCs (Fleck et al. 2021).

Contractions of seminiferous tubules, induced by extracellular ATP, can transport luminal fluid and immotile sperm cells. Even in basal conditions, a luminal flow was detected in the tubules, but additional ATP evoked an intensified flow. The movement along the tubules has a wave-like unidirectional motion, coinciding with Ca^{2+}-signals in speed and direction (Fleck et al. 2021). Most of the measurements were performed - due to availability and feasibility - in the mouse testis. To study contraction of HTPCs, collagen gel lattices were used which enable measurement and quantification of contractions of embedded cells (Tung and Fritz 1987; Ailenberg et al. 1990; Schell et al. 2010). Collagen gels reduced their surface size massively after ATP incubation. In addition, live cell imaging of cultured HTPCs revealed a shrinking of the cells and a rapid decrease of their cell surface after exposure with ATP (Fleck et al. 2021). Although, differences between human and mouse testis exist regarding structure and the spermatogonial stem cell system (Tung and Fritz 1990; Ehmcke et al. 2006; Weinbauer et al. 2009; Mayerhofer 2013), the findings of tubular motion in the mouse are likely transferable to the human system.

3.2 The role of testicular adenosine in peritubular cells

Testicular disorders, acquired or congenital ones, affect men's fertility. Inflammatory processes in the testis are likely a cause or a consequence of testicular disorders. In any way, they negatively influence male reproduction. Therefore, the present study indicates a direct association of the purinergic system with inflammation in the testis and suggests the potential consequence of related disturbances in male fertility.

Extracellular ATP is not only a mediator of contraction of peritubular cells (Fleck et al. 2021), it is also a danger signal causing a strong pro-inflammatory response in these cells and therefore may contribute to sterile inflammation (Walenta et al. 2018). Regulated release mechanisms or cell disruption can lead to an accumulation of extracellular ATP. However, the stability of ATP and therefore its range of action can be limited, as ectonucleotidases are located on cell surfaces and ensure a rapid degradation of ATP into its metabolites (Zimmermann 1992; Colgan et al. 2006; Grinthal and Guidotti 2006; Allard et al. 2017). Several sources of extracellular ATP are present in the testis and in the closer environment of peritubular cells, including Sertoli

cells, mast cells, nerve fibers and continuous apoptosis of germ cells (Mayerhofer et al. 1999; Meineke et al. 2000; Baum et al. 2005; Gelain et al. 2005; Xiong et al. 2009).

Similar to the action of ATP on peritubular cells, its final metabolite adenosine was found to induce strong pro-inflammatory responses *via* upregulated pro-inflammatory cytokine levels (Missel et al. 2021). The two ectonucleotidases CD39 and CD73 are ubiquitously expressed membrane-bound enzymes and responsible for the conversion of ATP to the final metabolite adenosine (Zimmermann et al. 2012). Their presence in testicular cells, especially in the human testis has not been described yet. However, peritubular cells of mice express both enzymes (Martin-Satue et al. 2009; Martin-Satue et al. 2010). Missel et al. (2021) found expression of CD39 and CD73 in HTPCs, which implied the possibility of the breakdown of ATP in the peritubular compartment of men. Peritubular cells are located directly adjacent to tubular and interstitial areas. In this setting, actions of ATP were already described in rodent Sertoli, Leydig and germ cells (Casali et al. 2001; Zamoner et al. 2006; Veitinger et al. 2011; Fleck et al. 2016).

Dephosphorylation of ATP, ADP and AMP generates free phosphate groups, which can be measured using the malachite green assay, a sensitive method based on a complex formed by malachite green, molybdate, and free orthophosphate (Cogan et al. 1999). Using this method in HTPCs gave clear evidence that breakdown of ATP, ADP and AMP occurs, a direct hint to the activity of the ectonucleotidases CD39 and CD73 and therefore the possible generation of adenosine in the peritubular compartment (Missel et al. 2021).

Active ectonucleotidases regulate the concentration of extracellular ATP and enable the generation of metabolites to affect cells in adjacent compartments. ATP exposure in a previous study of rat Sertoli cells resulted in much weaker adenosine accumulation than in peritubular cells of rats. In their study, ectonucleotidase activity after ATP exposure, revealed stronger effects of adenosine generation in both germ cells and peritubular cells than in Sertoli cells, indicating activity of CD39 and CD73 in the peritubular compartment (Gelain et al. 2003). The present study in HTPCs confirmed these findings regarding CD39, as its inhibition by POM-1 blocked both the release of extracellular phosphate levels and pro-inflammatory cytokine levels after

ATP and ADP addition in HTPCs (Missel et al. 2021). POM-1 is an effective and specific blocker and already showed beneficial effects in several other conditions (Reutershan et al. 2009; d'Almeida et al. 2016; Pimenta-Dos-Reis et al. 2017; Yang et al. 2020).

Adenosine exposure of isolated peritubular cells of human and mouse, as well as organotypic testes cultures of mice, induced severe upregulations of pro-inflammatory cytokine levels (Missel et al. 2021). Secretion of these cytokines can initiate immune cell infiltration and negatively influence spermatogenesis. For instance, adenosine has a significant impact on the expression of the prototypical pro-inflammatory cytokine IL-1B, which is described to induce a decrease in testosterone production in the testis (Fraczek and Kurpisz 2015). Further, IL-1B in turn is a possible inducer of MCP3, MCP1 and IL-6 synthesis (Polentarutti et al. 1997; Weber et al. 2010). Elevated cytokines can affect the permeability of the blood-testis barrier and, thus, facilitate their transport into the tubular compartment. Acting on Sertoli cells and germ cells, cytokines can modulate FSH levels, induce apoptosis of spermatogonial stem cells or reduce the fertilizing capacity of sperm cells (Petersen et al. 2004; Jacobo et al. 2011). Therefore, cytokines are necessary to tightly control spermatogenesis (Petersen et al. 2004), but a dysregulation in the ejaculate can disturb spermatogenesis and elevated levels are a possible indicator for testicular disorders (Pilatz et al. 2013).

3.2.1 The adenosine receptors ADORA and inflammation

Adenosine can activate the four G protein-coupled adenosine receptors A1, A2A, A2B and A3. It can also be deaminated to inosine by ADA. In HTPCs, inosine treatment resulted in no pro-inflammatory response in contrast to adenosine. Binding of adenosine to the associated receptors seems more likely, as the use of NECA, an analogue of adenosine and activator of the adenosine receptors, increased pro-inflammatory cytokines, as adenosine did (Missel et al. 2021). Rodent studies already found adenosine in the testis and suggested a function in sperm physiology (Conti et al. 1989; Dixon et al. 1996). So far unknown, mRNA expression of all four adenosine receptors was found in the human testis and except for A3, they are also expressed in peritubular cells. Both, mouse whole testis and peritubular cells express all four

adenosine receptors (Missel et al. 2021). Variations in the expression of A3 are known to differ significantly among species (Ramkumar et al. 1993).

The A2B receptor was determined as the prime candidate for being activated by adenosine in TPCs. Merely an agonist of A2B resulted in significantly increased pro-inflammatory cytokine levels, the agonists of A1 and A2A did not. Also, several commercial antibodies for A1 and A2A yielded non-specific results, in contrast to A2B-antibodies. A2B was localized in the tubular wall *in situ* on paraffin-embedded human testis samples. It is the only adenosine receptor that was activated by an agonist *in vitro* in HTPCs, resulting in pro-inflammatory effects, similar to those after adenosine exposure. A downregulation of A2B in HTPCs decreased those pro-inflammatory cytokines (Missel et al. 2021). Influence of A1 and A2A cannot, however, be excluded, as heteromerization of adenosine receptors can occur (Moriyama and Sitkovsky 2010; Smith and Milligan 2010).

Different to other tissues, where adenosine signalling is mainly described as a dampener of acute inflammation and tissue injury induced by ATP (Ohta and Sitkovsky 2001; Flogel et al. 2012), studies in peritubular cells revealed strong pro-inflammatory actions of both adenosine and ATP. Further insights into the network of testicular cells and the peritubular environment were employed by organotypic tissue cultures of mouse testis fragments. Stable Leydig cell and Sertoli cell markers in combination with elevated cytokine levels support the pro-inflammatory role of adenosine in the whole testis (Missel et al. 2021). Despite species dependent differences in expression profiles and tissue structures in the testis of mouse and human, the contribution of peritubular cells to the pro-inflammatory role of adenosine was also examined in isolated TPCs of the mouse. Similar to the results in human TPCs, strong pro-inflammatory actions of adenosine and a comparable action of ATP appeared in MTPCs, suggesting the generation of active ATP metabolites (Missel et al. 2021).

3.3 An immortalized translational model for peritubular cells

The described studies demonstrate the difficulties researchers are exposed to. It is almost impossible to perform organotypic tissue cultures of the human testis, due to the lack of whole testis samples. Furthermore, patient samples differ significantly with respect to age, lifestyle and health status. HTPCs are patient-derived cells and show clear heterogeneity regarding secreted products like steroids and cytokines (Landreh et al. 2014; Welter et al. 2014; Mayer et al. 2016). Rodent models are more convenient and often used in biomedical studies, as they overcome issues concerning tissue availability and heterogeneity. Nevertheless, in terms of testicular studies, species dependent differences hamper translation into the human situation. Already earlier studies indicated notable differences of rodent and man, regarding testicular structures and the spermatogonial stem cell system (Tung and Fritz 1990; Ehmcke et al. 2006; Weinbauer et al. 2009; Mayerhofer 2013). Recently, it was shown, that gene expression of the testis has one of the largest differences between mouse and human, compared to other mammalian species and organs (Cardoso-Moreira et al. 2019).

Non-human primates show smaller differences regarding testicular gene expression and a higher similarity to humans with respect to testicular structure, germ cell characteristic, architecture of the peritubular wall and spermatogenesis (Millar et al. 2000; Wistuba et al. 2003; Zuhlke and Weinbauer 2003; Cardoso-Moreira et al. 2019). MKTPCs are isolated peritubular cells from the marmoset monkey *Callithrix jacchus*, and were shown to be a suitable tool to study peritubular cells (Schmid et al. 2018). They have the advantage that they stem from marmosets which were grown up in an environment of documented nutrition and medical history.

HTPCs, MTPCs and MKTPCs are altogether well examined cellular models and each one has delivered important insights into peritubular cells of the testis. However, their use is limited, as they all have in common that they undergo senescence-associated changes (Schmid et al. 2019). Replicative senescence is the result of progressive telomere shortening (Allsopp et al. 1995) and can be avoided by immortalization using the insertion and therefore overexpression of *hTERT* (Kim et al. 1994; Petkov et al. 2018).

In this study, MKTPCs were immortalized (iMKTPCs) with a *piggyBac* transposon containing *hTERT*, and characterized regarding their usability and comparability to HTPCs (Schmid et al. 2020). iMKTPCs can be cultured over more than 50 passages without any evidence for cellular senescence. A high degree of similarity between iMKTPCs and MKTPCs was demonstrated on the proteome level, proving that they retain their phenotype despite immortalization. Expression of the receptors P2X4 and P2X7, and increasing pro-inflammatory cytokines after ATP exposure, indicated that iMKTPCs are an ideal model for in-depth studies of the purinergic system (Schmid et al. 2020).

3.4 Summary

The present study indicates that the purinergic system – although not fully explored yet – is involved in the regulation of inflammatory events in the testis and luminal sperm transport. On the one side, ATP is one of the main stimuli of contractile forces in the testis and on the other side, adenosine is a pro-inflammatory molecule. Both results raise the question regarding the mechanistic basis of tubule contractions, and their involvement in testicular sperm transport as well as of the role of the intermediate metabolites ADP and AMP.

In summary, three types of contractions in the seminiferous tubules were shown by Fleck et al. (2021): Spontaneous contractions, as well as those induced by intracellular Ca^{2+}-increase and by extracellular ATP. Therefore, luminal sperm transport in seminiferous tubules has to be mediated by paracrine purinergic signalling. Described reduced sperm counts in the ejaculate (Levine et al. 2017) may be one factor of disturbances in luminal sperm transport. As numbers of sperm are measured in the ejaculate and not at the site of spermatogenesis, the whole genital tract can affect sperm count, and contractility in seminiferous tubules can be one causal factor. Therefore, in addition to previous findings, that intracellular ATP (acting on the dynein arms in the flagellum) is a main player in the propulsion of sperm (Chan and Wang 1987), the present study found that extracellular ATP is an important player of sperm transport out of the testis (Fleck et al. 2021).

Adenosine is a pro-inflammatory molecule and sterile inflammation contributes to idiopathic infertility (Pelliccione et al. 2011; Milardi et al. 2017; Pilatz et al. 2019). Hence, if the results of these studies are transferable to the human situation *in vivo*, disturbances in this system can lead to male infertility. The inhibition of adenosine generation in the extracellular space, by blocking CD39, is only one possible target. Also, A2B, as the main receptor involved in adenosine signalling in the testis, is suitable to impair pro-inflammatory actions by receptor blockers or therapeutic antibodies (Wendell et al. 2020).

No single cellular model can mirror the complete situation in a tissue or organ, but they can allow relevant insights and are therefore of great importance and non-substitutable for basic research. One goal in science should be to either avoid animal studies or at least reduce their number of animals used for the experiment. In this line, following the 3R rule (replacement, reduction and refinement), formulated by Russel and Burch (1959), iMKTPCs are a suitable and long-lasting translational tool for the study of peritubular cells.

3.5 Future perspectives

This work gained new insights into the complex purinergic system in the testis. However, several questions still remain or can now be asked based on the findings of this study. Future experiments should address, whether ATP metabolites are also involved in contractile mechanisms and morphological changes of TPCs, and if a coordination of the contractile forces exists, for example by a coupling of TPCs by gap junctions.

Holistic approaches of adenosine treated TPCs, like proteome analyses and single-cell sequencing, could confirm and complete findings of the pro-inflammatory role of adenosine in the testis. While extracellular levels of adenosine activate the A2B receptor, an involvement of the other adenosine receptors, ADA and the transporters CNT and ENT cannot be ruled out and still has to be examined. Expression and activity of the ectonucleotidases was demonstrated in HTPCs with a clear indication of a generation of metabolites of ATP. However, the amount of the generated products is

still unclear. A measurement of ADP, AMP and adenosine concentrations after ATP exposure would solve this issue.
Primary cells such as HTPCs and MTPCs are not appropriate for knockout studies. The stable cellular model iMKTPC is the first TPC model with the possibility to modify the gene of interest using the CRISPR/Cas9 technology. An inactivation of P1 and P2 receptors would be the first step to strengthen the findings regarding ATP and adenosine of the present studies.

Insights into the purinergic system in the human testis open up a variety of new possibilities of therapeutical use in both infertility treatment and birth control. Male contraceptives are to date limited to condoms and vasectomies. Despite ongoing research in hormonal male contraception, efficiency rates are insufficient to outweigh androgenic side effects (Abbe et al. 2020). P2X1 receptors were already identified as candidates for non-hormonal contraceptives, due to their contractile function in the *vas deferens* (Mulryan et al. 2000; Burnstock 2017). As P2-receptors are also involved in luminal sperm transport inside the testis (Fleck et al. 2021), they could be also potential targets to limit the amount of sperm cells migrating to the epididymis. The control of sperm output in the ejaculate, dependent upon contractile events, may also be useful to treat male infertility, as the action of receptors, involved in luminal sperm transport, could be enhanced by ATP-potentiating agents or specific agonists.

There is a high prevalence of inflammatory disorders in the testis with an associated risk for irreversible male infertility. However, therapeutics are to date still rare (Fijak et al. 2018; Haidl et al. 2019). Therefore, the present study indicates new approaches, using inhibition of the ectonucleotidase CD39 or the adenosine receptor A2B, as promising therapeutic targets to treat inflammatory events in the male testis.

In conclusion, the purinergic system in the testis is involved in the regulation of testicular function. Therefore, the understanding of molecular processes of tubular contraction, testicular inflammation and the purinergic system, involved in both situations, would be an important step towards a better treatment for male (in)fertility.

4 REFERENCES

Abbe, C. R., S. T. Page, and A. Thirumalai. 2020. 'Male Contraception', *Yale J Biol Med*, 93: 603-13.

Abbracchio, M. P., and G. Burnstock. 1994. 'Purinoceptors: are there families of P2X and P2Y purinoceptors?', *Pharmacol Ther*, 64: 445-75.

Adam, M., J. U. Schwarzer, F. M. Köhn, L. Strauss, M. Poutanen, and A. Mayerhofer. 2011. 'Mast cell tryptase stimulates production of decorin by human testicular peritubular cells: possible role of decorin in male infertility by interfering with growth factor signaling', *Hum Reprod*, 26: 2613-25.

Adam, M., H. F. Urbanski, V. T. Garyfallou, U. Welsch, F. M. Köhn, J. Ullrich Schwarzer, L. Strauss, M. Poutanen, and A. Mayerhofer. 2012. 'High levels of the extracellular matrix proteoglycan decorin are associated with inhibition of testicular function', *Int J Androl*, 35: 550-61.

Ailenberg, M., P. S. Tung, and I. B. Fritz. 1990. 'Transforming growth factor-beta elicits shape changes and increases contractility of testicular peritubular cells', *Biol Reprod*, 42: 499-509.

Albert, S., J. Ehmcke, J. Wistuba, K. Eildermann, R. Behr, S. Schlatt, and J. Gromoll. 2010. 'Germ cell dynamics in the testis of the postnatal common marmoset monkey (Callithrix jacchus)', *Reproduction*, 140: 733-42.

Albrecht, M., R. Ramsch, F. M. Köhn, J. U. Schwarzer, and A. Mayerhofer. 2006. 'Isolation and cultivation of human testicular peritubular cells: a new model for the investigation of fibrotic processes in the human testis and male infertility', *J Clin Endocrinol Metab*, 91: 1956-60.

Allard, B., M. S. Longhi, S. C. Robson, and J. Stagg. 2017. 'The ectonucleotidases CD39 and CD73: Novel checkpoint inhibitor targets', *Immunol Rev*, 276: 121-44.

Allsopp, R. C., E. Chang, M. Kashefi-Aazam, E. I. Rogaev, M. A. Piatyszek, J. W. Shay, and C. B. Harley. 1995. 'Telomere shortening is associated with cell division in vitro and in vivo', *Exp Cell Res*, 220: 194-200.

Anthony, C. T., and M. K. Skinner. 1989. 'Cytochemical and biochemical characterization of testicular peritubular myoid cells', *Biol Reprod*, 40: 811-23.

Antonioli, L., P. Pacher, E. S. Vizi, and G. Hasko. 2013. 'CD39 and CD73 in immunity and inflammation', *Trends Mol Med*, 19: 355-67.

Ballesteros-Yanez, I., C. A. Castillo, S. Merighi, and S. Gessi. 2017. 'The Role of Adenosine Receptors in Psychostimulant Addiction', *Front Pharmacol*, 8: 985.

Banks, F. C., G. E. Knight, R. C. Calvert, C. S. Thompson, R. J. Morgan, and G. Burnstock. 2006a. 'The purinergic component of human vas deferens contraction', *Fertil Steril*, 85: 932-9.

Banks, F. C., G. E. Knight, R. C. Calvert, M. Turmaine, C. S. Thompson, D. P. Mikhailidis, R. J. Morgan, and G. Burnstock. 2006b. 'Smooth muscle and purinergic contraction of the human, rabbit, rat, and mouse testicular capsule', *Biol Reprod*, 74: 473-80.

Baum, J. S., J. P. St George, and K. McCall. 2005. 'Programmed cell death in the germline', *Semin Cell Dev Biol*, 16: 245-59.

Becht, E., L. McInnes, J. Healy, C. A. Dutertre, I. W. H. Kwok, L. G. Ng, F. Ginhoux, and E. W. Newell. 2018. 'Dimensionality reduction for visualizing single-cell data using UMAP', *Nat Biotechnol*.

Boisen, K. A., M. Kaleva, K. M. Main, H. E. Virtanen, A. M. Haavisto, I. M. Schmidt, M. Chellakooty, I. N. Damgaard, C. Mau, M. Reunanen, N. E. Skakkebaek, and J. Toppari. 2004. 'Difference in prevalence of congenital cryptorchidism in infants between two Nordic countries', *Lancet*, 363: 1264-9.

Bonnans, C., J. Chou, and Z. Werb. 2014. 'Remodelling the extracellular matrix in development and disease', *Nat Rev Mol Cell Biol*, 15: 786-801.

Boockfor, F. R., D. Wang, T. Lin, M. L. Nagpal, and B. L. Spangelo. 1994. 'Interleukin-6 secretion from rat Leydig cells in culture', *Endocrinology*, 134: 2150-5.

Borea, P. A., S. Gessi, S. Merighi, and K. Varani. 2016. 'Adenosine as a Multi-Signalling Guardian Angel in Human Diseases: When, Where and How Does it Exert its Protective Effects?', *Trends Pharmacol Sci*, 37: 419-34.

Borea, P. A., S. Gessi, S. Merighi, F. Vincenzi, and K. Varani. 2018. 'Pharmacology of Adenosine Receptors: The State of the Art', *Physiol Rev*, 98: 1591-625.

Bundesamt, Statistisches. 2021. "Ungewollte Kinderlosigkeit 2020. Leiden - Hemmungen - Lösungen." In *Bundesministerium für Familie, Frauen und Jugend. Referat Öffentlichkeitsarbeit*.

Burnstock, G. 1972. 'Purinergic nerves', *Pharmacol Rev*, 24: 509-81.

———. 2009. 'Purinergic signalling: past, present and future', *Braz J Med Biol Res*, 42: 3-8.

———. 2014. 'Purinergic signalling in the reproductive system in health and disease', *Purinergic Signal*, 10: 157-87.

———. 2017. 'Purinergic Signalling: Therapeutic Developments', *Front Pharmacol*, 8: 661.

Burnstock, G., and C. Kennedy. 1985. 'Is there a basis for distinguishing two types of P2-purinoceptor?', *Gen Pharmacol*, 16: 433-40.

Bustos-Obregon, E. 1976. 'Ultrastructure and function of the lamina propria of mammalian seminiferous tubules', *Andrologia*, 8: 179-85.

Capogrosso, P., E. Ventimiglia, L. Boeri, W. Cazzaniga, F. Chierigo, F. Pederzoli, N. Frego, C. Abbate, F. Deho, F. Montorsi, and A. Salonia. 2019. 'Age at First Presentation for Erectile Dysfunction: Analysis of Changes over a 12-yr Period', *Eur Urol Focus*, 5: 899-905.

Cardoso-Moreira, M., J. Halbert, D. Valloton, B. Velten, C. Chen, Y. Shao, A. Liechti, K. Ascencao, C. Rummel, S. Ovchinnikova, P. V. Mazin, I. Xenarios, K. Harshman, M. Mort, D. N. Cooper, C. Sandi, M. J. Soares, P. G. Ferreira, S. Afonso, M. Carneiro, J. M. A. Turner, J. L. VandeBerg, A. Fallahshahroudi, P. Jensen, R. Behr, S. Lisgo, S. Lindsay, P. Khaitovich, W. Huber, J. Baker, S. Anders, Y. E. Zhang, and H. Kaessmann. 2019. 'Gene expression across mammalian organ development', *Nature*, 571: 505-09.

Casali, E. A., T. R. da Silva, D. P. Gelain, G. R. Kaiser, A. M. Battastini, J. J. Sarkis, and E. A. Bernard. 2001. 'Ectonucleotidase activities in Sertoli cells from immature rats', *Braz J Med Biol Res*, 34: 1247-56.

Chan, S. Y., and C. Wang. 1987. 'Correlation between semen adenosine triphosphate and sperm fertilizing capacity', *Fertil Steril*, 47: 717-9.

Chiba, K., N. Enatsu, and M. Fujisawa. 2016. 'Management of non-obstructive azoospermia', *Reprod Med Biol*, 15: 165-73.

Clermont, Y. 1972. 'Kinetics of spermatogenesis in mammals: seminiferous epithelium cycle and spermatogonial renewal', *Physiol Rev*, 52: 198-236.

Cogan, E. B., G. B. Birrell, and O. H. Griffith. 1999. 'A robotics-based automated assay for inorganic and organic phosphates', *Anal Biochem*, 271: 29-35.

Colgan, S. P., H. K. Eltzschig, T. Eckle, and L. F. Thompson. 2006. 'Physiological roles for ecto-5'-nucleotidase (CD73)', *Purinergic Signal*, 2: 351-60.

Conti, M., C. Boitani, D. Demanno, S. Migliaccio, L. Monaco, and C. Szymeczek. 1989. 'Characterization and function of adenosine receptors in the testis', *Ann N Y Acad Sci*, 564: 39-47.

Cutolo, M., E. Balleari, M. Giusti, E. Intra, and S. Accardo. 1991. 'Androgen replacement therapy in male patients with rheumatoid arthritis', *Arthritis Rheum*, 34: 1-5.

d'Almeida, S. M., G. Kauffenstein, C. Roy, L. Basset, L. Papargyris, D. Henrion, V. Catros, N. Ifrah, P. Descamps, A. Croue, P. Jeannin, M. Gregoire, Y. Delneste, and

J. Tabiasco. 2016. 'The ecto-ATPDase CD39 is involved in the acquisition of the immunoregulatory phenotype by M-CSF-macrophages and ovarian cancer tumor-associated macrophages: Regulatory role of IL-27', *Oncoimmunology*, 5: e1178025.

Davidoff, M. S., H. Breucker, A. F. Holstein, and K. Seidl. 1990. 'Cellular architecture of the lamina propria of human seminiferous tubules', *Cell Tissue Res*, 262: 253-61.

DePierre, J. W., and M. L. Karnovsky. 1974. 'Ecto-enzyme of granulocytes: 5'-nucleotidase', *Science*, 183: 1096-8.

Di Persio, S., T. Tekath, L. M. Siebert-Kuss, J. F. Cremers, J. Wistuba, X. Li, G. Meyer Zu Horste, H. C. A. Drexler, M. J. Wyrwoll, F. Tüttelmann, M. Dugas, S. Kliesch, S. Schlatt, S. Laurentino, and N. Neuhaus. 2021. 'Single-cell RNA-seq unravels alterations of the human spermatogonial stem cell compartment in patients with impaired spermatogenesis', *Cell Rep Med*, 2: 100395.

Dinarello, C. A. 2007. 'Historical insights into cytokines', *Eur J Immunol*, 37 Suppl 1: S34-45.

Dixon, A. K., A. K. Gubitz, D. J. Sirinathsinghji, P. J. Richardson, and T. C. Freeman. 1996. 'Tissue distribution of adenosine receptor mRNAs in the rat', *Br J Pharmacol*, 118: 1461-8.

Drury, A. N., and A. Szent-Gyorgyi. 1929. 'The physiological activity of adenine compounds with especial reference to their action upon the mammalian heart', *J Physiol*, 68: 213-37.

Ehmcke, J., J. Wistuba, and S. Schlatt. 2006. 'Spermatogonial stem cells: questions, models and perspectives', *Hum Reprod Update*, 12: 275-82.

Eubler, K., C. Herrmann, A. Tiefenbacher, F. M. Köhn, J. U. Schwarzer, L. Kunz, and A. Mayerhofer. 2018. 'Ca(2+) Signaling and IL-8 Secretion in Human Testicular Peritubular Cells Involve the Cation Channel TRPV2', *Int J Mol Sci*, 19.

Fernandez, D., M. V. Bertoldi, L. Gomez, A. Morales, E. Callegari, and L. A. Lopez. 2008. 'Identification and characterization of Myosin from rat testicular peritubular myoid cells', *Biol Reprod*, 79: 1210-8.

Ferre, S., F. Ciruela, J. Borycz, M. Solinas, D. Quarta, K. Antoniou, C. Quiroz, Z. Justinova, C. Lluis, R. Franco, and S. R. Goldberg. 2008. 'Adenosine A1-A2A receptor heteromers: new targets for caffeine in the brain', *Front Biosci*, 13: 2391-9.

Fijak, M., A. Pilatz, M. P. Hedger, N. Nicolas, S. Bhushan, V. Michel, K. S. K. Tung, H. C. Schuppe, and A. Meinhardt. 2018. 'Infectious, inflammatory and 'autoimmune' male factor infertility: how do rodent models inform clinical practice?', *Hum Reprod Update*, 24: 416-41.

Filippini, A., A. Tripiciano, F. Palombi, A. Teti, R. Paniccia, M. Stefanini, and E. Ziparo. 1993. 'Rat testicular myoid cells respond to endothelin: characterization of binding and signal transduction pathway', *Endocrinology*, 133: 1789-96.

Fleck, D., L. Kenzler, N. Mundt, M. Strauch, N. Uesaka, R. Moosmann, F. Bruentgens, A. Missel, A. Mayerhofer, D. Merhof, J. Spehr, and M. Spehr. 2021. 'ATP activation of peritubular cells drives testicular sperm transport', *Elife*, 10.

Fleck, D., N. Mundt, F. Bruentgens, P. Geilenkirchen, P. A. Machado, T. Veitinger, S. Veitinger, S. M. Lipartowski, C. H. Engelhardt, M. Oldiges, J. Spehr, and M. Spehr. 2016. 'Distinct purinergic signaling pathways in prepubescent mouse spermatogonia', *J Gen Physiol*, 148: 253-71.

Flenkenthaler, F., S. Windschüttl, T. Fröhlich, J. U. Schwarzer, A. Mayerhofer, and G. J. Arnold. 2014. 'Secretome analysis of testicular peritubular cells: a window into the human testicular microenvironment and the spermatogonial stem cell niche in man', *J Proteome Res*, 13: 1259-69.

Flogel, U., S. Burghoff, P. L. van Lent, S. Temme, L. Galbarz, Z. Ding, A. El-Tayeb, S. Huels, F. Bonner, N. Borg, C. Jacoby, C. E. Müller, W. B. van den Berg, and J. Schrader. 2012. 'Selective activation of adenosine A2A receptors on immune cells by a CD73-dependent prodrug suppresses joint inflammation in experimental rheumatoid arthritis', *Sci Transl Med*, 4: 146ra08.

Fraczek, M., and M. Kurpisz. 2007. 'Inflammatory mediators exert toxic effects of oxidative stress on human spermatozoa', *J Androl*, 28: 325-33.

———. 2015. 'Cytokines in the male reproductive tract and their role in infertility disorders', *J Reprod Immunol*, 108: 98-104.

Fredholm, B. B., M. P. Abbracchio, G. Burnstock, J. W. Daly, T. K. Harden, K. A. Jacobson, P. Leff, and M. Williams. 1994. 'Nomenclature and classification of purinoceptors', *Pharmacol Rev*, 46: 143-56.

Fredholm, B. B., G. Arslan, L. Halldner, B. Kull, G. Schulte, and W. Wasserman. 2000. 'Structure and function of adenosine receptors and their genes', *Naunyn Schmiedebergs Arch Pharmacol*, 362: 364-74.

Fredholm, B. B., B. G. Frenguelli, R. Hills, A.P. lJzerman, K. A. Jacobson, K.N. Klotz, J. Linden, C.E. Müller, U. Schwabe, and G. L. Stiles. 2019. 'Adenosine receptors (version 2019.2) in the IUPHAR/BPS Guide to Pharmacology Database', *IUPHAR/BPS Guide to Pharmacology*.

Gelain, D. P., E. A. Casali, R. B. de Oliveira, L. F. de Souza, F. Barreto, F. Dal-Pizzol, and J. C. Moreira. 2005. 'Effects of follicle-stimulating hormone and vitamin A upon purinergic secretion by rat Sertoli cells', *Mol Cell Biochem*, 278: 185-94.

Gelain, D. P., L. F. de Souza, and E. A. Bernard. 2003. 'Extracellular purines from cells of seminiferous tubules', *Mol Cell Biochem*, 245: 1-9.

Goossens, E., and H. Tournaye. 2013. 'Adult stem cells in the human testis', *Semin Reprod Med*, 31: 39-48.

Grenz, A., H. Zhang, M. Hermes, T. Eckle, K. Klingel, D. Y. Huang, C. E. Müller, S. C. Robson, H. Osswald, and H. K. Eltzschig. 2007. 'Contribution of E-NTPDase1 (CD39) to renal protection from ischemia-reperfusion injury', *FASEB J*, 21: 2863-73.

Grinthal, A., and G. Guidotti. 2006. 'CD39, NTPDase 1, is attached to the plasma membrane by two transmembrane domains. Why?', *Purinergic Signal*, 2: 391-8.

Gruschwitz, M. S., R. Brezinschek, and H. P. Brezinschek. 1996. 'Cytokine levels in the seminal plasma of infertile males', *J Androl*, 17: 158-63.

Guo, J., E. J. Grow, H. Mlcochova, G. J. Maher, C. Lindskog, X. Nie, Y. Guo, Y. Takei, J. Yun, L. Cai, R. Kim, D. T. Carrell, A. Goriely, J. M. Hotaling, and B. R. Cairns. 2018. 'The adult human testis transcriptional cell atlas', *Cell Res*, 28: 1141-57.

Guo, J., E. Sosa, T. Chitiashvili, X. Nie, E. J. Rojas, E. Oliver, DonorConnect, K. Plath, J. M. Hotaling, J. B. Stukenborg, A. T. Clark, and B. R. Cairns. 2021. 'Single-cell analysis of the developing human testis reveals somatic niche cell specification and fetal germline stem cell establishment', *Cell Stem Cell*, 28: 764-78 e4.

Haidl, G., F. Haidl, J. P. Allam, and H. C. Schuppe. 2019. 'Therapeutic options in male genital tract inflammation', *Andrologia*, 51: e13207.

Hargrove, J. L., J. H. MacIndoe, and L. C. Ellis. 1977. 'Testicular contractile cells and sperm transport', *Fertil Steril*, 28: 1146-57.

Harris, G. C., and H. D. Nicholson. 1998. 'Stage-related differences in rat seminiferous tubule contractility in vitro and their response to oxytocin', *J Endocrinol*, 157: 251-7.

Hasko, G., J. Linden, B. Cronstein, and P. Pacher. 2008. 'Adenosine receptors: therapeutic aspects for inflammatory and immune diseases', *Nat Rev Drug Discov*, 7: 759-70.

Hearn, J. P., D. H. Abbott, P. C. Chambers, J. K. Hodges, and S. F. Lunn. 1978. 'Use of the common marmoset, Callithrix jacchus, in reproductive research', *Primates Med*, 10: 40-9.

Hedger, M. P., and A. Meinhardt. 2003. 'Cytokines and the immune-testicular axis', *J Reprod Immunol*, 58: 1-26.

Hess, R. A., and L. Renato de Franca. 2008. 'Spermatogenesis and cycle of the seminiferous epithelium', *Adv Exp Med Biol*, 636: 1-15.

Holt, W. V., and H. D. Moore. 1984. 'Ultrastructural aspects of spermatogenesis in the common marmoset (Callithrix jacchus)', *J Anat*, 138 (Pt 1): 175-88.

Holtmann, H., and K. Resch. 1995. 'Cytokines', *Naturwissenschaften*, 82: 178-87.

Hong, C. Y., J. H. Park, R. S. Ahn, S. Y. Im, H. S. Choi, J. Soh, S. H. Mellon, and K. Lee. 2004. 'Molecular mechanism of suppression of testicular steroidogenesis by proinflammatory cytokine tumor necrosis factor alpha', *Mol Cell Biol*, 24: 2593-604.

Hovatta, O. 1972. 'Contractility and structure of adult rat seminiferous tubules in organ culture', *Z Zellforsch Mikrosk Anat*, 130: 171-9.

Hunsucker, S. A., B. S. Mitchell, and J. Spychala. 2005. 'The 5'-nucleotidases as regulators of nucleotide and drug metabolism', *Pharmacol Ther*, 107: 1-30.

Jacobo, P., V. A. Guazzone, M. S. Theas, and L. Lustig. 2011. 'Testicular autoimmunity', *Autoimmun Rev*, 10: 201-4.

Jacobson, K. A., R. Balasubramanian, F. Deflorian, and Z. G. Gao. 2012. 'G protein-coupled adenosine (P1) and P2Y receptors: ligand design and receptor interactions', *Purinergic Signal*, 8: 419-36.

Jow, W. W., J. Steckel, P. N. Schlegel, M. S. Magid, and M. Goldstein. 1993. 'Motile sperm in human testis biopsy specimens', *J Androl*, 14: 194-8.

Junger, W. G. 2011. 'Immune cell regulation by autocrine purinergic signalling', *Nat Rev Immunol*, 11: 201-12.

Jungwirth, A., A. Giwercman, H. Tournaye, T. Diemer, Z. Kopa, G. Dohle, C. Krausz, and Infertility European Association of Urology Working Group on Male. 2012. 'European Association of Urology guidelines on Male Infertility: the 2012 update', *Eur Urol*, 62: 324-32.

Kandil, H., A. Agarwal, R. Saleh, F. Boitrelle, M. Arafa, P. Vogiatzi, R. Henkel, A. Zini, and R. Shah. 2021. 'Editorial Commentary on Draft of World Health Organization Sixth Edition Laboratory Manual for the Examination and Processing of Human Semen', *World J Mens Health*.

Kim, N. W., M. A. Piatyszek, K. R. Prowse, C. B. Harley, M. D. West, P. L. Ho, G. M. Coviello, W. E. Wright, S. L. Weinrich, and J. W. Shay. 1994. 'Specific association of human telomerase activity with immortal cells and cancer', *Science*, 266: 2011-5.

Kisseleva, T., and D. A. Brenner. 2008. 'Mechanisms of fibrogenesis', *Exp Biol Med (Maywood)*, 233: 109-22.

Kocak, I., C. Yenisey, M. Dundar, P. Okyay, and M. Serter. 2002. 'Relationship between seminal plasma interleukin-6 and tumor necrosis factor alpha levels with semen parameters in fertile and infertile men', *Urol Res*, 30: 263-7.

Kohler, D., T. Eckle, M. Faigle, A. Grenz, M. Mittelbronn, S. Laucher, M. L. Hart, S. C. Robson, C. E. Müller, and H. K. Eltzschig. 2007. 'CD39/ectonucleoside triphosphate diphosphohydrolase 1 provides myocardial protection during cardiac ischemia/reperfusion injury', *Circulation*, 116: 1784-94.

Kormano, M., and O. Hovatta. 1972. 'Contractility and histochemistry of the myoid cell layer of the rat seminiferous tubules during postnatal development', *Z Anat Entwicklungsgesch*, 137: 239-48.

Landreh, L., K. Spinnler, K. Schubert, M. R. Hakkinen, S. Auriola, M. Poutanen, O. Soder, K. Svechnikov, and A. Mayerhofer. 2014. 'Human testicular peritubular cells host putative stem Leydig cells with steroidogenic capacity', *J Clin Endocrinol Metab*, 99: E1227-35.

Le Moal, J., S. Goria, A. Guillet, A. Rigou, and J. Chesneau. 2021. 'Time and spatial trends of operated cryptorchidism in France and environmental hypotheses: a nationwide study from 2002 to 2014', *Hum Reprod*, 36: 1383-94.

Lee, S. Y., A. Fiene, W. Li, T. Hanck, K. A. Brylev, V. E. Fedorov, J. Lecka, A. Haider, H. J. Pietzsch, H. Zimmermann, J. Sevigny, U. Kortz, H. Stephan, and C. E. Müller. 2015. 'Polyoxometalates--potent and selective ecto-nucleotidase inhibitors', *Biochem Pharmacol*, 93: 171-81.

Leslie, S. W., H. Sajjad, and C. A. Villanueva. 2021. 'Cryptorchidism.' in, *StatPearls* (Treasure Island (FL)).

Levine, H., N. Jorgensen, A. Martino-Andrade, J. Mendiola, D. Weksler-Derri, I. Mindlis, R. Pinotti, and S. H. Swan. 2017. 'Temporal trends in sperm count: a systematic review and meta-regression analysis', *Hum Reprod Update*, 23: 646-59.

Li, L. H., J. M. Donald, and M. S. Golub. 2005. 'Review on testicular development, structure, function, and regulation in common marmoset', *Birth Defects Res B Dev Reprod Toxicol*, 74: 450-69.

Li, Y., and J. Liu. 2020. 'Aptamer-based strategies for recognizing adenine, adenosine, ATP and related compounds', *Analyst*, 145: 6753-68.

Maegawa, M., M. Kamada, M. Irahara, S. Yamamoto, S. Yoshikawa, Y. Kasai, Y. Ohmoto, H. Gima, C. J. Thaler, and T. Aono. 2002. 'A repertoire of cytokines in human seminal plasma', *J Reprod Immunol*, 54: 33-42.

Maggi, M., T. Barni, C. Orlando, G. Fantoni, G. Finetti, G. B. Vannelli, R. Mancina, L. Gloria, L. Bonaccorsi, M. Yanagisawa, and et al. 1995. 'Endothelin-1 and its receptors in human testis', *J Androl*, 16: 213-24.

Martin-du Pan, R. C., and A. Campana. 1993. 'Physiopathology of spermatogenic arrest', *Fertil Steril*, 60: 937-46.

Martin-Satue, M., E. G. Lavoie, M. Fausther, J. Lecka, E. Aliagas, F. Kukulski, and J. Sevigny. 2010. 'High expression and activity of ecto-5'-nucleotidase/CD73 in the male murine reproductive tract', *Histochem Cell Biol*, 133: 659-68.

Martin-Satue, M., E. G. Lavoie, J. Pelletier, M. Fausther, E. Csizmadia, O. Guckelberger, S. C. Robson, and J. Sevigny. 2009. 'Localization of plasma membrane bound NTPDases in the murine reproductive tract', *Histochem Cell Biol*, 131: 615-28.

Martinez-Prado, E., and M. I. Camejo Bermudez. 2010. 'Expression of IL-6, IL-8, TNF-alpha, IL-10, HSP-60, anti-HSP-60 antibodies, and anti-sperm antibodies, in semen of men with leukocytes and/or bacteria', *Am J Reprod Immunol*, 63: 233-43.

Mayer, C., M. Adam, L. Glashauser, K. Dietrich, J. U. Schwarzer, F. M. Köhn, L. Strauss, H. Welter, M. Poutanen, and A. Mayerhofer. 2016. 'Sterile inflammation as a factor in human male infertility: Involvement of Toll like receptor 2, biglycan and peritubular cells', *Sci Rep*, 6: 37128.

Mayer, C., M. Adam, L. Walenta, N. Schmid, H. Heikelä, K. Schubert, F. Flenkenthaler, K. G. Dietrich, S. Gruschka, G. J. Arnold, T. Fröhlich, J. U. Schwarzer, F. M. Köhn, L. Strauss, H. Welter, M. Poutanen, and A. Mayerhofer. 2018. 'Insights into the role of androgen receptor in human testicular peritubular cells', *Andrology*, 6: 756-65.

Mayerhofer, A. 2013. 'Human testicular peritubular cells: more than meets the eye', *Reproduction*, 145: R107-16.

Mayerhofer, A., M. B. Frungieri, S. Fritz, A. Bulling, B. Jessberger, and H. J. Vogt. 1999. 'Evidence for catecholaminergic, neuronlike cells in the adult human testis: changes associated with testicular pathologies', *J Androl*, 20: 341-7.

Mayerhofer, A., L. Walenta, C. Mayer, K. Eubler, and H. Welter. 2018. 'Human testicular peritubular cells, mast cells and testicular inflammation', *Andrologia*, 50: e13055.

McGlynn, K. A., S. S. Devesa, A. J. Sigurdson, L. M. Brown, L. Tsao, and R. E. Tarone. 2003. 'Trends in the incidence of testicular germ cell tumors in the United States', *Cancer*, 97: 63-70.

McInnes, L., and J. Healy. 2018. 'Uniform Manifold Approximation and Projection for Dimension Reduction', *ArXiv e-prints*.

Meineke, V., M. B. Frungieri, B. Jessberger, H. Vogt, and A. Mayerhofer. 2000. 'Human testicular mast cells contain tryptase: increased mast cell number and altered distribution in the testes of infertile men', *Fertil Steril*, 74: 239-44.

Menzies, R. I., F. W. Tam, R. J. Unwin, and M. A. Bailey. 2017. 'Purinergic signaling in kidney disease', *Kidney Int*, 91: 315-23.

Milardi, D., G. Luca, G. Grande, M. Ghezzi, N. Caretta, G. Brusco, G. De Filpo, R. Marana, A. Pontecorvi, R. Calafiore, C. Foresta, and A. Garolla. 2017. 'Prednisone treatment in infertile patients with oligozoospermia and accessory gland inflammatory alterations', *Andrology*, 5: 268-73.

Millar, M. R., R. M. Sharpe, G. F. Weinbauer, H. M. Fraser, and P. T. Saunders. 2000. 'Marmoset spermatogenesis: organizational similarities to the human', *Int J Androl*, 23: 266-77.

Missel, A., L. Walenta, K. Eubler, N. Mundt, H. Heikelä, U. Pickl, M. Trottmann, B. Popper, M. Poutanen, L. Strauss, F. M. Köhn, L. Kunz, M. Spehr, and A. Mayerhofer. 2021. 'Testicular adenosine acts as a pro-inflammatory molecule: role of testicular peritubular cells', *Mol Hum Reprod*, 27.

Monaco, L., and M. Conti. 1986. 'Localization of adenosine receptors in rat testicular cells', *Biol Reprod*, 35: 258-66.

Moriyama, K., and M. V. Sitkovsky. 2010. 'Adenosine A2A receptor is involved in cell surface expression of A2B receptor', *J Biol Chem*, 285: 39271-88.

Mruk, D. D., and C. Y. Cheng. 2004. 'Sertoli-Sertoli and Sertoli-germ cell interactions and their significance in germ cell movement in the seminiferous epithelium during spermatogenesis', *Endocr Rev*, 25: 747-806.

Müller, C. E., J. Iqbal, Y. Baqi, H. Zimmermann, A. Rollich, and H. Stephan. 2006. 'Polyoxometalates--a new class of potent ecto-nucleoside triphosphate diphosphohydrolase (NTPDase) inhibitors', *Bioorg Med Chem Lett*, 16: 5943-7.

Mulryan, K., D. P. Gitterman, C. J. Lewis, C. Vial, B. J. Leckie, A. L. Cobb, J. E. Brown, E. C. Conley, G. Buell, C. A. Pritchard, and R. J. Evans. 2000. 'Reduced vas deferens contraction and male infertility in mice lacking P2X1 receptors', *Nature*, 403: 86-9.

Murphy, K. M., and S. H. Snyder. 1981. 'Adenosine receptors in rat testes: labeling with 3H-cyclohexyladenosine', *Life Sci*, 28: 917-20.

Naz, R. K., and L. Evans. 1998. 'Presence and modulation of interleukin-12 in seminal plasma of fertile and infertile men', *J Androl*, 19: 302-7.

Newby, A.C. 1984. 'Adenosine and the concept of 'retaliatory metabolites'', *Trends in Biochemical Sciences*, 9: 42-44.

Nieschlag, E. 2009. 'Aufgaben und Ziele der Andrologie.' in Eberhard Nieschlag, Hermann M. Behre and Susan Nieschlag (eds.), *Andrologie - Grundlagen und Klinik der reproduktiven Gesundheit des Mannes* (Springer, Berlin, Heidelberg).

Nieschlag, E., and H. M. Behre. 2009. 'Anamnese und körperliche Untersuchung.' in Eberhard Nieschlag, Hermann M. Behre and Susan Nieschlag (eds.), *Andrologie - Grundlagen und Klinik der reproduktiven Gesundheit des Mannes*.

Nieschlag, E., H. M. Behre, P. Wieacker, D. Meschede, A. Kamischke, and S. Kliesch. 2009. 'Störungen im Bereich der Testes.' in Eberhard Nieschlag, Hermann M. Behre and Susan Nieschlag (eds.), *Andrologie - Grundlagen und Klinik der reproduktiven Gesundheit des Mannes* (Springer, Berlin, Heidelberg).

O'Bryan, M. K., S. Schlatt, O. Gerdprasert, D. J. Phillips, D. M. de Kretser, and M. P. Hedger. 2000. 'Inducible nitric oxide synthase in the rat testis: evidence for potential roles in both normal function and inflammation-mediated infertility', *Biol Reprod*, 63: 1285-93.

O'Donnell, L., P. K. Nicholls, M. K. O'Bryan, R. I. McLachlan, and P. G. Stanton. 2011. 'Spermiation: The process of sperm release', *Spermatogenesis*, 1: 14-35.

Oatley, J. M., and R. L. Brinster. 2012. 'The germline stem cell niche unit in mammalian testes', *Physiol Rev*, 92: 577-95.

Ohta, A., and M. Sitkovsky. 2001. 'Role of G-protein-coupled adenosine receptors in downregulation of inflammation and protection from tissue damage', *Nature*, 414: 916-20.

Okano, H., K. Hikishima, A. Iriki, and E. Sasaki. 2012. 'The common marmoset as a novel animal model system for biomedical and neuroscience research applications', *Semin Fetal Neonatal Med*, 17: 336-40.

Okuma, Y., K. Saito, A. E. O'Connor, D. J. Phillips, D. M. de Kretser, and M. P. Hedger. 2005. 'Reciprocal regulation of activin A and inhibin B by interleukin-1 (IL-1) and follicle-stimulating hormone (FSH) in rat Sertoli cells in vitro', *J Endocrinol*, 185: 99-110.

Orsi, A., D. Rees, I. Andreini, S. Venturella, S. Cinelli, and G. Oberto. 2011. 'Overview of the marmoset as a model in nonclinical development of pharmaceutical products', *Regul Toxicol Pharmacol*, 59: 19-27.

Pelliccione, F., A. d'Angeli, B. Cinque, S. Falone, A. Micillo, F. Francavilla, F. Amicarelli, L. Gandini, and S. Francavilla. 2011. 'Activation of the immune system and sperm DNA fragmentation are associated with idiopathic oligoasthenoteratospermia in men with couple subfertility', *Fertil Steril*, 95: 2676-9 e1-3.

Petersen, C., B. Froysa, and O. Soder. 2004. 'Endotoxin and proinflammatory cytokines modulate Sertoli cell proliferation in vitro', *J Reprod Immunol*, 61: 13-30.

Petkov, S., T. Kahland, O. Shomroni, T. Lingner, G. Salinas, S. Fuchs, K. Debowski, and R. Behr. 2018. 'Immortalization of common marmoset monkey fibroblasts by piggyBac transposition of hTERT', *PLoS One*, 13: e0204580.

Pierik, F. H., A. M. Van Ginneken, G. R. Dohle, J. T. Vreeburg, and R. F. Weber. 2000. 'The advantages of standardized evaluation of male infertility', *Int J Androl*, 23: 340-6.

Pilatz, A., C. Hudemann, F. Wagenlehner, H. C. Schuppe, T. Diemer, W. Weidner, H. Renz, and T. Bschleipfer. 2013. '[Seminal cytokines: is quantification useful in urogenital disorders?]', *Urologe A*, 52: 359-66.

Pilatz, A., J. Kilb, H. Kaplan, D. Fietz, H. Hossain, C. G. Schuttler, T. Diemer, M. Bergmann, E. Domann, W. Weidner, F. Wagenlehner, and H. C. Schuppe. 2019. 'High prevalence of urogenital infection/inflammation in patients with azoospermia does not impede surgical sperm retrieval', *Andrologia*, 51: e13401.

Pimenta-Dos-Reis, G., E. J. L. Torres, P. G. Quintana, L. O. Vidal, B. A. F. Dos Santos, C. S. Lin, N. Heise, P. M. Persechini, and J. Schachter. 2017. 'POM-1 inhibits P2 receptors and exhibits anti-inflammatory effects in macrophages', *Purinergic Signal*, 13: 611-27.

Polentarutti, N., M. Introna, S. Sozzani, R. Mancinelli, G. Mantovani, and A. Mantovani. 1997. 'Expression of monocyte chemotactic protein-3 in human monocytes and endothelial cells', *Eur Cytokine Netw*, 8: 271-4.

Premanandan, C., and R. Jennings. 2017. *Veterinary Histology* (Ohio State University Libraries).

Ramkumar, V., G. L. Stiles, M. A. Beaven, and H. Ali. 1993. 'The A3 adenosine receptor is the unique adenosine receptor which facilitates release of allergic mediators in mast cells', *J Biol Chem*, 268: 16887-90.

Ramphul, K., and S. G. Mejias. 2021. 'Sertoli-Cell-Only Syndrome.' in, *StatPearls* (Treasure Island (FL)).

Reddy, M. M., S. V. Mahipal, J. Subhashini, M. C. Reddy, K. R. Roy, G. V. Reddy, P. R. Reddy, and P. Reddanna. 2006. 'Bacterial lipopolysaccharide-induced oxidative stress in the impairment of steroidogenesis and spermatogenesis in rats', *Reprod Toxicol*, 22: 493-500.

Reutershan, J., I. Vollmer, S. Stark, R. Wagner, K. C. Ngamsri, and H. K. Eltzschig. 2009. 'Adenosine and inflammation: CD39 and CD73 are critical mediators in LPS-induced PMN trafficking into the lungs', *FASEB J*, 23: 473-82.

Rivkees, S. A. 1994. 'Localization and characterization of adenosine receptor expression in rat testis', *Endocrinology*, 135: 2307-13.

Romano, F., A. Tripiciano, B. Muciaccia, P. De Cesaris, E. Ziparo, F. Palombi, and A. Filippini. 2005. 'The contractile phenotype of peritubular smooth muscle cells is locally controlled: possible implications in male fertility', *Contraception*, 72: 294-7.

Ross, M. H., and I. R. Long. 1966. 'Contractile cells in human seminiferous tubules', *Science*, 153: 1271-3.

Rossi, F., A. Ferraresi, P. Romagni, L. Silvestroni, and V. Santiemma. 2002. 'Angiotensin II stimulates contraction and growth of testicular peritubular myoid cells in vitro', *Endocrinology*, 143: 3096-104.

Russel, W.M.S, and R.L. Burch. 1959. 'The principles of humane experimental technique', *Methuen & Co Ltd, London, UK*.

Russell, L. D., H. Chiarini-Garcia, S. J. Korsmeyer, and C. M. Knudson. 2002. 'Bax-dependent spermatogonia apoptosis is required for testicular development and spermatogenesis', *Biol Reprod*, 66: 950-8.

Sarkar, O., J. Bahrainwala, S. Chandrasekaran, S. Kothari, P. P. Mathur, and A. Agarwal. 2011. 'Impact of inflammation on male fertility', *Front Biosci (Elite Ed)*, 3: 89-95.

Schaeffer, D. J., K. M. Gilbert, J. S. Gati, R. S. Menon, and S. Everling. 2019. 'Intrinsic Functional Boundaries of Lateral Frontal Cortex in the Common Marmoset Monkey', *J Neurosci*, 39: 1020-29.

Schell, C., M. Albrecht, C. Mayer, J. U. Schwarzer, M. B. Frungieri, and A. Mayerhofer. 2008. 'Exploring human testicular peritubular cells: identification of secretory products and regulation by tumor necrosis factor-alpha', *Endocrinology*, 149: 1678-86.

Schell, C., M. Albrecht, S. Spillner, C. Mayer, L. Kunz, F. M. Köhn, U. Schwarzer, and A. Mayerhofer. 2010. '15-Deoxy-delta 12-14-prostaglandin-J2 induces hypertrophy and loss of contractility in human testicular peritubular cells: implications for human male fertility', *Endocrinology*, 151: 1257-68.

Schetinger, M. R., V. M. Morsch, C. D. Bonan, and A. T. Wyse. 2007. 'NTPDase and 5'-nucleotidase activities in physiological and disease conditions: new perspectives for human health', *Biofactors*, 31: 77-98.

Schlatt, S., and J. Ehmcke. 2014. 'Regulation of spermatogenesis: an evolutionary biologist's perspective', *Semin Cell Dev Biol*, 29: 2-16.

Schmid, N., F. Flenkenthaler, J. B. Stockl, K. G. Dietrich, F. M. Köhn, J. U. Schwarzer, L. Kunz, M. Luckner, G. Wanner, G. J. Arnold, T. Fröhlich, and A. Mayerhofer. 2019. 'Insights into replicative senescence of human testicular peritubular cells', *Sci Rep*, 9: 15052.

Schmid, N., A. Missel, S. Petkov, J. B. Stockl, F. Flenkenthaler, G. J. Arnold, T. Fröhlich, R. Behr, and A. Mayerhofer. 2020. 'A translational cellular model for the study of peritubular cells of the testis', *Reproduction*, 160: 259-68.

Schmid, N., J. B. Stockl, F. Flenkenthaler, K. G. Dietrich, J. U. Schwarzer, F. M. Köhn, C. Drummer, T. Frohlich, G. J. Arnold, R. Behr, and A. Mayerhofer. 2018. 'Characterization of a non-human primate model for the study of testicular peritubular cells-comparison with human testicular peritubular cells', *Mol Hum Reprod*, 24: 401-10.

Schuppe, H. C., A. Pilatz, H. Hossain, A. Meinhardt, M. Bergmann, G. Haidl, and W. Weidner. 2010. '[Orchitis and male infertility]', *Urologe A*, 49: 629-35.

Seshadri, S., M. Bates, G. Vince, and D. I. Jones. 2009. 'The role of cytokine expression in different subgroups of subfertile men', *Am J Reprod Immunol*, 62: 275-82.

Shami, A. N., X. Zheng, S. K. Munyoki, Q. Ma, G. L. Manske, C. D. Green, M. Sukhwani, K. E. Orwig, J. Z. Li, and S. S. Hammoud. 2020. 'Single-Cell RNA Sequencing of Human, Macaque, and Mouse Testes Uncovers Conserved and Divergent Features of Mammalian Spermatogenesis', *Dev Cell*, 54: 529-47 e12.

Shimogori, T., A. Abe, Y. Go, T. Hashikawa, N. Kishi, S. S. Kikuchi, Y. Kita, K. Niimi, H. Nishibe, M. Okuno, K. Saga, M. Sakurai, M. Sato, T. Serizawa, S. Suzuki, E. Takahashi, M. Tanaka, S. Tatsumoto, M. Toki, M. U, Y. Wang, K. J. Windak, H. Yamagishi, K. Yamashita, T. Yoda, A. C. Yoshida, C. Yoshida, T. Yoshimoto, and H. Okano. 2018. 'Digital gene atlas of neonate common marmoset brain', *Neurosci Res*, 128: 1-13.

Skakkebaek, N. E., E. Rajpert-De Meyts, G. M. Buck Louis, J. Toppari, A. M. Andersson, M. L. Eisenberg, T. K. Jensen, N. Jorgensen, S. H. Swan, K. J. Sapra, S. Ziebe, L. Priskorn, and A. Juul. 2016. 'Male Reproductive Disorders and Fertility Trends: Influences of Environment and Genetic Susceptibility', *Physiol Rev*, 96: 55-97.

Skinner, M. K., P. S. Tung, and I. B. Fritz. 1985. 'Cooperativity between Sertoli cells and testicular peritubular cells in the production and deposition of extracellular matrix components', *J Cell Biol*, 100: 1941-7.

Smith, N. J., and G. Milligan. 2010. 'Allostery at G protein-coupled receptor homo- and heteromers: uncharted pharmacological landscapes', *Pharmacol Rev*, 62: 701-25.

Soderstrom, K. O. 1986. 'Tubular hyalinization in human testis', *Andrologia*, 18: 97-103.

Sohni, A., K. Tan, H. W. Song, D. Burow, D. G. de Rooij, L. Laurent, T. C. Hsieh, R. Rabah, S. S. Hammoud, E. Vicini, and M. F. Wilkinson. 2019. 'The Neonatal and Adult Human Testis Defined at the Single-Cell Level', *Cell Rep*, 26: 1501-17 e4.

Spinnler, K., F. M. Köhn, U. Schwarzer, and A. Mayerhofer. 2010. 'Glial cell line-derived neurotrophic factor is constitutively produced by human testicular

peritubular cells and may contribute to the spermatogonial stem cell niche in man', *Hum Reprod*, 25: 2181-7.

Spychala, J. 2000. 'Tumor-promoting functions of adenosine', *Pharmacol Ther*, 87: 161-73.

Stephan, J. P., V. Syed, and B. Jegou. 1997. 'Regulation of Sertoli cell IL-1 and IL-6 production in vitro', *Mol Cell Endocrinol*, 134: 109-18.

Syed, V., J. P. Stephan, N. Gerard, A. Legrand, M. Parvinen, C. W. Bardin, and B. Jegou. 1995. 'Residual bodies activate Sertoli cell interleukin-1 alpha (IL-1 alpha) release, which triggers IL-6 production by an autocrine mechanism, through the lipoxygenase pathway', *Endocrinology*, 136: 3070-8.

t Hart, B. A., M. van Meurs, H. P. Brok, L. Massacesi, J. Bauer, L. Boon, R. E. Bontrop, and J. D. Laman. 2000. 'A new primate model for multiple sclerosis in the common marmoset', *Immunol Today*, 21: 290-7.

Trautmann, A. 2009. 'Extracellular ATP in the immune system: more than just a "danger signal"', *Sci Signal*, 2: pe6.

Travison, T. G., A. B. Araujo, S. A. Hall, and J. B. McKinlay. 2009. 'Temporal trends in testosterone levels and treatment in older men', *Curr Opin Endocrinol Diabetes Obes*, 16: 211-7.

Travison, T. G., A. B. Araujo, A. B. O'Donnell, V. Kupelian, and J. B. McKinlay. 2007. 'A population-level decline in serum testosterone levels in American men', *J Clin Endocrinol Metab*, 92: 196-202.

Tripiciano, A., A. Filippini, Q. Giustiniani, and F. Palombi. 1996. 'Direct visualization of rat peritubular myoid cell contraction in response to endothelin', *Biol Reprod*, 55: 25-31.

Tsai, M. C., Y. S. Cheng, T. Y. Lin, W. H. Yang, and Y. M. Lin. 2012. 'Clinical characteristics and reproductive outcomes in infertile men with testicular early and late maturation arrest', *Urology*, 80: 826-32.

Tung, P. S., and I. B. Fritz. 1987. 'Morphogenetic restructuring and formation of basement membranes by Sertoli cells and testis peritubular cells in co-culture: inhibition of the morphogenetic cascade by cyclic AMP derivatives and by blocking direct cell contact', *Dev Biol*, 120: 139-53.

———. 1990. 'Characterization of rat testicular peritubular myoid cells in culture: alpha-smooth muscle isoactin is a specific differentiation marker', *Biol Reprod*, 42: 351-65.

———. 1991. 'Transforming growth factor-beta and platelet-derived growth factor synergistically stimulate contraction by testicular peritubular cells in culture in serum-free medium', *J Cell Physiol*, 146: 386-93.

Veitinger, S., T. Veitinger, S. Cainarca, D. Fluegge, C. H. Engelhardt, S. Lohmer, H. Hatt, S. Corazza, J. Spehr, E. M. Neuhaus, and M. Spehr. 2011. 'Purinergic signalling mobilizes mitochondrial Ca(2)(+) in mouse Sertoli cells', *J Physiol*, 589: 5033-55.

Walenta, L., D. Fleck, T. Frohlich, H. von Eysmondt, G. J. Arnold, J. Spehr, J. U. Schwarzer, F. M. Köhn, M. Spehr, and A. Mayerhofer. 2018. 'ATP-mediated Events in Peritubular Cells Contribute to Sterile Testicular Inflammation', *Sci Rep*, 8: 1431.

Weber, A., P. Wasiliew, and M. Kracht. 2010. 'Interleukin-1 (IL-1) pathway', *Sci Signal*, 3: cm1.

Weber, J. E., L. D. Russell, V. Wong, and R. N. Peterson. 1983. 'Three-dimensional reconstruction of a rat stage V Sertoli cell: II. Morphometry of Sertoli--Sertoli and Sertoli--germ-cell relationships', *Am J Anat*, 167: 163-79.

Weinbauer, G.F., C.M. Luetjens, M. Simoni, and E. Nieschlag. 2009. 'Physiologie der Hodenfunktion.' in Eberhard Nieschlag, Hermann M. Behre and Susan Nieschlag (eds.), *Andrologie - Grundlagen und Klinik der reproduktiven Gesundheit des Mannes* (Springer, Berlin, Heidelberg).

Welsh, M., L. Moffat, K. Belling, L. R. de Franca, T. M. Segatelli, P. T. Saunders, R. M. Sharpe, and L. B. Smith. 2012. 'Androgen receptor signalling in peritubular myoid cells is essential for normal differentiation and function of adult Leydig cells', *Int J Androl*, 35: 25-40.

Welter, H., A. Huber, S. Lauf, D. Einwang, C. Mayer, J. U. Schwarzer, F. M. Köhn, and A. Mayerhofer. 2014. 'Angiotensin II regulates testicular peritubular cell function via AT1 receptor: a specific situation in male infertility', *Mol Cell Endocrinol*, 393: 171-8.

Welter, H., C. Kampfer, S. Lauf, R. Feil, J. U. Schwarzer, F. M. Köhn, and A. Mayerhofer. 2013. 'Partial loss of contractile marker proteins in human testicular peritubular cells in infertility patients', *Andrology*, 1: 318-24.

Wendell, S. G., H. Fan, and C. Zhang. 2020. 'G Protein-Coupled Receptors in Asthma Therapy: Pharmacology and Drug Action', *Pharmacol Rev*, 72: 1-49.

WHO. 2020. 'Infertility - Key facts'.

———. 2021. 'WHO laboratory manual for the examination and processing of human semen', Sixth Edition.

Wildt, D. E., P. Comizzoli, B. Pukazhenthi, and N. Songsasen. 2010. 'Lessons from biodiversity--the value of nontraditional species to advance reproductive science, conservation, and human health', *Mol Reprod Dev*, 77: 397-409.

Wistuba, J., A. Schrod, B. Greve, J. K. Hodges, H. Aslam, G. F. Weinbauer, and C. M. Luetjens. 2003. 'Organization of seminiferous epithelium in primates: relationship to spermatogenic efficiency, phylogeny, and mating system', *Biol Reprod*, 69: 582-91.

Wong, C. H., and C. Y. Cheng. 2005. 'The blood-testis barrier: its biology, regulation, and physiological role in spermatogenesis', *Curr Top Dev Biol*, 71: 263-96.

Wosnitzer, M., M. Goldstein, and M. P. Hardy. 2014. 'Review of Azoospermia', *Spermatogenesis*, 4: e28218.

Wu, A. R., J. Wang, A. M. Streets, and Y. Huang. 2017. 'Single-Cell Transcriptional Analysis', *Annu Rev Anal Chem (Palo Alto Calif)*, 10: 439-62.

Xia, W., D. D. Mruk, W. M. Lee, and C. Y. Cheng. 2005. 'Cytokines and junction restructuring during spermatogenesis--a lesson to learn from the testis', *Cytokine Growth Factor Rev*, 16: 469-93.

Xiong, W., H. Wang, H. Wu, Y. Chen, and D. Han. 2009. 'Apoptotic spermatogenic cells can be energy sources for Sertoli cells', *Reproduction*, 137: 469-79.

Yang, R., S. Elsaadi, K. Misund, P. Abdollahi, E. N. Vandsemb, S. H. Moen, A. Kusnierczyk, G. Slupphaug, T. Standal, A. Waage, T. S. Slordahl, T. B. Ro, E. Rustad, A. Sundan, C. Hay, Z. Cooper, A. G. Schuller, R. Woessner, A. Borodovsky, E. Menu, M. Borset, and A. M. Sponaas. 2020. 'Conversion of ATP to adenosine by CD39 and CD73 in multiple myeloma can be successfully targeted together with adenosine receptor A2A blockade', *J Immunother Cancer*, 8.

Yoon, J. C., J. L. Casella, M. Litvin, and A. S. Dobs. 2019. 'Male reproductive health in cystic fibrosis', *J Cyst Fibros*, 18 Suppl 2: S105-S10.

Zamoner, A., A. N. Bruno, E. A. Casali, P. F. Corbelini, G. P. Diniz, M. L. Barreto-Chaves, F. R. Silva, J. J. Sarkis, and R. Pessoa-Pureur. 2006. 'Genomic-independent action of thyroid hormones on NTPDase activities in Sertoli cell cultures from congenital hypothyroid rats', *Life Sci*, 80: 51-8.

Zebisch, M., M. Krauss, P. Schafer, and N. Strater. 2012. 'Crystallographic evidence for a domain motion in rat nucleoside triphosphate diphosphohydrolase (NTPDase) 1', *J Mol Biol*, 415: 288-306.

Zhao, H., C. Bo, Y. Kang, and H. Li. 2017. 'What Else Can CD39 Tell Us?', *Front Immunol*, 8: 727.

Zimmermann, H. 1992. '5'-Nucleotidase: molecular structure and functional aspects', *Biochem J*, 285 (Pt 2): 345-65.

———. 2021. 'Ectonucleoside triphosphate diphosphohydrolases and ecto-5'-nucleotidase in purinergic signaling: how the field developed and where we are now', *Purinergic Signal*, 17: 117-25.

Zimmermann, H., M. Zebisch, and N. Strater. 2012. 'Cellular function and molecular structure of ecto-nucleotidases', *Purinergic Signal*, 8: 437-502.

Zuhlke, U., and G. Weinbauer. 2003. 'The common marmoset (Callithrix jacchus) as a model in toxicology', *Toxicol Pathol*, 31 Suppl: 123-7.

ADDITIONAL PROJECT

Single-cell analysis of HTPCs

In recent years the powerful method of single-cell RNA-seq was established, using next-generation sequencing technologies on thousands of individual cells. This method enables studies on entire organs with no need for prior sorting. It also allows one to study cells of *in vitro* cultures and to identify their expression profiles, to uncover heterogeneity of cell clusters and to indicate developmental trajectories (Wu et al. 2017).

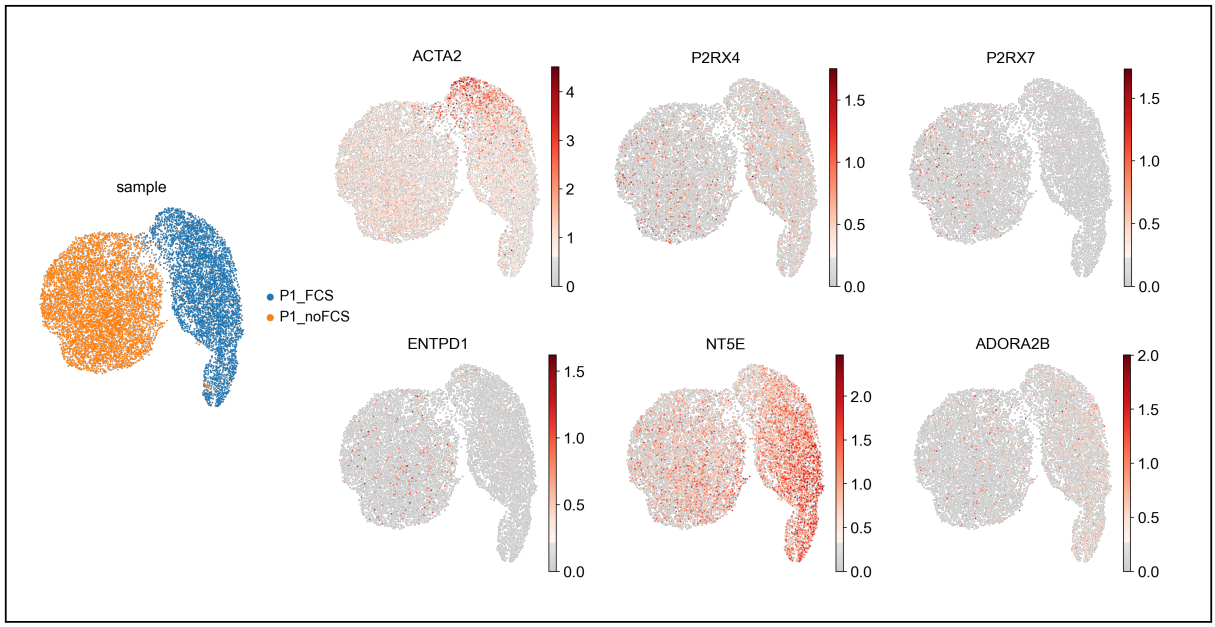

Figure 10. UMAP plot of the single-cell HTPC dataset.

HTPC samples exposed to two conditions, were integrated after single-cell sequencing and visualized using UMAP (blue: cultivated with FCS; orange: serum starved). Expression patterns of the typical peritubular marker gene ACTA2, the P2-receptors P2X4 and P2X7, the ectonucleotidases CD39 (ENTPD1) and CD73 (NT5E), and the adenosine receptor A2B are shown. Grey points indicate low or no expression and red points higher expression.

Employing a single-cell sequencing approach, HTPCs were analysed in a pilot study. Cells stem from a testicular sample which displayed normal spermatogenesis, and were exposed to two conditions: ('FCS') cultivation in standard conditions containing

5% FCS (Fetal calf serum) or ('noFCS') serum starvation for 24 h. 10,000 cells of each sample were loaded into a Chromium Single Cell Chip A (10x Genomics). After cDNA synthesis, library construction and sequencing, raw data was filtered regarding different quality control metrics and normalized. Based on a principal component analysis, a sheared neighbour graph was constructed and final data was visualized using the non-linear dimensional reduction method UMAP (Becht et al. 2018; McInnes and Healy 2018).

Figure 10 shows preliminary unpublished results. Expression of the typical peritubular marker gene *ACTA2* proves the cellular identity of HTPCs. Furthermore, the receptors *P2X4, P2X7, A2B* and ectonucleotidases *CD39* (*ENPTD1*) and *CD73* (*NT5E*), as part of the purinergic system, were detected in HTPCs. Differences in expression profiles between both conditions are detectable and require further evaluation. Each sample provides information of more than 6,000 cellular transcriptomes with more than 17,000 measured genes.

Single-cell sequencing enables a wide range of opportunities allowing in-depth insights into peritubular cells. Therefore, next to one-dimensional expression profiles of various genes, high-dimensional vectors like RNA-velocity can be analysed, indicating future states of individual cells. Single-cell studies of whole testis samples have recently been published, profiling developmental and pathological aspects (Guo et al. 2018; Sohni et al. 2019; Shami et al. 2020; Di Persio et al. 2021; Guo et al. 2021). As peritubular cells represent only a small proportion of testicular cells, the analysis of isolated and *in vitro* cultivated peritubular cells, compared to the *in vivo* situation will extend previous findings.

LIST OF FIGURES

ACKNOWLEDGEMENTS

"Creative people express themselves, in science or art."
(Geoffrey Burnstock)

Sincere gratitude to Prof. Dr. Artur Mayerhofer. I am very grateful for the chance you gave me, when I came to your lab as a practical student with no experience in cellular biology. The last years were full of continuous support, discussions, guidance, motivation, and a wide range of possibilities. Thank you for this great project, your trust in my work, and the freedom you gave me to bring the proper amount of creativity into these studies.

Further, I would like to extend my sincere thanks to PD Dr. Lars Kunz as my mentor in this thesis. You always had an open ear for all the challenges in the last years, you came up with new ideas, a critical view in proof reading of the thesis, a lot of patience and many helpful discussions.

I would like to thank Prof. Dr. Gisela Grupe for the helpful discussions in all the TAC-meetings, for the great support, and the new perspectives. Big thanks to Prof. Dr. Annette Müller-Taubenberger for all the motivating discussions during these studies. Also, thank you Prof. Dr. Jörg Nickelsen and Prof. Dr. Christof Osman for joining the examining board.

Furthermore, I am thankful for my collaborators and the amazing projects, which contributed to this work. Prof. Dr. Marc Spehr, thank you and your group for the great teamwork, the invitation to your lab and stunning insights into your work. Also, thanks to Prof. PhD Matti Poutanen and PhD Leena Strauss for providing the mouse testis samples, the great insights into your lab in Turku and the wonderful time with you and your group in Mathildedal. Thanks to PD Dr. Matthias Trottmann and Dr. Manfred Schleyer for the continuous supply of human testis samples. I want to thank Prof. Dr. Rüdiger Behr and Dr. Stoyan Petkov for the great collaboration in the study of the iMKTPCs and the inspiring visit at the Primatenzentrum in Göttingen. To

Prof. Dr. Jovica Ninkovic, Christina Koupourtidou as well as PhD Jingtao Guo, thank you for the collaboration in the fascinating single-cell sequencing projects.

This work would not have been possible and this fun without the Mayerhofer lab group and their wonderful atmosphere. First of all, thank you Dr. Lena Walenta for the initial supervision and guidance. Big thanks to my iMKTPC partner Dr. Nina Schmid and to our technicians Kim Dietrich, Astrid Tiefenbacher, Carola Herrmann and Nicole Kreitmair for their continuous help and support. To all of our current and former lab members – Daniel Aigner, Dr. Konstantin Bagnjuk, Sarah Beschta, Dr. Theresa Buck, Katja Eubler, Theo Hack, Verena Kast, Benedikt Mach, Melanie Kaseder, Karin Metzrath, Merit Müür, Moritz Offner, Pia Seßenhausen, Dr. Harald Welter – thank you for all the helpful discussions, fun excursions, Christmas parties, Mölkky games, pretzels, cakes, sparkling wine, and the overall great atmosphere, even in our daily lab routine. Special thanks to my proof-reading team Pia and Nina.

The most special gratitude goes to Michael and my family. You gave me the best emotional support during this time and without you this project wouldn't have been possible in this way.

APPENDIX

List of additional publications

Nie, X., S. K. Munyoki, M. Sukhwani, N. Schmid, **A. Missel**, B. R. Emery, Donor Connect, J.-B. Stukenborg, A. Mayerhofer, K. E. Orwig, K. I. Aston, J. M. Hotaling, B. R. Cairns and J. Guo. 2021. 'Single-Cell Analysis of Human Testis Aging, and Impact of Elevated Body Mass Index', bioRxiv, doi: 10.1101/2021.10.19.464550

Eubler, K., P. Rantakari, H. Gerke, C. Herrmann, **A. Missel**, N. Schmid, L. Walenta, S. Lahiri, A. Imhof, L. Strauss, M. Poutanen, and A. Mayerhofer. 2021. 'Exploring the Ion Channel TRPV2 and Testicular Macrophages in Mouse Testis', *Int J Mol Sci*, 22.

Welter, H., C. Herrmann, N. Dellweg, **A. Missel**, C. Thanisch, H. F. Urbanski, F. M. Köhn, J. U. Schwarzer, A. Müller-Taubenberger, and A. Mayerhofer. 2020. 'The Glucocorticoid Receptor NR3C1 in Testicular Peritubular Cells is Developmentally Regulated and Linked to the Smooth Muscle-Like Cellular Phenotype', *J Clin Med*, 9.

Scientific posters

European Testis Workshop (ETW), 2021

Miniposter: Exploring the purinergic system of the testis: Ectonucleotidases CD39/CD73 and ADORA receptors (**Missel A.,** Walenta L., Pickl U., Trottmann M., Köhn F.M., Mayerhofer A.) **Registration fee grant** (sponsored by the International Society of Andrology)

American Society of Andrology (ASA), 46th Annual Conference, 2021

Poster presentation: Adenosine Acts as a Pro-Inflammatory Molecule in the Testis: Role of Testicular Peritubular Cells (**Missel A.,** Walenta L., Eubler K., Mundt N., Pickl U., Trottmann M., Popper B., Poutanen M., Köhn F.M., Kunz L., Spehr M., Mayerhofer A.)

32. German Congress of Andrology (DGA), 2020

Poster presentation: Adenosine is a pro-inflammatory molecule in human testicular peritubular cells (**Missel A.,** Walenta L., Trottmann M., Pickl U., Köhn F.M., Mayerhofer A.)

62. Symposium of German Association of Endocrinology (DGE), Göttingen, 2019

Poster: A translational cellular model for the study of the peritubular cells of the testis (**Missel A.**, Schmid N., Petkov S., Stöckl JB., Arnold GJ., Fröhlich T., Behr R., Mayerhofer A.) **Best poster award**

61. Symposium of German Association of Endocrinology (DGE), Bonn, 2018

Poster: Inhibition of the ectonucleotidase CD39 reduces inflammatory effects of ATP in human testicular peritubular cells (**Missel A.,** Walenta L., Schwarzer JU., Köhn F.M., Mayerhofer A.) **Best poster award**